AN ABSTRACT OF THE DISSERTATION OF

Rebecca L. Maher for the degree of Doctor of Philosophy in Microbiology presented on June 7, 2021.

Title: Multiple Stressors Drive Changes in Coral Microbiome Diversity and Composition Demonstrating the Role of a Bacterial Symbiont in Microbial Community Sensitivity and Resilience.

Abstract approved:

_____

Rebecca L. Vega Thurber

On coral reefs, disturbances rarely occur in isolation. Global stressors such as increasing seawater temperature often coincide with local stressors like nutrient pollution. In the face of increasing anthropogenic stress, corals can function as environmental sentinels, although little is known about how multiple stressors interact to disrupt their associated bacterial communities and how symbiotic bacteria contribute to coral resistance and resilience to stress. Previous studies have shown that coral microbiomes under stress demonstrate shifts to more disease-associated states, increases in community variability, compromised function of beneficial microbiota, and selection for potentially pathogenic bacteria. Given that coral microbiota are thought to play an important role in host nutrient cycling and antimicrobial protection, it is important to understand how their response to individual and combined stressors can mitigate or exacerbate host susceptibility. My dissertation work coupled ecological experiments with DNA sequencing, bioinformatics, and multivariate statistics to describe compositional changes in coral

microbiomes under various combinations of stressors and to infer the role of symbiotic bacteria in holobiont sensitivity and resilience to environmental disturbance.

Ecological literature classifies interactions between combinations of individual stressors as synergistic, antagonistic, or having no interaction. We utilized common multivariate analyses to apply this multiple stressor framework to host-associated microbial communities. We conducted multiple stressor experiments both in mesocosm tanks and in the field on corals in Mo'orea, French Polynesia to evaluate how their microbiomes change compositionally with increasing and interacting levels of perturbation. We applied either no stress or single, double, or triple stressors of nutrient enrichment, simulated predation, and increased seawater temperature in mesocosm tanks to the coral *Pocillopora meandrina* for 21 days. We predicted that when sequentially adding stressors to the experimental system, we would observe a compounding increase in changes to the microbiome. In contrast, we found that microbiome disruption or variation from healthy controls does not scale positively with increasing number of stressors. In contrast to more heterogeneous communities that may be more robust to changes due to high diversity and functional redundancy, healthy *P. meandrina* controls were so dominated by Endozoicomonas, a proposed beneficial symbiont, such that any amount or type of stress was sufficient to increase community evenness. Single stressors of high temperature and scarring produced the largest shifts in community structure and additional stressors acted antagonistically to produce a less-than-additive response. We found that microbiome variability or dispersion increased with any number of stressors and community

dysbiosis is characterized by a proliferation of opportunistic bacteria such as *Rhodobacteraceae* and *Desulfovibrionaceae* rather than a depletion of the dominant taxon, *Endozoicomonas*.

To study this phenomenon *in situ,* we enriched corals on the reef before, during, and after a natural thermal stress event in 2016 to observe changes in the microbiome of *Acropora*, *Pocillopora*, and *Porites* corals undergoing concurrent temperature and nutrient stress. Concurrent work showed that corals exposed to nitrate exhibited more frequent bleaching, bleaching for longer duration, and were more likely to die. However, as observed in the tank experiment, we found that nutrients are less important for shaping the microbial community than temperature. The addition of nitrate and urea to the water column had no effect on the coral microbiome and did not interact with temperature. The three coral hosts displayed varying degrees of sensitivity to warm temperatures suggesting alternate strategies for coping with stress. Overall, post-stress microbiomes did not return to pre-stress community composition, but rather were less diverse and increasingly dominated by *Endozoicomonas* which could suggest its ability to utilize host metabolic products of thermal stress for a sustained competitive advantage against other microbial taxa. While we are only beginning to uncover the functional role of *Endozoicomonas*, these results suggest it may contribute to microbiome resilience to thermal stress.

Endozoicomonas species associate with a wide variety of marine hosts, and within corals, are hypothesized to breakdown dimethylsulfoniopropionate (DMSP) which the coral host produces during thermal stress. To investigate this role and other potential roles in nutrition and defense, I used culture-independent methods of

genome sequencing, metagenomics, to assemble the *Endozoicomonas* symbiont residing in *Pocillopora meandrina* corals in Mo'orea. Comparative genomics was subsequently conducted on all available *Endozoicomonas* genomes to better understand their shared and distinct functional characteristics. Despite their large genomes, *Endozoicomonas* species do not appear to contribute significantly to the cycling of carbon, nitrogen, or sulfur within the holobiont. Instead, they have many genomic features that could facilitate the maintenance of a stable symbiosis with their marine eukaryotic hosts. Only two *Endozoicomonas* species, not including our MAG (metagenome-assembled genome), encode genes involved in the breakdown of DMSP. Thus, we found no obvious genomic features that would suggest susceptibility or tolerance of this symbiont to thermal stress.

In this dissertation, I demonstrate how a dominant member of the coral host-associated microbial community can drive patterns in community diversity and variability, ultimately influencing community resistance and resilience. While I investigate the genetic potential of this dominant taxon, genomic features that contribute to community sensitivity or resilience remain elusive. Overall, this work highlights the complexity of possible interaction outcomes for environmental stressors to coral reefs when assessed at the microbial scale and presents foundational patterns in microbiome dysbiosis and recovery that can inform reef persistence into the future.

Multiple Stressors Drive Changes in Coral Microbiome Diversity and Composition Demonstrating the Role of a Bacterial Symbiont in Microbial Community Sensitivity and Resilience

by
Rebecca L. Maher

A DISSERTATION

submitted to

Oregon State University

in partial fulfillment of
the requirements for the
degree of

Doctor of Philosophy

Presented June 7, 2021
Commencement June 2021

Doctor of Philosophy dissertation of Rebecca L. Maher presented on June 7, 2021.

APPROVED:

Major Professor, representing Microbiology

Head of the Department of Microbiology

Dean of the Graduate School

I understand that my dissertation will become part of the permanent collection of Oregon State University libraries. My signature below authorizes release of my dissertation to any reader upon request.

Rebecca L. Maher, Author

ACKNOWLEDGEMENTS

This dissertation work was generously funded by the NSF Graduate Research Fellowship Program and the Ford Foundation Dissertation Fellowship. I would like to thank my adviser Dr. Rebecca Vega Thurber for giving me incredible research opportunities and knowledge as a graduate student. Thank you very much to my committee members, Dr. Ryan Mueller, Dr. Virginia Weis, Dr. Jeff Anderson, and Dr. Katie McLaughlin. I have had numerous mentors who helped shape me into the scientist I am today and were great friends along the way, including: Dr. Stephanie Rosales, Dr. Ryan McMinds, Dr. Mallory Rice, Dr. Lëila Ezzat, and Dr. Adrienne Correa. I would also like to thank past and present members of the Vega Thurber Lab, especially Adriana Messyasz, Grace Klinges, Emily Schmeltzer, and Dr. Lydia Baker. To Adriana and Grace, I am so incredibly grateful to have gone through this graduate journey together and to be leaving with so many wonderful memories. Thank you to all my grad student friends in the Department of Microbiology and in Corvallis. I would also like to thank Dr. Krista Nichols and researchers at the Northwest Fisheries Science Center to taking me in during my Graduate Research Internship. Thank you to all the incredible scientists I met at various conferences that always made me so excited to be a scientist. Lastly, I want to thank my parents, my sister, and my partner. With your endless love and support, I have always felt like I could do anything.

CONTRIBUTION OF AUTHORS

Dr. Mallory M. Rice conceived of, designed, and conducted the experiment in Chapter 2 and reviewed the manuscript. Dr. Ryan McMinds assisted in bioinformatic and statistical analysis for Chapters 2 & 3. Dr. Deron E. Burkepile conceived of and designed the experiments in Chapter 2 and 3. He helped interpret the data and reviewed the manuscripts. Emily R. Schmeltzer and Sonora Meiling conducted the labwork in Chapter 3. Dr. Leïla Ezzat assisted in interpreting the data for Chapter 3 and reviewed the manuscript. Dr. Andrew A. Shantz and Dr. Thomas C. Adam conducted the experiment in Chapter 3 and reviewed the manuscript. Dr. Russel J. Schmitt and Dr. Sally J. Holbrook conceived of and designed the experiment in Chapter 3 and reviewed the manuscript.

TABLE OF CONTENTS

TABLE OF CONTENTS (Continued)

TABLE OF CONTENTS (Continued)

TABLE OF CONTENTS (Continued)

LIST OF FIGURES

LIST OF TABLES

LIST OF APPENDIX FIGURES

LIST OF APPENDIX TABLES

LIST OF APPENDIX TABLES (Continued)

DEDICATION

I dedicate this dissertation to my parents who shared with me their love for knowledge and curiosity about the natural world and gave me the opportunity to follow my passions.

CHAPTER 1 GENERAL INTRODUCTION

1.1. Threats to coral reef ecosystems and the services they provide

Corals are the main builders of reef structure through the deposition of calcium carbonate. This framework creates a three-dimensional, complex habitat that serves as the basis for one of the most biodiverse and productive ecosystems (Reaka-Kudla, 1997). Coral reefs provide essential goods and services both to marine nations and to the global human population. These ecosystems provide a home for nearly a third of the worlds marine fish species, a fundamental source of protein through reef fisheries, a source of income for coastal nations through tourism-based industries, a form of coastal protection from physical degradation, and, lastly, a source of aesthetic and cultural value (Moberg and Folke, 1999). Unfortunately, coral reefs are critically threatened by various anthropogenic impacts that jeopardize these invaluable goods and services.

Increasing numbers of reefs worldwide are in decline as unprecedented environmental changes are fundamentally altering the composition of coral reefs (Ainsworth and Gates, 2016). According to the 2011 *Reefs at Risk Revisited* report from the World Resources Institute, more than 60% of coral reefs around the world are threatened from local sources by overfishing, destructive fishing, coastal development, and watershed- or marine-based pollution. Overfishing is the most pervasive and immediate local threat and can lead to the alteration of the trophic food web in reef ecosystems such that the persistence of healthy reef substrate is jeopardized. For instance, the over-harvesting of predatory fish allowed their rock-

boring sea urchin prey to rapidly proliferate, thereby excluding herbivorous fish and increasing the erosion of reef substrate (McClanahan and Kurtis, 1991). While overfishing of herbivorous fish is considered the primary mechanism driving the shift from coral- to macroalgal-dominated reefs, nutrient loading can also give algae the competitive advantage over slow-growing corals, and the combination of overfishing and nutrient loading can interact to magnify these effects (Burkepile and Hay, 2006; Vermeij et al., 2010). Water quality and turbidity, as affected by land clearing, coastal urbanization, agriculture, and the associated pollution, is also a major regional driver of coral fitness and reef health (De'ath and Fabricius, 2010).

In contrast to local threats, global threats resulting from climate change including ocean warming and acidification are widespread and cannot be mitigated by local or regional policy or management (De'ath et al., 2012). Rising sea surface temperature caused by anthropogenic global warming not only increases the frequency and severity of tropical storm events but also is a major cause of coral bleaching, or the breakdown of the relationship between corals and their endosymbiotic algae, Symbiodiniaceae (Hoegh-Guldberg, 1999; Knutson et al., 2010; Heron et al., 2016). Temperature-induced bleaching results from excessive production of reactive oxygen species by the algal symbiont leading to oxidative stress within the holobiont and the expulsion of the symbiont by the coral host (Weis, 2008; Nielsen et al., 2018). Bleaching events can cause mass coral mortality, reduce coral species diversity, and alter the species assemblage on a reef (Grottoli et al., 2014; Hughes et al., 2017). Adding to concern, global climate models based on current emission

scenarios forecast that the majority of the world's coral reefs will bleach annually within 30-50 years (van Hooidonk et al., 2013). Although bleached corals can recover once thermal stress is alleviated, global warming is increasing the frequency and intensity of thermal stress events thereby shortening the recovery period for bleached corals (Heron et al., 2016; Hughes et al., 2018). Further, the coral-Symbiodiniaceae relationship depends on a delicate balance and exchange of nutrients within the holobiont. Independent of oxidative stress, environmental enrichment of nitrate and/or phosphate limitation can cause changes in autotrophic metabolism and total carbon translocation to the host, resulting in coral bleaching (Morris et al., 2019). Additionally, evidence exists that the combination of nutrients that weaken the coral-algal symbiosis and thermal stress can act synergistically to further reduce translocation and increase the severity of bleaching (Burkepile et al., 2019). The combination of local impacts and global climate shifts places the future of coral reef ecosystems and the services they provide in jeopardy. Therefore, it is of critical import to investigate the ecological resistance and resilience of corals to these current threats.

1.2. Coral microbiome spatial and temporal patterns

The fundamental role of corals as ecosystem engineers depends heavily on the dynamic relationship of the coral animal and its associated microorganisms. Decades of research into animal-microbe symbioses have shown that microbial symbionts profoundly influence the growth and development of their eukaryotic hosts and contribute to energy metabolism, nutrition, digestion, defense, and immune system

modulation (Chu and Mazmanian, 2013; McFall-Ngai et al., 2013; Russell et al., 2014; Burkepile and Thurber, 2019). Similarly, corals have a mutually beneficial symbiosis with photosynthetic dinoflagellates (Symbiodiniaceae) which fix carbon and provide organic matter to their coral hosts thus allowing the coral to survive in the nutrient-poor waters that characterize coral reefs (Davy et al., 2012; van Oppen and Blackall, 2019). In addition to this well-studied symbiosis, corals are also associated with bacteria, archaea, fungi, protists, and viruses, collectively referred to as the coral holobiont (Rohwer et al., 2002).

Given the preponderance of evidence linking the health and function of living organisms and their microbiomes, combined with the global decline of coral reefs, there has been a recent surge in published studies investigating the diversity and function of coral-associated microorganisms (reviewed in van Oppen and Blackall, 2019). While researchers have been attempting to describe and isolate bacteria from corals for over 60 years, studies investigating the coral-associated microbial community began roughly 15 years ago facilitated by the application of next-generation sequencing (NGS) (Disalvo, 1969; Wegley et al., 2007; Thurber et al., 2009; van Oppen and Blackall, 2019). Numerous studies using 16S rRNA gene metabarcoding have begun to uncover the taxonomic diversity of bacteria and archaea associated with corals. With 39 described and candidate bacterial phyla and two archaeal phyla identified to date, corals are one of the most phylogenetically diverse animal microbiomes (Huggett and Apprill, 2019a). The most common bacterial associates reside within the Gammaproteobacteria, Alphaproteobacteria,

Bacteroidetes, Cyanobacteria, Firmicutes, and Tenericutes (Huggett and Apprill, 2019a). However, individual coral hosts are commonly dominated by two or three bacterial classes which is strong evidence for taxonomic, and likely functional, redundancy within the coral microbiome (Hernandez-Agreda et al., 2018).

The current challenge facing coral microbiome researchers involves uncovering spatial and temporal patterns in microbial community diversity and structure, as well as the drivers of these patterns. Bacterial communities change throughout the life cycle of the coral host, with adults demonstrating decreased diversity and increased temporal stability compared to juveniles of the same species (Epstein et al., 2019a). This indicates a "winnowing" process throughout host development by which bacterial assemblages are fine-tuned to meet the needs of a specific host in the local environmental conditions (Lema et al., 2014; Epstein et al., 2019a). Coral associated bacterial communities vary at spatial scales of millimeters due to differences between coral compartments: mucus, tissue, gastrovascular cavity, and skeleton up to spatial scales of thousands of kilometers along different biogeographical regions (Li et al., 2013; Pollock et al., 2018). Among coral compartments or microhabitats, the coral surface mucus layer and skeleton likely house the highest densities of bacteria (Garren and Azam, 2010; Yang et al., 2019), while skeleton-associated communities have the highest diversity (Pollock et al., 2018). Coral-associated bacterial communities are taxonomically distinct from those of the surrounding seawater and sediments, however, the mucus microbiome is more strongly influenced by environmental factors, while the tissue and skeleton

microbiomes are more influenced by host species and functional traits (Pollock et al., 2018). In general, abiotic factors in the environment such as water quality, light, and temperature can account for a significant portion of the variability within the coral microbiome (Littman et al., 2009; Hernandez-Agreda et al., 2016, 2018). One study estimated that >96% of the coral microbiome is composed of a diverse and transient assemblage that is environmentally responsive (Hernandez-Agreda et al., 2018).

Evidence exists for both coral species-specificity and a coral core microbiome (Mouchka et al., 2010; van Oppen and Blackall, 2019). However, interindividual variability is very high, for instance, one study found that only 2 to 3% of the total number of bacteria associated with the specific host species are found in any individual colony (Hernandez-Agreda et al., 2018). While various thresholds and definitions have been used to characterize the coral core microbiome, it likely consists of few, low abundance taxa potentially spanning both the Pacific and Atlantic oceans (Ainsworth et al., 2015; Chu and Vollmer, 2016; Hernandez-Agreda et al., 2018; Huggett and Apprill, 2019b). Two proposed core symbionts are Candidatus *Amoebophilus* and *Endozoicomonas*, the latter of which has held particularly attention due to its global distribution and high relative abundance in many coral hosts (Pollock et al., 2018; van Oppen and Blackall, 2019).

1.3. Functional roles of bacteria in the coral holobiont

While many bacteria or consortia of bacteria have been implicated in infectious diseases in corals, evidence exists for a multitude of potential services by which bacteria contribute to holobiont functioning in healthy corals. For instance,

bacterial dynamics in the mucus layer actively structure the microbiome by providing nutrients that promote the growth of beneficial bacteria, while also synthesizing and releasing antimicrobial compounds that inhibit the growth of invading harmful microorganisms (Ritchie, 2006; Teplitski and Ritchie, 2009). Certain coral-associated bacteria can enhance larval recruitment and settlement thereby playing a critical role in larval ecology and the survival of early coral life stages (Sharp et al., 2015). Coral bacteria are also involved in the cycling and/or provisioning of essential nutrients including carbon, nitrogen, sulfur, and phosphate to the coral host or algal symbiont, Symbiodiniaceae, as well as the essential passage of trace metals and vitamins (Bourne et al., 2016; McDevitt-Irwin et al., 2017a). Although the coral animal can receive up to 60% of their carbon requirements through heterotrophy or up to 100% through photoautotrophy mediated by Symbiodiniaceae, bacterial and archaeal genes involved in carbon fixation and degradation have been found (Falkowski et al., 1984; Palardy et al., 2008; Kimes et al., 2010).

Corals require nitrogen supplementation in addition to the photosynthates translocated from the algal symbiont, and the coral host exerts control over the density of Symbiodiniaceae by limiting nitrogen availability within the holobiont, among other nutrients (Falkowski et al., 1984, 1993). Therefore, nitrogen-cycling microbes may contribute to holobiont functioning and the stability of the coral-algal symbiosis. Microbial taxa that regulate nitrogen are ubiquitous and consistent in the coral microbiome, contributing to nitrogen fixation, nitrification, and denitrification (Rädecker et al., 2015). Diazotrophic (nitrogen-fixing) assemblages include taxa

within the *Rhizobiales* and endosymbiotic cyanobacteria related to *Synechococcus* spp. and *Prochlorococcus* spp., and can provide an estimated 11% of the nitrogen requirements of Symbiodiniaceae (Lesser et al., 2004, 2007; Lema et al., 2012, 2014; Cardini et al., 2015).

Coral reefs contribute to the global biogeochemical cycling of sulfur, and a large component of the sulfur pool within the coral holobiont is DMSP (dimethylsulfoniopropionate) (Van Alstyne et al., 2006). The breakdown of DMSP in the marine sulfur pool to gaseous DMS (dimethyl sulfide) allows for the transfer of sulfur from the ocean to the atmosphere providing a flow of sulfur from marine to terrestrial systems and contributing to climate regulation by facilitating cloud formation (Lovelock et al., 1972). Raina et al. (2009) identified putative DMSP-degrading bacteria in coral microbiomes primarily in the *Gammaproteobacteria* including *Alteromonas*-, *Pseudomonas*-, *Roseobacter*-, and *Spongiobacter* (*Endozoicomonas*)-related organisms. Further, several taxa show chemotaxis towards DMSP including *Rhizobiales*, *Roseobacter* sp., and *Vibrio coralliilyticus*, a coral pathogen. Thus, coral-derived DMSP likely structures the bacterial communities within the holobiont and mediates the interplay between corals and their bacteria (Bourne et al., 2016).

Although there are many proposed functional roles for bacteria in the coral microbiome, the lack of an axenic host model and the difficulty of bacterial cultivation prevents the experimental manipulation necessary to verify the links between microbial identity and function within the holobiont. Modern -omics

strategies offer a means to uncover the functional potential of the coral microbiome. Genome reconstruction through single-cell genomics or metagenomics can uncover the genetic repertoire of individual symbionts to entire communities, while metatranscriptomics and metabolomics can identify genes, metabolites, or proteins that are central to the microbial contribution to holobiont functioning (Bourne et al., 2016).

1.4. Environmental stress and the coral microbiome

Given the tight association between corals and their associated microorganisms, coral microbiomes have considerable potential to serve as indicators of environmental stress and as monitoring tools for coral health (Glasl et al., 2017, 2018, 2019). Changes in the environment that alter resource availability can predictably induce differential abundances of specific microbial taxa or shifts in community composition to prioritize specific microbial traits (Martiny et al., 2015). Similarly, researchers find distinct shifts in coral microbiome composition and function across gradients of anthropogenic impacts (Dinsdale et al., 2008; Kelly et al., 2014; Ziegler et al., 2016). In an effort to assess the role of the microbiome in coral health and resilience, many such studies have described patterns in microbiome variability across various local and global reef stressors including thermal stress, overfishing and nutrient pollution.

Perhaps the most well-documented pattern in the response of coral microbiomes to stress is the sensitivity of these communities to elevated seawater temperature. Vega Thurber et al. (2009) demonstrated that elevated temperatures

altered both the composition and functional potential of the microbiome of the coral *Porites compressa* in experimental aquarium manipulations. Changes in functional genes determined by metagenomic sequencing were driven primarily by metabolic shifts in low abundance *Vibrio* spp., and changes in composition reflected a disease-associated state with increased potential for opportunistic pathogenesis. While *Vibrio* spp. are present in apparently healthy coral microbiomes, they are commonly associated with corals experiencing thermal stress and disease (Ritchie, 2006). Ritchie (2006) found that after increases in temperature on the reef coral mucus samples were dominated by *Vibrio* isolates and antibiotic capabilities of mucus were lost. Thus, thermal stress may result in the proliferation of opportunists and the relative decrease of beneficial bacteria whose beneficial functions are correspondingly decreased. Thermal stress can also result in coral bleaching, and early analyses investigating the response of microbial communities to coral bleaching found that communities can shift to being *Vibrio*-dominated even before visual signs of bleaching in the host (Bourne et al., 2008). The microbial community can also shift from autotrophy to heterotrophy during bleaching due to an increase in genes associated with the metabolism of fatty acids, proteins, simple carbohydrates, phosphorus and sulfur, as well as an increase in virulence genes (Littman et al., 2011). This demonstrates that bleaching can alter microbial biogeochemical pathways within the holobiont and increase the potential for pathogenesis. Despite the potential detrimental effects of these changes on coral holobiont health, corals are able to recover from bleaching and the microbiome can shift back to its state prior to bleaching (Bourne et al., 2008;

Littman et al., 2011). The conditions and mechanisms which allow for this recovery depend on the severity of the bleaching event and are actively under investigation.

Thermal stress does not always coincide with overall changes in microbiome composition, especially when the stress does not result in coral bleaching (Webster et al., 2016; Hadaidi et al., 2017; Ziegler et al., 2017; Epstein et al., 2019a). Even when coral microbiome structure demonstrates resistance to thermal stress, however, individual taxon abundance or community species richness may vary (Tracy et al., 2015). Otherwise stable *Acropora* microbiomes exhibited increases in the disease- and stress-associated taxa *Alteromonadales, Vibrionales, and Flavobacteriales* in response to 10 days of high seawater temperatures (Gajigan et al., 2017a). In contrast, Epstein et al. (2019b) found that *Porites acuta* colonies during peak bleaching in the central Great Barrier Reef were distinguished by the high abundance and prevalence of a number of potentially beneficial taxa including Actinobacteria and several diazotrophs, although the colonies themselves did not bleach and their microbiomes remained stable. Therefore, coral microbiomes can be flexible in terms of the presence and abundance of individual taxa, while still maintaining overall microbial community stability during thermal stress. Researchers hypothesize that microbiome flexibility can allow the coral holobiont to shuffle its microbial members as a rapid adaptive response to changing environmental conditions (Reshef et al., 2006). Whether this restructuring is due to an active response by the coral host, perhaps through regulation of the chemical and biological characteristics of its tissues (Agostini et al., 2012), or due to microbial interactions such as the production of

antibiotics (Teplitski & Ritchie, 2009) has yet to be determined. This flexibility may function as a short-term mechanism for corals to develop resistance to disease or tolerance to stress (Ziegler et al., 2019). In contrast, high microbiome stability and diversity may also be indicative of a thermal stress tolerant coral holobiont where tolerance can result from the coral's previous exposure to higher temperatures in their native environment (Ziegler et al., 2017; Grottoli et al., 2018; Epstein et al., 2019b).

Increased seawater temperature, as well as excess nutrients and sedimentation, have been linked to increased reports of coral disease (Bruno et al., 2003, 2007; Kuntz et al., 2005; Littman et al., 2011; Furby et al., 2014). For instance, the coral pathogen *Vibrio coralliilyticus* induced tissue lysis in the coral *Pocillopora damicornis* during high temperatures (Ben-Haim et al., 2003). Adding to the detrimental effects of global warming, researchers hypothesize that high temperatures hinder the coral's ability to fight infection, increase pathogen virulence, and cause changes in the healthy microbiome, thereby increasing coral disease susceptibility and driving outbreaks (Bourne et al., 2009; Mouchka et al., 2010). As disease outbreaks are a major contributor to global coral decline, researchers have been investigating the etiological role of many bacteria associated with diseased corals, however, proving causation has been difficult (Bourne et al., 2009). For instance, acroporid corals in the Western Atlantic have been particularly devastated by White Band Disease, and implicated microbes from an order of obligate intracellular parasites, Rickettsiales, have been found in high abundance in both visually healthy and diseased corals (Casas et al., 2004; Godoy-Vitorino et al., 2017).

Local practices that promote overfishing and nutrient runoff can also impact corals down to the microbial scale, especially when in combination with global thermal stress. Both elevated nutrients and overfishing of herbivorous fish can increase the abundance of macroalgae and turf algae that compete with corals for space on the reef (Smith et al., 2010). Fleshy algae can release dissolved nutrients that stimulate microbial activity and rapid population growth within coral tissues, creating a zone of hypoxia on the surface of the coral and eventually leading to coral tissue mortality (Smith et al., 2006). Increased microbial activity or increased available nutrients in the water column could also result in increased nitrogen fixation rates within the holobiont. This may increase the nitrogen to phosphate ratio in corals and lead to the breakdown of the coral-algal symbiosis which relies on a delicate balance of nutrients within the holobiont (Rädecker et al., 2015).

Regardless of the type of stressor, consistent responses in coral microbiome structure and taxonomic composition have been found. Generally, anthropogenic impacts on coral reefs disrupt the functioning of the microbiome and result in an increase in the alpha (within-sample) diversity of the coral microbiome (McDevitt-Irwin et al., 2017a). The invasion of foreign microbes can increase microbial species richness, while the opportunistic growth of minor microbial members and shifts in taxonomic composition can increase microbial species evenness (Meron et al., 2011; Röthig et al., 2016; Welsh et al., 2017). Further, stressors commonly increase beta (between-sample) diversity either through shifts to an alternative community stable state and/or through the destabilization of the microbiome (Morrow et al., 2013;

Zaneveld et al., 2016). In contrast to a shift from a healthy to a dysbiotic stable state, microbiome destabilization refers to the variability induced by stochastic changes, perhaps resulting from an inability of the host to regulate its microbiome (Zaneveld et al., 2017). Stress commonly induces a decrease in the relative abundance of the proposed beneficial coral symbiont, *Endozoicomonas* (Order: *Oceanospirillales*) and an increase in opportunistic and pathogenic bacteria including *Vibrionales*, *Flavobacteriales*, *Rhodobacterales*, *Alteromonadales*, *Rhizobiales*, *Rhodospirillales*, and *Desulfovibrionales* (McDevitt-Irwin et al., 2017a).

In ecological communities, compounded perturbations which occur simultaneously or within short succession can push ecosystems with low resistance and resilience to an alternative, potentially compromised, stable state with reduced chance of recovery (Paine et al., 1998). For instance, in a three-year field study Zaneveld et al. (2016) found that overfishing and nutrient pollution not only reduce coral recruitment, growth, and survivorship, but also destabilize the coral microbiome, elevate putative pathogen loads, and increase disease prevalence and mortality. Further, these effects were exacerbated by thermal stress with 80% of coral mortality occurring during the warmest seasons. This study highlights the importance of considering multiple environmental stressors when assessing microbiome resistance and resilience. With the increasing anthropogenic impacts to natural ecosystems, understanding how local and global stressors interact to drive changes in the coral microbiome is crucial to understanding the degree to which coral

microbiomes can restructure under cumulative stress while maintaining host health and long-term survival.

1.5. Dissertation outline

As previously described, the coral holobiont is a dynamic assemblage of the coral animal and its associated microorganisms. In this dissertation, I focus specifically on the bacterial component of the holobiont and its response to environmental stressors. I use traditional statistical tools in community ecology as well as statistical tools that are explicitly designed to address the specific nature of microbiome data. I utilize both 16S amplicon sequencing to profile bacterial communities and metagenomic sequencing to uncover functional potential from a bacterial genome.

In Chapters 2 and 3 of my dissertation, I analyze the microbiomes of dominant reef-building corals in manipulative experiments both in controlled aquaria and in the field involving thermal stress and its interaction with local contributors to coral decline including nutrient enrichment, physical scarring, and disease. In chapter two, I present an analytical framework for characterizing the type of interactions between major reef stressors using various measures of microbiome diversity and taxon differential abundance. I apply ecological theory of multiple stressor interactions to characterize the two-way and three-way interactions between increased seawater temperature, physical scarring, and nutrient pollution as additive, synergistic, antagonistic, or having no interaction. Contrary to our expectations, I found that multiple stressors generally do not interact synergistically to exacerbate the effects of

a single stress. Instead, the severe response of the microbiome to thermal stress or physical scarring likely precludes any further dysbiosis due to nutrient enrichment. This experiment was conducted on a single coral species, *Pocillopora meandrina*, in a controlled mesocosm system in Mo'orea, French Polynesia. To extend the generality of our conclusions, we enriched colonies from three coral genera which span a range of host stress tolerance, *Pocillopora*, *Porites*, and *Acropora*, with nutrients on the reef in Mo'orea before, during, and after a natural thermal stress event. Similarly, nutrient enrichment did not interact to exacerbate the effects of the increasing temperatures. As I discuss in Chapter 3, we found no effects of nutrients on the structure and composition of the microbiome, while we captured the greatest changes over time as the seawater temperature rose and fell over a period of five months. In both studies, control corals (Chapter 2) and recovered corals (Chapter 3) were dominated by the proposed beneficial microbial symbiont, *Endozoicomonas*.

In Chapter 4, I explore the functional potential of *Endozoicomonas* in an effort to uncover the role this taxon plays in a healthy and stressed coral holobiont. I produce the first *Endozoicomonas* metagenome-assembled genome (MAG) from the coral *Pocillopora meandrina* in Mo'orea. I present a phylogenomic and pangenomic comparison of this MAG with all available *Endozoicomonas* genomes from a variety of marine hosts, including several coral species, and assembled from both isolate cultures and metagenomic reads. I found that *Endozoicomonas* genomes do not differentiate functionally or phylogenetically by host taxonomic group or geography, however, a subset of *Endozoicomonas* species from *Pocillopora* and *Stylophora*

corals were closely related. While *Endozoicomonas* species have no obvious genetic capabilities that suggest tolerance or susceptibility to thermal stress, our MAG encodes for a variety of antioxidants that may benefit the coral holobiont during periods of heat-induced oxidative stress and encodes for several unique genes with eukaryotic-like domains that may facilitate the maintenance of stable symbiosis.

CHAPTER 2 MULTIPLE STRESSORS INTERACT PRIMARILY THROUGH ANTAGONISM TO DRIVE CHANGES IN THE CORAL MICROBIOME

Rebecca L. Maher

Mallory M. Rice

Ryan McMinds

Deron E. Burkepile

Rebecca Vega Thurber

Scientific Reports

4 Crinan Street London N1 9XW

Vol. 9

2.1. Abstract

Perturbations in natural systems generally are the combination of multiple interactions among individual stressors. However, methods to interpret the effects of interacting stressors remain challenging and are biased to identifying synergies which are prioritized in conservation. Therefore we conducted a multiple stressor experiment (no stress, single, double, triple) on the coral *Pocillopora meandrina* to evaluate how its microbiome changes compositionally with increasing levels of perturbation. We found that effects of nutrient enrichment, simulated predation, and increased temperature are antagonistic, rather than synergistic or additive, for a variety of microbial community diversity measures. Importantly, high temperature and scarring alone had the greatest effect on changing microbial community composition and diversity. Using differential abundance analysis, we found that the main effects of stressors increased the abundance of opportunistic taxa, and two-way interactions among stressors acted antagonistically on this increase, while three-way interactions acted synergistically. These data suggest that: 1) multiple statistical analyses should be conducted for a complete assessment of microbial community dynamics, 2) for some statistical metrics multiple stressors do not necessarily increase the disruption of microbiomes over single stressors in this coral species, and 3) the observed stressor-induced community dysbiosis is characterized by a proliferation of opportunists rather than a depletion of a proposed coral symbiont of the genus *Endozoicomonas*.

2.2. Introduction

In natural systems, disturbances or stressors rarely occur in isolation. Anthropogenic impacts disrupt individual animal physiology, alter whole populations or community dynamics, and drive shifts in system-level processes thereby putting biodiversity in peril (Folt et al., 1999; Vinebrooke et al., 2004; Martínez-Ramos et al., 2016; Galic et al., 2018). Therefore, it is imperative to characterize how multiple stressors interact to disrupt natural systems. We are using the operational definitions of types of interactions between multiple stressors as defined by Folt et al. (Folt et al., 1999) and Vinebrooke et al. (Vinebrooke et al., 2004). An additive effect, or null interaction, occurs when the combined effect equals the sum of the separate effects. A synergistic interaction occurs when the combined effect of multiple stressors is greater than the additive effect. And lastly, an interaction is deemed antagonistic when combined stressors produce a biological response that is less than the additive effect.

Despite the existence of multiple interaction outcomes, synergies are often emphasized in conservation literature, perhaps due to the risk of negative feedbacks accelerating ecosystem decline and degradation (Côté et al., 2016). A balanced research agenda that looks for synergies and antagonisms is necessary to fully understand how mitigating local stressors will or will not compensate for global stressors (Brown et al., 2013). For instance, improving water quality and decreasing water turbidity in seagrass systems may exacerbate the damaging effects of heat stress from global warming (Brown et al., 2013). Similarly, marine invertebrates and their microbiomes are often faced with global stressors associated with climate change and

local stressors such as nutrient pollution or overfishing (Lesser et al., 2016; Zaneveld et al., 2016; McDevitt-Irwin et al., 2017b). Yet few studies empirically test the individual and combinatorial effects of more than two stressors on host microbiomes (Lesser et al., 2016; Zaneveld et al., 2016; McDevitt-Irwin et al., 2017; Wang et al., 2018).

Current statistical methods and models for microbiome studies (Xia and Sun, 2017), such as those that evaluate alpha and beta diversity and differential abundance, can be combined with multi-stressor experimental designs and used to statistically quantify the interacting effects of multiple stressors. For instance, patients with Crohn's, a disease associated with gut microbiome dysbiosis, were treated with either antibiotics or a diet of exclusive enteral nutrition (Lewis et al., 2015). The two therapies likely disrupt the gut microbiome through different mechanisms and are independently associated with dysbiosis. In one case, the stressors produced opposite responses in the abundance of a single bacterial genus, *Alistipes*. Yet, an antagonistic interaction was not tested for but easily could be with a crossed design with patients receiving both therapies. In an environmental example, warm- or cold-stressed oysters crossed with bacterial infection by vibrios showed evidence of synergy as warm-stressed oysters experienced the highest mortality following infection (Lokmer and Wegner, 2015). When evaluating the oyster hemolymph microbiome, an interaction term of stress × infection in the univariate analysis of alpha diversity and multivariate analysis of beta diversity was not included, but if included in statistical methods, would clarify the type of interaction between the two stressors.

Using robust statistical methods and interaction models benchmarked in the microbiome field (Knight et al., 2018), we investigated how a global stressor, thermal stress, interacts with local stressors, nutrient pollution and predation, to alter the coral microbiome. Corals, currently experiencing major threats of climate change and nutrient pollution, can function as environmental sentinels and are thereby prime candidates for multiple stressor experiments. Previous studies of the coral microbiome have shown that stress tends to increase species richness (Meron et al., 2011; Morrow et al., 2015; Welsh et al., 2016; Zaneveld et al., 2016; McDevitt-Irwin et al., 2017) and cause shifts in community composition from potentially beneficial symbiotic bacteria that dominate healthy corals to potentially opportunistic or pathogenic bacteria that dominate stressed corals (Sunagawa et al., 2009; Morrow et al., 2015; Webster et al., 2016; Welsh et al., 2016; Zaneveld et al., 2016; Gajigan et al., 2017; McDevitt-Irwin et al., 2017). Beta diversity, or species turnover between samples, has also been reported to increase with stress (Klaus et al., 2007; Lesser et al., 2016; Zaneveld et al., 2016, 2017), and stressed corals have microbial communities distinct from control corals (Ritchie, 2006; Bourne et al., 2008; Thurber et al., 2009; Rosenberg and Kushmaro, 2011).

Therefore, we designed a fully-crossed experiment to investigate biological responses including alpha and beta diversity indices and differential abundance modeling of individual taxa with stress. For the purposes of this study, we define a stressor to be any external disturbance from the host's environment that causes a quantifiable change in microbial community structure. We utilized univariate and

multivariate statistical techniques to parse the main effects and interactions among stressors. The coral *Pocillopora meandrina* was exposed to increased seawater temperatures, pulse nitrate and ammonium enrichment, and simulated predation in a factorial mesocosm tank experiment with all possible combinations of these stressors. We hypothesized that local stressors like nutrient pollution and predation would interact synergistically with thermal stress to reduce the host's ability to regulate its microbial community which would be manifested by: 1) an increase in the compositional heterogeneity and variability (beta diversity) among stressed corals compared to the controls, and 2) an increase in community evenness in stressed corals as a result of 3) shifts from few dominant symbiotic bacterial taxa to a myriad of potentially opportunistic bacterial taxa that bloom and become overrepresented in stressed corals.

2.3. Materials and Methods

2.3.1. Experimental design and sampling of coral tissue for microbial analysis

To test the individual and interactive effects of increased temperature, nutrient enrichment, and predation on coral microbiomes, a fully crossed tank experiment (Supplementary Figure 2.1) was conducted at the University of California Gump Research Station (17°29'26.04"S, 149°49'35.10"W) in Mo'orea, French Polynesia. The experiment was conducted in September of 2016 using twelve independent 150 L flow-through, temperature controlled mesocosms with natural locally-sourced sea water at a flow rate of 448.1 ± 24.1 mL per minute and run under a 12:12 light:dark cycle with ~700 μmol quanta per m^2 per second. Each of the twelve tanks was

independently regulated for temperature (chilling loop and heater) and for light. Ten *Pocillopora meandrina* colonies were collected from 3-4 m on the Mo'orea north shore fore reef and transported by boat to the Gump Research Station to be immediately fragmented. Each colony was fragmented into twelve coral nubbins (~5cm in length), epoxied with Z-Spar to vertically stand on plastic mesh, and distributed to each of mesocosm tanks at 26°C ± 1°C for a total of ten nubbins per tank.

After a 24-hour acclimation period, five (half) of the nubbins in each tank were randomly selected and mechanically scarred on the branch tip with 8 mm snub nose pliers. Therefore, each tank contained two treatments: control or scarred with a specific temperature and nutrient regime (Supplementary Figure 2.1). Pliers were sterilized between each scarring to prevent cross-contamination. The resulting scars were ~2 mm deep and removed the tissue layer and portions of the skeletal structure. These scars are representative of corallivory by parrotfishes and pufferfishes, two of the most common scraping corallivores on these reefs. Half of the tanks were then randomly selected and heated to 29°C (ca. <1°C change per hour) to mimic temperatures associated with thermal stress on Mo'orean reefs (Pratchett et al., 2013). Next, each tank was assigned one of three nutrient treatments: pulse of 4 µM of nitrate (NO_3^-), pulse of 4 µM of ammonium (NH_4^+), or no enrichment controls. For 21 days, each enriched tank was spiked with either nitrate or ammonium twice a day every 12 hr. Flow in all mesocosms was ceased for an hour immediately following

the nutrient additions. This resulted in a twice daily hour-long nutrient pulse, followed by 5 hours of steady dilution and 6 hours of ambient concentration.

For microbial analysis, a subset of the nubbins (n = 6 per treatment) were randomly selected while controlling for source tank and colony to minimize samples while ensuring sufficient replication after 21 days of exposure to stressors (Supplementary Figure 2.1, Supplementary Table 2.1). For microbial analysis, a healthy branch tip was clipped off of each unscarred nubbin and the branch tip around the scar was collected for scarred samples. These samples were frozen and shipped to Oregon State University.

2.3.2. 16S library preparation and sequencing, quality control, and initial data processing

DNA was extracted using the MoBio Powersoil® DNA Isolation Kit according to the manufacturer's recommendations. Polymerase Chain Reaction (PCR) was performed on the V4 region of the 16S rRNA gene using the primer pair 515F (5'-GTG CCA GCM GCC GCG GTA A-3') and 806Rb (5'-GGA CTA CHV GGG TWT CTA AT-3') that targets bacterial and archaeal communities (Apprill et al., 2015; Parada et al., 2016). Amplicons were barcoded with barcoding primers with Nextera adapters, pooled in equal volumes for sequencing (Kozich et al., 2013), and purified with AMPure XP beads. Amplicon pools were paired-end sequenced on the Illumina MiSeq sequencing platform, 2 × 300 bp end version 3 chemistry according to the manufacturer's specifications at the Oregon State University's Center for Genome Research and Biocomputing (CGRB) Core Laboratories.

QIIME (v1.9) (Caporaso et al., 2010b) was used for quality control and selection of operational taxonomic units (OTUs). Demultiplexed raw reads were trimmed of adapter and primer sequences and pair-end sequences merged. Sequences with a total expected error or total sum of the error probabilities >1 for all bases were discarded. Chimeras were removed and 97%-similarity OTUs were picked using USEARCH 6.1 (Edgar, 2010), the 97% GreenGenes 13_8 reference database (McDonald et al., 2012), and QIIME's subsampled open-reference OTU-picking protocol (Rideout et al., 2014). In this protocol, sequences that failed to hit the reference collection are randomly subsampled for de novo clustering. Taxonomy was assigned using UCLUST, and reads were aligned against the GreenGenes database using PyNAST (Caporaso et al., 2010a). The GreenGenes reference database is commonly used in microbiome analysis (Knight et al., 2018) and has been validated on animal and coral microbiomes in numerous studies (Ziegler et al., 2016; Moitinho-Silva et al., 2017; Brown et al., 2019; Morelan et al., 2019). FastTreeMP (Price et al., 2010) was used to create a bacterial phylogeny with constraints defined by the GreenGenes reference phylogeny.

Both a rarefied and unrarefied OTU table were created for downstream analyses. First, OTUs were filtered out of the starting table if their representative sequences failed to align with PyNAST to the GreenGenes database or if they were annotated as mitochondrial or chloroplast sequences. After this step, the number of reads per sample ranged from 1 to 87262 with a median of 9742 per sample and 3383 unique reads. OTUs with less than 100 counts were then removed from the OTU table

resulting in a total of 430 unique reads, and a histogram of reads by samples was plotted (Supplementary Figure 2.2). We did not find that any one OTU was associated with one particular sample. Samples with less than 1000 reads were considered undersampled and discarded from the table resulting in an unbalanced experimental design (Supplementary Table 2.1). Two OTU tables were created from this parent table using the package *phyloseq* (McMurdie and Holmes, 2013) (v1.20.1) in R (v3.4.0). First, the parent table was used as the unrarefied OTU table in downstream dominant taxa and differential OTU abundance analysis. Second, the parent table was rarefied to the minimum sample sequencing depth corresponding to exactly 1070 sequences per sample. This depth was chosen to maximize sample sequencing depth while preserving replication. This rarefied table was then used to calculate a Weighted UniFrac (Lozupone and Knight, 2005; Lozupone et al., 2007) pairwise dissimilarity matrix. Also from this rarefied table, alpha diversity metrics including Faith's phylogenetic diversity (Faith, 1992), Chao1 statistic (Chao and Chiu, 2016), and Simpson's diversity index were calculated in *phyloseq*.

2.3.3. Statistical analyses investigating alpha and beta diversity

To determine how dominant taxa within the community respond to stressors, the rarefied OTU table was first transformed to proportions to identify the five OTUs with the highest relative abundances. These OTUs were then evaluated for changes with treatment using generalized linear mixed-effects models (GLMM) which allow for inclusion of random effects. Raw OTU counts from the unrarefied table were then included as the response variable in the GLMM with an offset by the log of total

sequencing depth to reflect relative abundances. Offset variables are commonly used in count models to adjust for differential exposure times and, for these purposes, to adjust for different sequencing depths. Each OTU count distribution was evaluated for normality with quantile-quantile plots and the Shapiro-Wilk test for normality (Royston, 1982). A logistic regression with unrarefied count data with an offset was selected over a linear regression with proportion data from the rarefied table since the data were not normally distributed and evidence suggests logistic regressions perform better than arcsine-transformed data in linear regressions (Shi et al., 2013). For all models, temperature, nutrients, and scarring were assessed as fixed effects and factorial interaction terms and tank and colony as separate random effects. For the most abundant OTU in the dataset, OTU-Endo, a poisson distribution was used since it resulted in normal residuals using *lme4* (Bates et al., 2014) (v1.1.15) and *lmerTest* (v2.0.36) to obtain P-values. For the remaining four OTUs a zero-inflated negative binomial regression was used to account for the excess of zeros in the data using *glmmTMB* (v0.2.2.0). The negative binomial distribution was also evaluated based on normality of residuals. A single zero-inflation parameter was modeled for all observations.

To improve normality of alpha diversity metrics, Chao1 and Faith's phylogenetic distance were log-transformed, while Simpson's index was arcsine-transformed. Stressor effects on each alpha diversity metric were assessed with linear mixed effect models (LMM) using *lme4* with temperature, nutrients, and scarring as

fixed effects and factorial interaction terms and tank and colony as separate random effects. P-values were approximated with the *lmerTest* (v2.0.36).

For beta diversity analyses, the Weighted Unifrac dissimilarity matrix generated in *phyloseq* (v1.23.1) was used to test for location and dispersion effects acting on the microbial community. First, differences between treatments were assessed with permutational multivariate analysis of variance (PERMANOVA) using the adonis function in the package *vegan* (v2.4.6) both with treatment as the single factor and with pairwise comparisons between treatments (Anderson, 2001). Next, permutation tests for homogeneity in multivariate dispersion (PERMDISP) were performed using the betadisper function in the package *vegan* both with treatment as the single factor and with pairwise comparisons between treatments (Anderson, 2006). For visualizing differences in beta diversity, mean distance-to-centroid values by treatment were extracted from the betadisper results, and mean separation from communities in other treatments or between-group distances were averaged by treatment from the pairwise dissimilarity matrix generated in *phyloseq*. Together, PERMANOVA and PERMDISP provide a comprehensive analysis of deterministic and stochastic changes to the microbiome by evaluating between-group differences and within-group dispersions, respectively. For comparability, the two tests were run with treatment as the single factor, since PERMDISP does not allow for a specified model formula. Pairwise analysis of variance for the PERMANOVA test were conducted using a modified version of *pairwiseAdonis* (Martinez Arbizu, 2017) (v0.0.1), and for the PERMDISP test with the permutest command in *vegan*.

Distance-to-centroid was also regressed against the arcsine-transformed relative abundance of OTU-Endo to determine the correlation between community dispersion and the dominant taxon. Lastly, stressor main effects and interactions were evaluated with PERMANOVA by fitting a linear model to the distance matrices using factorial interaction terms. All diversity analyses were conducted in *R* (v3.4.0).

2.3.4. Differential OTU abundance analysis

To analyze differences in abundance of bacterial taxa across stressors and stressor interactions, a negative binomial generalized linear model (GLM) was fitted with the R package *DESeq2* (v1.16.1) using the unrarefied OTU table (Love et al., 2014). *DESeq2* does not support random effects and therefore a mixed model was not used. All rare taxa that were present in fewer than 15 samples were excluded from this table to create a pre-filtered, unrarefied OTU table. In the *DESeq2* method, raw counts are modeled with a negative binomial distribution which is commonly used for overdispersed count data (Cameron and Trivedi, 2013). Additionally, "size factors" or normalization factors are calculated with a median-of-ratios method to normalize differences in sequencing depth between samples (Love et al., 2014). The GLM design specified nutrient regime, temperature, scarring, and their interactions as factors with beta priors set to false. Wald post-hoc tests were used to identify factors in the model that significantly affected each taxon compared to the control level by building a results table from a specified treatment contrast. To control the rate of false positives due to multiple comparisons, differentially abundant taxa within each treatment contrast were identified as significant with Benjamini-Hochberg FDR p-

values less than 0.05 (Benjamini and Hochberg, 1995). The pre-filtered, unrarefied OTU table was summarized to Family and Genus level using the tax_glom command in *phyloseq*. The DESeq2 method was then applied to these two tables to demonstrate accordance between significant changes at the OTU level with significant changes at higher taxonomic levels.

2.4. Results

2.4.1. Stressors drive symbiont decreases and opportunist increases in relative abundance

To test the individual and interactive effects of increased temperature, nutrient enrichment, and predation on coral microbiomes, replicates of the coral *Pocillopora meandrina* were exposed to each combination of individual, double, and triple stressors in a fully crossed tank experiment (Supplementary Figure 2.1). Patterns in the relative abundance of different microbial taxa were assessed with generalized linear mixed-effects models (GLMM) and clearly revealed a dominant member of the coral community (Fig. 1). A single OTU assigned according to the Greengenes database to the family *Endozoicimonaceae* (OTU-Endo, genus *Endozoicomonas*) was present in every sample unit with relative abundances ranging from 0.093-99.44%, with an average 67.52 ± 3.55%. Members of the genus *Endozoicomonas* are proposed bacterial symbionts with coral, and are typically underrepresented in stressed corals (Lee et al., 2012; Bayer et al., 2013; D Ainsworth et al., 2015; McDevitt-Irwin et al., 2017b). All control corals were dominated by OTU-Endo with an average relative abundance of 94.88 ± 0.86% (Figure 2.1). The main effects of high temperature,

scarring, and NO_3^- all significantly decreased the relative abundance of OTU-Endo in the GLMM ($p<0.001$, $p<0.001$, $p<0.05$; Supplementary Table 2.2, Figure 2.1). Compared to control corals, the relative abundance of the dominant OTU-Endo decreased by more than 50% in the high temperature treatment (41.19 ± 16.61%) and decreased nearly 50% in the scarred treatment (48.21 ± 16.61%). High temperature and scarring interact to reduce the sum of the independent effects on the dominant taxon ($p<0.01$; Supplementary Table 2.2), decreasing OTU-Endo by only ~25% (70.67 ± 5.44) compared to controls. In fact, all two-way interactions were antagonistic and significantly reduced the magnitude of the response predicted by main effects (Supplementary Table 2.2). Alternatively, both three-way interactions significantly increased the response of the individual stressors on OTU-Endo after accounting for all main effects and two-way interactions (Supplementary Table 2.2).

The decreases observed in OTU-Endo closely mirror increases in the second most abundant OTU of the family *Desulfovibrionaceae* (OTU-Desulfo). For instance, all four main effects significantly increased the relative abundance of OTU-Desulfo (Supplementary Table 2.3) with high temperature causing the greatest change in this OTU from control corals with 0.09 ± 0.09% to 25.56 ± 13.44%, followed by NO_3^- (10.62 ± 10.18%) and scarring (9.92 ± 6.30%). Alternatively, the interaction of high temperature and scarring only increased the relative abundance of OTU-Desulfo to 1.51 ± 0.78%. Two-way and three-way interactions showed similar significant, but opposite directional changes as those observed for OTU-Endo (Supplementary Table 2.3). For the third most abundant OTU of the family *Enterobacteriaceae*, the main

effect of scarring caused significant increases in abundance and significant interactions between scarring and nutrient treatments (Supplementary Table 2.3). The OTU from family *Amoebophilaceae* significantly increased in scarring and high temperature and the three-way interaction with NH_4^+ was significant (Supplementary Table 2.3). And lastly, the OTU from family *Moraxellaceae* significantly increased in the NH_4^+ treatment and two-way interactions with scarring and nutrient treatments were significant (Supplementary Table 2.3). For all OTUs, significant two-way interactions were antagonistic, or less than the sum of the main effects, and three-way interactions were synergistic when accounting for main effects and two-way interactions. When evaluating changes in relative abundance, the microbial community under stress is marked both by a decrease in the dominant symbiont and increases in lower abundant opportunistic taxa.

2.4.2. High temperature and scarring drive changes in community diversity

Alpha diversity metrics were assessed with linear mixed effects models (LMM) and showed the absence of synergisms. On average, Chao1 estimates found that control corals had a mean of 40.42 ± 3.48 unique OTUs and had the lowest standard error across all treatments (Supplementary Fig. 2.3). Neither main effects nor interactions were significant predictors in the LMM with Chao1 index as the response variable (Supplementary Table 2.4). Faith's phylogenetic diversity ranged from 4.09 ± 0.55 in control corals to 8.99 ± 1.81 for corals in high temperature. The main effects of high temperature and scarring significantly increased Faith's phylogenetic diversity ($p<0.05$, $p<0.05$; Supplementary Table 2.4). Additionally, the

interaction between high temperature and NH_4^+ showed a significantly antagonistic response on Faith's phylogenetic diversity ($p<0.05$, Supplementary Table 2.4). Although evidence suggests that stressors generally increase microbial species richness in coral microbiomes (McDevitt-Irwin et al., 2017b), we found no significant differences in species richness, but rather changes in phylogenetic diversity with stressors.

All treatments tended to increase Simpson's index or community diversity (3- to 7-fold) compared to the controls, with an index of 0.10 ± 0.02 (Figure 2.2a). Patterns in community diversity closely match those of the dominant OTU-Endo and reflect changes in community 'evenness' which is accounted for when calculating the Simpson's index. Both high temperature and scarring significantly increased Simpson's Index compared to the controls ($p<0.01$ and $p<0.01$; Supplementary Table 2.4). High temperature and scarred treatments produced the highest mean community diversity (0.62 ± 0.16 and 0.67 ± 0.11, respectively), greater than 6 times that of the controls. Interestingly, scarring and high temperature interact to reduce the independent effects in the regression analysis ($p<0.01$; Supplementary Table 2.4). This interaction can be observed with interaction plots and described in two ways: 1) high temperature reverses the effect of increased community diversity from control to scarred corals (Figure 2.2b), or 2) scarring decreases the difference in community diversity between corals in ambient to high temperature seawater (Figure 2.2c). Enrichment with NH_4^+ or NO_3^- also significantly interacts to reverse the main effect of scarring, thereby decreasing community diversity in scarred corals compared to

controls ($p<0.01$, $p<0.05$; Supplementary Table 2.4; Supplementary Figure 2.4). The two three-way interactions between scarring, high temperature, and nutrient enrichment also produced a significant result ($p<0.05$, $p<0.05$; Supplementary Table 2.4), suggesting that the interaction between any two stressors depends on the level of the third stressor. In the linear model framework, interaction type is not directly interpretable with the less-than- or greater-than-additive definition since three-way interactions in the model account for all main effects and two-way interactions. Therefore, the three-way interaction increased community diversity after accounting for all antagonistic two-way interactions, although the triple stressor treatments are less than most single stressor treatments (Figure 2.2a). Despite the significant main effects and interactions in the LMM, no pairwise treatment comparisons were significant with a Tukey post hoc test.

2.4.3. Beta diversity measures show less-than-additive effects during microbiome exposure to multiple stressors

PERMANOVA results, with treatment as the predicting factor, showed the presence of distinct microbial communities (Figure 2.3a p-value, Supplementary Table 2.5). To visualize differences in community location, mean separation from communities in other treatments (between-group-distance) was calculated (Figure 2.3a). Control corals had low average between-group distances and were significantly different from single stressors of NH_4^+, high temperature, and scarring (Figure 2.3a, Supplementary Table 2.5). However, unlike our hypothesis that with additional amounts of stress microbiomes would become increasingly distinct, single stressors of scarring and high temperature produced the greatest mean between-group distances

rather than interacting stressors (Figure 2.3a, yellow versus purple and red boxes). In fact, high temperature and scarring combined was significantly different from controls but not from either high temperature or scarring alone (Figure 2.3a, Supplementary Table 2.5). Additionally, triple stressors (red boxes) were not significantly different from single stressors (Figure 2.3a, Supplementary Table 2.5). Therefore, the combination of multiple stressors had less-than-additive effects on the change in composition of the microbial communities. And, while a true synergism is not possible for relative distance measures with a maximum value of 1.0, combined stressors are generally less than single stressors. The linear model PERMANOVA results showed that in corals experiencing the main effect of high temperature, microbial communities were significantly distinct from controls ($p<0.05$; Supplementary Table 2.6). The three-way interaction between temperature, nutrients, and scarring was also significant ($p<0.05$; Supplementary Table 2.6), suggesting that the biological response to a single stressor is influenced by the other two. Like double stressor treatments, triple stressors (Figure 2.3a red boxes) interact antagonistically to produce less community distance or distinctness than scarring or high temperature alone. Our results suggest that the high temperature as a main effect and high temperature and scarring as independent treatments have the most influential effect on shifting microbial communities.

PERMDISP results also showed significant differences among treatments in dispersion magnitude (Figure 2.3b p-value, Supplementary Table 2.7). Distance to group centroid measures showed that control corals harbored microbial communities

that were more homogenous, and therefore less dispersed, than those belonging to stressed corals (Figure 2.3b). The addition of stressors (with the exception of NO_3 and scarring combined) increased distance-to-centroid and increased variance suggesting that stress causes dispersion or destabilization of the microbiome. These stochastic changes may show evidence of the Anna Karenina Principle (AKP) in which dysbiotic animal microbiomes vary more in community composition than healthy microbiomes (Zaneveld et al., 2017). When considering the dominance of OTU-Endo within the community (Figure 2.1), however, evidence suggests that the single taxon is driving the dispersion effect. In fact, the relative abundance of OTU-Endo was significantly negatively correlated with sample distance-to-centroid measurements (estimate: -0.35, $p<0.001$). The ability to detect statistically meaningful variance in other taxa is marginal due to the dominance of OTU-Endo. Instead, dispersion may be artificially increased in stressed corals due to an increase in the relativized number of rare taxa and the reduction in OTU-Endo dominance.

2.4.4. Differential abundance analysis shows stress is marked by an increase in opportunists

From differential abundance analysis with DESeq2, a total of 56 unique OTUs were differentially abundant in one or more of the treatments or interactions (Figure 2.4, Supplementary Table 2.8). On average, main effects resulted in a 2.80 log2 fold-change in the differentially abundant OTUs (yellow-colored line; Figure 2.4). This increase was driven primarily by high temperature and scarred treatments which have an average log2 fold-change of 6.35 and 7.23, respectively (yellow-dashed lines, Figure 2.4). In contrast, NO_3^- and NH_4^+ treatments on average significantly decreased

taxa compared to controls (-5.92 and -10.06, respectively, yellow-dashed line, Figure 2.4). The NH_4^+ treatment resulted in the fewest differentially abundant OTUs (Figure 2.4), suggesting that the microbial communities under NH_4^+ enrichment are most similar to the control corals. Ammonium (NH_4^+) is a fish-derived form of nitrogen that can be beneficial to corals (Shantz and Burkepile, 2014), which likely would reflect a healthy microbial community. A single OTU from the proposed symbiont family of *Endozoicimonaceae* increased in abundance in high temperature, however, this taxon was not the same dominant OTU-Endo from Figure 2.1. In fact, OTU-Endo was not identified as having significantly changed in any treatments. When differential abundance analysis was repeated with an OTU table summarized by Family and Genus, higher-level significant changes generally agree with those of individual OTUs (Supplementary Table 2.9). Therefore, the average increase in abundance of OTUs from families such as *Rhodobacteraceae*, *Sphingomonadaceae*, and *Desulfovibrionaceae* (Figure 2.4), suggests that the changes in relative abundance and dysbiosis resulting from stressors are characterized by an enrichment of pathogenic or opportunistic bacteria rather than a depletion of symbionts.

2.4.5. Interaction type depends on the type and number of stressors

The response of bacterial taxa in two-way interactions was variable depending on family of OTU, OTU, and type of interacting stressors. Generally, two-way interactions between stressors were antagonistic in nature aside from the interaction between NO_3^- and high temperature which produced a synergistic average increase in taxa (purple-colored box, Figure 2.4). In the linear framework model, zero log2-fold

change between two main effects (grey lines in purple-colored box, Figure 2.4) signifies no interaction or the additive model (sum of the two main effects). Instead, the model shows that the average log2-fold change in bacterial taxa for two-way interactions was less than the sum of the individual main effects by -4.95 (purple-colored line, Figure 2.4). This suggests that when combined, two individual stressors act antagonistically to dampen the main effects. The family *Rhodobacteraceae* had the most differentially abundant OTUs. A total of 10 and 14 OTUs from this family significantly increased in abundance in the high temperature and scarred treatments, respectively, whereas, 11 of these shared OTUs decreased in the two-way interaction. Likewise, three OTUs of the family *Desulfovibrionaceae* all increased in the high temperature and scarred treatments. However, in the two-way interaction, two of these OTUs decreased compared to the expected additive model.

The GLM model, however, also shows that three-way interactions between stressors are generally synergistic when considering changes in taxa abundances (red-colored box, Figure 2.4). The three-way interaction takes into account the main effects and each of the two-way interactions. The null model predicts that the addition of a third stressor has no effect on the interaction of the other two stressors. Compared to this null model, the three-way interactions of high temperature, scarring, and nutrients resulted in an average 19.55 log2 fold increase in taxa (red-colored line, Figure 2.4). Numerous differently abundant OTUs in the two-way and three-way interactions have a 30 log-fold change. These results may, however, be a caveat of the DESeq2 method to calculate a change in abundance associated with the presence of a

taxon that was formerly absent in the treatment contrast. Notably, the magnitude of the average log2 fold-change increases with increasing number of stressors (yellow-, purple-, and red-colored lines, Figure 2.4), which likely results from reduced power from the consecutive addition of interaction terms, thereby, requiring a larger change for a significant statistical result. Regardless of these differences in the magnitude of the response, the evaluation of factorial interactions with a GLM agree with results from the dominant taxa (Supplementary Table 2.2 & 2.3) and Simpson's Index (Supplementary Table 2.4) in characterizing double stressors as antagonistic and triple stressors as synergistic.

2.5. Discussion

Contrary to our hypothesis, our overall results suggest the global and local stressors tested in this tank experiment generally do not act synergistically to induce dysbiosis in the coral microbiome of *Pocillopora meandrina*. In fact, we find that the biological response in the microbial community to stress does not scale positively with increasing number of stressors. We predicted that when sequentially adding stressors to the system, we would see a concurrent increase in deterministic changes to the microbiome (Figure 2.5a,c,e). For beta diversity, deterministic changes would produce clusters with increasingly distant locations from the control community (Figure 2.5a). Stochastic changes would likewise produce communities that were more dispersed or variable (Figure 2.5c). Instead, we found that the greatest deterministic changes in the microbial community resulted from single stressors, while interactions produced an intermediate level of change resulting in antagonisms

that decreased the individual effects (Figure 2.5b). For stochastic changes, any environmental stressor was sufficient to induce dispersion around the centroid of healthy corals (Figure 2.5d), although this dispersion was likely a result of the single dominant taxon (Figure 2.1). The changes in alpha diversity, however, did not scale positively with the number of stressors, and single stressors appear to increase community diversity more than two or three stressors combined (Figure 2.5e,f). We also found that stress induced a myriad of opportunists to invade the community, shifting species dominance away from coral symbionts. The dynamics observed in species' abundance profiles of the microbial community following a perturbation may be explained by each particular microbes' nutrient preference and competitive ability (Goyal et al., 2018).

In contrast to more heterogeneous communities that may be more robust to changes in community evenness, the control corals were dominated by a single taxon initially and thus exhibited low evenness. We would predict then that any perturbation to the system would only increase evenness reflected in higher Simpson's diversity (e.g., Figure 2.2). As such, when stressors were applied to the coral host, bacterial community evenness increased when the dominance shifted from the OTU-Endo symbiont to other taxa such as *Desulfovibrionaceae* (Garren et al., 2009; Gajigan et al., 2017b; McDevitt-Irwin et al., 2017b), *Enterobacteraceae* (Sunagawa et al., 2009; Rosenberg and Kushmaro, 2011), *Amoebophilaceae* (Sweet and Bythell, 2015; Ziegler et al., 2016), *Moraxellaceae* (Koren and Rosenberg, 2008; Li et al., 2015b), and *Rhodobacteraceae* (Meron et al., 2011; McDevitt-Irwin et al.,

2017b; Pollock et al., 2017; Welsh et al., 2017) (Figure 2.1). Contrary to previous work (McDevitt-Irwin et al., 2017b), we did not see an increase in species richness with stress. This may be a result of the mesocosm tanks restricting natural presence/absence dynamics on the reef. Instead, the results suggest a reshuffling of microbial members rather than an increase of new species. Many microbiome studies seek to understand whether dysbiosis, or an imbalance in microbiota, is marked by an invasion or proliferation of pathogens or a depletion of beneficial bacteria (Olesen and Alm, 2016; Duvallet et al., 2017). Yet taxon relative abundance measures alone do not provide enough information to answer this question.

Individual responses of taxa to stress and their contribution to microbiome dysbiosis can be assessed with differential abundance analysis (Welsh et al., 2017; Wipperman et al., 2017; Gurry et al., 2018). Unlike diversity measures which are driven by the changes of dominant taxa in the community, differential abundance testing can identify changes in minor players in the community. DESeq2 can be used to model the abundance of each taxon independently, while accounting for the discrete positive nature of count data and the compositionality of the community using a generalized linear model (GLM) (Love et al., 2014). Using the linear model framework, we expected main effects to increase opportunistic bacteria, and interactions to produce synergistic effects as the community becomes increasingly compromised (Figure 2.5g). Instead, we found that two-way interactions produced antagonistic responses among opportunistic taxa. This apparent antagonism may be a result of a dominance effect, in which one stressor accounts for most or all of the

biological response, changing susceptible taxa such that the second stressor has no additional effect (Côté et al., 2016). Stressors may provide some benefit or resource that normally limits the abundance of opportunistic taxa. For instance, high temperature may increase bacterial reproduction and metabolic rate, while scarring may increase free nutrients in the form of amino acids or open niches. These results suggest that opportunists such as *Rhodobacter* or *Desulfovibrio* spp. are not co-limited by the resources provided by high temperature and scarring. For instance, opportunistic taxa may be proliferating at such a high rate due to increased temperature and increased reproductive rates, that additional free nutrients from scarring do not compound the effect. In contrast, three-way interactions resulted in synergies as invading taxa continued to increase in abundance (Figure 2.5h). This suggests that opportunistic taxa that had maximized their biological response under two stressors, were in fact co-limited by some resource provided by a third stressor. For instance, the addition of nitrogen may have allowed some opportunistic taxa to surpass the maximum threshold of reproductive or metabolic potential set by high temperature and scarring. Alternatively, the difference in interaction type between two-way and three-way interactions may be a result from the coral host's compromised immune system (Bourne et al., 2009; Bosch, 2013; Krediet Cory J. et al., 2013). The coral host effectively regulates it's associated microbial community under two stressors with a heightened immune response. However, with the addition of a third stressor, innate immunity could be overwhelmed, and the host could no

longer regulate its community, thereby allowing a synergistic proliferation of opportunists.

Despite the current bias in interaction literature toward identifying synergies (Côté et al., 2016), our study highlights multivariate and univariate statistical tools that can be combined with standard methods in microbial ecology to more accurately characterize interaction types to host-microbiome systems. Community diversity measures are standardly conducted in microbiome research (Knight et al., 2018), however, they have rarely been used to explicitly test for antagonisms or synergisms between environmental stressors using a microbiome dataset (Lewis et al., 2015; Lokmer and Wegner, 2015; Lesser et al., 2016; Zaneveld et al., 2016; Welsh et al., 2017). Although there is no evidence that these measures respond linearly to stress, these analyses revealed unexpected patterns of community response to increasing amounts of stress. This study presents an initial evaluation of the utility of these community diversity measures in characterizing interactions between different combinations of stressors that are known to damage the coral host and produce compositional changes in its microbiome.

2.6. Funding

This work was funded by: NSF CAREER Award (#OCE-1547952) to DEB, a Dimensions of Biodiversity NSF grant (#1442306) to RVT, an NSF Ocean Sciences grant (#1635913) to RVT, and NSF Graduate Fellowships to both RLM (#1314109-DGE) and MMR (#1650114-DGE). Support was also provided by NSF grants #OCE-

1236905 and #OCE-1637396 to the Mo'orea Coral Reef LTER. Lastly this work was funded by the Riverbanks Zoo & Garden Conservation Support Fund to MMR.

2.7. Acknowledgements

We thank Brendan Bohannan, Beth Miller, and Kyle Meyer at the University of Oregon for useful discussions and feedback. We are grateful to Katherine McLaughlin at Oregon State University for advice on statistical analysis. Lastly, we thank Andrew Shantz at Penn State for assistance with the tank experiment.

2.8. Data availability statement

Microbial data is available at NCBI Sequence Read Archive under the BioProject ID PRJNA549489.

2.9. Author contributions

MMR, DEB, and RVT conceived of and designed the experiment. MMR conducted the experiment. RLM conducted labwork and bioinformatic and statistical analysis with assistance from RVT and RM. RLM, RVT, DEB, and RM interpreted the data. RLM wrote the manuscript. All authors reviewed the manuscript.

2.10. Figures

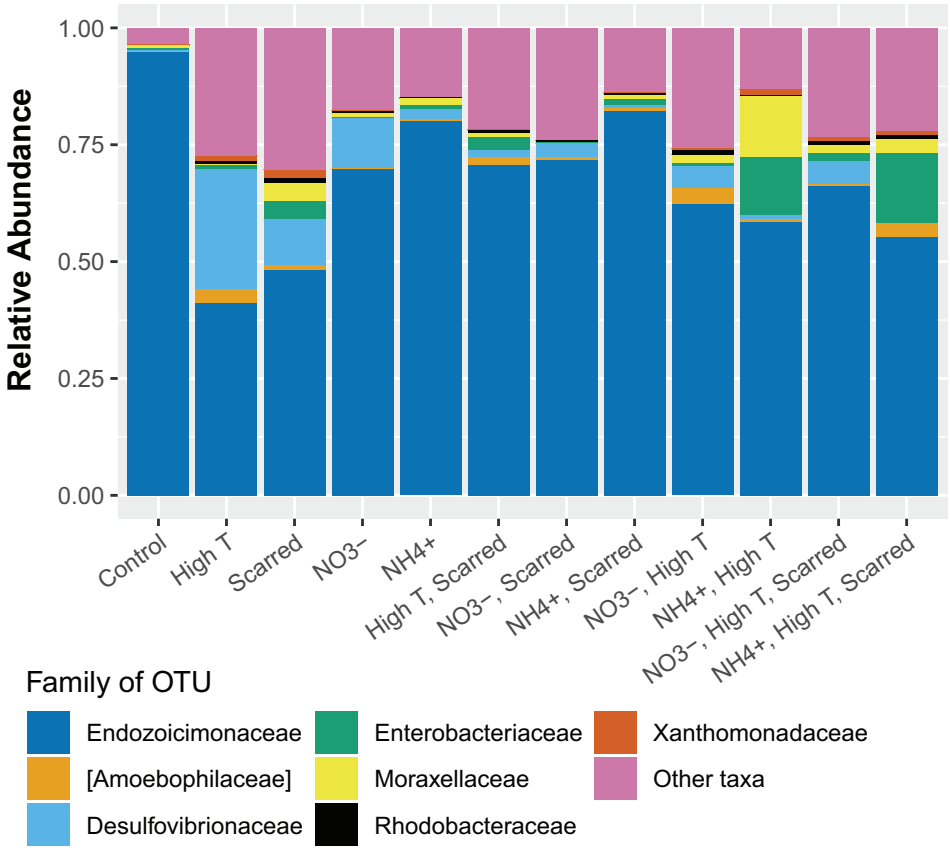

Figure 2.1. Distribution of the relative abundance of dominant OTUs across the twelve experimental treatments from the rarefied OTU table. The top nine OTUs with a mean relative abundance >0.005 are plotted and colored by family. Three of the top OTUs belong to the family *Moraxellaceae*. All other family labels represent a single OTU. All other OTUs are grouped in "Other taxa" to visualize 100% of the community.

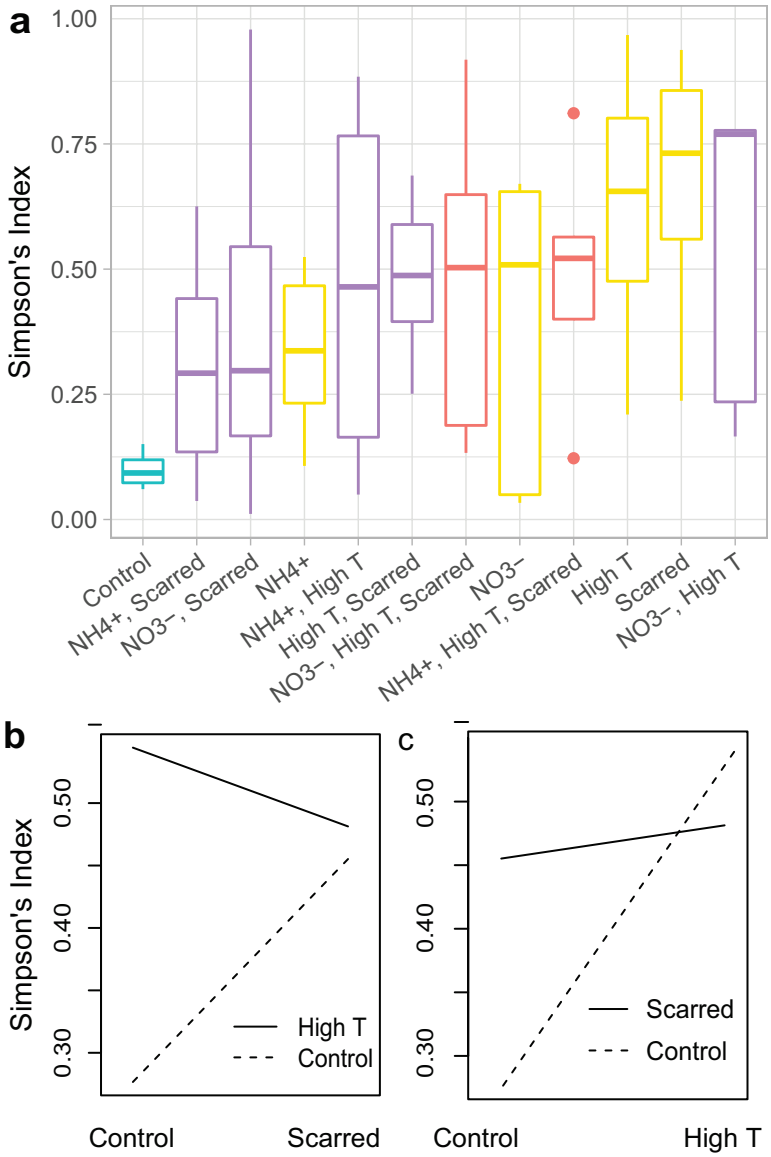

Figure 2.2. Patterns in community alpha diversity. a) Average Simpson's index by treatment. Box colors represent the type of stressor combination applied to the corals: none=teal, single=yellow, double=purple, triple=red. No pairwise treatment comparisons were significant, however, several main effects and interactions were significant in the linear mixed effects model (Supplementary Table 2.4), including the interaction between scarring and temperature. b & c) Interaction plots of interaction between scarring and temperature on Simpson's Index visualized two ways.

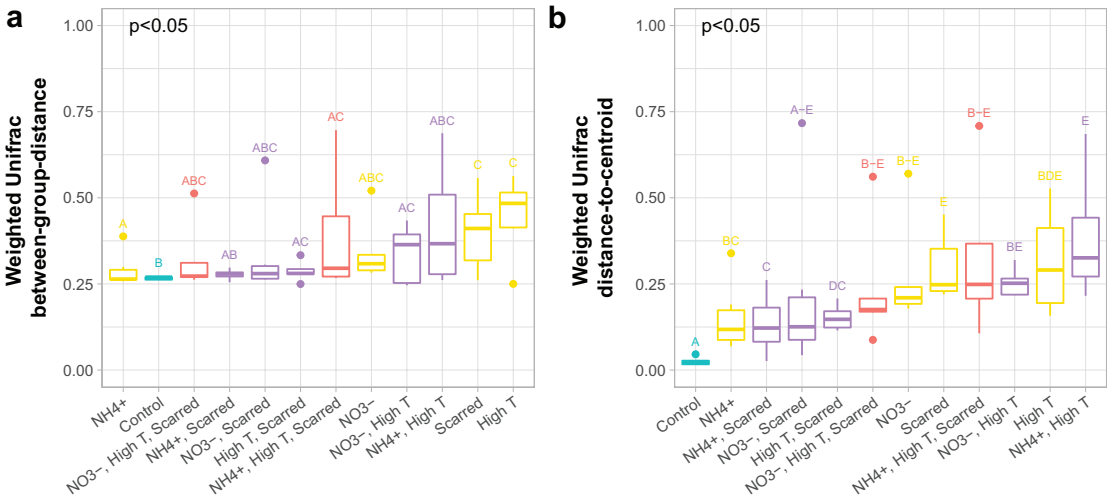

Figure 2.3. Patterns in community beta diversity. a) Mean between-group distances from Weighted Unifrac community dissimilarity by treatment. P-values denote the significance of treatment group in a PERMANOVA using adonis. Significance codes for each treatment are assigned based on the results of pairwise treatment comparisons with adonis (Supplementary Table 2.5). b) Weighted Unifrac mean distance-to-centroid by treatment. P-values denote the significance of treatment group in a PERMDISP using betadisper. Pairwise betadisper was used to assign significance codes for group distances (Supplementary Table 2.7). Groups sharing a letter are not significantly different from each other. Box colors represent the type of stressor combination applied to the corals: none=teal, single=yellow, double=purple, triple=red. Distances are ordered by increasing median, and note that red (triple stressor) treatments are not clustered on the far left.

Figure 2.4. Differential abundance of OTUs with significant response to stressors using DESeq2 and the generalized linear model framework. Only OTUs present in greater than 15 samples were included in the analysis. Each point represents a single OTU that increased or decreased significantly (FDR corrected $p<0.05$) with the stressor or stressor interaction. Each row and dot color corresponds to a microbial family (i.e. multiple OTUs from a single family are increased in multiple treatments). Family name in [] represents a recommended taxonomic annotation by GreenGenes. Box colors represent the stressor type: main effect=yellow, two-way interaction=purple, three-way interaction=red. The colored line within each box represents the mean log2FoldChange for OTUs with significant changes in that stressor type. The dashed colored line within comparisons represents the mean log2FoldChange for OTUs with significant changes within the individual stressor effects and interactions. The gray colored line at 0 log2FoldChange denotes no effect or no interaction.

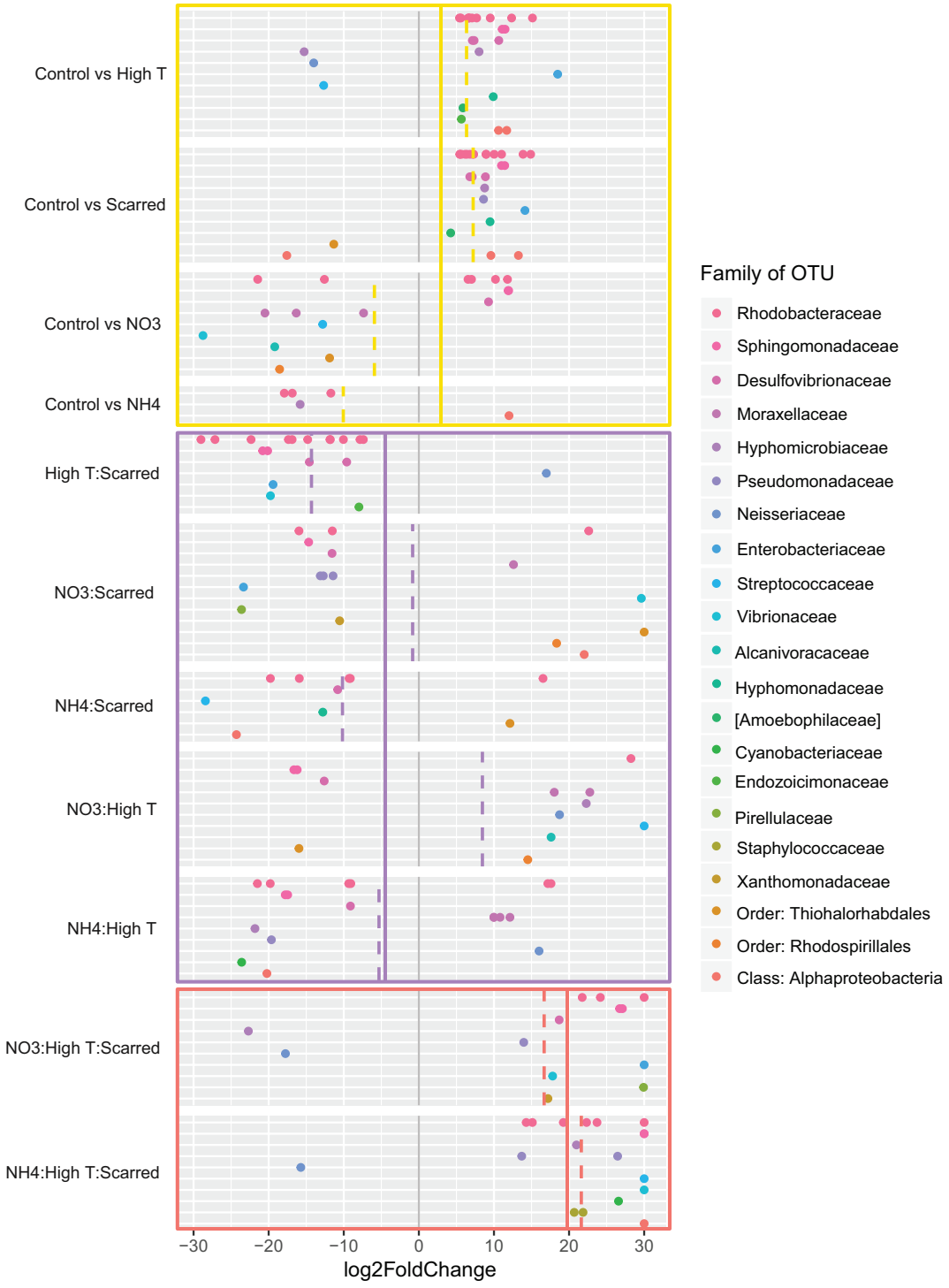
Control vs High T
Control vs Scarred
Control vs NO3
Control vs NH4
High T:Scarred
NO3:Scarred
NH4:Scarred
NO3:High T
NH4:High T
NO3:High T:Scarred
NH4:High T:Scarred
−30
−20
−10
0
10
20
30
log2FoldChange
Family of OTU
Rhodobacteraceae
Sphingomonadaceae
Desulfovibrionaceae
Moraxellaceae
Hyphomicrobiaceae
Pseudomonadaceae
Neisseriaceae
Enterobacteriaceae
Streptococcaceae
Vibrionaceae
Alcanivoracaceae
Hyphomonadaceae
[Amoebophilaceae]
Cyanobacteriaceae
Endozoicimonaceae
Pirellulaceae
Staphylococcaceae
Xanthomonadaceae
Order: Thiohalorhabdales
Order: Rhodospirillales
Class: Alphaproteobacteria

Figure 2.4.

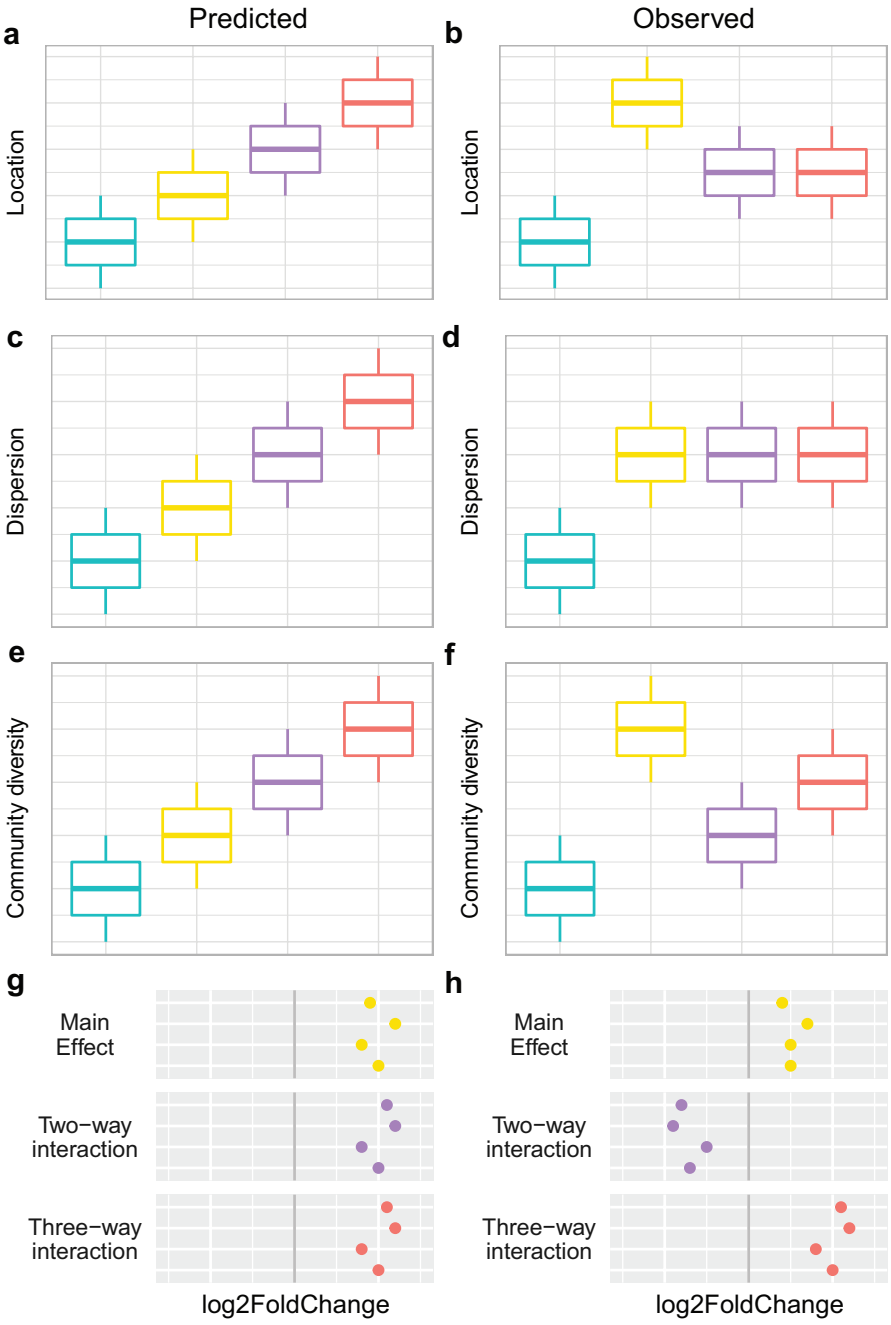

Figure 2.5. Conceptual description of predicted (a,c,e,g) vs observed (b,d,f,h) patterns with multiple stressors. Location (a,b) and dispersion (c,d) effects represent measures of beta diversity. Community evenness (e,f) represents patterns in Simpson's index. Patterns in taxa differential abundance in log2FoldChange using the generalized linear model framework are displayed in g and h with the gray line denoting no effect or no interaction. Colors represent the type of stressor combination applied to the corals: none=teal, single=yellow, double=purple, triple=red.

CHAPTER 3 CORAL MICROBIOMES DEMONSTRATE FLEXIBILITY AND RESILIENCE THROUGH A REDUCTION IN COMMUNITY DIVERSITY FOLLOWING A THERMAL STRESS EVENT

Rebecca L. Maher

Emily R. Schmeltzer

Sonora Meiling

Ryan McMinds

Leïla Ezzat

Andrew A. Shantz

Thomas C. Adam

Russell J. Schmitt

Sally J. Holbrook

Deron E. Burkepile

Rebecca Vega Thurber

Frontiers in Ecology and Evolution

Avenue du Tribunal Fédéral 34, 1005 Lausanne Switzerland

Vol. 8

3.1. Abstract

Thermal stress increases community diversity, community variability, and the abundance of potentially pathogenic microbial taxa in the coral microbiome. Nutrient pollution such as excess nitrogen can also interact with thermal stress to exacerbate host fitness degradation. However, it is unclear how different forms of nitrogen (nitrate vs. ammonium/urea) interact with bleaching-level temperature stress to drive changes in coral microbiomes, especially on reefs with histories of resilience. We used a 13-month field experiment spanning a thermal stress event in the Austral summer of 2016 on the oligotrophic fore reef of Mo'orea, French Polynesia to test how different forms of nitrogen (nitrate vs. urea) impact the resistance and resilience of coral microbiomes. For *Acropora*, *Pocillopora*, and *Porites* corals, we found no significant differences in diversity metrics between control, nitrate- and urea-treated corals during thermal stress. In fact, thermal stress may have overwhelmed any effects of nitrogen. Although all three coral hosts were dominated by the bacterial clade *Endozoicomonas* which is a proposed beneficial coral symbiont, each host differed through time in patterns of community diversity and variability. These differences between hosts may reflect different strategies for restructuring or maintaining microbiome composition to cope with environmental stress. Contrary to our expectation, post-stress microbiomes did not return to pre-stress community composition, but rather were less diverse and increasingly dominated by *Endozoicomonas.* The dominance of *Endozoicomonas* in microbiomes 10 months after peak sea surface temperatures may suggest its ability to utilize host metabolic

products of thermal stress for a sustained competitive advantage against other microbial members. If *Endozoicomonas* is a beneficial coral symbiont, its proliferation after warm summer months could provide evidence of its ability to mitigate coral holobiont dysbiosis to thermal stress and of resilience in coral microbiomes.

3.2. Introduction

Coral reef ecosystems are exceptionally vulnerable to rapid increases in sea surface temperatures. Driven by climate change, coral bleaching events are increasing in frequency and intensity, inspiring extensive efforts to understand the breakdown of the symbiotic association between the coral host and its photosynthetic dinoflagellate endosymbionts of the family Symbiodiniaceae (Bourne et al., 2008; Hughes et al., 2018; Sully et al., 2019). Similarly, bacterial members of the coral holobiont are sensitive to changing environmental conditions but have been evaluated less extensively under increasing seawater temperatures. Research on bacterial community dynamics under temperature stress demonstrates shifts to more disease-associated states, increases in community variability, compromised function of beneficial microbiota, and selection for potentially pathogenic bacteria (Ritchie, 2006; Bourne et al., 2008; Thurber et al., 2009; Mouchka et al., 2010; Maher et al., 2019). Given that coral microbiota are thought to play an important role in nutrient cycling and antimicrobial protection (Ritchie, 2006; Wegley et al., 2007), it is important to understand how their response to thermal stress events can mitigate or exacerbate host survival and ecosystem resilience.

Nutrient enrichment resulting from human activities is an important contributor to coral reef decline (Szmant, 2002; Fabricius, 2011). Elevated inorganic nutrients (i.e. nitrogen and phosphorus) can induce profound changes in the benthic communities of coastal ecosystems, fostering the growth of macroalgae and increasing the prevalence of coral diseases (McCook et al., 2001; Burkepile and Hay, 2006; Vega Thurber et al., 2014). In addition, nutrient enrichment may affect coral physiological traits such as growth and reproductive effort and may impair coral thermal tolerance to bleaching (Wooldridge, 2009; Cunning and Baker, 2013; D'Angelo and Wiedenmann, 2014). That said, recent studies indicate these effects may depend on the chemical form (i.e. nitrate, ammonium, urea) and source of nitrogen, as well as on the stoichiometry of the N:P (Wiedenmann et al., 2013; Shantz and Burkepile, 2014). Both laboratory and field experiments show negative effects of elevated nitrate levels derived from anthropogenic sources on coral growth rate, bleaching prevalence and duration - especially when coupled with low levels of phosphorus (Wiedenmann et al., 2013; Ezzat et al., 2015; Burkepile et al., 2019). In contrast, fish-derived nutrients such as ammonium and urea have either neutral or beneficial effects on coral growth, photosynthesis and bleaching tolerance (Béraud et al., 2013; Shantz and Burkepile, 2014; Ezzat et al., 2015; Allgeier et al., 2017; Burkepile et al., 2019; Ezzat et al., 2019c).

While the effects of excess nitrogen levels on coral physiology have been well documented, less is known about their potential to alter coral-associated bacterial communities, especially when combined with stressors such as ocean warming. For

corals maintained in aquaria, both nitrate and ammonium were sufficient to destabilize the coral-associated bacterial community, although ammonium-treated corals remained more similar compositionally to controls than nitrate-treated corals (Maher et al., 2019; Rice et al., 2019). In the Florida Keys, nitrogen and phosphorous enrichment made corals more susceptible to mortality from predation, above-average seawater temperatures, and bacterial opportunism (Zaneveld et al., 2016). In fact, during that multi-year experimental enrichment, nutrient loading increased both the prevalence and severity of coral disease and bleaching (Vega Thurber et al., 2014).

To understand the interacting effects of nutrients and bleaching on coral microbiomes in a coral depauperate reef, we previously enriched corals with nutrients during a 2014 bleaching event in the Florida Keys (Wang et al., 2018). The Florida Keys, like many Caribbean reefs, have experienced deterioration since the 1980s leading to phase shifts from coral- to algal-dominated reefs that show little evidence of reversibility or recovery (Rogers and Miller, 2006; Maliao et al., 2008). From *Siderastrea siderea* coral metagenomes, we found that nutrient enrichment alone increased microbial community beta diversity throughout the bleaching event but had no interacting effects with temperature. This supports mounting evidence that microbial community diversity increases with stress (McDevitt-Irwin et al., 2017b) potentially reflecting microbiome destabilization or dysbiosis (van Oppen and Blackall, 2019). In sharp contrast to the Florida Keys which remain in a state of low total coral cover, the fore reef of Mo'orea, French Polynesia, has recovered from numerous landscape-scale perturbations within about a decade with total coral cover

reaching ~50% in 2019 (Adjeroud et al., 2002, 2009; Berumen and Pratchett, 2006; Penin et al., 2007; Adam et al., 2011, 2014; Trapon et al., 2011; Holbrook et al., 2018). Mesocosm experiments on *Pocillopora meandrina* microbiomes in Mo'orea showed that while nutrients and the interaction between nutrient enrichment and high temperature had an effect on individual members of the microbiome, temperature alone had the strongest effect on alpha and beta diversity overall (Maher et al., 2019). However, the temperature stress applied in the experiment was not sufficient to induce bleaching or mortality (Rice et al., 2019). To extend this previous work to a natural system, we assessed the response of coral microbiomes to combined nutrient and thermal stress *in situ* on the historically resilient fore reef of Mo'orea.

This study investigated how the availability of different types of nitrogen (nitrate vs. urea) influenced the community composition of coral microbiomes during a bleaching event on the oligotrophic fore reef in Mo'orea, French Polynesia. We included coral genera susceptible to thermal stress, *Acropora* and *Pocillopora*, and a more resistant genus, *Porites* (Burkepile et al., 2019). Over 13 months, we sampled members of each species from plots that were either maintained as controls or continuously enriched with nitrate or urea. We used high taxonomic resolution based on sub-operational taxonomic units to assess the compositional variability of *Acropora*, *Pocillopora*, and *Porites* microbiomes before, during, and after a bleaching event in the 2016 Austral summer. The goal of our study was to evaluate how different nitrogen sources interact with seawater warming to drive changes in bacterial community dynamics. We hypothesized that stress would lead to dysbiosis

of the microbial community resulting in increased diversity and between-sample variability, and that communities would demonstrate resilience by returning to their initial state after the stress event. Additionally, we expected nitrate to exacerbate community dysbiosis induced by increased seawater temperatures compared to ambient nutrient conditions, while urea would have no interacting effects with temperature.

3.3. Materials and Methods

3.3.1. Design of the nutrient enrichment experiment

To test how temperature stress interacted with nitrate and urea enrichment to reorganize coral microbiomes, we conducted a 13-month enrichment experiment at 10 m depth on the north shore of Mo'orea, French Polynesia (17°30'S, 149°50'W) (Burkepile et al., 2019). Mo'orea is a high-relief volcanic island at the eastern end of the Society Island archipelago with a well-developed lagoon and barrier reef formation. Conditions on the fore reef are relatively oligotrophic (0.28 ± 0.19 uM DIN (mean ± SE); 0.14 ± 0.05 uM SRP; Alldredge 2019) with coral cover approaching 50% at the study site when our experiment began (Holbrook et al., 2018). The coral community was dominated by *Acropora* spp. (primarily *Acropora retusa*, *Acropora hyacinthus*, *Acropora globiceps*), *Pocillopora* spp. (primarily *Pocillopora verrucosa*, *Pocillopora meandrina*, and *Pocillopora eydouxi*), and *Porites lobata* complex; therefore we set out to examine the impacts of enrichment on the microbiome of representative corals from each of these three genera.

In January 2016, we enriched small sections of the benthos around individual focal corals with polymer coated, slow-release nitrate (Multicote 12-0-44, Haifa Chemicals Ltd) or urea (Apex 39-0-0, JR Simplot Company) fertilizers. To achieve localized enrichment, we created 'nutrient diffusers' by drilling holes in 4cm diameter PVC tubes which we then wrapped in window screen and filled with either 200 g of nitrate fertilizer or 62 g of urea fertilizer. Different amounts of each fertilizer were used to standardize the total amount of N delivered in both treatments. Nutrient diffusers were secured to the bottom within 15 cm of focal corals with cable ties attached to stainless steel all-thread posts or eyebolts drilled into the reef framework and epoxied in place. Empty diffusers containing no fertilizer were also deployed next to control colonies to account for any effects the diffusers may have had that were unrelated to the fertilizer. To ensure continuous enrichment, diffusers were exchanged every 10-12 weeks from January 2016 to September 2017. As described in Burkepile et al. 2019, nitrogen concentrations of enrichment treatments were quantified each week over a 10-week period following the deployment of a fresh nutrient diffuser at a subset (n=5) of control, nitrate, and urea plots.

Plots for enrichment were haphazardly selected between 10-12 m depth by identifying areas where *Porites, Pocillopora,* and *Acropora* were all growing within a 0.5 m radius of a central point where a diffuser could be deployed. However, because not all of the plots contained all three genera of corals, the total replication for our treatments differed by genera. For *Pocillopora*, replication was $n = 70$ for nitrate, $n = 63$ for urea, and $n = 67$ for controls. *Acropora* colonies were present in $n = 35$ nitrate

plots, n = 32 urea plots, and n = 40 control plots. *Porites* colonies were present in n = 59 nitrate, n = 55 urea, and n = 65 control plots. To facilitate re-sampling, focal corals were marked by epoxying stainless steel, numbered cattle tags at the base of each colony. All diffusers were separated by at least 1-2 m and spread over approximately 11,000 m^2. Sea water temperature was recorded every two minutes via two thermistors deployed at opposite ends of the site.

3.3.2. Tissue sampling for microbial communities

To track changes in the coral microbiome we collected tissue samples from a subset of the study's focal corals in January, March, May, and July of 2016 as well as January of 2017. For *Pocillopora* and *Acropora* spp., divers used bone cutters to clip off ~1 cm sections of branches from each focal coral. For massive *Porites,* ~1 cm^2 sections of tissue and skeleton were removed from focal colonies with a hammer and chisel or leather punch. Samples were collected underwater in individually labeled, sterile whirlpaks and transferred to the boat. On board the boat, the water was drained from each whirlpak and the samples were placed on ice, transported ~10 min to shore, and stored at -80° C until analysis.

3.3.3. Sample selection, DNA extraction, 16S library preparation and sequencing

For library preparation and sequencing, a subset of the focal coral samples was chosen to include only individual corals sampled at all five time points and within each nutrient treatment. Therefore, this subset only included corals with no observed mortality either due to bleaching or some stochastic process for the duration of the experiment (280 samples total). See Supplementary Table 3.1 for replication by

treatment. Subsamples of frozen fragments were taken and preserved in individual bead-beating garnet tubes from MoBio PowerSoil® DNA Isolation Kit (now QIAgen PowerSoil® DNA Isolation Kit). DNA was extracted from each sample according to the MoBio PowerSoil® DNA Isolation Kit protocol. To target bacterial and archaeal communities, the V4 region of the hypervariable16S rRNA gene was amplified via 2-step PCR coupling forward and reverse primers 515F (5'-GTG YCA GCM GCC GCG GTA A-3') (Parada et al., 2016) and 806R (5'-GGA CTA CNV GGG TWT CTA AT-3') (Apprill et al., 2015). First-step reactions (12.5 µl reaction volume) included 6.25 µl AccuStart II ToughMix (2X), 1.25 µl forward primer (10 µM), 1.25 µl reverse primer (10 µM), 0.5 µl sample DNA, and 3.25 µl PCR-grade water. Sample DNA concentrations ranged widely from 0.07 to 10.0 µg/mL. Thermocycler reaction protocol was performed with 3 min denaturation at 94° C; 35 cycles of 45 s at 94° C, 60s at 50° C, and 90 s at 72° C; followed by 10 min at 72° C and a 4º C hold. Amplified products were run on a 1.5% agarose gel and manually excised. Following gel purification using Wizard® SV Gel and PCR Clean-Up System (Promega), products were barcoded with dual indices with custom multiple amplicon adapters in a 12-cycle PCR reaction (12.5 µl AccuStart II ToughMix (2X), 9.5 µl PCR-grade water, 1 µl (10 µM) each of forward and reverse barcodes, 1 µl of gel-purified DNA). After pooling amplicons in equivolume ratios, we used Agencourt® AMPure XP beads in a final clean-up step on the single resulting pool. Libraries were sequenced at Oregon State University (OSU) by the Center for Genome Research and

Biocomputing (CGRB) with v.3 reagent 2 x 300 bp read chemistry on Illumina MiSeq.

3.3.4. Quality control, and initial data processing

A total of 280 samples were sequenced, quality filtered, and run through the Deblur workflow (Supplementary Table 3.1). Raw reads were first demultiplexed using the fastq-multx tool from ea-utils (http://code.google.com/p/eautils/) resulting in a total of 12,079,654 reads. Then reads were trimmed of primers and adapters using Cutadapt v1.12 (Martin, 2011). The following quality control steps were conducted using VSEARCH v2.8.1 (Rognes et al., 2016). Sequences were truncated at the first position having a quality score ≤10, and paired-end reads were merged resulting in 5,989,931 reads. Next, sequences with a total expected error >1 per base or with >1 N were discarded. The resulting 5,388,863 reads underwent the Deblur workflow to trim quality-controlled sequences to 250 base pairs, to identify exact sequences with single-nucleotide resolution, and to filter de novo chimeras (Amir et al., 2017). The Deblur workflow is a novel method for obtaining sequences that describe community composition at the sub-operational taxonomic unit (sOTU) level using Illumina error profile (Amir et al., 2017). A total of 1,110,070 reads remained across the 280-sample dataset with 2,016 unique sequences from the Deblur workflow. The loss of ~80% of reads in the workflow likely reflects the large proportion of host coral mitochondrial sequences (<250 base pairs) amplified by the primers, which is a known issue in using the 515F-806R primers on coral tissues.

The resulting sOTU table from the Deblur workflow was processed in QIIME 2 2019.7 (Bolyen et al., 2019). Taxonomy was assigned with the q2-feature-classifier plugin (Bokulich et al., 2018) which employs the classify-sklearn naïve Bayes taxonomy classifier against the Silva 132 99% OTUs reference sequences from the 515F/806R region (Quast et al., 2012). Next, sOTUs were removed from the dataset if they annotated as mitochondrial or chloroplast sequences or were only present in a single sample further reducing the number of reads per sample to a median value of 1,210 with a variance of 1.2.

The remaining sOTUs were aligned with mafft (Katoh et al., 2002) (via q2-alignment) and used to construct a phylogeny with fasttree2 (Price et al., 2010) (via q2-phylogeny). Alpha rarefaction curves were visualized using the q2-diversity plugin to pick a minimum frequency of 881 reads per sample as a sufficient rarefying depth (Supplementary Table 3.1, Supplementary Figure 3.1). The sOTU table was rarefied resulting in 159 remaining samples with unbalanced replication across treatments and coral hosts (Table 3.1) using the package *phyloseq* (v1.28.0) (McMurdie and Holmes, 2013). Alpha diversity metrics including Faith's phylogenetic diversity (Faith, 1992), Chao1 statistic (Chao and Chiu, 2016), and Simpson's diversity index (Heip et al., 2001), and beta diversity metrics including weighted UniFrac (Lozupone et al., 2007), unweighted UniFrac (Lozupone and Knight, 2005), Binary Jaccard distance, and Bray-Curtis dissimilarity were calculated after log-transformation in *phyloseq*.

3.3.5. Statistical analyses

To improve normality of alpha diversity metrics, Chao1 and Faith's phylogenetic diversity were square root-transformed, while Simpson's index was arcsine-transformed. Experimental group effects on each alpha diversity metric were assessed with linear mixed effect models (LMM) using *lme4* (v1.1.21) (Bates et al., 2014) with month, coral genus, and nutrient treatment as fixed effects and factorial interaction terms and individual colony as a random effect. Multiple comparisons were performed with estimated marginal means (EMMs) using the *emmeans* (v1.4) package. For beta diversity metrics, Permutational Analyses of Variance (PERMANOVA; Anderson, 2001) were conducted to test differences in bacterial community compositions between groups and group factorial interactions. In addition, Permutational Analyses of Multivariate Dispersions (PERMDISP; Anderson, 2006) were used to test for homogeneity of multivariate dispersions between groups. PERMANOVA and PERMDISP were performed using the functions adonis and betadisper in the package *vegan* (v2.5.5) followed by a pairwise analysis of variance with *pairwiseAdonis* (v0.01) and permutest in *vegan*, respectively, with FDR adjusted p-values. The betadisper command also was used to calculate the distance to centroid for each sampling group.

All analyses were initially conducted on all microbiome data controlling for host taxa so that patterns of change driven by time and treatment were assessed across all samples with coral genus (*Porites*, *Acropora*, or *Pocillopora*) as an independent variable. When there was a significant interaction between treatment and coral genus, analyses were repeated for each individual host genus to discern differences in main

effects between coral genera that may have been masked when all genera were combined. Due to the opportunistic nature of field sampling, replication across coral genera, treatment, and month vary widely with *Acropora* corals having the highest replication and *Porites* corals having no samples from January 2016 (Table 3.1). Samples from January 2016 were collected pre-treatment and were therefore analyzed as controls.

Additionally, changes in the abundance of different bacterial genera across month and treatment in all three corals combined, and within each coral genus were assessed with analysis of composition of microbiomes (ANCOM) with controls for false discovery rate (Mandal et al., 2015). For differential abundance analysis with ANCOM, an unrarefied sOTU table was used including samples with 881 or more reads. While treatment and the interaction between month and treatment were assessed in ANCOM models, significant differentially abundant taxa were only identified in the ANCOM model with month as a single predictor and individual colony as a random effect.

3.4. Results

3.4.1. Sea surface temperatures, thermal stress, and nitrogen exposure

The 2015/2016 El Niño event increased the probability that corals would experience thermal stress and bleaching, providing us with an opportunity to test the effects of nutrient enrichment and bleaching on the coral microbiome. As reported in Burkepile et al. 2019, the daily average sea surface temperature (SST) at our experimental site peaked in late March at 29.7° C, and remained at or above 29° C

through May of 2016. These temperature thresholds correlate with thermal stress and coral bleaching in Mo'orea (Pratchett et al., 2013). Thus, for a total of 45 days, including 37 consecutive days from mid-March to mid-April, corals at our site experienced thermal stress sufficient to cause bleaching. Average monthly SST is reported in Table 3.1 and a graph of average daily temperatures during the experiment can be found in Supplementary Figure 3.2. Of the corals analyzed here, only 7 colonies bleached (*Acropora*: n=6, *Porites*: n=1) in May 2016 all of which had no signs of bleaching in July 2016 (Supplementary Table 3.1). Due to this low sample size of bleached corals and the absence of bleaching-induced mortality in the dataset, bleaching was not included in statistical analyses.

Over a 10-week period, nutrient diffusers in nitrate and urea plots increased the concentrations of nitrogen in the surrounding seawater compared to control plots (Burkepile et al. 2019). Analysis of concentrations in Burkepile et al. 2019 showed that nitrogen exposures in nitrate and urea plots were similar and significantly distinct from control plots, and treatments were consistent throughout the 10-week diffuser deployment. Total water-column nitrogen concentrations ranged from approximately 1-3 uM, 3-8 uM, and 3-11 uM Nitrogen for control, urea, and nitrate plots, respectively, over the 10-week period (see Figure 2 in Burkepile et al. 2019).

3.4.2. Bacterial community composition varied over time

The dominant bacterial taxon in the dataset (n=159) belonged to the genus *Endozoicomonas* (mean relative abundance 0.448 ± 0.033 SEM); this genus was present in all but 21 samples (Figure 3.1). The next most abundant taxa across the

dataset belonged to the genera *Vibrio* (0.060 ± 0.011), *Acinetobacter* (0.059 ± 0.008), *Pseudomonas* (0.049 ± 0.006), and *Candidatus Amoebophilus* (0.038 ± 0.011). Generally, *Endozoicomonas* relative abundance was lowest in March (0.277 ± 0.050) and July 2016 (0.186 ± 0.047) and highest in January 2017 (0.817 ± 0.058) for all corals combined. Despite low replication for *Pocillopora* samples in May of 2016 (Table 3.1), coral samples from all three genera had high relative abundance of *Endozoicomonas*. The decrease in relative abundance of *Endozoicomonas* in March, May, and July coincided with an increase in the relative abundance of minor taxa including *Vibrio*, *Pseudomonas*, *Staphylococcus*, and *Halobacteriovorax*, all of which decreased or disappeared in January 2017 (Figure 3.1). In contrast, other taxa such as *Acinetobacter*, *Candidatus Amoebophilus*, and *Corynebacterium* were present throughout the sampling period. Figure 3.1 does not reflect the high variance in relative abundance across samples, for instance, taxa such as *Spiroplasma*, *Halomonas*, and *Tenacibaculum* dominated a single sample within a genus/treatment/month combination (Supplementary Figure 3.3).

3.4.3. Patterns in microbiome alpha diversity differed among coral host genera during thermal stress

Analyses of bacterial species richness and evenness suggested seasonal variation in alpha diversity, although the patterns varied by coral host genus (Figure 3.2). Pooled by coral genus, *Porites* corals had the highest Chao1 diversity index (mean 33.983 ± 2.88 SEM, n=39) and Faith's phylogenetic diversity (4.289 ± 0.302) compared to *Acropora* (27.910 ± 2.211 and 3.643 ± 0.211, respectively, n=74) and *Pocillopora* (21.085 ± 1.806 and 3.118 ± 0.225, respectively, n=46). By contrast,

Acropora had the highest Simpson's diversity index (0.679 ± 0.027) compared to *Pocillopora* (0.580 ± 0.050) and *Porites* (0.557 ± 0.046). In LMMs with nutrient treatment, month, and coral genus as fixed effects, nutrient treatment was not a significant predictor for Chao1 ($p = 0.470$, $F_{(2,64.7)}=0.765$), Simpson's diversity ($p = 0.085$, $F_{(2,122)}=2.516$), or Faith's phylogenetic diversity ($p = 0.694$, $F_{(2,58.3)}=0.368$) (Supplementary Table 3.2). Instead, the interaction between month and coral genus was a significant predictor for Chao1 ($p < 0.01$, $F_{(7,109.4)}=3.133$), Simpson's diversity ($p < 0.01$, $F_{(8,122)}=3.469$), and Faith's phylogenetic diversity ($p < 0.01$, $F_{(7,106.8)}=3.108$), suggesting that patterns across time differed between coral genera (Figure 3.2). For this reason, we evaluated patterns of alpha diversity across time with LMMs within each coral genus. Due to loss of samples during bioinformatic filtering, replication varied widely between time points (Table 3.1).

3.4.4. Temporal patterns in alpha diversity were similar to patterns in the relative abundance of Endozoicomonas

In *Acropora* samples, month was a significant predictor of Chao1 ($p < 0.001$, $F_{(4,57.9)}=18.476$), Simpson's diversity ($p < 0.001$, $F_{(4,69)}=7.483$), and Faith's phylogenetic diversity ($p < 0.001$, $F_{(4,57.5)}=23.265$, Supplementary Table 3.3). In pairwise comparisons, the last time point, January 2017, was significantly lower than March, May, and July of 2016 for both Chao1 and Simpson's diversity and was significantly lower than all other time points for Faith's phylogenetic diversity (Figure 3.2). Initially, in January 2016, before bleaching, *Acropora* samples had a mean Chao1 of 19.724 ± 2.671 which increased significantly to 40.844 ± 4.275 in May 2016 and decreased significantly to 9.586 ± 1.045 in January 2017 (Figure

3.2A). Similarly, *Acropora* samples had the lowest Simpson's diversity in January 2017 (0.465 ± 0.048), although January, May, and July 2016 were variable with some low diversity samples (Figure 3.2B). These patterns closely mirrored the temporal pattern in relative abundance of *Endozoicomonas* in *Acropora* samples where initial mean relative abundance of 0.747 ± 0.143 decreased to 0.277 ± 0.079 in July 2016 and increased to 0.972 ± 0.011 in the final sampling point (Figure 3.1).

Porites samples showed similar patterns to *Acropora* with month as a significant predictor of Chao1 ($p < 0.05$, $F_{(3,35)}=4.354$), Simpson's diversity ($p < 0.05$, $F_{(4,26.2)}=5.105$), and Faith's phylogenetic diversity ($p < 0.001$, $F_{(3,35)}=8.203$, Supplementary Table 3.4). All three diversity metrics significantly decreased from May or July to January 2017 in *Porites* (Figure 3.2). Similar to the pattern displayed by *Acropora*, the highest relative abundance of *Endozoicomonas* was during the month with lowest diversity in January 2017 (0.533 ± 0.136) (Figure 3.1).

In contrast to *Acropora* and *Porites*, *Pocillopora* exhibited low alpha diversity in May 2016 as well as January 2017 (Figure 3.2). Month was a significant predictor of Chao1 ($p < 0.001$, $F_{(4,41)}=11.724$), Simpson's diversity ($p < 0.001$, $F_{(4,41)}=17.740$), and Faith's phylogenetic diversity ($p < 0.001$, $F_{(4,35.85)}=18.986$, Supplementary Table 3.5). For all three measures, alpha diversity significantly decreased from March to May, increased from May to July, and decreased from July to January 2017 (Figure 3.2). The low replication in May compared to March and July for *Pocillopora* samples may contribute to this pattern. However, all three samples from May were consistently dominated by *Endozoicomonas* (0.960 ± 0.026) as in January 2017

(0.875 ± 0.109), compared to March (0.143 ± 0.072) and July (0.105 ± 0.064) (Figure 3.1).

3.4.5. Thermal stress and recovery produced distinct microbial communities in all three coral hosts

PERMANOVA results, with month as the predicting factor, showed the presence of distinct microbial communities for all four measures of community dissimilarity. Month explained the most variance using weighted UniFrac distances (PERMANOVA; $p < 0.001$, $R^2 = 0.270$, Supplementary Table 3.6), and pairwise comparisons showed that all months were significantly different from one another. Coral host genus ($p < 0.001$, $R^2 = 0.072$, Figure 3.3A) and the interaction between genus and month ($p < 0.001$, $R^2 = 0.074$) were also significant using weighted UniFrac distances. In fact, all four dissimilarity measures found month, host genus, and their interaction significant for predicting distinct microbial communities. Nutrient treatment did not produce distinct communities for any dissimilarity measure.

For all four dissimilarity measures, month produced distinct communities in *Acropora* corals, while treatment and the interaction between month and treatment did not (Supplementary Table 3.7). Month explained the most variance with weighted UniFrac distances (PERMANOVA; $p < 0.001$, $R^2 = 0.403$), and pairwise comparisons showed that all pairwise comparisons of month were different (Figure 3.3B). Likewise, month produced distinct communities for *Pocillopora* ($p < 0.001$, $R^2 = 0.427$, Supplementary Table 3.8) and *Porites* ($p < 0.001$, $R^2 = 0.249$, Supplementary Table 3.9) samples using weighted UniFrac distances (Figure 3.3C&D). All four

months were significantly different from each other for *Porites* samples from pairwise comparisons. For *Pocillopora* samples, January 2016 was not different from May 2016, nor were March and July 2016 or May 2016 and January 2017.

3.4.6. Community dispersion varied among coral hosts over time

Across all corals, community dispersion was significantly different over time but only for the Binary Jaccard presence/absence measure (PERMDISP; $p < 0.01$, $F = 3.609$). Dispersion varied by coral genus with weighted UniFrac ($p < 0.01$, $F = 4.766$, Figure 4A), Bray-Curtis ($p < 0.01$, $F = 4.911$), and Binary Jaccard ($p < 0.01$, $F = 5.880$). Additionally, there were no differences in dispersion by nutrient treatment across all coral hosts and any dissimilarity measure (Table 3.10). Dispersion differed significantly among sampling periods for *Acropora* corals based on the weighted UniFrac distances ($p < 0.001$, $F = 13.009$, Figure 3.4B), but was not significantly different among nutrient treatments ($p = 0.386$, $F = 0.964$, Supplementary Table 3.11). Pairwise comparisons showed that community dispersion in January 2017 was significantly less than in all other months and dispersion in May 2016 was significantly less than in January 2016 ($p < 0.01$). Dispersion did not significantly differ among months for *Pocillopora* samples ($p = 0.671$, $F = 0.591$, Figure 3.4C). Dispersion was also significantly different between months for *Porites* samples ($p < 0.05$, $F= 3.459$, Supplementary Table 3.11) with May having the lowest dispersion and January 2017 having the highest although no pairwise comparisons were significant after correction (Figure 3.4D).

3.4.7. Differentially abundant taxa increased during thermal stress and decreased during recovery

Differential abundance analysis with ANCOM was performed on *Acropora*, *Pocillopora*, *Porites*, and combined coral samples to assess if specific bacterial genera significantly changed in abundance relative to other genera in the community. There were no differences in taxon abundance by nutrient treatment for combined and individual coral communities. However, there were differentially abundant bacterial genera between months ($p < 0.05$, $W=0.9$). A total of 14 bacterial genera were significantly differentially abundant in all coral samples combined (Figure 3.5A, Supplementary Table 3.12). *Acropora* corals had 11 differentially abundant taxa with month, while *Pocillopora* and *Porites* corals had 2 and 3 differentially abundant taxa, respectively (Figure 3.5B-D). *Endozoicomonas* was differentially abundant across all corals combined, *Acropora* alone, and *Pocillopora* alone, but not *Porites* corals alone. *Candidatus Amoebophilus* was only differentially abundant within *Pocillopora* samples, while *Streptococcus* was only differentially abundant within *Porites* samples and all corals combined. Interestingly, *Pseudoxanthomonas* was differentially abundant for *Acropora* alone and all corals combined and was found exclusively in May 2016 (Figure 3.5A&B). Based on relative abundance (Figure 3.5), differentially abundant taxa across all samples appear to fall into three categories: a) moderate decreases in May 2016 and severe decreases in January 2017 compared to March and July (i.e. *Acinetobacter*, *Pseudomonas*, *Corynebacterium*), b) nearly exclusive occurrence in May 2016 (i.e. *Paenibacillus*, *Alteromonas*, *Reyranella*,

Pseudoxanthomonas), c) increased abundance and occurrence in January 2017 (i.e. *Endozoicomonas*).

3.5. Discussion

We tracked the composition and stability of microbiomes associated with *Acropora*, *Pocillopora*, and *Porites* corals throughout a thermal stress event under ambient nutrient conditions and nitrogen enrichment. We found that microbiomes varied widely across months, potentially due to the temperature fluctuations that contributed to the stress event. Periods of thermal stress were accompanied by increased alpha diversity and community heterogeneity. Coral microbiomes returned to a state of reduced diversity, dominated by *Endozoicomonas*, some months following the event. Neither nitrate nor urea exposure had any effects on community diversity or abundance of individual taxa despite experimental evidence that nitrate and urea diffusers increase the concentration of nitrogen in the surrounding seawater over a 10-week period (Burkepile et al. 2019). Contrary to our hypothesis, nitrogen did not interact with month, which is inherently connected with seawater temperatures. Instead, temperature likely overwhelmed any effects of nutrients. Although conclusions presented here are limited by reduced sample sizes in some groups (Table 3.1), our data demonstrate the importance of collecting time series datasets across several coral hosts and with sufficient sampling periods to capture the dynamics of microbiome recovery post stress.

3.5.1. Alpha diversity changes under seasonal thermal stress vary between coral genera

Microbiome species richness of Mo'orean corals varied significantly among months and host genus. SST peaked in March 2016 and decreased slightly but maintained bleaching-level temperatures until May. Interestingly, mean microbial species richness peaked in May 2016 for *Acropora* and *Porites* corals. A similar result was found in a study of *Agaricia* corals in the Florida Keys, where microbial species richness was highest in the month following temperature and bleaching highs (Wang et al., 2018). This could suggest that the colonization or establishment of temperature-sensitive opportunistic taxa into a stressed coral microbiome may be delayed following peak thermal stress. Two putative examples of such opportunistic taxa are *Paenibacillus* and *Reyranella*, which occurred almost exclusively in May in both *Acropora* and *Porites* corals (Figure 3.5B&D). Alternatively, opportunistic taxa may become established stochastically throughout the duration of stress events, with species richness gradually increasing as long as the event lasts. To distinguish between these patterns, future microbial time series will be required which span bleaching events with sufficiently fine-scale repetitive sampling.

Time series should also consider including multiple coral host species, since the patterns in diversity observed in Mo'orea varied by host (Figures 3.2&3.3). Contrary to the response of *Acropora* and *Porites* microbiomes, *Pocillopora* microbiomes experienced a drastic decrease in alpha diversity following peak temperatures (Figure 3.2). The reduction in observed species richness was accompanied by a much higher relative abundance of the putative coral symbiont *Endozoicomonas* (Figure 3.5). This pattern could be the result of an active regulatory

response to exclude heat-associated opportunists, possibly mediated by *Endozoicomonas* (Neave et al., 2016). However, it is also possible that drastically increased absolute abundance of *Endozoicomonas* outcompeted the rest of the community (with unknown implications for host health), or even simply overwhelmed signatures of other taxa with relative abundances too low to detect at our sequencing depths. If an active regulatory mechanism were responsible, the increased diversity in July could reflect the eventual failure of this response to exclude or reduce opportunists such as *Vibrio*, *Pseudomonas*, and *Staphylococcus*, which subsequently increased in relative abundance at that time (Figure 3.1). If a drastic increase in *Endozoicomonas* absolute abundance was responsible for the patterns, these opportunists could have been present throughout March, May, and July but gone undetected in May. Distinguishing between these possibilities could be a target of future studies that sequence samples to much greater depths.

3.5.2. Dynamics of Endozoicomonas abundance drive community variability and resilience

Our results add to mounting evidence supporting the importance of *Endozoicomonas* in shaping coral microbiomes (Neave et al., 2016; McDevitt-Irwin et al., 2017b; Pollock et al., 2018; Maher et al., 2019). For both *Acropora* and *Pocillopora* corals, the abundance of *Endozoicomonas* significantly changed over the thermal stress event (Figure 3.5B&C). Most notably, January 2017 samples of both corals were dominated almost exclusively by *Endozoicomonas*. For *Acropora* corals, this was accompanied by a significant reduction in the sample-to-sample variability (Figure 3.4B). *Pocillopora* samples also appear to be less variable during January

2017, although low replication may have prevented us from detecting a response in dispersion (Figure 3.4C) (Anderson and Walsh, 2013). In contrast, *Porites* samples during this time point were highly variable (Figure 3.4D). Interestingly, *Endozoicomonas* abundances in *Porites* did not significantly change over the thermal stress event (Figure 3.5D). Experiments and surveys on *Porites lobata* in Mo'orea have shown a similar community response under various stressors, including mechanical wounding, predation, corallivore feces deposition, and combinations of stressors (Ezzat et al., 2019a, 2020). In these experiments, Hahellaceae (family of *Endozoicomonas*) was a dominant member of the coral microbiome but was generally not differentially abundant with stress. Hahellaceae only decreased significantly 3 hours after corals were exposed to feces, but recovered to control levels within 48 hours (Ezzat et al., 2019a). This suggests that while the dominant symbiont *Endozoicomonas* fluctuates in abundance during stress for *Acropora* and *Pocillopora* corals, this taxon is generally less variable in *Porites* corals. However, the relative proportion of this taxon did still change in *Porites* samples, particularly in July (Figure 3.1). Thus, despite lower variability, these changes could still result in shifts in the relative contribution of *Endozoicomonas* to microbiome function in *Porites*.

The dynamics of *Endozoicomonas* throughout this experiment combined with evidence of its involvement in holobiont sulfur cycling suggest its potential functional role in microbiome resilience (Bourne et al., 2016). The dominance of *Endozoicomonas* at the final month for *Acropora* and *Pocillopora* corals may be explained by sulfur cycling processes in the coral holobiont. Corals are significant

sources of dimethylsulfoniopropionate (DMSP) and dimethylsulfide (DMS) in reef waters (Broadbent and Jones, 2004). Research shows that coral DMSP and DMS production is upregulated during oxidative stress, such as warming events and bleaching (Lesser, 2006; Deschaseaux et al., 2014). Some *Endozoicomonas* species can metabolize DMSP to DMS, using DMSP as a carbon source for growth and survival (Tandon et al., 2020). Increased DMSP production during stress could provide substrate for *Endozoicomonas* to proliferate and confer the taxon a competitive advantage over other coral-associated taxa. This could explain the dominance of *Endozoicomonas* by January 2017 to levels that surpass those of pre-bleaching communities.

The increase in abundance of *Endozoicomonas* during oxidative stress could confer benefits to their coral host that may provide resilience during thermal stress. For instance, the breakdown of DMSP to DMS by *Endozoicomonas* produces carbon (Tandon et al., 2020) which could provide the coral with an alternative carbon source during recovery from thermal stress to partially compensate for the loss of energy-supplying algal symbionts. Furthermore, the coral pathogen *Vibrio coralliilyticus* uses DMSP as a strong cue to find heat-stressed hosts through chemotaxis and chemokinesis (Garren et al., 2014). The increased metabolism of DMSP by growing *Endozoicomonas* populations after thermal stress could reduce the amount of chemoattractant for *Vibrio* spp. to detect, potentially helping to alleviate *Vibrio* infection. However, we did not find any evidence *Vibrio* spp. abundance was influenced by *Endozoicomonas* and the idea that *Endozoicomonas* provide benefits to

their coral hosts remains speculative. Future investigation is warranted to determine what role *Endozoicomonas* plays in holobiont sulfur cycling and overall health during temperature stress.

3.5.3. Dynamics of opportunistic microbiota differentiate hosts' responses to stress

The number of bacterial genera that significantly fluctuated throughout the thermal stress event may provide evidence for coral host-specific mechanisms for coping with environmental change. For instance, *Acropora* samples had more differentially abundant bacterial taxa than *Pocillopora* or *Porites*. This could be related to the fact that *Acropora* were also the most sensitive of the three coral genera to bleaching (Burkepile et al., 2019). *Acropora* corals have been described as microbiome conformers by adapting to changing environmental conditions while *Pocillopora* corals were described as microbiome regulators by remaining stable through change (Ziegler et al., 2019). For instance, Ziegler et al. 2019 found the microbiome of *A. hemprichii* to be readily "responding" and variable across different anthropogenic impacts and flexible upon transplantation. It remains to be determined whether microbiome restructuring is a deterministic mechanism for beneficial holobiont adaptation or plasticity or if it is a stochastic response to dysbiosis. However, *Acropora* corals were less variable than *Pocillopora* or *Porites* corals (Figure 3.4A) suggesting that more deterministic changes were driving *Acropora* community dynamics (Zaneveld et al., 2017). Based on our evaluation of the number of individual bacterial taxa that changed in abundance, *Porites* may fall closer to the 'microbiome regulator' side of the two proposed stress-response mechanisms.

However, differentiating conformers from regulators may require a closer look at the identity and function of those individual bacterial taxa.

The high microbiome flexibility in *Acropora* may leave the host-associated community vulnerable to the loss of important or beneficial symbionts and their corresponding functions or to the acquisition of pathogens. For instance, bacterial genera present in March and/or May 2016 including *Pseudomonas*, *Acinetobacter*, *Sphingomonas*, *Corynebacterium 1*, *Alteromonas*, and *Vibrio* have each been association with various coral stressors including elevated seawater temperature and ocean acidification (Grottoli et al., 2018), hyper-salinity (Röthig et al., 2016), bleaching (Koren and Rosenberg, 2008), bacterial challenge (Wright et al., 2017), and coral disease (Sweet et al., 2013). However, these associations with stress are not always consistent across studies and stressors. For example, *Acinetobacter*, *Corynebacterium 1*, and *Vibrio* have been found both in association and not associated with Dark Spot Syndrome (Sweet et al., 2013; Meyer et al., 2016) and *Acinetobacter* has also been found in high abundance with healthy corals (Cai et al., 2018). Similarly, *Pseudomonas* was found to be positively associated with hyper-salinity but negatively associated with bleaching (Ritchie et al., 1994; Röthig et al., 2016). The coarse classification of bacterial taxa to the genus-level in these studies as well as the study presented here limit our ability to detect finer scale functional differences, for instance at the species or strain level. Although these taxa are associated with thermal stress in this study, future functional analysis at the sOTU

level would better discern their potential positive or negative contributions to holobiont health.

In contrast, although taxa changed in relative abundance, we did not detect differentially abundant stress-associated bacterial taxa in *Pocillopora* corals (Figure 3.5, Figure 3.1). This may be due to our reduced replication for *Pocillopora* samples in May 2016. Alternatively, this may represent the coral host's or microbiome's ability to strategically maintain a stable and robust microbial community during stress. That said, abundance of the dominant symbiont *Endozoicomonas* changed throughout temperature stress despite evidence that the globally conserved association between *Pocillopora verrucosa* and *Endozoicomonas* remains unchanged during bleaching or mortality (Pogoreutz et al., 2018; Maher et al., 2019). However, evidence from previous studies is based on short-term (<1 month) aquaria experiments that may not reflect microbiome dynamics on the reefs over realistic timescales (Pogoreutz et al., 2018; Maher et al., 2019). Additionally, the abundance of the taxon *Candidatus Amoebophilus* which has been associated with diseased and healthy corals (Apprill et al., 2016) significantly changed in *Pocillopora* with decreases in abundance and occurrence in March and May (Figure 3.4). This taxon is a member of the core microbiome for Australian corals and an intracellular symbiont of eukaryotes with genomic evidence of a symbiotic lifestyle (Schmitz-Esser et al., 2010; Pollock et al., 2018). Its reduction in March and May could reflect an interaction with Symbiodiniaceae within the coral tissue (Apprill et al., 2016) which are then lost during thermal stress. The decrease of putative symbionts in *Pocillopora*

corals contrasts sharply with the increase of potential opportunists in *Acropora* and *Porites* corals further supporting differential host responses to thermal stress.

3.5.4. Effects of temperature may overwhelm those of nutrients

Elucidating the combined effects of nitrogen pollution and thermal stress on corals is critical to predicting how coral reefs will respond to increasing levels of anthropogenic stress. Previously, a superset of the corals evaluated in the present study were surveyed for bleaching response over the mild bleaching event during the austral summer of 2016 in Mo'orea, French Polynesia. This study found that, compared to corals in ambient conditions, *Acropora* and *Pocillopora* corals that were exposed to nitrate exhibited more frequent bleaching, bleached for longer duration, and were more likely to die (Burkepile et al., 2019). In contrast, we found that under combined and prolonged heat and nitrogen stress, enrichment with either ammonium or nitrate had no discernable effect on the composition of the coral microbiome. Previous work supports the hypothesis that the coral host and microbiome have parallel responses under stress (Ziegler et al., 2017). Our selection of samples that survived the 2016 bleaching event may have inadvertently biased our dataset to corals that did not bleach (bleached n = 7). This may have prevented us from detecting any effects by nitrogen on the microbiome that parallel the significant interaction between temperature and nitrate and the significant differences between nitrate and urea observed in the coral host response (Burkepile et al., 2019).

Our results suggest that thermal stress likely overwhelmed the coral microbiome such that additional nutrient stress had no measurable effect. We found

no significant interactions on microbiome diversity between nitrogen enrichment and increased seawater temperatures. This corroborates work on *Pocillopora meandrina* in tanks in Mo'orea and *Agaricia* spp. on the reef during severe bleaching in the Florida Keys (Wang, 2006; Maher et al., 2019). Importantly, this result is consistent on the coral reefs studied regardless of disturbance history and during both moderate and severe bleaching events. We show that even under a mild thermal stress event, nutrients do not differentially affect the coral microbiome. However, since few bleached corals were included in our study and because we could not control for temperature, we cannot eliminate the possibility that bleaching response itself may impose some stress-exposure threshold that allows for interactions with nutrients and temperature in terms of changing microbial community dynamics.

3.5.5. Future research implications

With thermal stress events increasing in severity and frequency, future research should investigate if and how the homogenization of coral microbiomes after thermal stress will prepare coral holobionts for future stress events. After exposure to a warmer, more variable environment, *Acropora* corals in American Samoa were themselves more tolerant to a subsequent acute heat stress in the laboratory, exhibiting a robust and stable microbiome (Ziegler et al., 2017). This suggests that corals surviving one heat stress may have increased tolerance to future heat stress events. Whether tolerance of the host coral is conferred or promoted through microbiome composition remains to be determined (Ziegler et al., 2017). Burkepile et al. 2019 observed nitrate-treated *Acropora* corals in Mo'orea bleaching for longer

duration in the more severe 2017 bleaching event. Evaluation of microbiome dynamics in time series over repetitive stress events could help determine if microbiome tolerance can be developed through stress exposure and if an *Endozoicomonas*-dominated community plays a role in microbiome tolerance.

3.6. Funding

This work was funded by the National Science Foundation Grants #1442306 to RV, #OCE-1635913 to RV, #1314109-DGE to RLM, #OCE-1619697 to SH, DB, and RS, OCE-1547952 to DB, and OCE-1236905 and OCE-1637396 for the Mo'orea Coral Reef LTER to RS and SH. This work was also funded by the Swiss National Science Foundation Fellowship #P400PB_ 183867 to LE.

3.7. Acknowledgements

We thank M. Anskog, A. Duran, C. Fuchs, K. Landfield, S. Leung, K. Neumann, K. Seydel, A. M. S. Correa, A. T. S. Tang, A. Thurber, R. Welsh, and S. Wise for field and laboratory assistance. We are grateful to T. Lamy for his assistance in preliminary data analysis. Research was completed under permits issued by the Territorial Government of French Polynesia (Délégation à la Recherche) and the Haut-commissariat de la République en Polyneésie Francaise (DTRT) (Protocole d'Accueil 2015–2017).

3.8. Data availability statement

The datasets and code generated for this study can be found in the online repositories. The names of the repositories and accession number can be found below:

https://www.ncbi.nlm.nih.gov/, PRJNA627248; https://github.com/maherrl/RAPID-analysis.

3.9. Author contributions

R.V.T., D.E.B., S.J.H., and R.J.S. conceived of and designed the experiment. A.A.S. and T.C.A. conducted the experiment. E.S and S.M. conducted the labwork. R.L.M. conducted bioinformatic and statistical analysis with assistance from R.V.T., R.M., S.M., A.A.S. and L.E. R.L.M., R.V.T., and D.E.B. interpreted the data. R.L.M wrote the manuscript. All authors reviewed the manuscript.

3.10. Table

Table 3.1. Sample sizes and mean daily sea surface temperature (SST) with standard error across months, coral hosts, and nutrient treatments.

Month	**SST Mean & SE**	**Treatment**	***Acropora***	***Pocillopora***	***Porites***
January 2016	28.4 ± 0.15° C	Control	6	4	0
March 2016	29.0 ± 0.08° C	Control	7	6	2
		Nitrate	6	6	3
		Urea	6	3	3
May 2016	28.4 ± 0.02° C	Control	6	1	5
		Nitrate	6	0	3
		Urea	7	2	5
July 2016	26.9 ± 0.02° C	Control	6	7	2
		Nitrate	5	4	2
		Urea	4	4	4
January 2017	28.9 ± 0.05° C	Control	5	3	4
		Nitrate	5	4	3
		Urea	5	2	3

3.11. Figures

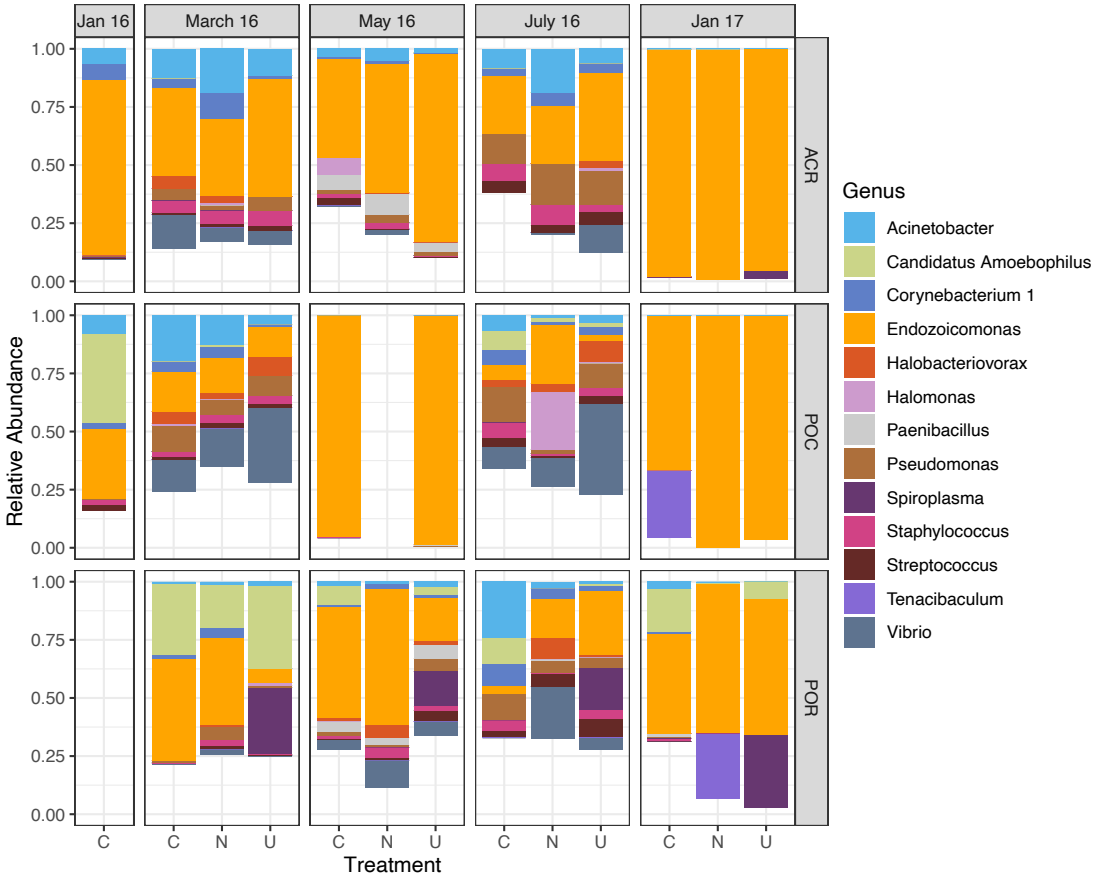

Figure 3.1. Relative abundance of dominant microbial genera varies over time across all corals. Data are organized by month, coral host (ACR: *Acropora*, POC: *Pocillopora*, POR: *Porites*), and nutrient treatment (C: Control, N: Nitrate, U: Urea). Only genera with a mean relative abundance greater than 0.10 are included. Sample sizes are reported in Table 3.1.

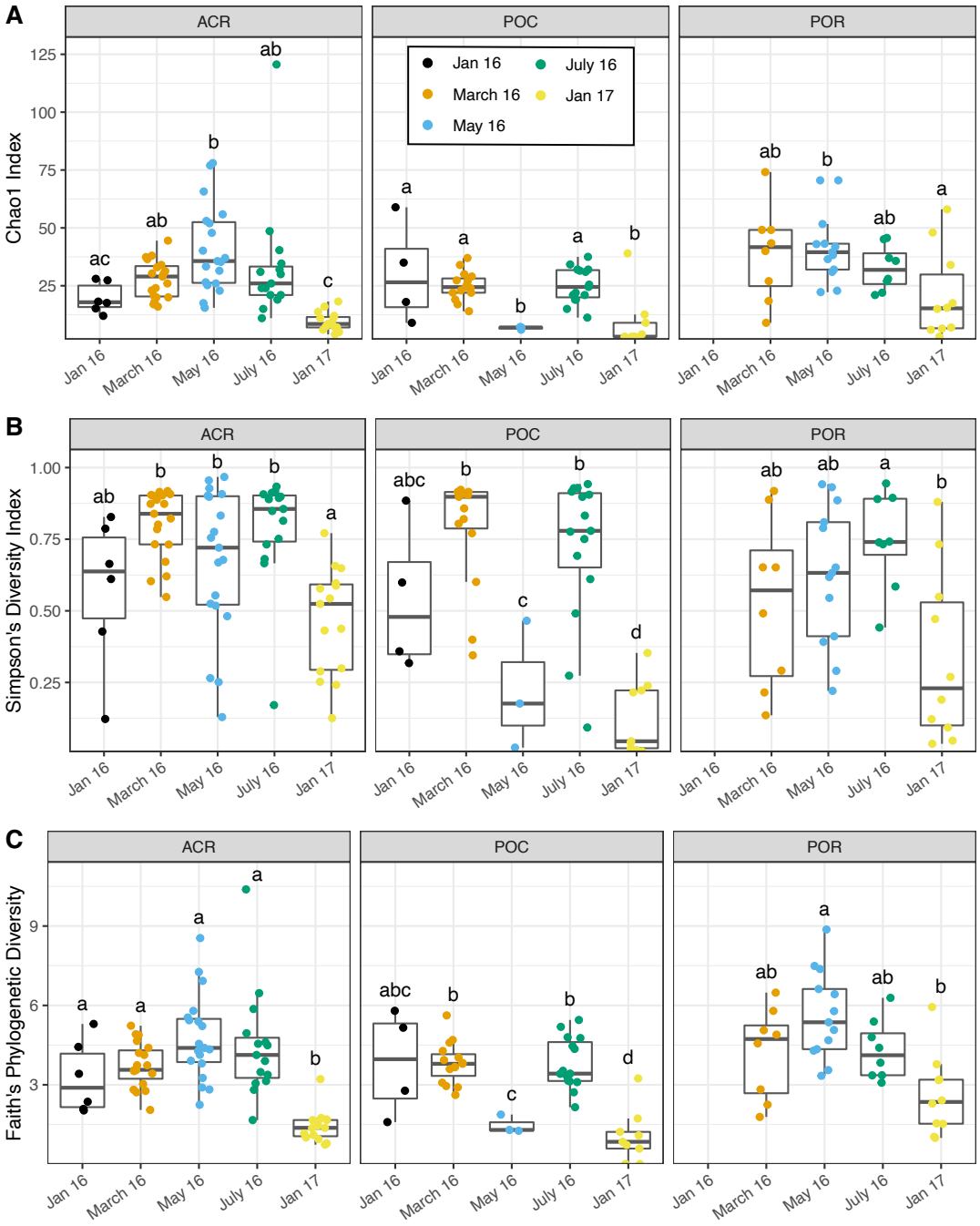

Figure 3.2. Microbiome alpha diversity varies by time and between coral genera. Due to a significant interaction effect between month and genus, significant differences were determined between months within each coral genus using linear mixed-effects models and pairwise comparisons. Boxes sharing a letter are not significantly different from one another and are only comparable within genus. (A) Chao1 index versus month. (B) Simpson's diversity index versus month. (C) Faith's phylogenetic diversity versus month.

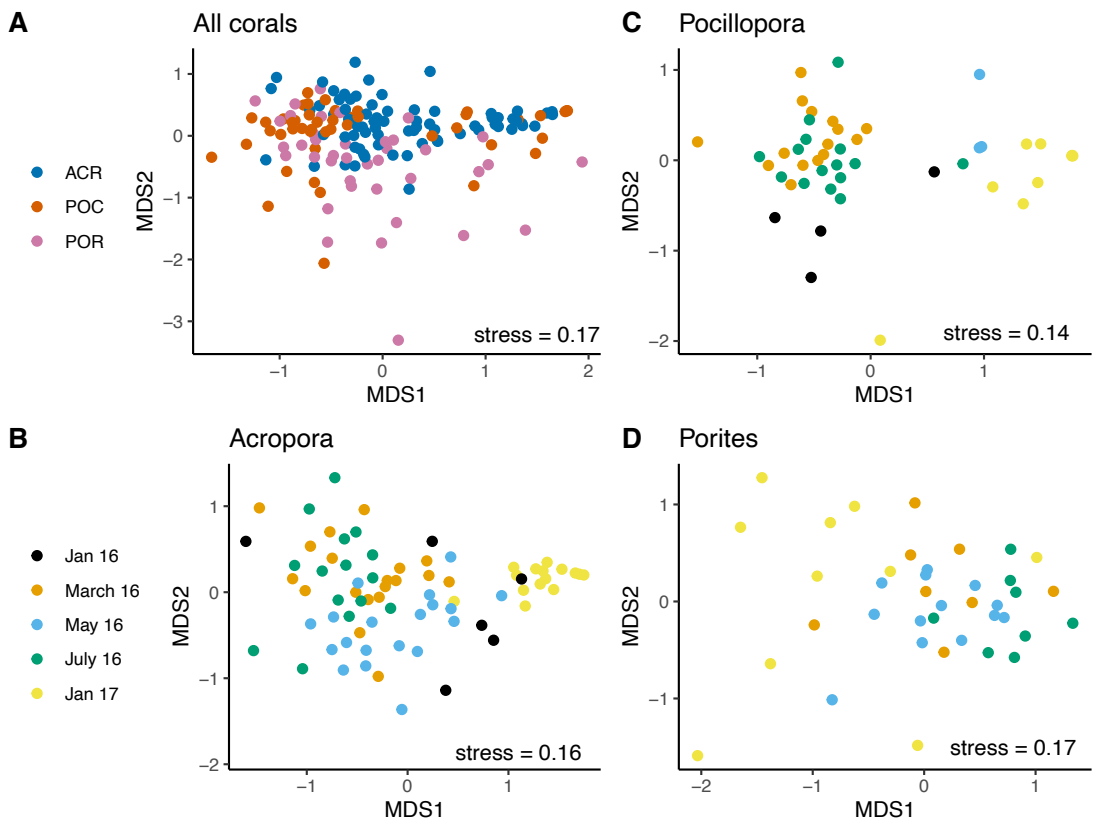

Figure 3.3. Coral microbiomes are distinct across month and between coral genera. The bacterial community data were first log-transformed and dissimilarity was calculated using weighted UniFrac. NMDS ordination of (A) All corals combined by genus, (B) *Acropora* samples by time, (C) *Pocillopora* samples by time, and (D) *Porites* samples by time.

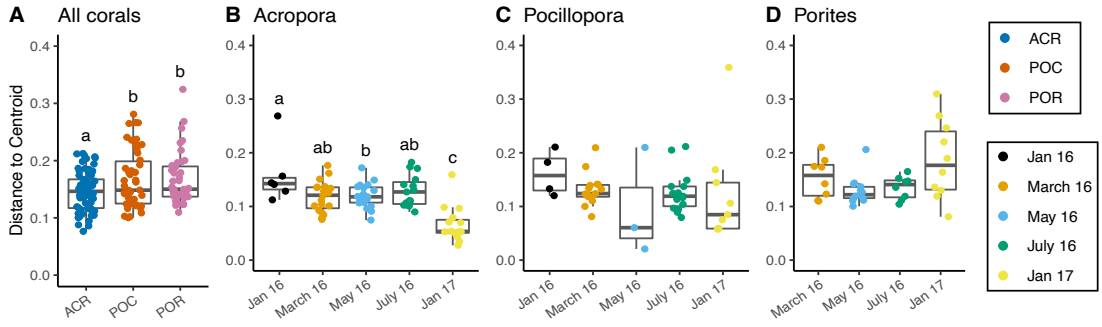

Figure 3.4. Microbiome dispersion varies by coral host and over time. (A) All corals combined by genus, (B) *Acropora* corals by time, (C) *Pocillopora* corals by time, (D) *Porites* corals by time. Boxes sharing a letter are not significantly different from one another. Dispersion was not significant for *Pocillopora* samples, but was significant for *Porites* samples, although there were no significant pairwise differences.

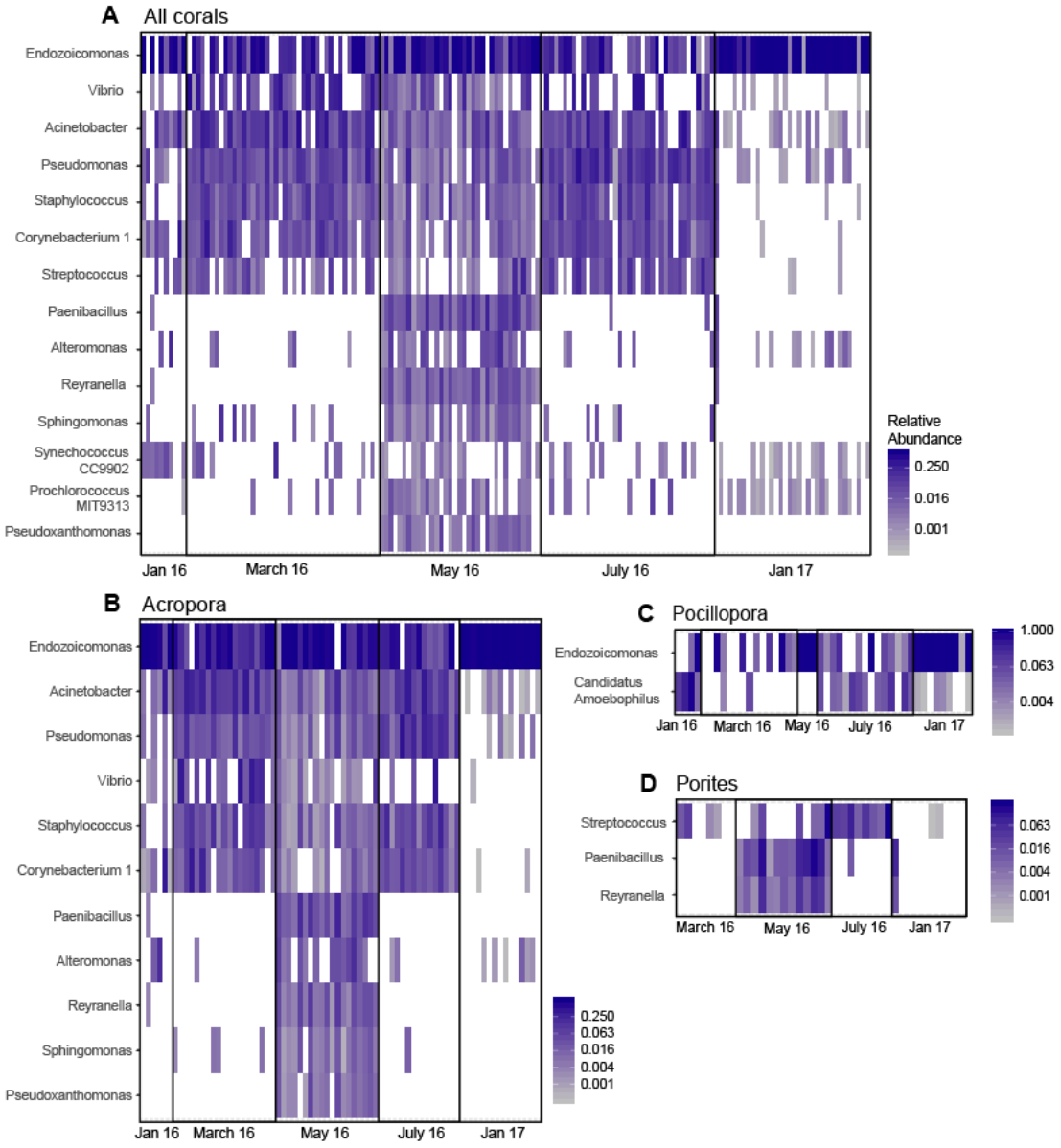

Figure 3.5. Differentially abundant taxa across month identified by ANCOM. Significant taxa were identified for (A) all samples combined, (B) *Acropora* samples only, (C) *Pocillopora* samples only, and (D) *Porites* samples only. Cells are scaled by the relative abundance and white cells indicate an absence of that taxon in the sample.

CHAPTER 4 GENOMIC INSIGHT INTO THE HOST-ENDOSYMBIONT RELATIONSHIP OF *ENDOZOICOMONAS* SPECIES WITH THEIR MARINE EUKARYOTIC HOSTS

4.1. Abstract

Endozoicomonas bacteria are globally distributed in a diversity of marine hosts and are commonly found in high abundance in healthy corals. While there are several proposed functions of this endosymbiont, including nutrient cycling and regulation of bacterial colonization within their hosts, there is little genomic or experimental evidence to support these functions. Recent work experimentally verified the ability of *E. acroporae*, isolated from *Acropora* corals in Taiwan, to metabolize dimethylsulfoniopropionate (DMSP). We previously showed that *Endozoicomonas* species in Mo'orean corals were resilient to thermal stress and hypothesized that the recovery in *Endozoicomonas* abundance was due to its ability to metabolize DMSP which is produced by the coral host under oxidative stress. To test this hypothesis, I assembled a metagenome-assembled genome (MAG) from the Mo'orean coral *Pocillopora meandrina* and conducted comparative genomics with all available *Endozoicomonas* genomes. While the MAG does not encode genes for the metabolism of DMSP, we found genome-specific genes involved in the maintenance of a stable symbiosis with a eukaryotic host. Interestingly, *Endozoicomonas* species do not differentiate by host taxonomic group or by location, however, some coral hosts and their *Endozoicomonas* symbionts demonstrate evidence of cophylogeny. Further, we found that *Endozoicomonas* species may contribute essential nutrients including B vitamins and amino acids to their eukaryotic hosts.

4.2. Introduction

Animal-bacterial symbioses are increasingly recognized as fundamental components of processes ranging from animal evolution and development to ecosystem functioning (McFall-Ngai et al., 2013). Symbiotic bacteria from the genus *Endozoicomonas* are of particular interest to coral microbial ecologists as these microbes often dominate the microbiomes of coral animals that engineer coral reef ecosystems (Neave et al., 2017b). *Endozoicomonas* (i.e. monad living inside an animal) was phenotypically and phylogenetically characterized as a novel genus of Gammaproteobacteria after isolation from the sea slug *Elysia ornata* and 16S rRNA gene sequencing (Kurahashi and Yokota, 2007). Since its characterization, a rapidly growing number of studies have demonstrated that the bacterial genus is a ubiquitous and abundant member of the microbiome of many marine organisms, including cnidarians, poriferans, molluscs, annelids, tunicates, and fish (Jensen et al., 2010; Morrow et al., 2012; Forget and Juniper, 2013; Fiore et al., 2015; Katharios et al., 2015). *Endozoicomonas* are found in all major oceans of the world from abyssal depths to warm photic zones (Neave et al., 2016, 2017b). Microscopy studies demonstrate that *Endozoicomonas* symbionts aggregate deep within their hosts' tissues, aggregating extracellularly in ascidians, inside the nucleus of mussels, and within a thin tightly enveloping membrane in fish and snails, all of which suggest an intimate symbiosis with their hosts (Zielinski et al., 2009; Bayer et al., 2013; Mendoza et al., 2013; Beinart et al., 2014; Katharios et al., 2015; Schreiber et al., 2016b). Within corals, *Endozoicomonas* form similar structures to cell-associated

microbial aggregates (CAMAs) and are found in gastrodermal tissues or bordering the epidermis and gastrodermis (Neave et al., 2016, 2017b).

Given their ubiquity across various marine hosts, *Endozoicomonas* species are under investigation for their ecological and functional roles. *Endozoicomonas* species are hypothesized to be beneficial symbionts, particularly within coral holobionts, as this bacterium is underrepresented in diseased or stressed corals and in corals from environments of high anthropogenic impact (Vezzulli et al., 2013; Morrow et al., 2015; Webster et al., 2016; Ziegler et al., 2016; Maher et al., 2020). In fact, *Endozoicomonas* species can comprise >90% of the microbiome of apparently healthy corals (Pogoreutz et al., 2018; Maher et al., 2019). However, *Endozoicomonas* species have also been associated with diseased fish in aquaculture facilities and can cause rapid and significant host mortality (Mendoza et al., 2013; Katharios et al., 2015). *Endozoicomonas* has also been detected in seawater samples (Schreiber et al., 2016). Thus, *Endozoicomonas* species appear to be involved in facultative symbioses with various marine eukaryotic hosts with functions ranging from commensal symbionts to pathogens.

Before the sequencing of the first *Endozoicomonas* genomes in 2014 (Neave et al., 2014), researchers hypothesized that these organisms were involved in nutrient cycling and provisioning within their invertebrate hosts (Forget and Juniper, 2013; Nishijima et al., 2013; Morrow et al., 2015), regulation of holobiont bacterial colonization through the production of bioactive secondary metabolites (Mohamed et al., 2008; Rua et al., 2014), or competitive exclusion of pathogenic bacteria (Bourne

et al., 2008). Raina et al. (2009) demonstrated that various Gammaproteobacteria including *Endozoicomonas*-related isolates from *Acropora millepora* coral tissues have the ability to metabolize dimethylsulfoniopropionate (DMSP) to dimethyl sulfide (DMS) by successfully isolating the bacteria on media with DMSP as the sole carbon source. Reef-building corals and their symbiotic dinoflagellates, *Symbiodiniaceae*, are significant producers of DMSP and DMS in reef waters, both of which are key compounds in the global sulfur cycle (Raina et al., 2013). Therefore, genomic investigations in *Endozoicomonas* species have explicitly searched for genes involved in DMSP degradation in an effort to link these species to sulfur cycling within the holobiont and uncover functional evidence for their apparent ubiquity and dominance in some marine invertebrate hosts.

Comparative genomics of *Endozoicomonas* species has recently produced nearly complete and draft genomes (Neave et al., 2014, 2017a; Ding et al., 2016; Tandon et al., 2020). Importantly, Tandon et al. (2020) demonstrated that three strains of the species *Endozoicomonas acroporae* from *Acropora* corals were able to metabolize media with a select range of DMSP concentrations into volatile DMS and identified the DMSP lyase, *dddD*, within the genomes. Of the ten other *Endozoicomonas* genomes available at the time, no other species possessed genes for this process, suggesting that metabolization of DMSP to DMS is not a hallmark of *Endozoicomonas* species but instead is restricted to certain *Endozoicomonas* lineages and thus only functionally relevant in some host-bacterial symbioses. Further, DMSP and DMS can function as antioxidants and may mitigate the oxidative stress

experienced by corals during thermal stress (Sunda et al., 2002; Lesser, 2006; Deschaseaux et al., 2014).

From differential abundances of *Endozoicomonas* sequences throughout a mild coral bleaching event in Mo'orea, French Polynesia, we observed the post-stress recovery of *Endozoicomonas* to a higher relative abundance than in the pre-stress community (Maher et al., 2020). We hypothesized that these temperature-responsive *Endozoicomonas* species may have been able to utilize the DMSP produced by their coral hosts during the bleaching-induced oxidative stress to proliferate and outcompete other bacterial symbionts to dominant the microbiome. To investigate this hypothesis, we assembled the genome of an *Endozoicomonas* species associated with the reef-building coral *Pocillopora meandrina* from metagenomic samples collected in Mo'orea, French Polynesia and searched for genes involved in DMSP metabolism. Further, we collected all currently available *Endozoicomonas* genomes and conducted phylogenomic and pangenomic analyses on the genus to assess the functional contribution of this genus to holobiont dynamics and to infer possible contributions to coral resistance and resilience to stress.

4.3. Materials and Methods

4.3.1. Coral sampling, DNA extraction, library preparation, and sequencing

To assemble the genome of *Endozoicomonas* from *Pocillopora meandrina* corals in Mo'orea, French Polynesia, this study utilized samples from the *Tara* Pacific expedition that explored 32 islands across the entire Pacific over a period of 2.5 years from 2016 to 2018 (Planes et al., 2019). All coral sampling, DNA extraction and

quantification, library preparation, and sequencing methods were conducted as part and according to the *Tara* Pacific metagenomic pipeline. Briefly, nine colonies from three sites around the island of Mo'orea (17.5388° S, 149.8295° W, Supplementary Figure 4.1) were sampled by collecting a coral fragment with sterile bone cutters. On board, coral samples were preserved in DNA/RNA Shield™ (Zymo Research, Irvine, CA, USA) with Lysing Matrix A beads (MP Biomedicals, USA) in 15ml tubes and stored at -20°C. Once in lab, coral cells were homogenized by the high-speed benchtop homogenizer, the FastPrep-24™5G Instrument (MP Biomedicals, USA) which used the simultaneous multidirectional striking of the Lysis Matrix A beads. Coral DNA was purified using a commercial Quick-DNA/RNA Kit (Zymo Research, Irvine, CA, USA) supplemented by an enzymatic digestion step using a homemade enzymatic cocktail which optimizes lysis of prokaryotic cells of the microbiome present in low proportion in coral. DNA was then quantified using Qubit 2.0 Flurometer instrument with Qubit dsDNA BR (Broad range) and HS (High sensitivity) Assays (ThermoFisher Scientific, Waltham, MA). DNA was then sheared to a target mean size of 380 bp using a Covaris E210 instrument (Covaris, Inc., USA) and visualized on an Agilent Bioanalyzer DNA High Sensitivity chip. Fragments were end-repaired and 3'-adenylated, and then NEXTflex™ DNA barcoded adaptors (Bioo Scientific, Austin, TX, USA) were added by using NEBNext Ultra™ II DNA library preparation kit (New England Biolabs, Ipswich, MA, USA) for Illumina. After two consecutive 1x AMPure clean ups, the ligated products were PCR-amplified with NEBNext Ultra™ II Q5 Master Mix, followed by 0.8x AMPure XP purification. For

samples with >500ng of starting DNA, ligated products were instead amplified with Kapa Hifi HotStart NGS library Amplification kit (Kapa Biosystems, Wilmington, MA) followed by 0.6x AMPure XP purification. Libraries were sequenced on the Illumina HiSeq platform at the French National Sequencing Center, Genoscope, in Évry, France.

4.3.2. Metagenomic assembly, contig identification, and MAG refinement

In order to generate a metagenome-assembled genome (MAG), libraries underwent the following bioinformatic pipeline (Supplementary Figure 4.2). Paired end reads obtained from Illumina HiSeq were iteratively filtered using BBDuk v38.06 (sourceforge.net/projects/bbmap/) to remove Illumina adapters (k=23, mink=11) and PhiX Control (k=31) using normal mode. Next, reads were quality-trimmed to Q14, and reads containing more than one 'N', or with quality scores averaging less than 20 over the read length, or length under 45bp after trimming were discarded. Two assembly pipelines were used to obtain a co-assembly (i.e. reads from all samples assembled together) and multi-assembly (i.e. reads from each sample assembled individually). For co-assembly, quality-filtered paired end reads were merged using BBMerge v38.06 (sourceforge.net/projects/bbmap/) and a minimum overlap of 16. Merged reads, and forward and reverse reads that were not mergeable from each of the nine samples were co-assembled with MEGAHIT v1.1.1 (Li et al., 2015a). Multi-assembly was performed according to the Tara metagenomics pipeline. Briefly, quality-filtered paired end and singleton reads were normalized using BBNorm v38.06 with a target average depth of 40x and zero minimum depth. Forward and

reverse paired end reads and singletons from each sample were assembled individually with metaSPAdes v3.12 (Nurk et al., 2017). Next, targeted binning was then performed on contigs from all ten assemblies (nine multi- and one co-assembly). Coding sequences from the genomes of *E. acroporae* Acr-14, *E. acroporae* Acr-1, *E. acroporae* Acr-5, *E. elysicola* DSM 222380, *E. montiporae* LMG 24815, and *E. numazuensis* DSM 25634 were downloaded from the Pathosystems Resource Integration Center (PATRICBRC.org), concatenated, and used to build a blast database. Co-assembled and multi-assembled contigs containing *Endozoicomonas* genes were identified using blastn v2.11.0 (Altschul et al., 1990) with a maximum E-value cutoff of $1e^{-6}$. Assemblies were then evaluated for completion using CheckM v1.1.3 (Parks et al., 2015), and the single, co-assembly of *Endozoicomonas* contigs was further refined and used in downstream analysis.

Our co-assembled *Endozoicomonas* MAG was refined using the Anvi'o pipeline (Eren et al., 2015). Fasta headers of the blast-identified contigs were simplified using the simplify-fasta script from the Binsanity v0.4.4 (Graham et al., 2017) suite of tools. Input reads to the MEGAHIT assembly from each sample were then individually mapped to the blast-identified contigs using bowtie2 v2.4.1 (Langmead and Salzberg, 2012) to produce SAM files that were converted to BAM, sorted, and indexed with samtools v1.10 (Li et al., 2009). Blast-identified contigs and sample BAM files were then imported into Anvi'o v7 following the metagenomic workflow pipeline to refine the MAG (Eren et al., 2015). Briefly, a contigs database was generated using anvi-gen-contigs-database which uses Prodigal v2.6.3 (Hyatt et

al., 2010) to identify open reading frames and was decorated with hits from HMM models with anvi-run-hmms which uses HMMER v3.3.2 (Finn et al., 2011). Genes in the contig database were annotated with functions from the NCBI's Clusters of Orthologous Groups (Tatusov et al., 2000) using anvi-run-ncbi-cogs and from the EMBL-EBI's Pfam database (Mistry et al., 2021) using anvi-run-pfams. Single-copy core genes in the contig database were associated with taxonomy information using anvi-run-scg-taxonomy. Note, Anvi'o annotations were used solely for MAG refinement and not in downstream functional analyses. Sample-specific information about contigs was stored in profile databases by profiling each BAM file with anvi-profile. Anvi'o profiles were merged with the contig database using the anvi-merge command. Finally, anvi-interactive and anvi-refine were used to visualize and refine a single MAG based on taxonomic assignment and completion and redundancy estimates. Ribosomal RNA genes identified by the Anvi'o pipeline that were not in the final MAG were manually inspected for inclusion based on taxonomic annotation.

4.3.3. Annotation and identification of genomic characteristics of Endozoicomonas *genomes*

All available *Endozoicomonas* genomes (17) were downloaded from the NCBI genomes database (last accessed March 2021). Additionally, four *Endozoicomonas* genome assemblies from Neave et al. (2017a) were obtained from the author, and a putative *Endozoicomonas* species (MAG Plut_88861) assembled in Robbins et al. (2019) was obtained from http://refuge2020.reefgenomics.org (data accessibility in Supplementary Table 4.2). All genomes (22), including our MAG, were quality checked for completeness, contamination, and strain heterogeneity using

taxonomy_wf from CheckM v1.1.3 (Parks et al., 2015) with marker genes from all genomes within the bacterial order Oceanospirillales. Amino acid identity (AAI) among the genomes was calculated with CompareM (https://github.com/dparks1134/CompareM). Average nucleotide identity (ANI) between genomes was calculated with the pyANI metric (Pritchard et al., 2015) with blastn v2.10.1 for alignment. Several microbial gene annotation pipelines were employed for maximum annotation recovery. Gene prediction and annotation on all genomes used in this study was performed with Prodigal v2.6.3 (Hyatt et al., 2010) wrapped in Prokka v1.14.6 (Seemann, 2014) with default settings. KEGG Orthologs (Kanehisa et al., 2017) were assigned to Prokka-predicted genes using KofamKOALA (Aramaki et al., 2020) and BLAST+ against the KEGG GENES database with the BBH (bi-directional best hit) method on the KAAS server (Moriya et al., 2007). Output from KofamKOALA and KAAS were combined, duplicate KO identifiers were removed, and pathways were visualized with KEGG-decoder (Graham et al., 2018). Up-to-date high level functional categories at subsystem levels were obtained from rapid annotation using the subsystem technology (RAST) server and the RAST tool kit (Aziz et al., 2008; Brettin et al., 2015). Lastly, DRAM (Distilled and Refined Annotation of Metabolism) which is designed to facilitate the annotation of microbial and viral MAGs was run on the assemblies (Shaffer et al., 2020).

4.3.4. Comparative genomic analysis

In order to determine the phylogenetic relationships between gene sequences in our *Endozoicomonas* genome assemblies, we used OrthoFinder v2.5.2 (Emms and Kelly, 2015, 2019) to identify orthogroups common to all genomes, including the outgroup *Parendozoicomonas haliclonae* S-B4-1U^{T}. An orthogroup is a set of genes from multiple species that are descended from a single gene in the last common ancestor (LCA) of that set of species, compared to an ortholog which is a set of genes from a pair of species that are descended from a single gene in the LCA of the two species (Emms and Kelly, 2019). DNA sequences of single-copy orthologous genes (orthogroups with a single gene member) common to all genomes were used to generate a phylogenomic tree. The nucleotide sequences of each single-copy orthogroup from each *Endozoicomonas* genome were aligned using MAFFT v4.475 (Katoh and Standley, 2013). Genes were concatenated by genome, and a tree was constructed using IQ-TREE v2.1.2 (Minh et al., 2020) with 1000 bootstrap replicates using UFBoot2 (Hoang et al., 2018). Within IQ-TREE, ModelFinder (Kalyaanamoorthy et al., 2017) determined the most likely model was the general time reversible model with empirical base and codon frequencies, allowing for a proportion of invariable sites, and a discrete Gamma model with default four rate categories (GTR+F+I+G4). Tree visualization and rooting was completed using FigTree v1.4.4 (http://tree.bio.ed.ac.uk/software/figtree/).

OrthoFinder was run a second time with a subset of the genomes to identify unique and shared orthogroups between genomes we could confidently identify as *Endozoicomonas* based on ANI and phylogenomics. Orthogroups were plotted using

the R v3.6.1 package UpSetR v1.4.10 (Conway et al., 2017; R Core Team, 2019). Orthogroups of interest that were unique to our MAG were interrogated based on functional annotation from Prokka, KofamKOALA, and DRAM.

GraftM v0.13.1 (https://github.com/geronimp/graftM) was used to search the *Endozoicomonas* genomes for DMSP lyase (*ddd**, which included *dddD*, *dddL*, *dddK*, *dddP*, *dddQ*, *dddW*, and *dddY*), and DMSP demethylase (*dmdA*) gene sequences. GraftM uses gene packages made up of gene-specific HMMs constructed from full-length reference sequences to identify matches in an assembly. The gene-specific packages were previously generated in Robbins et al. (2019) and accessed from (https://data.ace.uq.edu.au/public/ graftm/7/).

4.4. Results and Discussion

4.4.1. Co-assembly of multiple samples recovers a nearly complete Endozoicomonas *genome*

Herein, I assembled the first *Endozoicomonas* MAG from a dominant reef-building coral on the island of Mo'orea, French Polynesia. Blastn and the interactive Anvi'o visualization interface were used to obtain an assembly of an *Endozoicomonas* genome with 94.6% completeness and low contamination from nine *Pocillopora meandrina* co-assembled metagenomes (Table 4.1, Supplementary Figure 4.3). Read counts for each step in the bioinformatic pipeline are reported in Supplementary Table 4.1. The MAG, referred to as *Endozoicomonas meandrina*, was assembled into 679 contigs with a total of 5.45 Mb, and Prokka predicted 4,191 genes (avg. length: 995 bp), including 4,121 coding sequences (CDS) and 62 tRNAs with a

gene density of 769 genes per Mb. Co-assembly of metagenomic reads from all nine samples in a single Megahit run recovered more of the *Endozoicomonas* genome than multi-assembly of individual samples. Individual assemblies recovered genomes ranging from 4.18 to 61.97% completeness and 0.95 to 6.28 % contamination as assessed by Oceanospirillales marker genes with CheckM (Supplementary Table 4.1). Co-assembly of multiple metagenome samples to generate a single set of contigs has recently been recommended, particularly through the Anvi'o pipeline, as an alternative to individual assembly. Proponents highlight this method as a way to attain higher read depths and greater genome recovery, to facilitate comparison across samples, and to improve binning of genomes through differential coverage. Hofmeyr et al. (2020) demonstrated that co-assembly enables the recovery of a larger genome fraction resulting in more complete genomes and lower error rates, particularly for low-abundance, rare genomes. However, individual assembly is considered superior at recovering more strain variation in abundant genomes. Neave et al. (2017) determined that two strains were present in the metagenome-assembled *Endozoicomonas* genome from the coral *P. verrucosa* in which ~65% of marker genes were present in two copies (CheckM contamination, Table 4.1) and ~64% of these copies were from the same organism (CheckM strain heterogeneity). However, the two strains were not able to be differentiated with binning. In fact, the differentiation of strains in heterogeneous populations with metagenomics is challenging, and strain heterogeneity can compromise genome assembly of a target population (Luo et al., 2012; Albertsen et al., 2013). Based on contamination levels

alone, multiple strains were not detected in our assembly of *E. meandrina*. Analysis of strain level variation among *Endozoicomonas* species in the *P. meandrina* corals sampled here is difficult given the low completion in the individually assembled genomes. The ability to differentiate strain-level variation from metagenomic datasets will be continually improved with corresponding improvements in sequencing read length and quality (Albertsen et al., 2013).

To conduct comparative genomics within the genus *Endozoicomonas*, all available genome assemblies (21) were downloaded from the NCBI taxonomy database, for which host, sampling location, and library source information were available (Table 4.1, Figure 4.1A). Two genomes were assembled from single-cell genomics, five from metagenomes, and all others from culture isolates. Fourteen of the assemblies were more complete than *E. meandrina* (>94.6%) and were all sequenced from cultured isolates. Generally, genomes assembled from metagenomic binning or single-cell genomics were shorter and less complete than our *E. meandrina* co-assembled MAG and genomes assembled from culture isolates. Genomes ranged in size from 2.3 Mbp (*E. humilis*) to 6.8 Mbp (*E.* SM1973). Several genomes assembled from metagenomic binning and single-cell genomics were relatively fragmented with up to 3,343 contigs in the assembly (*E. verrucosa*) and an N50 as low as 1,686 (*E. humilis*). Lower genome recovery for these genomes was attributed to limitations associated with these methodologies such as PCR amplification bias in single-cell genomics and strain differentiation and eukaryotic contamination in metagenomic binning (Neave et al., 2017a). Thus, the large range in genome sizes for

the species evaluated here are likely a product of methodology rather than biological variation. In contrast, several assemblies from culture isolates were able to assemble few, long scaffolds due to the inclusion of short Illumina reads and long Pacific Biosciences reads (*E. montiporae* CL33, 1 scaffold/3 contigs) or inclusion of paired-end and mate-pair Illumina libraries (*E. elysicola*, *E. numazuensis*, *E. montiporae* LMG 24815, and *E. ascidiicola* species). Given the difficulty in culturing *Endozoicomonas* from host tissues, culture-independent methods offer alternatives that can increase our understanding of the functional gene repertoire. The key to recovering complete genomes will be increasing read depth, perhaps through co-assembly, and utilization of long-read or mate-pair read technologies.

4.4.2. Endozoicomonas *species differentiate by host species*

Average ANI and AAI values among the *Endozoicomonas* species were ~75 and ~70%, respectively, which agrees with previous observations of high genomic diversity (Figure 4.1B&C) (Tandon et al., 2020). Species based on ANI relationships (>95%) were confirmed for strains of *E. acroporae*, *E. montiporae*, *E. arenosclerae*, and *E. ascidiicola* (Figure 4.1B). Interestingly, *Endozoicomonas* strains A and B from the same colony of the coral *Stylophora pistillata* had an ANI of 93% and did not meet the 95% ANI cut-off for putative species assignments (Jain et al., 2018), nor did *Endozoicomonas* strains from *Pocillopora verrucosa* and *P. meandrina* corals (88% ANI). Thus, ANI values suggest that coral-associated *E. meandrina* is a novel species. Further, *E. elysicola* from the sea slug *Elysia ornata* and *E. cretensis* from the Sharpsnout seabream *Diplodus puntazzo* had a relatively high ANI of 93%. The

Endozoicomonas genome from the coral *Porites lutea*, herein referred to as *E. lutea*, and *Endozoicomonas* sp. SM1973 from sediment had the lowest ANI to all other genomes with 71% and 70%, respectively, which was lower than the ANI of the outgroup, *Parendozoicomonas haliclonae* (not included in Figure 4.1B&C) to all other genomes (72%). Robbins et al. (2019) identified the 16S rRNA gene from *E. lutea* as family Endozoicomonadaceae with no genus assignment and inferred the taxonomic assignment of *Endozoicomonas* from a core gene phylogeny. The assembly *Endozoicomonas* spp. SM1973 from sediment was downloaded from NCBI with no corresponding publication. ANI values suggest that *E. lutea* and *Endozoicomonas* spp. SM1973 may be within the family Endozoicomonadaceae, but not within the genus *Endozoicomonas.* These data were congruent with a phylogenomic tree built from concatenated sequences of the computationally-determined single-copy orthologous genes (Figure 4.1D).

4.4.3. Endozoicomonas *species do not predictably differentiate by geography or host taxonomic group*

Single-copy orthogroup (n = 94)-based phylogenetic analysis reflected the host phylogeny in some cases, and also suggested high genomic divergence within the species of genus *Endozoicomonas* (Figure 4.1D). While *Endozoicomonas* genomes clustered tightly together based on host species, e.g. *Montiporae aequituberculata* or *Arenosclera brasiliensis*, genomes did not cluster based on host phylogeny as previously reported (Neave et al., 2017a). For instance, *Endozoicomonas* species from different coral genera are more phylogenetically similar to species from other marine invertebrates than to each other.

Endozoicomonas species from *P. meandrina*, *P. verrucosa*, and *S. pistillata* are an exception to this observation. Findings from a previous study profiling the 16S community of *P. verrucosa* and *S. pistillata* corals across their geographic range, may explain these observations (Neave et al., 2017b). *Endozoicomonas* was the dominant bacterial symbiont in both species, and *S. pistillata* harbored *Endozoicomonas* OTUs that were geographically specific, while *P. verrucosa* harbored the same *Endozoicomonas* OTUs across a large geographic region, spanning from the Red Sea to American Samoa. It was suggested that the high gene connectivity and long planktonic stage of *Pocillopora* species may account for the weaker geographic structuring (Pinzón et al., 2013; Neave et al., 2017b). These patterns in geographic structuring may explain why the *Endozoicomonas* species from *P. verrucosa* in the Red Sea was more similar to our recovered species from *P. meandrina* in Mo'orea, French Polynesia than to species from *S. pistillata* in the Red Sea (Figure 4.1). However, Neave et al. (2017b) found that for corals in the Red Sea, one *Endozoicomonas* OTU from *S. pistillata* was more similar to a lineage of *Endozoicomonas* OTUs from *P. verrucosa* than to other OTUs from *S. pistillata*. Thus, there may be some symbiont sharing between coral hosts within the Red Sea, and our data suggests that some *Endozoicomonas* genomes from the Red Sea are from the same lineage. This is in stark contrast to distantly related *Endozoicomonas* species from *Acropora* and *Montipora* corals from the same sampling location off the coast of Taiwan (Figure 4.1).

Phylogenomic relatedness between symbionts obtained from Red Sea corals does not include the species *Acropora humilis* which shares a clade and high ANI values with several marine sponge species (Figures 4.1). Like *P. verrucosa* and *S. pistillata*, *A. humilis* microbiomes in the Red Sea are dominated by *Endozoicomonas* and contained one *Endozoicomonas* OTU that clustered phylogenetically with an OTU from a Caribbean *Acropora* coral (Bayer et al., 2013). Thus, *E. humilis* may be phylogenetically related to other coral-associated *Endozoicomonas* species whose genomes have yet to be sequenced. For instance, healthy *Acropora cervicornis* samples in the Caribbean are associated with high abundances of *Endozoicomonas* sequences (Gignoux-Wolfsohn et al., 2017).

Interestingly, *E. cretensis* and *E. elysicola* from a fish and sea slug, respectively, were closely related with high ANI values (Figure 4.1). *Ca.* E. cretensis is a vertebrate pathogen that causes epitheliocystis in fish larvae and is undergoing genome erosion through the massive expansion of insertion sequences (IS elements) and pseudogene formation (Qi et al., 2018). This may be indicative of the process of genome reduction that occurs in symbionts or pathogens with long-term host-association (McCutcheon and Moran, 2012). Alternatively, *E. elysicola* has relatively low frequencies of IS and pseudogenes which is indicative of free-living organisms (Ding et al., 2016). In fact, *Endozoicomonas* 16S rRNA sequences with high similarity to host-associated *Endozoicomonas* sequences have been found in the surrounding seawater suggesting a this facultative symbiosis was initiated through horizontal transmission (Schreiber et al., 2016a). We identified 1,033 IS elements in

the *E. cretensis* genome compared to only seven in the *E. elysicola* genome. Similarly, our *E. meandrina* assembly had eight IS elements, while *E. atrinae* had the second most IS elements (395) after *E. cretensis*. Most genomes had between six and 125 IS elements with no apparent relationship with genome size (Supplementary Figure 4.4). Further evaluation of pseudogenes could help uncover the stage of symbiont genome erosion of *E. meandrina*.

4.4.4. Phylogenomics suggests cophylogeny among symbionts from Pocillopora *corals*

While coral-specific or sponge-specific symbionts do not cluster in obvious lineages, evolutionary patterns within host taxonomic group could account for phylogenomic relationships (Figure 4.1D). The *Endozoicomonas* bacterial lineage has been hypothesized to have coevolved with their coral hosts (Bayer et al., 2013). Pollock & McMinds et al. (2018) explored evidence for cophylogeny, i.e. the association of groups of related microbes with groups of related hosts, within the coral microbiome. They found that only a subset of coral-associated bacteria demonstrated an interaction between bacterial phylogeny and host phylogeny, which included *Endozoicomonas*-like bacteria found in coral tissues. One subclade of *Endozoicomonas* were deemed 'host specific' with statistical evidence suggesting their cophylogeny with various coral genera including *Stylophora*, *Pocillopora*, and *Acropora*, while cophylogenetic signals were weaker for more cosmopolitan 'host generalist' *Endozoicomonas* symbionts that were abundant across various coral genera including *Montipora* and *Porites*. Thus, our phylogeny presents convincing evidence that the bacterial lineage hosting *E. meandrina* and *E. verrucosa* from

Pocillopora corals demonstrates cophylogeny (Figure 4.1D). Further, the clade including *E. meandrina*, *E. verrucosa*, and *E. pistillata* through to *E. acroporae* may coincide with the 'host specific' clade defined in Pollock & McMinds et al. (2018) with a strong cophylogenetic signal, and *E. montiporae* and *E. lutea* may coincide with the 'host generalist' clade. Host-specific *Endozoicomonas* species from Pollock & McMinds et al. (2018) were more closely related to some marine invertebrates including mollusks and marine sponges than to the host-generalist group, which suggests the evolution of multiple novel associations between *Endozoicomonas* and corals and may account for the genomic divergence between coral-associated species (Figure 4.1).

4.4.5. Pangenomic analysis highlights the differentiation of genetic potential by host species

Due to the distinction of *P. lutea* and *Endozoicomonas* spp. SM1973 from other *Endozoicomonas* species in the phylogeny and their low ANI values, these species were removed from pangenome analyses as they may not represent true *Endozoicomonas* species. Further, the *E. humilis* assembly was particularly fragmented with an N50 of 1,686 and was also not included. From the Prokka gene prediction and annotation of all remaining species, between 3,140 and 6,166 genes were annotated per sample, and 93.4% of 86,252 gene sequences were identified as belonging to 11,195 orthogroups (Figure 4.2). A total of 554 orthogroups were shared by all genomes and 237 of these sequences were identified as single-copy. There were 513 orthogroups made up of 1,604 genes exclusive to a specific genome. *E. verrucosa* had the greatest number of genome-specific orthogroups (115), and *E. acroporae*

Acr-1 had no genome-specific orthogroups. Most shared orthogroups were specific to genomes from the same host organism. For instance, 754 orthologs were shared between *Endozoicomonas* strains isolated from the marine sponge *Arenosclera brasiliensis*. As with ANI and the phylogeny, shared orthologs reflect host species relationships rather than host taxonomic group, although *Endozoicomonas* species from marine sponges shared a relatively high number of orthogroups (71). No other host taxonomic group shared orthogroups.

4.4.6. E. meandrina-*specific genes are likely involved in the maintenance of stable symbiosis*

Genome-specific genes were estimated to determine functional features unique to *E. meandrina*. Approximately 39 orthogroups comprised of 136 genes were unique to *E. meandrina* which amounted to 3.3% of the species total gene count. Recovery of gene annotations varied between annotation pipelines (Table 4.2). All of the genome-specific genes were predicted as hypothetical proteins with Prokka and KEGG Orthology. Further annotation with DRAM uncovered functional annotations for eight of the *E. meandrina* genome-specific orthogroups. Annotations included ankyrin repeats, zinc-finger double domain, ring finger domain, anaphase-promoting complex subunit 4 (APC4) WD40 domain, and Yersinia/Haemophilus virulence surface antigen. EffectiveT3 also identified 52 of the 136 genes as being type III secretion system (T3SS) effector proteins. T3SSs are integral to the establishment of host-associations as they allow bacteria to transport protein into the cytoplasm of eukaryotic cells (Preston, 2007).

Genome-specific genes, including the T3SS effector proteins, provide evidence for symbiosis and bacterial-host interactions between *E. meandrina* and its coral host. Ankyrin repeats (ARPs) are predominantly found in eukaryotes, but are also found in microbial proteins and likely facilitate stable microbial association with a host through the secretion of ARP-containing proteins into eukaryotic host cells that mimic or modulate host intracellular processes (Al-Khodor et al., 2010). For instance, bacterial symbionts in marine sponges likely escape digestion by the host through the expression of ARPs (Nguyen et al., 2014). Further, Ding et al. (2016) identified ARPs in both *E. elysicola* and *E. numazuensis*, but not *E. montiporae* CL33. In addition to the 14 genome-specific ARPs, 0.96% of protein coding genes in *E. meandrina* contain ARPs which is well above the 0.2% conservative threshold that is a hallmark of host-associated microorganisms (Jernigan and Bordenstein, 2014; Robbins et al., 2019). Other annotated genome-specific genes also encode for eukaryotic-like domains. Zinc-finger domains were originally discovered in eukaryotic transcription factors but also appear to regulate virulence and symbiosis gene transcription in the plant bacterial pathogens *Agrobacterium tumefaciens* and *Rhizobium etli*, respectively (Close et al., 1987; Bittinger et al., 1997; Malgieri et al., 2015). The ring finger domain is a type of zinc-finger domain with cognates in the eukaryotic ubiquitin system which involves the covalent modification of proteins (Burroughs et al., 2011; Callis, 2014). ACP4, which includes a WD40 domain in *E. meandrina*, is a ubiquitin-protein ligase complex in eukaryotes involved in the regulation of the cell cycle transitions and has yet to be characterized in bacteria (Alfieri et al., 2017). In fact,

WD40 domains are rarely encoded in bacterial genomes, however, proteins containing WD40 domains were found in sponge-associated *Poribacteria* and Crenarchaeota and have been shown to be involved in the bacterial infection process of plant root hairs (Hallam et al., 2006; Yano et al., 2009; Kamke et al., 2014). Further, ARPs and WD40 domains were enriched in bacterial MAGs associated with the coral *Porites lutea* compared to seawater-associated MAGs (Robbins et al., 2019). Lastly, surface antigens are generated by bacteria such as *Yersinia* and *Haemophilus* species to promote virulence in host cells through attachment, invasion, and evasion of host immune responses (Munson, 1990; Pettersson et al., 1999; Liu, 2015). The annotation of a virulence surface antigen in the set of genome-specific genes may present one mechanism by which *E. meandrina* can establish within the cells of its host. Thus, *E. meandrina* annotations provide further evidence for the presence of eukaryotic-like protein domains in bacteria associated with marine invertebrates which may strengthen the hypothesis that these domains are involved in the formation or maintenance of bacterial-eukaryotic symbiosis, be they commensal, mutualistic, or pathogenic.

4.4.7. Endozoicomonas *species have no discernible genetic advantage in the response to thermal stress*

Our previous work on coral-associated *Endozoicomonas* species in Mo'orea, French Polynesia shows that these populations can have low resistance and high resilience to thermal stress. During periods of peak seawater temperatures, the proportion of *Endozoicomonas* sequences in the coral microbiome decreased drastically, while relative abundances recovered even more drastically once the

thermal stress was eliminated (Maher et al., 2020). To test whether the spike in *Endozoicomonas* sequences after the recovery period resulted from the symbiont's ability to utilize a host metabolic product of thermal stress, DMSP, we searched for DMSP lyases involved in the DMSP to DMS cleavage pathway in the *Endozoicomonas* genomes (Supplementary Figure 4.5). The program GraftM correctly identified the lyase *dddD* in all three strains of *E. acroporae* with an E-value of $1.1e^{-174}$ as in Tandon et al. (2020). Additionally, the DMSP lyase *dddY* was identified in the *E. pistillata* B genome with an E-value of $4.4e^{-187}$. This gene corresponded to an *E. pistillata* B-specific singly copy orthogroup in the pangenomic analysis. GraftM allowed for the identification of this gene, whereas a previous annotation of this genome with RASTtk found no genes involved in the breakdown of DMSP (Neave et al., 2017a). Besides GraftM, the *dddY* gene was not identified by any other annotation methods used here. No other *Endozoicomonas* genome contained genes involved in DMSP metabolism. This is unexpected given that the *E. acroporae* 16S gene was found in microbiome profiles from *A. humilis* in the Great Barrier Reef and *P. verrucosa* in the Red Sea (Tandon et al., 2020). While the genomic capability to metabolize DMSP has thus been found in only four strains of *Endozoicomonas* species, further genome sequencing of different strains may uncover more. *Endozoicomonas* species from *Acropora* corals in Mo'orea should be especially targeted for genome sequencing as sequences from this host had the most striking proliferation after recovery from thermal stress (Maher et al., 2020). Additionally, *E. meandrina* should be cultured to verify the inability to metabolize

DMSP *in vivo*, as there may be lyase genes in the genome that are not yet characterized. Further, DMSP lyases have been identified in other bacteria commonly found in corals including Rhodobacterales, Pseudomonadales, and *Roseobacter* species (Tandon et al., 2020; Raina et al., 2009). Future work could investigate if the uptake and degradation of DMSP by these species can contribute to the availability of organic carbon to other non-DMSP degrading members of the microbiome, such as *E. meandrina*.

We used the stress response subsystems in RAST to evaluate any genetic potential for thermal stress tolerance in *Endozoicomonas* species. The RASTtk pipeline annotated 2,192 of 5,878 genes of CDS in the *E. meandrina* genome (Table 4.2), 864 of which were assigned to a subsystem. RAST annotation revealed the involvement of 49 genes in stress responses, including one in osmotic stress, 28 in oxidative stress, 11 in detoxification, 13 in general stress response, and 5 in the periplasmic stress response. While gene counts in the different stress categories varied between the *Endozoicomonas* species, all genomes had the most stress response genes involved in oxidative stress (Supplementary Figure 4.6).

Aerobic bacteria have developed mechanisms to effectively scavenge endogenous reactive oxygen species (ROS) and ROS from their environment (Imlay, 2019). Several of these mechanisms involved in defense against ROS were identified in *E. meandrina* under the oxidative stress subsystem including the enzyme superoxide dismutase, and the antioxidants thioredoxin peroxidase and glutathione. Heat- or light-induced overproduction of reactive oxygen species by the coral

endosymbiont and toxic accumulation of ROS in host tissues may play a central role in coral bleaching (Weis, 2008; Nielsen et al., 2018). Thus, antioxidant activity in *Endozoicomonas* species may be directed to reducing ROS in the holobiont, however, further screening to determine the proportion of antioxidant activity in *Endozoicomonas* species directed towards endogenously versus exogenously produced ROS is required. Additionally, both corals and their algal symbionts produce DMSP, and DMSP production is upregulated in corals experiencing oxidative stress (Raina et al., 2013). DMSP and its lysis and oxidation products, including DMS and DMSO, make up a highly effective antioxidant system (Supplementary Figure 4.5) (Sunda et al., 2002). While *E. meandrina* lacks the genetic capability to cleave DMSP to DMS, it does encode a DMSO reductase which converts DMSO to DMS that could facilitate the recycling or regeneration of the DMSP antioxidant system in the coral holobiont during thermal stress (Robbins et al., 2019).

4.4.8. Endozoicomonas *species may contribute essential nutrients to their hosts*

To assess the contribution of *Endozoicomonas* species to nutrient cycling within their hosts, DRAM annotations of metabolic pathways were explored (Figure 4.3A). While genes encoding enzymes involved in carbon fixation such as ribulose bisphosphate carboxykinase (Rubisco) and pathways including the Calvin-Benson-Bassham (CBB) cycle, the reverse tricarboxylic acid (rTCA), and hydroxypropionate/hydroxybutyrate pathway have been found in the genomes of bacteria associated with hosts such as corals (Kimes et al., 2010; Robbins et al.,

2019), *Endozoicomonas* species do not appear to be significant contributors of carbon to their hosts (Supplementary Figure 4.7). However, *Endozoicomonas* species possess a variety of genes for the utilization of various forms of carbon (carbohydrate active enzymes, Figure 4.3A). All genomes have the capability to degrade chitin, and most genomes have the capability to degrade arabinose. Chitin is the most abundant polysaccharide in the marine environment, and while chitin degradation is a ubiquitous process in the ocean, only a small fraction of marine host-associated bacteria have chitinolytic abilities (Souza et al., 2011; Raimundo et al., 2021). However, Gammaproteobacteria in octocorals have higher proportions of chitinase sequences and a MAG identified as the family Endozoicomonadaceae possessed chitinase genes (Raimundo et al., 2021). Given the differential capacities to process chitin among marine host-associated microbes, *Endozoicomonas* species may contribute to inter-species substrate cross-feeding through the degradation of chitin and thereby influence turnover of organic carbon and nitrogen within the holobiont (Raimundo et al., 2021). Beyond these capabilities, *Endozoicomonas* species are not major contributors to nitrogen-cycling or sulfur-cycling within their hosts (Figure 4.3A). Within nitrogen metabolism, *E.* OPT23 and *E.* SM1973 genomes each possess a functional pathway within nitrification, aerobic ammonia oxidation and nitrite reduction, respectively. Various genomes, excluding *E. meandrina* have functional pathways within denitrification including nitrate reduction to nitrite, nitrite reduction to nitric oxide, and nitric oxide reduction to nitrous oxide. There is no functional capacity for nitrogen fixation within the *Endozoicomonas* genus. Notably, several

coral-associated genomes, *E. meandrina*, *E. humilis*, *E. pistillata* A, *E. lutea*, and *E. verrucosa*, possess no functional pathways in nitrogen metabolism. Within sulfur metabolism, only *E. arenosclerae* species and *E. numazuensis*, both associated with marine sponges, have the capacity to oxidize thiosulfate to sulfate.

Animals lack the metabolic pathways to produce many nutritional compounds including B vitamins and many amino acids that are essential to meet their metabolic needs (Payne and Loomis, 2006; Moran, 2007). Just as bacterial symbionts or pathogens undergo genome erosion and depend on host metabolic capabilities, so too can hosts depend on their symbionts for supplementation (McCutcheon and Moran, 2012). In fact, many symbioses arose *de novo*, as opposed to having coevolved, due to the mutual advantages of differing sets of metabolic capabilities which are reflected in different gene contents of genomes (Moran, 2007). *Endozoicomonas* genomes possess genes involved in the metabolic pathways for a diversity of amino acids and B vitamins, although completion of these pathways varies (Figure 4.3B). KEGG annotation of the *E. meandrina* genome revealed complete or nearly complete pathways for the metabolism of thiamine (B_1), riboflavin (B_2), and biotin (B_7). *E. meandrina* may supplement its coral host with B vitamins as the prokaryotic microbiome is the only member of the coral holobiont capable of producing these essential nutrients (Robbins et al., 2019). In contrast, both bacterial symbionts and algal endosymbionts of corals can supplement the host with amino acids (Shinzato et al., 2011; Robbins et al., 2019). Several coral-associated species, including *E. meandrina*, *E. verrucosa*, and *E. pistillata* A and B, had notably fewer complete

pathways for the biosynthesis of amino acids than the rest of the species (Figure 4.3B). Thus, the algal symbiont may supply more of the host-required amino acids in those holobionts. Genome assembly of *P. meandrina* and the dominant Symbiodiniaceae species would help clarify the functional contributions of each member of the holobiont.

4.4.9. Conclusions

In a previous study (Maher et al., 2020), we showed with 16S amplicon sequencing that *Endozoicomonas* sequences decreased in relative abundance with a mild thermal stress event and recovered after alleviation of the thermal stress to abundances that were higher than the pre-stress community. Our hypothesis that the *Endozoicomonas* species used DMSP produced by the stressed coral host as a carbon source to proliferate and dominate the community with the coral *P. meandrina* was incorrect as our MAG does not encode for a DMSP lyase gene. Further, we did not uncover any genetic capabilities that would facilitate resilience of *Endozoicomonas* within a recovering coral host. Instead, *Endozoicomonas* species may simply proliferate to occupy open niche space left by opportunistic taxa such as *Vibrio* that decrease or disappear from the community when the holobiont is no longer in a stressed state (Bourne et al., 2016). Further, *Endozoicomonas* species may be able to proliferate to higher abundances and outcompete other taxa associated with healthy corals, such as *Candidatus Amoebophilus*, due to genomic features that promote colonization and persistence with a eukaryotic host and/or due to cophylogeny with

their hosts that facilitates stable symbiotic relationships across extended evolutionary time (Ding et al., 2016; Pollock et al., 2018).

In a comparative genomic analysis of all available *Endozoicomonas* genomes, we found that *Endozoicomonas* species do not predictably differentiate by host taxonomic group or geography. For instance, *Endozoicomonas* species from corals do not group together phylogenetically, nor do they share a specific set of orthogroups. Instead, we found evidence for cophylogeny between the *Pocillopora*, *Stylophora*, and *Acropora* coral hosts included in this study and their *Endozoicomonas* lineages. Upon closer functional annotation of our MAG, *E. meandrina*, we found that the symbiont has specific genomic features which include eukaryotic-like domains that may facilitate the maintenance of a stable symbiosis with its coral host. Further, there were no obvious genetic capabilities that suggest tolerance to thermal stress or that would explain the patterns we saw in 16S communities from a previous study (Maher et al., 2020). However, they do encode some antioxidant capabilities that while commonplace in aerobic bacteria, could be utilized in the holobiont response to oxidative stress.

4.5. Funding

This work was funded by the Ford Foundation Dissertation Fellowship to RLM.

4.6. Acknowledgements

I would like to thank the *Tara* Pacific Consortium for sample acquisition. I would also like to thank Dr. Lydia Baker, Dr. Kalia Bistolas, and Dr. Stephanie Rosales for assistance in data analysis.

4.7. Data availability statement

Metagenomic samples from Mo'orea, French Polynesia will be made available by the *Tara* Pacific Consortium at their discretion.

4.8. Tables

Table 4.1. Source data and genome assembly quality information for *Endozoicomonas* genomes.

Genome	Source	Host species	Comp (%)	Cont (%)	Assembly size (bp)	GC (%)	N50	Genes
Endozoicomonas numazuensis DSM 25634	Marine sponge	*Haliclona* sp.	100.0	2.06	6,342,227	0.47	917,146	5,466
Endozoicomonas sp. OPT23	Sponge	*Ophlitaspongia papilla*	100.0	2.55	4,938,102	0.47	737,835	4,175
Endozoicomonas elysicola DSM 22380	Sea slug	*Elysia ornata*	99.8	2.75	5,606,375	0.47	5,569,560	4,653
Endozoicomonas acroporae Acr-1	Coral	*Acropora* sp.	99.7	1.61	6,024,033	0.49	56,565	5,062
Endozoicomonas acroporae Acr-5	Coral	*Acropora* sp.	99.7	1.61	6,034,674	0.49	58,040	5,096
Endozoicomonas montiporae CL-33	Coral	*Montipora aequituberculata*	99.7	3.42	5,430,256	0.48	5,430,256	4,935
Endozoicomonas montiporae LMG24815	Coral	*Montipora aequituberculata*	99.7	3.42	5,602,297	0.48	1,015,541	5,070
Endozoicomonas atrinae WP70	Comb pen shell	*Atrina pectinata*	99.6	4.5	6,687,418	0.48	21,158	6,166
Endozoicomonas arenosclerae AB112	Marine sponge	*Arenosclera brasiliensis*	99.5	3.69	6,453,554	0.48	44,889	5,571
Endozoicomonas sp. SM1973	Sediment		99.5	2.04	6,824,910	0.40	101,917	5,961
Endozoicomonas ascidiicola AVMART05	Sea squirt	*Ascidiella sp.*	99.3	1.16	6,130,497	0.47	771,815	5,282
Endozoicomonas acroporae Acr-14	Coral	*Acropora* sp.	99.2	0.95	6,048,850	0.49	47,658	5,014
Endozoicomonas ascidiicola KASP37	Sea squirt	*Ascidiella scabra*	98.9	1.35	6,512,467	0.47	675,874	5,629
Ca. Endozoicomonas cretensis	Fish	*Diplodus puntazzo*	98.3	4.77	5,876,352	0.47	19,256	5,293
Endozoicomonas meandrina[*]	Coral	*Pocillopora meandrina*	94.6	3.85	5,450,934	0.51	13,235	4,121
Endozoicomonas sp. strain AB1[*]	Bryozoan	*Bugula neritina*	94.3	11.24	4,049,356	0.45	20,804	3,483
Endozoicomonas verrucosa[*]	Coral	*Pocillopora verrucosa*	89.8	65.06	5,277,290	0.54	2,052	5,019
Endozoicomonas arenosclerae E-MC227	Marine sponge	*Arenosclera brasiliensis*	87.1	7.31	6,216,773	0.47	4,718	5,874
Endozoicomonas humilis[*]	Coral	*Acropora humilis*	81.3	4.14	2,304,083	0.49	1,686	2,262
Endozoicomonas lutea[*]	Coral	*Porites lutea*	81.2	2.75	3,336,747	0.48	3,629	2,982
Endozoicomonas pistillata (Type B)[**]	Coral	*Stylophora pistillata*	75.6	3.48	3,535,298	0.51	17,786	3,140
Endozoicomonas pistillata (Type A)[**]	Coral	*Stylophora pistillata*	60.0	2.69	3,788,925	0.50	9,041	3,342

[*]Assembly from metagenomic sequencing reads.
[**]Assembly from single-cell genomics.

Table 4.2. Recovery of microbial gene annotations using various annotation tools.

Tool	Predicted genes	Annotated genes	% annotated
Prokka	4,121	1,665	40.4
RASTtk	5,878	2,192	37.3
KEGG Orthology	4,121	2,080	50.5
DRAM	4,034	2,682	66.5

4.9. Figures

Figure 4.1. Genomic and phylogenetic summary of available *Endozoicomonas* genomes. A) Source location for each sample, B) average nucleotide identity (ANI), and C) average amino acid identity (AAI). D) Organization of *Endozoicomonas* genomes based on phylogenomics using 94 single copy orthologs generated with OrthoFinder. Rooting was based on comparison to a previously published phylogeny (Tandon et al. 2020) and Parendozoicomonas haliclonae S-B4-IU was used as the outgroup. Genomes are colored by source material and letters correspond to the location the sample was obtained from on the map (A).

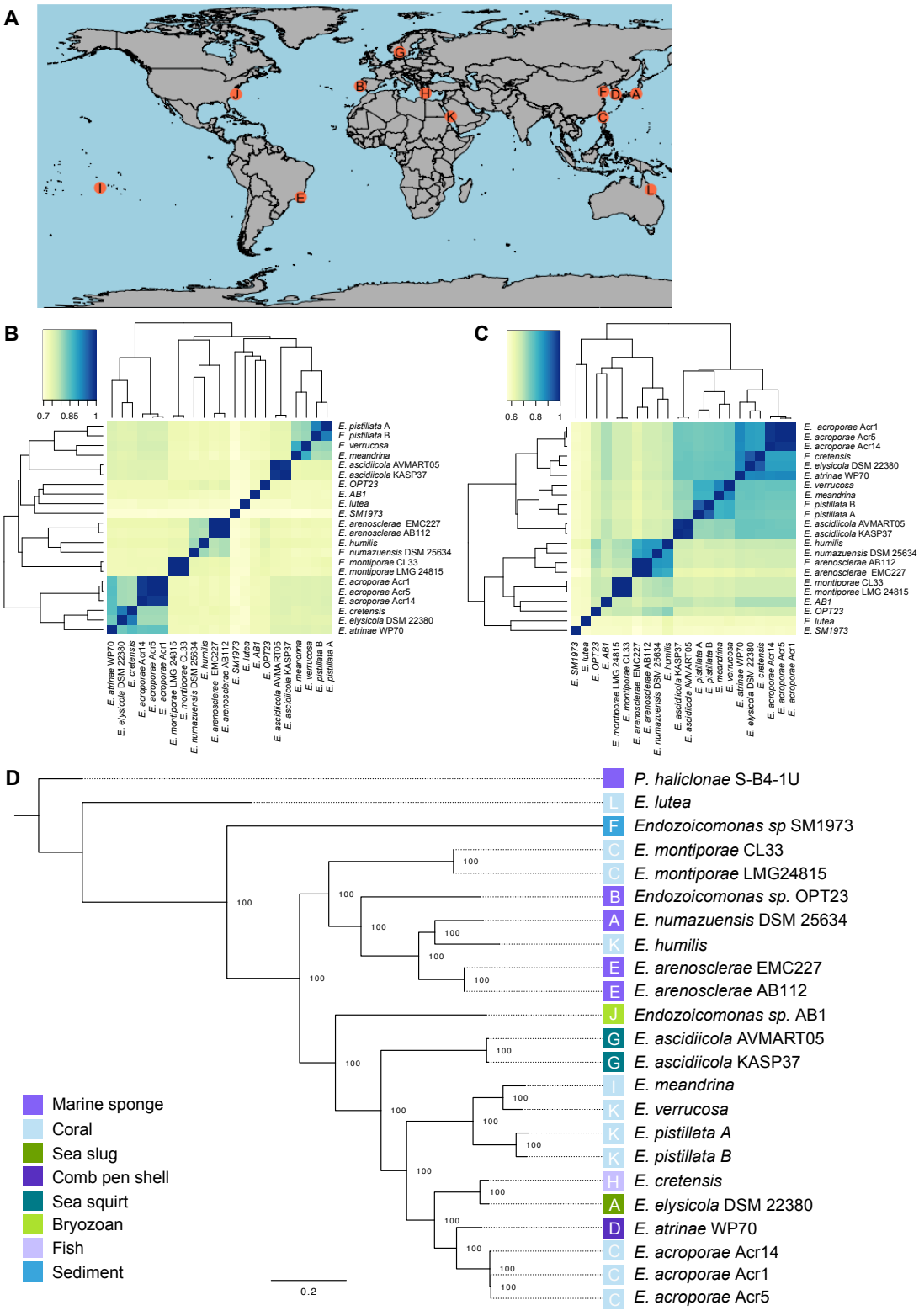
A
G
B
H
J
F
D
A
K
C
I
E
L
B
0.7
0.85
1
E. pistillata A
E. pistillata B
E. verrucosa
E. meandrina
E. ascidiicola AVMART05
E. ascidiicola KASP37
E. OPT23
E. AB1
E. lutea
E. SM1973
E. arenosclerae EMC227
E. arenosclerae AB112
E. humilis
E. numazuensis DSM 25634
E. montiporae CL33
E. montiporae LMG 24815
E. acroporae Acr1
E. acroporae Acr5
E. acroporae Acr14
E. cretensis
E. elysicola DSM 22380
E. atrinae WP70
C
0.6
0.8
1
E. acroporae Acr1
E. acroporae Acr5
E. acroporae Acr14
E. cretensis
E. elysicola DSM 22380
E. atrinae WP70
E. verrucosa
E. meandrina
E. pistillata B
E. pistillata A
E. ascidiicola AVMART05
E. ascidiicola KASP37
E. humilis
E. numazuensis DSM 25634
E. arenosclerae AB112
E. arenosclerae EMC227
E. montiporae CL33
E. montiporae LMG 24815
E. AB1
E. OPT23
E. lutea
E. SM1973
D
P. haliclonae S-B4-1U
E. lutea
Endozoicomonas sp SM1973
E. montiporae CL33
E. montiporae LMG24815
Endozoicomonas sp. OPT23
E. numazuensis DSM 25634
E. humilis
E. arenosclerae EMC227
E. arenosclerae AB112
Endozoicomonas sp. AB1
E. ascidiicola AVMART05
E. ascidiicola KASP37
E. meandrina
E. verrucosa
E. pistillata A
E. pistillata B
E. cretensis
E. elysicola DSM 22380
E. atrinae WP70
E. acroporae Acr14
E. acroporae Acr1
E. acroporae Acr5
100
0.2
Marine sponge
Coral
Sea slug
Comb pen shell
Sea squirt
Bryozoan
Fish
Sediment

Figure 4.1.

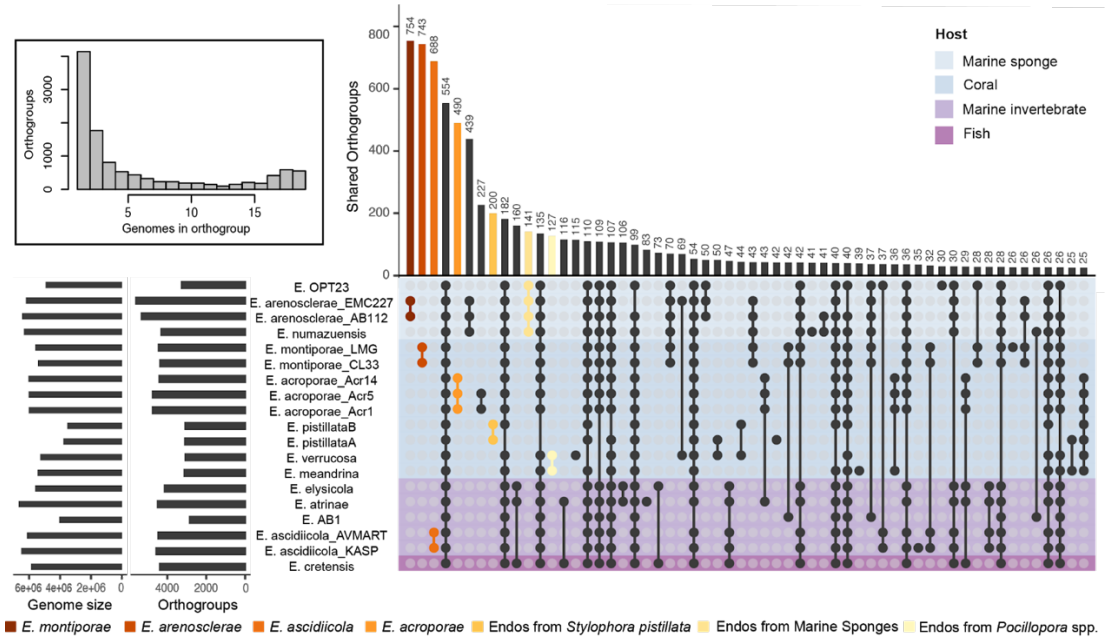

Figure 4.2. The number of orthologous genes in *Endozoicomonas* genome assemblies identified with OrthoFinder. Genome assemblies are grouped by host taxonomic group: Marine Sponge, Coral, Marine Invertebrate, Fish. Queries 1-6 represent orthologs shared between *Endozoicomonas* strains from the same species. Query 7 represents orthologs shared in all *Endozoicomonas* genomes from marine sponges. Only the top 58 sets of shared orthogroups are displayed.

Figure 4.3. Summary of metabolic capabilities for *Endozoicomonas* species. A) Presence/absence of functions involved in carbon utilization (carbohydrate active enzymes; CAZy), nitrogen metabolism, and sulfur metabolism based on DRAM annotations. B) Percent completion for pathways involved in transport and biosynthesis of vitamins and amino acids based on KEGG Orthology.

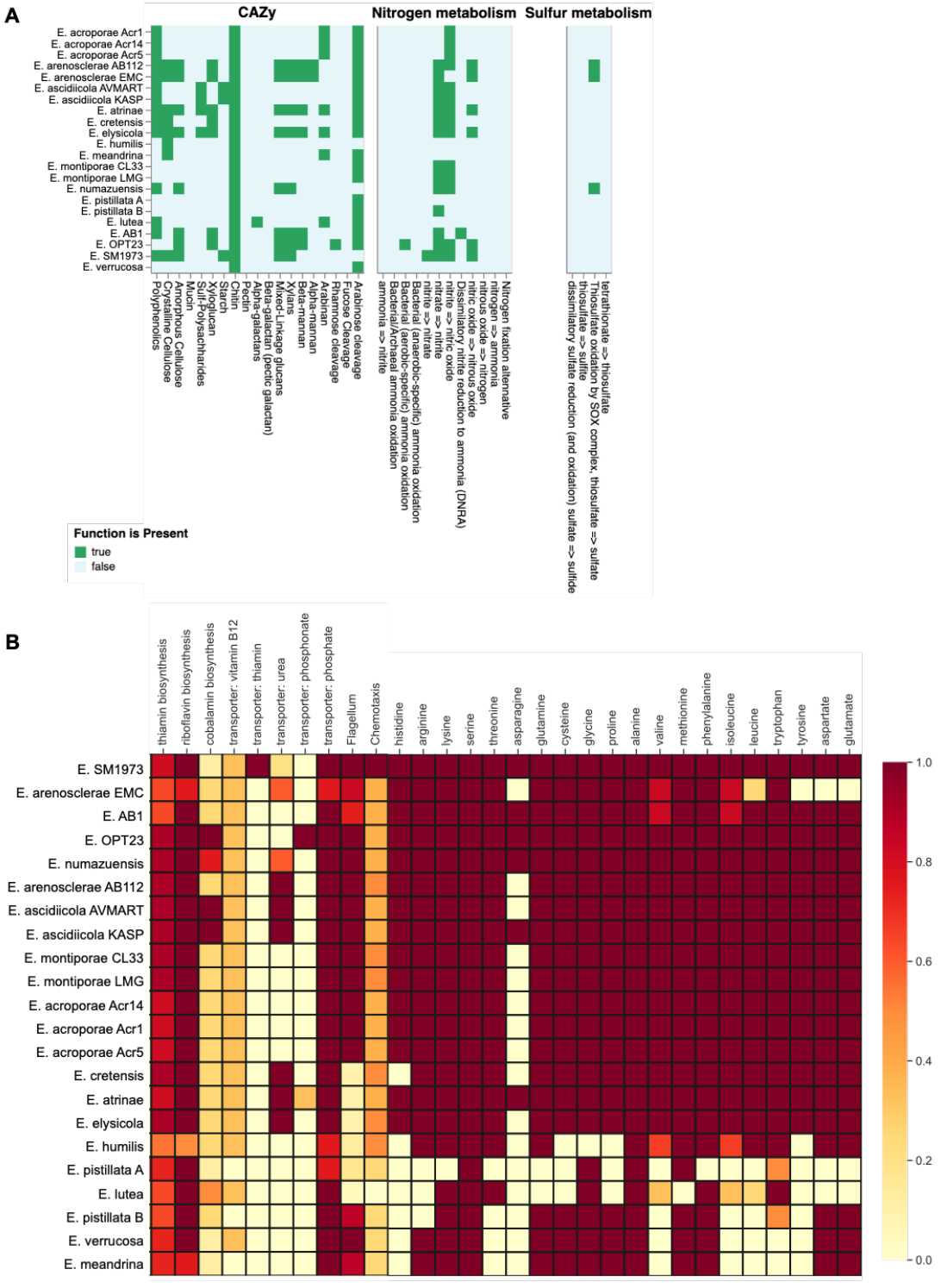
A
CAZy
Nitrogen metabolism
Sulfur metabolism
E. acroporae Acr1
E. acroporae Acr14
E. acroporae Acr5
E. arenosclerae AB112
E. arenosclerae EMC
E. ascidiicola AVMART
E. ascidiicola KASP
E. atrinae
E. cretensis
E. elysicola
E. humilis
E. meandrina
E. montiporae CL33
E. montiporae LMG
E. numazuensis
E. pistillata A
E. pistillata B
E. lutea
E. AB1
E. OPT23
E. SM1973
E. verrucosa
Polyphenolics
Crystaline Cellulose
Amorphous Cellulose
Mucin
Sulf-Polysaccharides
Xyloglucan
Starch
Chitin
Pectin
Alpha-galactans
Beta-galactan (pectic galactan)
Mixed-Linkage glucans
Xylans
Beta-mannan
Alpha-mannan
Rhamnose cleavage
Fucose Cleavage
Arabinose cleavage
Bacterial/Archaeal ammonia oxidation
ammonia => nitrite
Bacterial (aerobic-specific) ammonia oxidation
Bacterial (anaerobic-specific) ammonia oxidation
nitrite => nitrate
nitrate => nitrite
nitrite => nitric oxide
Dissimilatory nitrite reduction to ammonia (DNRA)
nitric oxide => nitrous oxide
nitrous oxide => nitrogen
nitrogen => ammonia
Nitrogen fixation alternative
dissimilatory sulfate reduction (and oxidation) sulfate => sulfide
thiosulfate => sulfite
Thiosulfate oxidation by SOX complex, thiosulfate => sulfate
tetrathionate => thiosulfate
Function is Present
true
false
B
thiamin biosynthesis
riboflavin biosynthesis
cobalamin biosynthesis
transporter: vitamin B12
transporter: thiamin
transporter: urea
transporter: phosphonate
transporter: phosphate
Flagellum
Chemotaxis
histidine
arginine
lysine
serine
threonine
asparagine
glutamine
cysteine
glycine
proline
alanine
valine
methionine
phenylalanine
isoleucine
leucine
tryptophan
tyrosine
aspartate
glutamate
E. SM1973
E. arenosclerae EMC
E. AB1
E. OPT23
E. numazuensis
E. arenosclerae AB112
E. ascidiicola AVMART
E. ascidiicola KASP
E. montiporae CL33
E. montiporae LMG
E. acroporae Acr14
E. acroporae Acr1
E. acroporae Acr5
E. cretensis
E. atrinae
E. elysicola
E. humilis
E. pistillata A
E. lutea
E. pistillata B
E. verrucosa
E. meandrina
1.0
0.8
0.6
0.4
0.2
0.0

Figure 4.3.

CHAPTER 5 GENERAL CONCLUSION

5.1. Summary of Research

In the chapters and appendices of this dissertation, I have explored the structure and dynamics of bacterial communities associated with apparently healthy and stressed coral hosts and focused investigations into the role of a specific dominant bacterial taxon within these communities. My dissertation focused on describing the individual and combined effects of major environmental stressors on coral reefs. In an effort to generalize my results, I utilize experimental simulation of stress and a natural stress event on three dominant genera of reef-building corals in Mo'orea, French Polynesia: *Pocillopora*, *Porites*, and *Acropora,* all of which I found to be dominated by a proposed bacterial symbiont in the genus *Endozoicomonas*. Given the predominance of *Endozoicomonas* in these Mo'orean corals, I then utilized -omics technologies to uncover the functional contribution of this species to the coral holobiont during environmental disturbances.

In this dissertation I have shown that local stressors of nitrate or ammonium enrichment and simulated coral predation do not act synergistically to compound the effect of global seawater temperature increases (**Chapter 2**). I found further evidence that nitrate and urea loading do not exacerbate microbiome dysbiosis that results from a natural thermal anomaly across coral genera of varying degrees of stress tolerance (**Chapter 3**). In both studies, I show how the dominant microbiome member, *Endozoicomonas*, drives patterns in community dissimilarity, variability, and composition under stress. Further, differential abundance analyses highlight how

stress can be characterized by a reduction in *Endozoicomonas* and/or a proliferation of potential opportunistic pathogens. Finally, I explore the functional potential of *Endozoicomonas* species from a Mo'orean coral and from a diversity of marine hosts through orthologous clustering of the protein sequences from assembled *Endozoicomonas* genomes (**Chapter 4**).

5.2. Overarching Research Aims

This dissertation work addresses four overarching research aims that are particularly urgent and relevant given the global degradation of coral reefs. First, I sought to thoroughly describe the response of the coral microbiome to stress (**Aim 1**). The 'stress' applied in my experiments was designed to simulate the major environmental threats prioritized in coral reef conservation literature, namely high sea surface temperatures and nutrient pollution. Second, I aimed to expand the microbiome stress literature by characterizing the interaction between multiple stressors (**Aim 2**). While I initially employed theory and developed hypotheses that did not differentiate between different types of stressors, in Chapter 2 I discovered that thermal stress was not only the most impactful, but also the most ecologically relevant stress facing corals and their microbiomes. Therefore, I modified my hypothesis in Chapter 3 to differentiate between stressors with the specific aim of evaluating whether nutrient stress exacerbates thermal stress. This hypothesis is particularly relevant to the current state of coral reefs given that any local management of environmental disturbance cannot alleviate the global threat of climate change. Third, I sought to evaluate the resistance and resilience of the coral

microbiome to stress (**Aim 3**). This was accomplished by employing timeseries sampling in Chapter 3 that captured both the stress exposure and a recovery period. And lastly, I aimed to characterize the role of the dominant bacterial taxon *Endozoicomonas* in both the coral microbiome itself, and the microbiome's response to stress (**Aim 4**). In characterizing the microbiome stress response and evaluating resistance and resilience to multiple stressors, I became intrigued by the contribution of this bacterial symbiont to the patterns in community composition that I observed in Aims 1-4 and to the overall functioning of the coral holobiont. Therefore, I evaluated the functional potential of a coral-associated *Endozoicomonas* genome and paid special attention to genes involved in the establishment of symbiosis and stress response.

5.2.1. Coral microbiome diversity and variability increases with stress

My results from Aim 1 largely clarify many of the patterns previously observed in the coral microbiome stress literature. Contrary to macroecological communities which commonly experience a loss in biodiversity with stress (Vinebrooke et al., 2004), the coral microbiomes evaluated here generally increased in species richness and evenness with stress. Stressed microbiomes were often more dissimilar and more variable than control microbiomes. Further, compositional changes were driven by the introduction or proliferation of opportunists within the community and by the corresponding decrease in the relative proportion of *Endozoicomonas*. Based on the work presented here and various studies I contributed to during my dissertation work (Ezzat et al., 2019b, 2020; Rice et al., 2019; Klinges et

al., 2020), I consider these trends to be the predominant response of the coral microbiome to stress, however, there is considerable variation in these responses. For instance, stress may cause community evenness to shift, while species richness remains constant (Maher et al., 2019). Stressed communities may become more variable than controls, but still not appear compositionally distinct from controls (Zaneveld et al., 2016). In some cases, stress may even cause communities to be less variable than controls (Ezzat et al., 2019b). Overall, these patterns may vary depending on the type or duration of stress applied which is understandable given that various stressors limit the response of bacteria in different ways. For instance, the addition of a limiting nutrient such as nitrate may result in the incremental increase in abundance of certain taxa that can utilize this resource, while rises in seawater temperature may surpass a threshold in which certain taxa cannot survive and disappear altogether from the community.

5.2.2. Multiple stressors do not interact synergistically with the dominant stress of high temperature

Fulfilling Aim 2, this dissertation demonstrates that the specific stressors of simulated predation and enrichment of nitrogen in various forms (i.e. nitrate, ammonium, and urea) do not act synergistically with thermal stress to induce dysbiosis in the coral microbiome. In Chapter 2, I showed an antagonistic response in which the combined effect of thermal stress and simulated predation was less than expected by the sum of the two individual responses for several metrics of alpha and beta diversity. Interestingly, simulated predation alone had an equal effect as high temperature alone on microbiome dysbiosis. The strong effects of simulated predation

should be considered in the context of coral reef ecology. Predation is highly localized on a coral colony, and evidence suggests that microbial community changes are largely restricted to the site of the wound (Clements et al., 2020). Coral predation is part of the natural dynamics of the reef and likely causes microbiome variation that is also part of the natural dynamics of the coral holobiont. However, corallivores can act as vectors by introducing pathogens into the microbiome at the predation scar (Nicolet et al., 2018; Ezzat et al., 2019b). From a conservation perspective, thermal stress is a much more formidable threat to corals since increasing seawater temperature has a pervasive effect on the coral holobiont compared to localized wounding.

In a concurrent paper, we explored several metrics of host performance in response to the different combinations of stressors. Coral growth rate and Symbiodiniaceae density were not affected by high temperature, simulated predation, nutrient enrichment, or their interactions. High temperatures caused a significant decrease in healing rates of the simulated predation wounds. However, the addition of ammonium or nitrate restored wound healing rates at high temperatures (Figure 5.1). Studies are beginning to uncover whether the coral and its microbiome experience parallel or causal responses to stress (Ziegler et al., 2017; Savary et al., 2021), however, the aim of this dissertation was to focus specifically on changes in the microbiome, independent of host.

In Chapter 3, I showed that nitrate and urea loading had no observable effect on the microbiomes of thermally stressed corals and therefore no interaction with

thermal stress. This was a very surprising result given that a superset of the corals we evaluated experienced a strong interaction between nitrate and temperature that exacerbated bleaching severity (Burkepile et al., 2019). For these Mo'orean corals, there was a disconnect between the hosts bleaching response to nitrate loading and the lack of a response of the microbiome to nitrate loading. In contrast, Shaver et al. (2017) found that for Caribbean *Acropora* corals, inorganic nitrogen and phosphorous caused significant changes to the microbiome, but did not affect coral mortality, tissue loss, growth rates, or algal colonization. These changes in the microbiome were driven by the bacterial parasite *Ca. Aquarickettsia rohweri* which proliferates under nutrient enrichment (Klinges et al., 2019). There is no evidence for the existence of such a dominant, nutrient-responsive bacterial symbiont in Mo'orean corals, perhaps due to the lack of chronic nutrient pollution in Mo'orea compared to the Caribbean (Haßler et al., 2019; Lapointe et al., 2019). In fact, the pervasive effects of thermal stress compared to the minimal response to nutrients in Mo'orean corals may be explained by sensitivity of the dominant taxon *Endozoicomonas* to changes in temperature and resistance to changes in nutrients as evidenced in Chapter 3 (Figure 3.1). While nutrients may be a strong driver of microbiome variation in Caribbean corals, my work demonstrates that nutrients may not have an ecologically relevant effect on the microbiome of corals in Mo'orea, especially in the face of rising seawater temperatures.

5.2.3. Despite low resistance, coral microbiomes may be resilient to thermal stress

There is strong evidence suggesting that the coral microbiome can recover from thermal stress (Bourne et al., 2008; Ziegler et al., 2019), and my work in Chapter 3 supports this and addresses Aim 3. Studies without a timeseries component, such as Chapter 2, capture the sensitivity of coral microbiomes to stress. After a defined period of thermal stress exposure, microbiome profiles are commonly characterized by reduced *Endozoicomonas* and increased opportunists, especially *Vibrio* species. Thus, coral microbiomes are not resistant to stress, however, the degree of flexibility that microbiomes have in responding to stress may vary depending on coral host (Ziegler et al., 2019; Maher et al., 2020). Timeseries sampling allows for an assessment of resilience, i.e. the rate or extent to which a community recovers to pre-stress or stable conditions. Bourne et al. (2008) described recovery of coral microbiomes as a return to a stable state which was marked by the reduction of *Vibrio* sequences back to pre-stress levels. Likewise, I assessed coral microbiome resilience in Chapter 3 as a return to pre-stress community composition, i.e. a state dominated by *Endozoicomonas*. While the coral microbiomes were resilient to stress, they recovered to a less diverse state with even higher proportions of *Endozoicomonas* than the pre-stress communities. Given the current state of coral reefs, coral microbiome resilience likely depends on the severity and frequency of environmental stress events. Severe stress events that cause coral mortality offer no chance for community recovery, and repeated stress events can shorten the recovery periods and thereby jeopardize resilience (Hughes et al., 2019). Back-to-back stress events could result in the development of stress tolerance or in exponential increases

in susceptibility. Microbiome timeseries sampling that spans multiple stress events will be crucial to understanding coral microbiome resilience to severe, repetitive, and/or prolonged thermal stress in the future.

5.2.4. The host-endosymbiont relationship facilitates microbiome stability and resilience

Endozoicomonas sequences often dominate the microbiomes of apparently healthy corals and contribute to high community stability and low community diversity even during exposure to environmental stress (Ziegler et al., 2016, 2019; Pogoreutz et al., 2018). This contrasts with an ecological hypothesis that higher diversity can lead to higher functional redundancy within a community which is positively correlated with stability and resilience (Biggs et al., 2020). Functionally redundant taxa can perform the ecosystem function of another taxon lost during disturbance. Variation in the microbial communities investigated in this dissertation are subject to host feedback and modulation that may alter traditional ecological patterns of community disturbance. In Chapter 4, I highlight how *Endozoicomonas* species associate with a diversity of marine hosts that do not differentiate geographically or by host taxonomic group (i.e. coral versus sponge). Instead, some *Endozoicomonas* lineages are host-specific and demonstrate cophylogeny with host lineages (Pollock et al., 2018). Thus, these marine hosts acquired a stable endosymbiotic association with *Endozoicomonas* and may enjoy the benefits of complementary metabolic capabilities such as supplementation of vitamins or amino acids. In addressing Aim 4, we found no stress response genes in *Endozoicomonas* that would suggest an active role in holobiont susceptibility or tolerance to stress.

Ultimately, the persistence and predominance of the coral-*Endozoicomonas* symbiosis may explain why *Endozoicomonas* sequences can recover after stress to dominate the community and drive stability and resilience in the coral holobiont.

5.3. Caveats and Considerations for the Analysis of Experimental 16S Amplicon Data

This dissertation used multiple statistical methods to interrogate the dynamics of coral microbiomes between treatments and overtime. Below, I detail some issues that arose during my studies in the context of coral-associated bacterial communities, but the considerations may be applicable to the broader animal-microbiome community. Further, I give recommendations for future researchers interested in conducting and analyzing 16S amplicon data.

5.3.1. Capturing stochasticity with tests for community dispersion

Most studies of the animal microbiome attempt to predict a shift from a healthy to a dysbiotic stable state in response to stress or perturbation. Characterization of predictable community shifts under certain stressors would no doubt facilitate the development of targeted microbial-mediated health interventions and conservation approaches such as the development of probiotics or ‘designer microbes’ aimed at enhancing resistance or resilience of holobionts. While deterministic changes that induce these shifts to alternate stable states are important to community dynamics, stochastic changes should also be considered as they provide insight into biologically meaningful dynamics that are often overlooked. Stochastic changes result in the spread or dispersion of community data points in multivariate

space and have been observed in systems ranging from corals and marine sponges to the lungs of patients suffering from HIV/AIDs (Zaneveld et al., 2016). In the statistical tradition, PERMANOVA assumes same "multivariate spread" among factors as with the assumption of variance homogeneity in the univariate ANOVA. Rather than using this test solely to detect a difference in means, PERMANOVA can be used to explain ecological phenomenon in which unequal dispersions within a group are considered part of the signal differentiating two groups (Anderson, 2001). In other words, a significant PERMANOVA test could mean both a significant change in community stable state and/or in sample-to-sample community variability. Further, PERMDISP explicitly tests if the average within-group dispersion is equivalent among groups using average distance to group centroid (Anderson, 2006).

In this dissertation, I uncover both dispersion and location effects for coral microbiomes undergoing various perturbations. For Chapters 2 & 3, group centroids shifted, and samples dispersed in ordination space under stress. This dispersion may result from the hosts inability to regulate its microbiome (Zaneveld et al., 2017). While there is strong evidence in the literature that dispersion effects are important in driving coral microbiome structure under stress, I encountered two issues in interpreting results from these tests that may be specific to microbiomes with similar structure as those examined here. First, corals in my dataset from Chapter 2 were highly dominated by a single taxon, an *Endozoicomonas* species, and samples were rarefied to a relatively low level (1,070 reads) in order to preserve replication. For control corals with ~95% of the community composed of a single *Endozoicomonas*

OTU (Figure 2.1), only 5% of the reads represented minor or low abundance taxa. In contrast, more reads were available to uncover minor members within stressed communities where the proportion of *Endozoicomonas* sequences was much lower. Therefore, the ability to detect variability due to the presence of rare taxa may depend on the dominance of *Endozoicomonas*. I used a linear regression to test this hypothesis and found that the relative abundance of *Endozoicomonas* sequences was significantly negatively correlated with sample distance-to-centroid measurements (i.e. dispersion). This has been documented in the literature in instances where small sample sizes and low sampling depth may artificially inflate beta-diversity when rare, shared species are only detected in a single sample and erroneously considered unique (Chao et al., 2005; Lozupone et al., 2011). This could be ameliorated by rarefying datasets to a level where the species accumulation curve has flattened as I demonstrate in Chapter 3 (Supplementary Figure 3.1).

Second, both PERMANOVA and PERMDISP can be sensitive to unbalanced experimental designs (Anderson and Walsh, 2013). PERMANOVA may be overly liberal in rejection rates when a smaller group has a larger dispersion than a larger group or overly conservative when the larger group has the greater dispersion (Anderson and Walsh 2013). Datasets in Chapters 2 & 3 had unbalanced designs as some samples failed to sequence entirely or were discarded due to low sequencing depth after removal of host contamination in 16S libraries. In Maher et al. (2020), *Acropora* corals sampled in 2016 had low replication and slightly larger dispersion which may have resulted a liberal rejection in the PERMANOVA test between

sampling months. However, NMDS visualizations show strong clustering that support the PERMANOVA test results (Figure 3.3). In a later co-first-authored paper, Klinges and Maher et al. (2020), I addressed the issue by down-sampling treatment groups with larger sample sizes to a balanced design and repeating PERMANOVA and PERMDISP tests for 1000 permutations. The results agreed with those of the unbalanced groups. The down-sampling procedure can be easily implemented to confirm the results of PERMANOVA and PERMDISP tests on unbalanced designs.

5.3.2. Methods for normalization of count data and identification of differentially abundant taxa

Microbiome data is often normalized prior to downstream analysis due to issues inherent to the data including: uneven sequencing depth (i.e., library size), sparsity resulting from a high proportion of zeroes, and compositionality as the number of reads does not represent absolute abundance. For instance, rarefying involves subsampling large sequencing libraries down to the smallest sample library size for comparability in diversity analyses. However, some researchers deem this process inadmissible as it discards valid available data and sequencing rarely saturates the full range of species (McMurdie and Holmes, 2014; Weiss et al., 2017). In Chapter 3, I use alpha rarefaction curves to demonstrate that the chosen rarefaction level roughly saturates the full range of species (Supplementary Figure 3.1), however, complete saturation is difficult given the range in sequencing depths among samples in amplicon sequencing. One alternative to alpha diversity estimation based on rarefaction is the R package DivNet which estimates species richness using a bias correction that incorporates unobserved taxa and a variance adjustment that models

measurement error (Willis and Martin, 2020). While I would recommend this method for analyzing 16S amplicon data, it is very computationally expensive, and rarefaction is still a common and accepted method. Further, when comparing alpha diversity estimates based on DivNet and rarefaction on a lab dataset, we found that while rarefaction can consistently underestimate species richness and discard rare taxa, it does not generally affect the patterns of alpha and beta diversity among treatments (Figure 5.2). Therefore, I used rarefaction to normalize microbiome data for diversity analyses, but opted for alternative methods for assessing the differential abundance of specific taxa.

Various statistical methods for comparing the (relative) taxon abundance between two groups (i.e. case vs. control) have been developed. Initially developed for RNAseq data, DESeq2 uses a scaling factor based on the taxon/gene of median absolute abundance to normalize –omics count data and then uses a negative binomial distribution to fit a generalized linear model (GLM) to each taxon/gene (Love et al., 2014). While DESeq2 can incorporate multiple explanatory variables and their interactions into the model, it cannot incorporate random effects. Alternatively, ANCOM uses the non-parametric Mann-Whitney test to compare the log-ratio of the abundance of each taxon to the abundance of every other taxon and allows for complex mixed model designs (Mandal et al., 2015). Random effects are often inherent to the design of manipulative experiments with corals as treatments can be replicated across tanks, individual corals sampled repeatedly overtime, or individual fragments from a single colony distributed across treatments. DESeq2 is optimized

for increased sensitivity on smaller datasets due to its development for RNAseq data, and has a higher false discovery rate (FDR) for library sizes that are large and/or highly uneven (Weiss et al., 2017). In Chapter 2, I used DESeq2 to identify 56 differentially abundant taxa across several treatment variables and their interactions. Alternatively, ANCOM is robust to changes in FDR based on library size, but has reduced sensitivity on small datasets (Weiss et al., 2017). In Chapter 3, I identified only 14 differentially abundant taxa within three different coral hosts across time. In Figure 5.3, I ran both methods on a coral microbiome dataset from Klinges and Maher et al. (2020) and found that DESeq2 identified many more differentially abundant taxa than ANCOM which calls into question the prevalence of false positives with DESeq2 and/or the overly conservativism on ANCOM. Many microbiome researchers have also criticized the use of DESeq2 for microbial count data since sequencing counts represent a fraction or random sample from the environment and should therefore by analyzed as composition data (Gloor et al., 2016). For future microbiome studies, I suggest that researchers carefully review the range in library sizes as well as the sample size of their datasets to assess which method has the most appropriate normalization technique and statistical test for their data. As there are many more options than the two mentioned here, I further advocate for using multiple differential abundance methods and considering the overlap between the methods as the most accurate prediction of differentially abundant taxa.

5.4. Figures

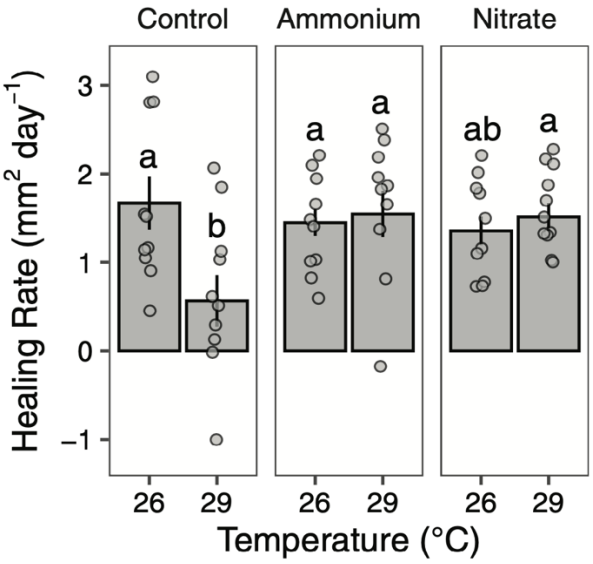

Figure 5.1. Wound healing rates of *Pocillopora meandrina*. The wound healing rates (mm^2 day^{-1}; mean ± SE) of wounded Pocillopora meandrina nubbins under different temperature and nutrient treatments. The points show the distribution of the data. Bars sharing a letter are not significantly different from each other. Figure from Rice and Maher et al. (2019).

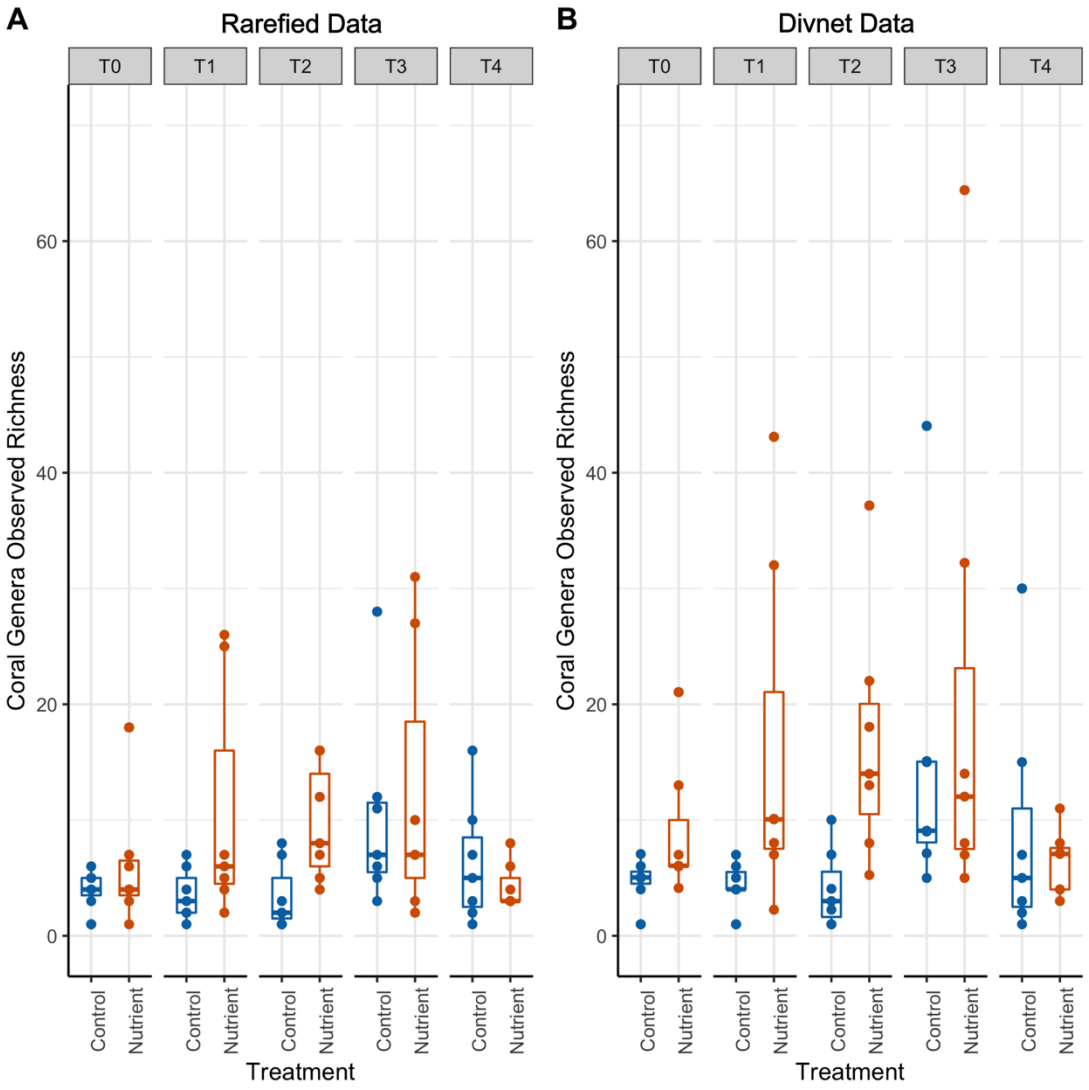

Figure 5.2. Observed richness of coral-associated bacterial genera from A) rarefied data and B) DivNet data. Figure was produced from a dataset tracking coral microbiomes in two treatments over five time points from Messyasz et al. (in prep).

Figure 5.3. Comparison of differential abundance with ANCOM and DESeq2. (A) Volcano plot of results from differential abundance analysis using ANCOM. The genus-level ASV table filtered to include taxa with a total count of 10 in at least 20% of samples (# taxa = 32) was used. ANCOM tests the null hypothesis that the average abundance of a given species in a group is equal to that in the other group. The W statistic represents the strength of the test for the 32 tested species and is the number of times the null-hypothesis was rejected for a given species. Taxa above the dashed line are significant with the null-hypothesis rejected 60% of the time. The x-axis value presents the effect size as the clr (centered log ratio) transformed mean difference in abundance of a given species between the two groups being compared. For the first panel, a positive x-axis value means the genus is abundant in Pre-Bleach Susceptible samples compared to Pre-bleached Resistant samples or vice versa for a negative x-axis value. (B) Significant results from differential abundance analysis using DESeq2. Each point is a bacterial genus colored by order. Contrasts show the log2 fold change difference between bleaching status/resistance combinations. ASVs were summarized to the genus level and included in the analysis if they had a total count of 10 in at least 20% of samples (# taxa = 32).

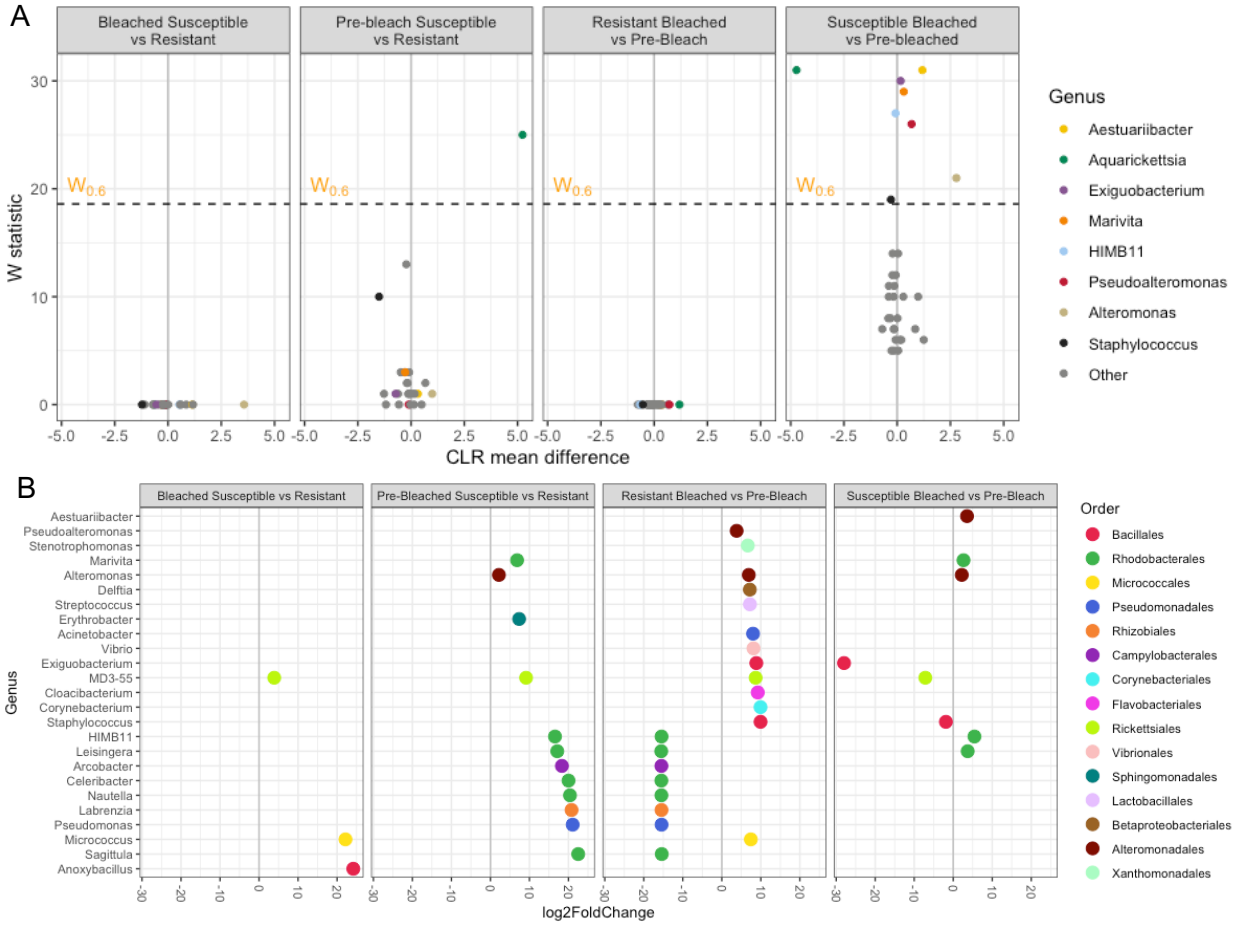
A
Bleached Susceptible vs Resistant
Pre-bleach Susceptible vs Resistant
Resistant Bleached vs Pre-Bleach
Susceptible Bleached vs Pre-bleached
W statistic
W0.6
CLR mean difference
Genus
Aestuariibacter
Aquarickettsia
Exiguobacterium
Marivita
HIMB11
Pseudoalteromonas
Alteromonas
Staphylococcus
Other
B
Bleached Susceptible vs Resistant
Pre-Bleached Susceptible vs Resistant
Resistant Bleached vs Pre-Bleach
Susceptible Bleached vs Pre-Bleach
Genus
log2FoldChange
Order
Bacillales
Rhodobacterales
Micrococcales
Pseudomonadales
Rhizobiales
Campylobacterales
Corynebacteriales
Flavobacteriales
Rickettsiales
Vibrionales
Sphingomonadales
Lactobacillales
Betaproteobacteriales
Alteromonadales
Xanthomonadales

Figure 5.3

BIBLIOGRAPHY

Adam, T. C., Brooks, A. J., Holbrook, S. J., Schmitt, R. J., Washburn, L., and Bernardi, G. (2014). How will coral reef fish communities respond to climate-driven disturbances? Insight from landscape-scale perturbations. *Oecologia* 176, 285–296. doi:10.1007/s00442-014-3011-x.

Adam, T. C., Schmitt, R. J., Holbrook, S. J., Brooks, A. J., Edmunds, P. J., Carpenter, R. C., et al. (2011). Herbivory, Connectivity, and Ecosystem Resilience: Response of a Coral Reef to a Large-Scale Perturbation. *PLOS ONE* 6, e23717. doi:10.1371/journal.pone.0023717.

Adjeroud, M., Augustin, D., Galzin, R., and Salvat, B. (2002). Natural disturbances and interannual variability of coral reef communities on the outer slope of Tiahura (Moorea, French Polynesia): 1991 to 1997. *Marine Ecology Progress Series* 237, 121–131. doi:10.3354/meps237121.

Adjeroud, M., Michonneau, F., Edmunds, P. J., Chancerelle, Y., de Loma, T. L., Penin, L., et al. (2009). Recurrent disturbances, recovery trajectories, and resilience of coral assemblages on a South Central Pacific reef. *Coral Reefs* 28, 775–780. doi:10.1007/s00338-009-0515-7.

Agostini, S., Suzuki, Y., Higuchi, T., Casareto, B. E., Yoshinaga, K., Nakano, Y., et al. (2012). Biological and chemical characteristics of the coral gastric cavity. *Coral Reefs* 31, 147–156. doi:10.1007/s00338-011-0831-6.

Ainsworth, T. D., and Gates, R. D. (2016). Corals' microbial sentinels. *Science* 352, 1518–1519. doi:10.1126/science.aad9957.

Ainsworth, T. D., Krause, L., Bridge, T., Torda, G., Raina, J. B., Zakrzewski, M., et al. (2015). The coral core microbiome identifies rare bacterial taxa as ubiquitous endosymbionts. *The ISME Journal* 9, 2261–2274. doi:10.1038/ismej.2015.39.

Albertsen, M., Hugenholtz, P., Skarshewski, A., Nielsen, K. L., Tyson, G. W., and Nielsen, P. H. (2013). Genome sequences of rare, uncultured bacteria obtained by differential coverage binning of multiple metagenomes. *Nature Biotechnology* 31, 533–538. doi:10.1038/nbt.2579.

Alex, A., and Antunes, A. (2019). Comparative Genomics Reveals Metabolic Specificity of Endozoicomonas Isolated from a Marine Sponge and the Genomic Repertoire for Host-Bacteria Symbioses. *Microorganisms* 7. doi:10.3390/microorganisms7120635.

Alfieri, C., Zhang, S., and Barford, D. (2017). Visualizing the complex functions and mechanisms of the anaphase promoting complex/cyclosome (APC/C). *Open Biology* 7, 170204. doi:10.1098/rsob.170204.

Al-Khodor, S., Price, C. T., Kalia, A., and Kwaik, Y. A. (2010). Ankyrin-repeat containing proteins of microbes: a conserved structure with functional diversity. *Trends Microbiol* 18, 132–139. doi:10.1016/j.tim.2009.11.004.

Allgeier, J. E., Burkepile, D. E., and Layman, C. A. (2017). Animal pee in the sea: consumer-mediated nutrient dynamics in the world's changing oceans. *Global Change Biology*. doi:10.1111/gcb.13625.

Altschul, S. F., Gish, W., Miller, W., Myers, E. W., and Lipman, D. J. (1990). Basic Local Alignment Search Tool. *Journal of Molecular Biology*, 8. doi:10.1016/S0022-2836(05)80360-2.

Amir, A., McDonald, D., Navas-Molina, J. A., Kopylova, E., Morton, J. T., Zech Xu, Z., et al. (2017). Deblur Rapidly Resolves Single-Nucleotide Community Sequence Patterns. *mSystems* 2. doi:10.1128/mSystems.00191-16.

Anderson, M. J. (2001). A new method for non-parametric multivariate analysis of variance. *Austral ecology* 26, 32–46. doi:10.1111/j.1442-9993.2001.01070.pp.x

Anderson, M. J. (2006). Distance-Based Tests for Homogeneity of Multivariate Dispersions. *Biometrics* 62, 245–253. doi:10.1111/j.1541-0420.2005.00440.x.

Anderson, M. J., and Walsh, D. C. (2013). PERMANOVA, ANOSIM, and the Mantel test in the face of heterogeneous dispersions: what null hypothesis are you testing? *Ecological monographs* 83, 557–574. doi:10.1890/12-2010.1.

Appolinario, L. R., Tschoeke, D. A., Rua, C. P. J., Venas, T., Campeão, M. E., Amaral, G. R. S., et al. (2016). Description of Endozoicomonas arenosclerae sp. nov. using a genomic taxonomy approach. *Antonie van Leeuwenhoek* 109, 431–438. doi:10.1007/s10482-016-0649-x.

Apprill, A., McNally, S., Parsons, R., and Weber, L. (2015). Minor revision to V4 region SSU rRNA 806R gene primer greatly increases detection of SAR11 bacterioplankton. *Aquatic Microbial Ecology* 75, 129–137. doi:10.3354/ame01753.

Apprill, A., Weber, L. G., and Santoro, A. E. (2016). Distinguishing between Microbial Habitats Unravels Ecological Complexity in Coral Microbiomes. *mSystems* 1. doi:10.1128/mSystems.00143-16.

Aramaki, T., Blanc-Mathieu, R., Endo, H., Ohkubo, K., Kanehisa, M., Goto, S., et al. (2020). KofamKOALA: KEGG Ortholog assignment based on profile HMM and adaptive score threshold. *Bioinformatics* 36, 2251–2252. doi:10.1093/bioinformatics/btz859.

Aziz, R. K., Bartels, D., Best, A. A., DeJongh, M., Disz, T., Edwards, R. A., et al. (2008). The RAST Server: Rapid Annotations using Subsystems Technology. *BMC Genomics* 9, 75. doi:10.1186/1471-2164-9-75.

Bates, D., Mächler, M., Bolker, B., and Walker, S. (2014). Fitting Linear Mixed-Effects Models Using lme4. *Journal of Statistical Software* 67, 1–48. doi:10.18637/jss.v067.i01.

Bayer, T., Neave, M. J., Alsheikh-Hussain, A., Aranda, M., Yum, L. K., Mincer, T., et al. (2013). The Microbiome of the Red Sea Coral Stylophora pistillata Is Dominated by Tissue-Associated Endozoicomonas Bacteria. *Appl. Environ. Microbiol.* 79, 4759–4762. doi:10.1128/AEM.00695-13.

Beinart, R. A., Nyholm, S. V., Dubilier, N., and Girguis, P. R. (2014). Intracellular Oceanospirillales inhabit the gills of the hydrothermal vent snail Alviniconcha with chemosynthetic, γ-Proteobacterial symbionts. *Environmental Microbiology Reports* 6, 656–664. doi:10.1111/1758-2229.12183.

Ben-Haim, Y., Thompson, F. L., Thompson, C. C., Cnockaert, M. C., Hoste, B., Swings, J., et al. (2003). Vibrio coralliilyticus sp. nov., a temperature-dependent pathogen of the coral Pocillopora damicornis. *International Journal of Systematic and Evolutionary Microbiology* 53, 309–315. doi:10.1099/ijs.0.02402-0.

Benjamini, Y., and Hochberg, Y. (1995). Controlling the False Discovery Rate: A Practical and Powerful Approach to Multiple Testing. *Journal of the Royal Statistical Society. Series B (Methodological)* 57, 289–300. doi:10.1111/j.2517-6161.1995.tb02031.x.

Béraud, E., Gevaert, F., Rottier, C., and Ferrier-Pagès, C. (2013). The response of the scleractinian coral Turbinaria reniformis to thermal stress depends on the nitrogen status of the coral holobiont. *Journal of Experimental Biology* 216, 2665–2674. doi:10.1242/jeb.085183.

Berumen, M. L., and Pratchett, M. S. (2006). Recovery without resilience: persistent disturbance and long-term shifts in the structure of fish and coral communities at Tiahura Reef, Moorea. *Coral Reefs* 25, 647–653. doi:10.1007/s00338-006-0145-2.

Biggs, C. R., Yeager, L. A., Bolser, D. G., Bonsell, C., Dichiera, A. M., Hou, Z., et al. (2020). Does functional redundancy affect ecological stability and resilience? A review and meta-analysis. *Ecosphere* 11, e03184. doi:10.1002/ecs2.3184.

Bittinger, M. A., Milner, J. L., Saville, B. J., and Handelsman, J. (1997). *rosR* , a Determinant of Nodulation Competitiveness in *Rhizobium etli*. *MPMI* 10, 180–186. doi:10.1094/MPMI.1997.10.2.180.

Bokulich, N. A., Kaehler, B. D., Rideout, J. R., Dillon, M., Bolyen, E., Knight, R., et al. (2018). Optimizing taxonomic classification of marker-gene amplicon sequences with QIIME 2's q2-feature-classifier plugin. *Microbiome* 6. doi:10.1186/s40168-018-0470-z.

Bolyen, E., Rideout, J. R., Dillon, M. R., Bokulich, N. A., Abnet, C. C., Al-Ghalith, G. A., et al. (2019). Reproducible, interactive, scalable and extensible microbiome data science using QIIME 2. *Nat Biotechnol* 37, 852–857. doi:10.1038/s41587-019-0209-9.

Bosch, T. C. G. (2013). Cnidarian-Microbe Interactions and the Origin of Innate Immunity in Metazoans. *Annual Review of Microbiology* 67, 499–518. doi:10.1146/annurev-micro-092412-155626.

Bourne, D. G., Garren, M., Work, T. M., Rosenberg, E., Smith, G. W., and Harvell, C. D. (2009). Microbial disease and the coral holobiont. *Trends in Microbiology* 17, 554–562. doi:10.1016/j.tim.2009.09.004.

Bourne, D. G., Morrow, K. M., and Webster, N. S. (2016). Insights into the Coral Microbiome: Underpinning the Health and Resilience of Reef Ecosystems. *Annual Review of Microbiology* 70, 317–340. doi:10.1146/annurev-micro-102215-095440.

Bourne, D., Iida, Y., Uthicke, S., and Smith-Keune, C. (2008). Changes in coral-associated microbial communities during a bleaching event. *The ISME Journal* 2, 350–363. doi:10.1038/ismej.2007.112.

Brettin, T., Davis, J. J., Disz, T., Edwards, R. A., Gerdes, S., Olsen, G. J., et al. (2015). RASTtk: A modular and extensible implementation of the RAST algorithm for building custom annotation pipelines and annotating batches of genomes. *Scientific Reports* 5, 8365. doi:10.1038/srep08365.

Broadbent, A. D., and Jones, G. B. (2004). DMS and DMSP in mucus ropes, coral mucus, surface films and sediment pore waters from coral reefs in the Great Barrier Reef. *Mar. Freshwater Res.* 55, 849–855. doi:10.1071/MF04114.

Brown, A. L., Lipp, E. K., and Osenberg, C. W. (2019). Algae dictate multiple stressor effects on coral microbiomes. *Coral Reefs*. doi:10.1007/s00338-019-01769-w.

Brown, C. J., Saunders, M. I., Possingham, H. P., and Richardson, A. J. (2013). Managing for Interactions between Local and Global Stressors of Ecosystems. *PLoS ONE* 8, e65765. doi:10.1371/journal.pone.0065765.

Bruno, J. F., Petes, L. E., and Harvell, C. D. (2003). Nutrient enrichment can increase the severity of coral diseases. 6, 1056–1061. doi:10.1046/j.1461-0248.2003.00544.x.

Bruno, J. F., Selig, E. R., Casey, K. S., Page, C. A., Willis, B. L., Harvell, C. D., et al. (2007). Thermal stress and coral cover as drivers of coral disease outbreaks. *PLoS Biol* 5, e124. doi:10.1371/journal.pbio.0050124.

Burkepile, D. E., and Hay, M. E. (2006). Herbivore Vs. Nutrient Control of Marine Primary Producers: Context-Dependent Effects. *Ecology* 87, 3128–3139. doi:10.1890/0012-9658(2006)87[3128:HVNCOM]2.0.CO;2.

Burkepile, D. E., Shantz, A. A., Adam, T. C., Munsterman, K. S., Speare, K. E., Ladd, M. C., et al. (2019). Nitrogen Identity Drives Differential Impacts of Nutrients on Coral Bleaching and Mortality. *Ecosystems*. doi:10.1007/s10021-019-00433-2.

Burkepile, D. E., and Thurber, R. V. (2019). Long Arm of Species Loss: How Will Defaunation Disrupt Ecosystems Down to the Microbial Scale? *BioScience* 69, 443–454. doi:10.1093/biosci/biz047.

Burroughs, A. M., Iyer, L. M., and Aravind, L. (2011). Functional diversification of the RING finger and other binuclear treble clef domains in prokaryotes and the early evolution of the ubiquitin system. *Mol. BioSyst.* 7, 2261–2277. doi:10.1039/C1MB05061C.

Cai, L., Tian, R.-M., Zhou, G., Tong, H., Wong, Y. H., Zhang, W., et al. (2018). Exploring coral microbiome assemblages in the South China Sea. *Scientific Reports* 8. doi:10.1038/s41598-018-20515-w.

Callis, J. (2014). The Ubiquitination Machinery of the Ubiquitin System. *Arabidopsis Book* 12. doi:10.1199/tab.0174.

Cameron, A. C., and Trivedi, P. K. (2013). *Regression Analysis of Count Data*. 2nd ed., Econometric Society Monograph. (Cambridge: Cambridge University Press), 1-566. doi:10.1017/CBO9781139013567.

Caporaso, J. G., Bittinger, K., Bushman, F. D., DeSantis, T. Z., Andersen, G. L., and Knight, R. (2010a). PyNAST: a flexible tool for aligning sequences to a template alignment. *Bioinformatics* 26, 266–267. doi:10.1093/bioinformatics/btp636.

Caporaso, J. G., Kuczynski, J., Stombaugh, J., Bittinger, K., Bushman, F. D., Costello, E. K., et al. (2010b). QIIME allows analysis of high-throughput community sequencing data. *Nature Methods* 7, 335–336. doi:10.1038/nmeth.f.303.

Cardini, U., Bednarz, V. N., Naumann, M. S., van Hoytema, N., Rix, L., Foster, R. A., et al. (2015). Functional significance of dinitrogen fixation in sustaining coral productivity under oligotrophic conditions. *Proceedings of the Royal Society B: Biological Sciences* 282, 20152257. doi:10.1098/rspb.2015.2257.

Casas, V., Kline, D. I., Wegley, L., Yu, Y., Breitbart, M., and Rohwer, F. (2004). Widespread association of a Rickettsiales-like bacterium with reef-building corals. *Environmental Microbiology* 6, 1137–1148. doi:10.1111/j.1462-2920.2004.00647.x.

Chao, A., Chazdon, R. L., Colwell, R. K., and Shen, T.-J. (2005). A new statistical approach for assessing similarity of species composition with incidence and abundance data. *Ecology Letters* 8, 148–159. doi:10.1111/j.1461-0248.2004.00707.x.

Chao, A., and Chiu, C.-H. (2016). "Species Richness: Estimation and Comparison," in *Wiley StatsRef: Statistics Reference Online*, eds. N. Balakrishnan, T. Colton, B. Everitt, W. Piegorsch, F. Ruggeri, and J. L. Teugels (Chichester, UK: John Wiley & Sons, Ltd), 1–26. doi:10.1002/9781118445112.stat03432.pub2.

Chu, H., and Mazmanian, S. K. (2013). Innate immune recognition of the microbiota promotes host-microbial symbiosis. *Nat Immunol* 14, 668–675. doi:10.1038/ni.2635.

Chu, N. D., and Vollmer, S. V. (2016). Caribbean corals house shared and host-specific microbial symbionts over time and space. *Environmental Microbiology Reports* 8, 493–500. doi:10.1111/1758-2229.12412.

Clements, C. S., Burns, A. S., Stewart, F. J., and Hay, M. E. (2020). Parasite-host ecology: the limited impacts of an intimate enemy on host microbiomes. *Animal Microbiome* 2, 42. doi:10.1186/s42523-020-00061-5.

Close, T. J., Rogowsky, P. M., Kado, C. I., Winans, S. C., Yanofsky, M. F., and Nester, E. W. (1987). Dual control of Agrobacterium tumefaciens Ti plasmid

virulence genes. *Journal of Bacteriology* 169, 5113–5118. doi:10.1128/JB.169.11.5113-5118.1987.

Conway, J. R., Lex, A., and Gehlenborg, N. (2017). UpSetR: an R package for the visualization of intersecting sets and their properties. *Bioinformatics* 33, 2938–2940. doi:10.1093/bioinformatics/btx364.

Côté, I. M., Darling, E. S., and Brown, C. J. (2016). Interactions among ecosystem stressors and their importance in conservation. *Proceedings of the Royal Society B: Biological Sciences* 283, 2015–2592. doi:10.1098/rspb.2015.2592.

Cunning, R., and Baker, A. C. (2013). Excess algal symbionts increase the susceptibility of reef corals to bleaching. *Nature Climate Change* 3, 259–262. doi:10.1038/nclimate1711.

D Ainsworth, T., Krause, L., Bridge, T., Torda, G., Raina, J.-B., Zakrzewski, M., et al. (2015). The coral core microbiome identifies rare bacterial taxa as ubiquitous endosymbionts. *ISME J* 9, 2261–2274. doi:10.1038/ismej.2015.39.

D'Angelo, C., and Wiedenmann, J. (2014). Impacts of nutrient enrichment on coral reefs: new perspectives and implications for coastal management and reef survival. *Current Opinion in Environmental Sustainability* 7, 82–93. doi:10.1016/j.cosust.2013.11.029.

Davy, S. K., Allemand, D., and Weis, V. M. (2012). Cell Biology of Cnidarian-Dinoflagellate Symbiosis. *Microbiol. Mol. Biol. Rev.* 76, 229–261. doi:10.1128/MMBR.05014-11.

De'ath, G., and Fabricius, K. (2010). Water quality as a regional driver of coral biodiversity and macroalgae on the Great Barrier Reef. *Ecological Applications* 20, 840–850. doi:10.1890/08-2023.1.

De'ath, G., Fabricius, K. E., Sweatman, H., and Puotinen, M. (2012). The 27–year decline of coral cover on the Great Barrier Reef and its causes. *PNAS* 109, 17995–17999. doi:10.1073/pnas.1208909109.

Deschaseaux, E. S. M., Jones, G. B., Deseo, M. A., Shepherd, K. M., Kiene, R. P., Swan, H. B., et al. (2014). Effects of environmental factors on dimethylated sulfur compounds and their potential role in the antioxidant system of the coral holobiont. *Limnology and Oceanography* 59, 758–768. doi:10.4319/lo.2014.59.3.0758.

Ding, J.-Y., Shiu, J.-H., Chen, W.-M., Chiang, Y.-R., and Tang, S.-L. (2016). Genomic Insight into the Host–Endosymbiont Relationship of Endozoicomonas montiporae CL-33T with its Coral Host. *Front. Microbiol.* 7. doi:10.3389/fmicb.2016.00251.

Dinsdale, E. A., Pantos, O., Smriga, S., Edwards, R. A., Angly, F., Wegley, L., et al. (2008). Microbial Ecology of Four Coral Atolls in the Northern Line Islands. *PLOS ONE* 3, e1584. doi:10.1371/journal.pone.0001584.

Disalvo, L. H. (1969). Isolation of Bacteria from the Corallum of *Porites lobata* (Vaughn) and Its Possible Significance. *Am Zool* 9, 735–740. doi:10.1093/icb/9.3.735.

Duvallet, C., Gibbons, S. M., Gurry, T., Irizarry, R. A., and Alm, E. J. (2017). Meta-analysis of gut microbiome studies identifies disease-specific and shared responses. *Nature Communications* 8. doi:10.1038/s41467-017-01973-8.

Edgar, R. C. (2010). Search and clustering orders of magnitude faster than BLAST. *Bioinformatics* 26, 2460–2461. doi:10.1093/bioinformatics/btq461.

Emms, D. M., and Kelly, S. (2015). OrthoFinder: solving fundamental biases in whole genome comparisons dramatically improves orthogroup inference accuracy. *Genome Biology* 16, 157. doi:10.1186/s13059-015-0721-2.

Emms, D. M., and Kelly, S. (2019). OrthoFinder: phylogenetic orthology inference for comparative genomics. *Genome Biol* 20, 238. doi:10.1186/s13059-019-1832-y.

Epstein, H. E., Torda, G., Munday, P. L., and van Oppen, M. J. H. (2019a). Parental and early life stage environments drive establishment of bacterial and dinoflagellate communities in a common coral. *The ISME Journal* 13, 1635–1638. doi:10.1038/s41396-019-0358-3.

Epstein, H. E., Torda, G., and van Oppen, M. J. H. (2019b). Relative stability of the Pocillopora acuta microbiome throughout a thermal stress event. *Coral Reefs* 38, 373–386. doi:10.1007/s00338-019-01783-y.

Eren, A. M., Esen, Ö. C., Quince, C., Vineis, J. H., Morrison, H. G., Sogin, M. L., et al. (2015). Anvi'o: an advanced analysis and visualization platform for 'omics data. *PeerJ* 3, e1319. doi:10.7717/peerj.1319.

Ezzat, L., Lamy, T., Maher, R. L., Munsterman, K. S., Landfield, K. M., Schmeltzer, E. R., et al. (2020). Parrotfish predation drives distinct microbial communities in reef-building corals. *Anim Microbiome* 2, 5. doi:10.1186/s42523-020-0024-0.

Ezzat, L., Lamy, T., Maher, R. L., Munsterman, K. S., Landfield, K., Schmeltzer, E. R., et al. (2019a). Surgeonfish feces increase microbial opportunism in reef-building corals. *Marine Ecology Progress Series* 631, 81–97. doi:10.3354/meps13119.

Ezzat, L., Lamy, T., Maher, R., Munsterman, K., Landfield, K., Schmeltzer, E., et al. (2019b). Surgeonfish feces increase microbial opportunism in reef-building corals. *Marine Ecology Progress Series* 631, 81–97. doi:10.3354/meps13119.

Ezzat, L., Maguer, J.F., Grover, R., and Ferrier-Pagès, C. (2015). New insights into carbon acquisition and exchanges within the coral–dinoflagellate symbiosis under NH4+ and NO3− supply. *Proc Biol Sci* 282. doi:10.1098/rspb.2015.0610.

Ezzat, L., Maguer, J.F., Grover, R., Rottier, C., Tremblay, P., and Ferrier-Pagès, C. (2019c). Nutrient starvation impairs the trophic plasticity of reef-building corals under ocean warming. *Functional Ecology* 33, 643–653. doi:10.1111/1365-2435.13285.

Fabricius, K. E. (2011). "Factors Determining the Resilience of Coral Reefs to Eutrophication: A Review and Conceptual Model," in *Coral Reefs: An Ecosystem in Transition*, eds. Z. Dubinsky and N. Stambler (Dordrecht: Springer Netherlands), 493–505. doi:10.1007/978-94-007-0114-4_28.

Faith, D. P. (1992). Conservation evaluation and phylogenetic diversity. *Biological Conservation* 61, 1–10. doi:10.1016/0006-3207(92)91201-3.

Falkowski, P. G., Dubinsky, Z., Muscatine, L., and McCloskey, L. (1993). Population Control in Symbiotic Corals. *BioScience* 43, 606–611. doi:10.2307/1312147.

Falkowski, P. G., Dubinsky, Z., Muscatine, L., and Porter, J. W. (1984). Light and the Bioenergetics of a Symbiotic Coral. *BioScience* 34, 705–709. doi:10.2307/1309663.

Finn, R. D., Clements, J., and Eddy, S. R. (2011). HMMER web server: interactive sequence similarity searching. *Nucleic Acids Research* 39, W29–W37. doi:10.1093/nar/gkr367.

Fiore, C. L., Labrie, M., Jarett, J. K., and Lesser, M. P. (2015). Transcriptional activity of the giant barrel sponge, Xestospongia muta Holobiont: molecular evidence for metabolic interchange. *Front. Microbiol.* 6. doi:10.3389/fmicb.2015.00364.

Folt, C. L., Chen, C. Y., Moore, M. V., and Burnaford, J. (1999). Synergism and antagonism among multiple stressors. *Limnology and Oceanography* 44, 864–877. doi:10.4319/lo.1999.44.3_part_2.0864.

Forget, N. L., and Juniper, S. K. (2013). Free-living bacterial communities associated with tubeworm (Ridgeia piscesae) aggregations in contrasting diffuse flow hydrothermal vent habitats at the Main Endeavour Field, Juan de Fuca Ridge. *MicrobiologyOpen* 2, 259–275. doi:10.1002/mbo3.70.

Furby, K. A., Apprill, A., Cervino, J. M., Ossolinski, J. E., and Hughen, K. A. (2014). Incidence of lesions on Fungiidae corals in the eastern Red Sea is related to water temperature and coastal pollution. *Marine Environmental Research* 98, 29–38. doi:10.1016/j.marenvres.2014.04.002.

Gajigan, A. P., Diaz, L. A., and Conaco, C. (2017a). Resilience of the prokaryotic microbial community of *Acropora digitifera* to elevated temperature. *MicrobiologyOpen* 6, e00478. doi:10.1002/mbo3.478.

Gajigan, A. P., Diaz, L. A., and Conaco, C. (2017b). Resilience of the prokaryotic microbial community of Acropora digitifera to elevated temperature. *Microbiologyopen* 6. doi:10.1002/mbo3.478.

Galic, N., Sullivan, L., Grimm, V., and Forbes, V. E. (2018). When things don't add up: quantifying impacts of multiple stressors from individual metabolism to ecosystem processing. *Ecology Letters* 21, 568–577. doi:10.1111/ele.12923.

Garren, M., and Azam, F. (2010). New Method for Counting Bacteria Associated with Coral Mucus. *Appl. Environ. Microbiol.* 76, 6128–6133. doi:10.1128/AEM.01100-10.

Garren, M., Raymundo, L., Guest, J., Harvell, C. D., and Azam, F. (2009). Resilience of Coral-Associated Bacterial Communities Exposed to Fish Farm Effluent. *PLoS ONE* 4, e7319. doi:10.1371/journal.pone.0007319.

Garren, M., Son, K., Raina, J.B., Rusconi, R., Menolascina, F., Shapiro, O. H., et al. (2014). A bacterial pathogen uses dimethylsulfoniopropionate as a cue to target heat-stressed corals. *The ISME Journal* 8, 999–1007. doi:10.1038/ismej.2013.210.

Gignoux-Wolfsohn, S. A., Aronson, F. M., and Vollmer, S. V. (2017). Complex interactions between potentially pathogenic, opportunistic, and resident bacteria emerge during infection on a reef-building coral. *FEMS Microbiol Ecol* 93. doi:10.1093/femsec/fix080.

Glasl, B., Bourne, D. G., Frade, P. R., Thomas, T., Schaffelke, B., and Webster, N. S. (2019). Microbial indicators of environmental perturbations in coral reef ecosystems. *Microbiome* 7, 94. doi:10.1186/s40168-019-0705-7.

Glasl, B., Bourne, D. G., Frade, P. R., and Webster, N. S. (2018). Establishing microbial baselines to identify indicators of coral reef health. *Microbiology Australia*. doi:10.1071/MA18011.

Glasl, B., Webster, N. S., and Bourne, D. G. (2017). Microbial indicators as a diagnostic tool for assessing water quality and climate stress in coral reef ecosystems. *Mar Biol* 164, 91. doi:10.1007/s00227-017-3097-x.

Gloor, G. B., Wu, J. R., Pawlowsky-Glahn, V., and Egozcue, J. J. (2016). It's all relative: analyzing microbiome data as compositions. *Annals of Epidemiology* 26, 322–329. doi:10.1016/j.annepidem.2016.03.003.

Godoy-Vitorino, F., Ruiz-Diaz, C. P., Rivera-Seda, A., Ramírez-Lugo, J. S., and Toledo-Hernández, C. (2017). The microbial biosphere of the coral Acropora cervicornis in Northeastern Puerto Rico. *PeerJ* 5, e3717. doi:10.7717/peerj.3717.

Goyal, A., Dubinkina, V., and Maslov, S. (2018). Multiple stable states in microbial communities explained by the stable marriage problem. *The ISME Journal* 12, 2823–2834. doi:10.1038/s41396-018-0222-x.

Graham, E. D., Heidelberg, J. F., and Tully, B. J. (2017). BinSanity: unsupervised clustering of environmental microbial assemblies using coverage and affinity propagation. *PeerJ* 5, e3035. doi:10.7717/peerj.3035.

Graham, E. D., Heidelberg, J. F., and Tully, B. J. (2018). Potential for primary productivity in a globally-distributed bacterial phototroph. *The ISME Journal* 12, 1861–1866. doi:10.1038/s41396-018-0091-3.

Grottoli, A. G., Martins, P. D., Wilkins, M. J., Johnston, M. D., Warner, M. E., Cai, W.-J., et al. (2018). Coral physiology and microbiome dynamics under combined warming and ocean acidification. *PLOS ONE* 13, e0191156. doi:10.1371/journal.pone.0191156.

Grottoli, A. G., Warner, M. E., Levas, S. J., Aschaffenburg, M. D., Schoepf, V., McGinley, M., et al. (2014). The cumulative impact of annual coral bleaching can turn some coral species winners into losers. *Global Change Biology* 20, 3823–3833. doi:10.1111/gcb.12658.

Gurry, T., Gibbons, S. M., Nguyen, L. T. T., Kearney, S. M., Ananthakrishnan, A., Jiang, X., et al. (2018). Predictability and persistence of prebiotic dietary supplementation in a healthy human cohort. *Scientific Reports* 8, 12699. doi:10.1038/s41598-018-30783-1.

Hadaidi, G., Röthig, T., Yum, L. K., Ziegler, M., Arif, C., Roder, C., et al. (2017). Stable mucus-associated bacterial communities in bleached and healthy corals of Porites lobata from the Arabian Seas. *Scientific Reports* 7, 45362. doi:10.1038/srep45362.

Hallam, S. J., Konstantinidis, K. T., Putnam, N., Schleper, C., Watanabe, Y., Sugahara, J., et al. (2006). Genomic analysis of the uncultivated marine crenarchaeote Cenarchaeum symbiosum. *PNAS* 103, 18296–18301. doi:10.1073/pnas.0608549103.

Haßler, K., Dähnke, K., Kölling, M., Sichoix, L., Nickl, A.-L., and Moosdorf, N. (2019). Provenance of nutrients in submarine fresh groundwater discharge on Tahiti and Moorea, French Polynesia. *Applied Geochemistry* 100, 181–189. doi:10.1016/j.apgeochem.2018.11.020.

Heip, C. H. R., Herman, P. M. J., and Soetaert, K. (2001). Indices of diversity and evenness. *Océanis* 24, 61–87.

Hernandez-Agreda, A., Leggat, W., Bongaerts, P., and Ainsworth, T. D. (2016). The Microbial Signature Provides Insight into the Mechanistic Basis of Coral Success across Reef Habitats. *mBio* 7. doi:10.1128/mBio.00560-16.

Hernandez-Agreda, A., Leggat, W., Bongaerts, P., Herrera, C., and Ainsworth, T. D. (2018). Rethinking the Coral Microbiome: Simplicity Exists within a Diverse Microbial Biosphere. *mBio* 9, e00812-18. doi:10.1128/mBio.00812-18.

Heron, S. F., Maynard, J. A., van Hooidonk, R., and Eakin, C. M. (2016). Warming Trends and Bleaching Stress of the World's Coral Reefs 1985–2012. *Scientific Reports* 6, 38402. doi:10.1038/srep38402.

Hoang, D. T., Chernomor, O., von Haeseler, A., Minh, B. Q., and Vinh, L. S. (2018). UFBoot2: Improving the Ultrafast Bootstrap Approximation. *Molecular Biology and Evolution* 35, 518–522. doi:10.1093/molbev/msx281.

Hoegh-Guldberg, O. (1999). Climate change, coral bleaching and the future of the world's coral reefs. *Mar. Freshwater Res.* doi:10.1071/MF99078.

Hofmeyr, S., Egan, R., Georganas, E., Copeland, A. C., Riley, R., Clum, A., et al. (2020). Terabase-scale metagenome coassembly with MetaHipMer. *Scientific Reports* 10, 10689. doi:10.1038/s41598-020-67416-5.

Holbrook, S. J., Adam, T. C., Edmunds, P. J., Schmitt, R. J., Carpenter, R. C., Brooks, A. J., et al. (2018). Recruitment Drives Spatial Variation in Recovery Rates of Resilient Coral Reefs. *Sci Rep* 8, 1–11. doi:10.1038/s41598-018-25414-8.

Huggett, M. J., and Apprill, A. (2019a). Coral microbiome database: Integration of sequences reveals high diversity and relatedness of coral-associated microbes. *Environmental Microbiology Reports* 11, 372–385. doi:10.1111/1758-2229.12686.

Huggett, M. J., and Apprill, A. (2019b). Coral microbiome database: Integration of sequences reveals high diversity and relatedness of coral-associated microbes. *Environmental Microbiology Reports* 11, 372–385. doi:10.1111/1758-2229.12686.

Hughes, T. P., Anderson, K. D., Connolly, S. R., Heron, S. F., Kerry, J. T., Lough, J. M., et al. (2018). Spatial and temporal patterns of mass bleaching of corals in the Anthropocene. *Science* 359, 80–83. doi:10.1126/science.aan8048.

Hughes, T. P., Kerry, J. T., Álvarez-Noriega, M., Álvarez-Romero, J. G., Anderson, K. D., Baird, A. H., et al. (2017). Global warming and recurrent mass bleaching of corals. *Nature* 543, 373–377. doi:10.1038/nature21707.

Hughes, T. P., Kerry, J. T., Connolly, S. R., Baird, A. H., Eakin, C. M., Heron, S. F., et al. (2019). Ecological memory modifies the cumulative impact of recurrent climate extremes. *Nature Climate Change* 9, 40–43. doi:10.1038/s41558-018-0351-2.

Hyatt, D., Chen, G.-L., LoCascio, P. F., Land, M. L., Larimer, F. W., and Hauser, L. J. (2010). Prodigal: prokaryotic gene recognition and translation initiation site identification. *BMC Bioinformatics* 11, 119. doi:10.1186/1471-2105-11-119.

Hyun, D.-W., Shin, N.-R., Kim, M.-S., Oh, S. J., Kim, P. S., Whon, T. W., et al. (2014). Endozoicomonas atrinae sp. nov., isolated from the intestine of a comb pen shell Atrina pectinata. *International Journal of Systematic and Evolutionary Microbiology* 64, 2312–2318. doi:10.1099/ijs.0.060780-0.

Imlay, J. A. (2019). Where in the world do bacteria experience oxidative stress? *Environmental Microbiology* 21, 521–530. doi:10.1111/1462-2920.14445.

Jain, C., Rodriguez-R, L. M., Phillippy, A. M., Konstantinidis, K. T., and Aluru, S. (2018). High throughput ANI analysis of 90K prokaryotic genomes reveals clear species boundaries. *Nature Communications* 9, 5114. doi:10.1038/s41467-018-07641-9.

Jensen, S., Duperron, S., Birkeland, N.-K., and Hovland, M. (2010). Intracellular Oceanospirillales bacteria inhabit gills of Acesta bivalves: Acesta excavata bivalve bacterium. *FEMS Microbiology Ecology* 74, 523–533. doi:10.1111/j.1574-6941.2010.00981.x.

Jernigan, K. K., and Bordenstein, S. R. (2014). Ankyrin domains across the Tree of Life. *PeerJ* 2, e264. doi:10.7717/peerj.264.

Kalyaanamoorthy, S., Minh, B. Q., Wong, T. K. F., von Haeseler, A., and Jermiin, L. S. (2017). ModelFinder: fast model selection for accurate phylogenetic estimates. *Nature Methods* 14, 587–589. doi:10.1038/nmeth.4285.

Kamke, J., Rinke, C., Schwientek, P., Mavromatis, K., Ivanova, N., Sczyrba, A., et al. (2014). The Candidate Phylum Poribacteria by Single-Cell Genomics: New Insights into Phylogeny, Cell-Compartmentation, Eukaryote-Like Repeat

Proteins, and Other Genomic Features. *PLOS ONE* 9, e87353. doi:10.1371/journal.pone.0087353.

Kanehisa, M., Furumichi, M., Tanabe, M., Sato, Y., and Morishima, K. (2017). KEGG: new perspectives on genomes, pathways, diseases and drugs. *Nucleic Acids Res* 45, D353–D361. doi:10.1093/nar/gkw1092.

Katharios, P., Seth-Smith, H. M. B., Fehr, A., Mateos, J. M., Qi, W., Richter, D., et al. (2015). Environmental marine pathogen isolation using mesocosm culture of sharpsnout seabream: striking genomic and morphological features of novel Endozoicomonas sp. *Scientific Reports* 5, 17609. doi:10.1038/srep17609.

Katoh, K., Misawa, K., Kuma, K., and Miyata, T. (2002). MAFFT: a novel method for rapid multiple sequence alignment based on fast Fourier transform. *Nucleic Acids Res* 30, 3059–3066. doi:10.1093/nar/gkf436

Katoh, K., and Standley, D. M. (2013). MAFFT Multiple Sequence Alignment Software Version 7: Improvements in Performance and Usability. *Mol Biol Evol* 30, 772–780. doi:10.1093/molbev/mst010.

Kelly, L. W., Williams, G. J., Barott, K. L., Carlson, C. A., Dinsdale, E. A., Edwards, R. A., et al. (2014). Local genomic adaptation of coral reef-associated microbiomes to gradients of natural variability and anthropogenic stressors. *PNAS* 111, 10227–10232. doi:10.1073/pnas.1403319111.

Kimes, N. E., Nostrand, J. D. V., Weil, E., Zhou, J., and Morris, P. J. (2010). Microbial functional structure of Montastraea faveolata, an important Caribbean reef-building coral, differs between healthy and yellow-band diseased colonies. *Environmental Microbiology* 12, 541–556. doi:10.1111/j.1462-2920.2009.02113.x.

Klaus, J. S., Janse, I., Heikoop, J. M., Sanford, R. A., and Fouke, B. W. (2007). Coral microbial communities, zooxanthellae and mucus along gradients of seawater depth and coastal pollution. *Environ. Microbiol.* 9, 1291–1305. doi:10.1111/j.1462-2920.2007.01249.x.

Klinges, G., Maher, R. L., Vega Thurber, R. L., and Muller, E. M. (2020). Parasitic ‘ *Candidatus* Aquarickettsia rohweri’ is a marker of disease susceptibility in *ACROPORA CERVICORNIS* but is lost during thermal stress. *Environmental Microbiology*. doi:10.1111/1462-2920.15245.

Klinges, J. G., Rosales, S. M., McMinds, R., Shaver, E. C., Shantz, A. A., Peters, E. C., et al. (2019). Phylogenetic, genomic, and biogeographic characterization of a novel and ubiquitous marine invertebrate-associated Rickettsiales parasite, Candidatus Aquarickettsia rohweri, gen. nov., sp. nov. *The ISME Journal* 13, 2938–2953. doi:10.1038/s41396-019-0482-0.

Knight, R., Vrbanac, A., Taylor, B. C., Aksenov, A., Callewaert, C., Debelius, J., et al. (2018). Best practices for analysing microbiomes. *Nature Reviews Microbiology* 16, 410–422. doi:10.1038/s41579-018-0029-9.

Knutson, T. R., McBride, J. L., Chan, J., Emanuel, K., Holland, G., Landsea, C., et al. (2010). Tropical cyclones and climate change. *Nature Geoscience* 3, 157–163. doi:10.1038/ngeo779.

Koren, O., and Rosenberg, E. (2008). Bacteria associated with the bleached and cave coral Oculina patagonica. *Microb. Ecol.* 55, 523–529. doi:10.1007/s00248-007-9297-z.

Kozich, J. J., Westcott, S. L., Baxter, N. T., Highlander, S. K., and Schloss, P. D. (2013). Development of a Dual-Index Sequencing Strategy and Curation Pipeline for Analyzing Amplicon Sequence Data on the MiSeq Illumina Sequencing Platform. *Applied and Environmental Microbiology* 79, 5112–5120. doi:10.1128/AEM.01043-13.

Krediet Cory J., Ritchie Kim B., Paul Valerie J., and Teplitski Max (2013). Coral-associated micro-organisms and their roles in promoting coral health and thwarting diseases. *Proceedings of the Royal Society B: Biological Sciences* 280, 20122328. doi:10.1098/rspb.2012.2328.

Kuntz, N., Kline, D., Sandin, S., and Rohwer, F. (2005). Pathologies and mortality rates caused by organic carbon and nutrient stressors in three Caribbean coral species. *Marine Ecology Progress Series* 294. doi:10.3354/meps294173.

Kurahashi, M., and Yokota, A. (2007). Endozoicomonas elysicola gen. nov., sp. nov., a γ-proteobacterium isolated from the sea slug Elysia ornata. *Systematic and Applied Microbiology* 30, 202–206. doi:10.1016/j.syapm.2006.07.003.

Langmead, B., and Salzberg, S. L. (2012). Fast gapped-read alignment with Bowtie 2. *Nat Meth* 9, 357–359. doi:10.1038/nmeth.1923.

Lapointe, B. E., Brewton, R. A., Herren, L. W., Porter, J. W., and Hu, C. (2019). Nitrogen enrichment, altered stoichiometry, and coral reef decline at Looe Key, Florida Keys, USA: a 3-decade study. *Mar Biol* 166, 108. doi:10.1007/s00227-019-3538-9.

Lee, O. O., Yang, J., Bougouffa, S., Wang, Y., Batang, Z., Tian, R., et al. (2012). Spatial and species variations in bacterial communities associated with corals from the Red Sea as revealed by pyrosequencing. *Appl. Environ. Microbiol.* 78, 7173–7184. doi:10.1128/AEM.01111-12.

Lema, K. A., Bourne, D. G., and Willis, B. L. (2014). Onset and establishment of diazotrophs and other bacterial associates in the early life history stages of the

coral Acropora millepora. *Molecular Ecology* 23, 4682–4695. doi:10.1111/mec.12899.

Lema, K. A., Willis, B. L., and Bourne, D. G. (2012). Corals Form Characteristic Associations with Symbiotic Nitrogen-Fixing Bacteria. *Applied and Environmental Microbiology* 78, 3136–3144. doi:10.1128/AEM.07800-11.

Lesser, M., Falcón, L., Rodríguez-Román, A., Enríquez, S., Hoegh-Guldberg, O., and Iglesias-Prieto, R. (2007). Nitrogen fixation by symbiotic cyanobacteria provides a source of nitrogen for the scleractinian coral Montastraea cavernosa. *Marine Ecology Progress Series* 346, 143–152. doi:10.3354/meps07008.

Lesser, M. P. (2006). Oxidative Stress In Marine Environments: Biochemistry and Physiological Ecology. *Annual Review of Physiology* 68, 253–278. doi:10.1146/annurev.physiol.68.040104.110001.

Lesser, M. P., Fiore, C., Slattery, M., and Zaneveld, J. (2016). Climate change stressors destabilize the microbiome of the Caribbean barrel sponge, Xestospongia muta. *Journal of Experimental Marine Biology and Ecology* 475, 11–18. doi:10.1016/j.jembe.2015.11.004.

Lesser, M. P., Mazel, C. H., Gorbunov, M. Y., and Falkowski, P. G. (2004). Discovery of Symbiotic Nitrogen-Fixing Cyanobacteria in Corals. *Science* 305, 997–1000. doi:10.1126/science.1099128.

Lewis, J. D., Chen, E. Z., Baldassano, R. N., Otley, A. R., Griffiths, A. M., Lee, D., et al. (2015). Inflammation, Antibiotics, and Diet as Environmental Stressors of the Gut Microbiome in Pediatric Crohn's Disease. *Cell Host & Microbe* 18, 489–500. doi:10.1016/j.chom.2015.09.008.

Li, D., Liu, C.-M., Luo, R., Sadakane, K., and Lam, T.-W. (2015a). MEGAHIT: an ultra-fast single-node solution for large and complex metagenomics assembly via succinct de Bruijn graph. *Bioinformatics* 31, 1674–1676. doi:10.1093/bioinformatics/btv033.

Li, H., Handsaker, B., Wysoker, A., Fennell, T., Ruan, J., Homer, N., et al. (2009). The Sequence Alignment/Map format and SAMtools. *Bioinformatics* 25, 2078–2079. doi:10.1093/bioinformatics/btp352.

Li, J., Chen, Q., Long, L.-J., Dong, J.-D., Yang, J., and Zhang, S. (2015b). Bacterial dynamics within the mucus, tissue and skeleton of the coral Porites lutea during different seasons. *Scientific Reports* 4. doi:10.1038/srep07320.

Li, J., Chen, Q., Zhang, S., Huang, H., Yang, J., Tian, X.-P., et al. (2013). Highly Heterogeneous Bacterial Communities Associated with the South China Sea

Reef Corals Porites lutea, Galaxea fascicularis and Acropora millepora. *PLOS ONE* 8, e71301. doi:10.1371/journal.pone.0071301.

Littman, R. A., Willis, B. L., Pfeffer, C., and Bourne, D. G. (2009). Diversities of coral-associated bacteria differ with location, but not species, for three acroporid corals on the Great Barrier Reef. *FEMS Microbiology Ecology* 68, 152–163. doi:10.1111/j.1574-6941.2009.00666.x.

Littman, R., Willis, B. L., and Bourne, D. G. (2011). Metagenomic analysis of the coral holobiont during a natural bleaching event on the Great Barrier Reef. *Environmental Microbiology Reports* 3, 651–660. doi:10.1111/j.1758-2229.2010.00234.x.

Liu, D. (2015). "Chapter 55 - Enterotoxin-Producing Staphylococcus aureus," in *Molecular Medical Microbiology (Second Edition)*, eds. Y.-W. Tang, M. Sussman, D. Liu, I. Poxton, and J. Schwartzman (Boston: Academic Press), 979–995. doi:10.1016/B978-0-12-397169-2.00055-X.

Lokmer, A., and Wegner, K. M. (2015). Hemolymph microbiome of Pacific oysters in response to temperature, temperature stress and infection. *The ISME journal* 9, 670. doi:10.1038/ismej.2014.160

Love, M. I., Huber, W., and Anders, S. (2014). Moderated estimation of fold change and dispersion for RNA-seq data with DESeq2. *Genome Biology* 15. doi:10.1186/s13059-014-0550-8.

Lovelock, J. E., Maggs, R. J., and Rasmussen, R. A. (1972). Atmospheric Dimethyl Sulphide and the Natural Sulphur Cycle. *Nature* 237, 452–453. doi:10.1038/237452a0.

Lozupone, C. A., Hamady, M., Kelley, S. T., and Knight, R. (2007). Quantitative and qualitative beta diversity measures lead to different insights into factors that structure microbial communities. *Appl. Environ. Microbiol.* 73, 1576–1585. doi:10.1128/AEM.01996-06.

Lozupone, C., and Knight, R. (2005). UniFrac: a New Phylogenetic Method for Comparing Microbial Communities. *Applied and Environmental Microbiology* 71, 8228–8235. doi:10.1128/AEM.71.12.8228-8235.2005.

Lozupone, C., Lladser, M. E., Knights, D., Stombaugh, J., and Knight, R. (2011). UniFrac: an effective distance metric for microbial community comparison. *The ISME Journal* 5, 169–172. doi:10.1038/ismej.2010.133.

Luo, C., Tsementzi, D., Kyrpides, N. C., and Konstantinidis, K. T. (2012). Individual genome assembly from complex community short-read metagenomic datasets. *The ISME Journal* 6, 898–901. doi:10.1038/ismej.2011.147.

Maher, R. L., Rice, M. M., McMinds, R., Burkepile, D. E., and Vega Thurber, R. (2019). Multiple stressors interact primarily through antagonism to drive changes in the coral microbiome. *Scientific Reports* 9, 6834. doi:10.1038/s41598-019-43274-8.

Maher, R. L., Schmeltzer, E. R., Meiling, S., McMinds, R., Ezzat, L., Shantz, A. A., et al. (2020). Coral Microbiomes Demonstrate Flexibility and Resilience Through a Reduction in Community Diversity Following a Thermal Stress Event. *Front. Ecol. Evol.* 8. doi:10.3389/fevo.2020.555698.

Malgieri, G., Palmieri, M., Russo, L., Fattorusso, R., Pedone, P. V., and Isernia, C. (2015). The prokaryotic zinc-finger: structure, function and comparison with the eukaryotic counterpart. *The FEBS Journal* 282, 4480–4496. doi:10.1111/febs.13503.

Maliao, R. J., Turingan, R. G., and Lin, J. (2008). Phase-shift in coral reef communities in the Florida Keys National Marine Sanctuary (FKNMS), USA. *Marine Biology* 154, 841–853. doi:10.1007/s00227-008-0977-0.

Mandal, S., Van Treuren, W., White, R. A., Eggesbø, M., Knight, R., and Peddada, S. D. (2015). Analysis of composition of microbiomes: a novel method for studying microbial composition. *Microb Ecol Health Dis* 26. doi:10.3402/mehd.v26.27663.

Martin, M. (2011). Cutadapt removes adapter sequences from high-throughput sequencing reads. *EMBnet.journal* 17, 10–12. doi:10.14806/ej.17.1.200.

Martinez Arbizu, P. (2017). pairwiseAdonis: Pairwise multilevel comparison using adonis. *R package version 0.0.1*.

Martínez-Ramos, M., Ortiz-Rodríguez, I. A., Piñero, D., Dirzo, R., and Sarukhán, J. (2016). Anthropogenic disturbances jeopardize biodiversity conservation within tropical rainforest reserves. *PNAS* 113, 5323–5328. doi:10.1073/pnas.1602893113.

Martiny, J. B. H., Jones, S. E., Lennon, J. T., and Martiny, A. C. (2015). Microbiomes in light of traits: A phylogenetic perspective. *Science* 350. doi:10.1126/science.aac9323.

McClanahan, T. R., and Kurtis, J. D. (1991). Population regulation of the rock-boring sea urchin Echinometra mathaei (de Blainville). *Journal of Experimental Marine Biology and Ecology* 147, 121–146. doi:10.1016/0022-0981(91)90041-T.

McCook, L., Jompa, J., and Diaz-Pulido, G. (2001). Competition between corals and algae on coral reefs: a review of evidence and mechanisms. *Coral Reefs* 19, 400–417. doi:10.1007/s003380000129.

McCutcheon, J. P., and Moran, N. A. (2012). Extreme genome reduction in symbiotic bacteria. *Nature Reviews Microbiology* 10, 13–26. doi:10.1038/nrmicro2670.

McDevitt-Irwin, J. M., Baum, J. K., Garren, M., and Vega Thurber, R. L. (2017a). Responses of Coral-Associated Bacterial Communities to Local and Global Stressors. *Front. Mar. Sci.* 4. doi:10.3389/fmars.2017.00262.

McDevitt-Irwin, J. M., Baum, J. K., Garren, M., and Vega Thurber, R. L. (2017b). Responses of Coral-Associated Bacterial Communities to Local and Global Stressors. *Frontiers in Marine Science* 4, 262. doi:10.3389/fmars.2017.00262.

McDonald, D., Price, M. N., Goodrich, J., Nawrocki, E. P., DeSantis, T. Z., Probst, A., et al. (2012). An improved Greengenes taxonomy with explicit ranks for ecological and evolutionary analyses of bacteria and archaea. *The ISME journal* 6, 610–618. doi:10.1038/ismej.2011.139

McFall-Ngai, M., Hadfield, M. G., Bosch, T. C. G., Carey, H. V., Domazet-Lošo, T., Douglas, A. E., et al. (2013). Animals in a bacterial world, a new imperative for the life sciences. *PNAS* 110, 3229–3236. doi:10.1073/pnas.1218525110.

McMurdie, P. J., and Holmes, S. (2013). phyloseq: An R Package for Reproducible Interactive Analysis and Graphics of Microbiome Census Data. *PLoS ONE* 8, e61217. doi:10.1371/journal.pone.0061217.

McMurdie, P. J., and Holmes, S. (2014). Waste not, want not: why rarefying microbiome data is inadmissible. *PLoS computational biology* 10, e1003531. doi:10.1371/journal.pcbi.1003531.

Mendoza, M., Güiza, L., Martinez, X., Caraballo, X., Rojas, J., Aranguren, L., et al. (2013). A novel agent (Endozoicomonas elysicola) responsible for epitheliocystis in cobia Rachycentrum canadum larvae. *Dis. Aquat. Org.* 106, 31–37. doi:10.3354/dao02636.

Meron, D., Atias, E., Iasur Kruh, L., Elifantz, H., Minz, D., Fine, M., et al. (2011). The impact of reduced pH on the microbial community of the coral Acropora eurystoma. *ISME J* 5, 51–60. doi:10.1038/ismej.2010.102.

Meyer, J. L., Rodgers, J. M., Dillard, B. A., Paul, V. J., and Teplitski, M. (2016). Epimicrobiota Associated with the Decay and Recovery of Orbicella Corals Exhibiting Dark Spot Syndrome. *Front. Microbiol.* 7. doi:10.3389/fmicb.2016.00893.

Miller, I. J., Weyna, T. R., Fong, S. S., Lim-Fong, G. E., and Kwan, J. C. (2016). Single sample resolution of rare microbial dark matter in a marine invertebrate metagenome. *Sci Rep* 6. doi:10.1038/srep34362.

Minh, B. Q., Schmidt, H. A., Chernomor, O., Schrempf, D., Woodhams, M. D., von Haeseler, A., et al. (2020). IQ-TREE 2: New Models and Efficient Methods for Phylogenetic Inference in the Genomic Era. *Molecular Biology and Evolution* 37, 1530–1534. doi:10.1093/molbev/msaa015.

Mistry, J., Chuguransky, S., Williams, L., Qureshi, M., Salazar, G. A., Sonnhammer, E. L. L., et al. (2021). Pfam: The protein families database in 2021. *Nucleic Acids Research* 49, D412–D419. doi:10.1093/nar/gkaa913.

Moberg, F., and Folke, C. (1999). Ecological goods and services of coral reef ecosystems. *Ecological Economics* 29, 215–233. doi:10.1016/S0921-8009(99)00009-9.

Mohamed, N. M., Cicirelli, E. M., Kan, J., Chen, F., Fuqua, C., and Hill, R. T. (2008). Diversity and quorum-sensing signal production of Proteobacteria associated with marine sponges. *Environmental Microbiology* 10, 75–86. doi:10.1111/j.1462-2920.2007.01431.x.

Moitinho-Silva, L., Nielsen, S., Amir, A., Gonzalez, A., Ackermann, G. L., Cerrano, C., et al. (2017). The sponge microbiome project. *Gigascience* 6, 1–7. doi:10.1093/gigascience/gix077.

Moran, N. A. (2007). Symbiosis as an adaptive process and source of phenotypic complexity. *PNAS* 104, 8627–8633. doi:10.1073/pnas.0611659104.

Morelan, I. A., Gaulke, C. A., Sharpton, T. J., Vega Thurber, R., and Denver, D. R. (2019). Microbiome Variation in an Intertidal Sea Anemone Across Latitudes and Symbiotic States. *Front. Mar. Sci.* 6. doi:10.3389/fmars.2019.00007.

Moriya, Y., Itoh, M., Okuda, S., Yoshizawa, A. C., and Kanehisa, M. (2007). KAAS: an automatic genome annotation and pathway reconstruction server. *Nucleic Acids Res* 35, W182-185. doi:10.1093/nar/gkm321.

Morrow, K., Liles, M., Paul, V., Moss, A., and Chadwick, N. (2013). Bacterial shifts associated with coral–macroalgal competition in the Caribbean Sea. *Marine Ecology Progress Series* 488, 117. doi:10.3354/meps10394.

Morrow, K. M., Bourne, D. G., Humphrey, C., Botté, E. S., Laffy, P., Zaneveld, J., et al. (2015). Natural volcanic CO2 seeps reveal future trajectories for host–microbial associations in corals and sponges. *ISME J* 9, 894–908. doi:10.1038/ismej.2014.188.

Morrow, K. M., Moss, A. G., Chadwick, N. E., and Liles, M. R. (2012). Bacterial Associates of Two Caribbean Coral Species Reveal Species-Specific Distribution and Geographic Variability. *Appl. Environ. Microbiol.* 78, 6438–6449. doi:10.1128/AEM.01162-12.

Morris, L. A., Voolstra, C. R., Quigley, K. M., Bourne, D. G., and Bay, L. K. (2019). Nutrient Availability and Metabolism Affect the Stability of Coral–Symbiodiniaceae Symbioses. *Trends in Microbiology* 27, 678–689. doi:10.1016/j.tim.2019.03.004.

Mouchka, M. E., Hewson, I., and Harvell, C. D. (2010). Coral-Associated Bacterial Assemblages: Current Knowledge and the Potential for Climate-Driven Impacts. *Integr Comp Biol* 50, 662–674. doi:10.1093/icb/icq061.

Munson, R. S. (1990). Haemophilus influenzae: surface antigens and aspects of virulence. *Can J Vet Res* 54 Suppl, S63-67.

Neave, M. J., Apprill, A., Ferrier-Pagès, C., and Voolstra, C. R. (2016). Diversity and function of prevalent symbiotic marine bacteria in the genus Endozoicomonas. *Appl Microbiol Biotechnol* 100, 8315–8324. doi:10.1007/s00253-016-7777-0.

Neave, M. J., Michell, C. T., Apprill, A., and Voolstra, C. R. (2014). Whole-Genome Sequences of Three Symbiotic Endozoicomonas Bacteria. *Genome Announc* 2. doi:10.1128/genomeA.00802-14.

Neave, M. J., Michell, C. T., Apprill, A., and Voolstra, C. R. (2017a). Endozoicomonas genomes reveal functional adaptation and plasticity in bacterial strains symbiotically associated with diverse marine hosts. *Sci Rep* 7, 40579. doi:10.1038/srep40579.

Neave, M. J., Rachmawati, R., Xun, L., Michell, C. T., Bourne, D. G., Apprill, A., et al. (2017b). Differential specificity between closely related corals and abundant Endozoicomonas endosymbionts across global scales. *The ISME Journal* 11, 186–200. doi:10.1038/ismej.2016.95.

Nguyen, M. T. H. D., Liu, M., and Thomas, T. (2014). Ankyrin-repeat proteins from sponge symbionts modulate amoebal phagocytosis. *Molecular Ecology* 23, 1635–1645. doi:10.1111/mec.12384.

Nicolet, K. J., Chong-Seng, K. M., Pratchett, M. S., Willis, B. L., and Hoogenboom, M. O. (2018). Predation scars may influence host susceptibility to pathogens: evaluating the role of corallivores as vectors of coral disease. *Scientific Reports* 8, 1–10. doi:10.1038/s41598-018-23361-y.

Nielsen, D. A., Petrou, K., and Gates, R. D. (2018). Coral bleaching from a single cell perspective. *The ISME Journal* 12, 1558–1567. doi:10.1038/s41396-018-0080-6.

Nishijima, M., Adachi, K., Katsuta, A., Shizuri, Y., and Yamasato, K. 2013 (2013). Endozoicomonas numazuensis sp. nov., a gammaproteobacterium isolated from marine sponges, and emended description of the genus Endozoicomonas Kurahashi and Yokota 2007. *International Journal of Systematic and Evolutionary Microbiology* 63, 709–714. doi:10.1099/ijs.0.042077-0.

Nurk, S., Meleshko, D., Korobeynikov, A., and Pevzner, P. A. (2017). metaSPAdes: a new versatile metagenomic assembler. *Genome Res* 27, 824–834. doi:10.1101/gr.213959.116.

Olesen, S. W., and Alm, E. J. (2016). Dysbiosis is not an answer. *Nature Microbiology* 1, 16228. doi:10.1038/nmicrobiol.2016.228.

Paine, R. T., Tegner, M. J., and Johnson, E. A. (1998). Compounded Perturbations Yield Ecological Surprises. *Ecosystems* 1, 535–545. doi:10.1007/s100219900049.

Palardy, J. E., Rodrigues, L. J., and Grottoli, A. G. (2008). The importance of zooplankton to the daily metabolic carbon requirements of healthy and bleached corals at two depths. *Journal of Experimental Marine Biology and Ecology* 367, 180–188. doi:10.1016/j.jembe.2008.09.015.

Parada, A. E., Needham, D. M., and Fuhrman, J. A. (2016). Every base matters: assessing small subunit rRNA primers for marine microbiomes with mock communities, time series and global field samples. *Environ. Microbiol.* 18, 1403–1414. doi:10.1111/1462-2920.13023.

Parks, D. H., Imelfort, M., Skennerton, C. T., Hugenholtz, P., and Tyson, G. W. (2015). CheckM: assessing the quality of microbial genomes recovered from isolates, single cells, and metagenomes. *Genome Res.* 25, 1043–1055. doi:10.1101/gr.186072.114.

Payne, S. H., and Loomis, W. F. (2006). Retention and Loss of Amino Acid Biosynthetic Pathways Based on Analysis of Whole-Genome Sequences. *Eukaryotic Cell* 5, 272–276. doi:10.1128/EC.5.2.272-276.2006.

Penin, L., Adjeroud, M., Schrimm, M., and Lenihan, H. S. (2007). High spatial variability in coral bleaching around Moorea (French Polynesia): patterns across locations and water depths. *Comptes Rendus Biologies* 330, 171–181. doi:10.1016/j.crvi.2006.12.003.

Pettersson, J., Holmström, A., Hill, J., Leary, S., Frithz-Lindsten, E., Euler-Matell, A. V., et al. (1999). The V-antigen of Yersinia is surface exposed before target cell contact and involved in virulence protein translocation. *Molecular Microbiology* 32, 961–976. doi:10.1046/j.1365-2958.1999.01408.x.

Pinzón, J. H., Sampayo, E., Cox, E., Chauka, L. J., Chen, C. A., Voolstra, C. R., et al. (2013). Blind to morphology: genetics identifies several widespread ecologically common species and few endemics among Indo-Pacific cauliflower corals (Pocillopora, Scleractinia). *Journal of Biogeography* 40, 1595–1608. doi:10.1111/jbi.12110.

Planes, S., Allemand, D., Agostini, S., Banaigs, B., Boissin, E., Boss, E., et al. (2019). The Tara Pacific expedition—A pan-ecosystemic approach of the "-omics" complexity of coral reef holobionts across the Pacific Ocean. *PLOS Biology* 17, e3000483. doi:10.1371/journal.pbio.3000483.

Pogoreutz, C., Rädecker, N., Cárdenas, A., Gärdes, A., Wild, C., and Voolstra, C. R. (2018). Dominance of Endozoicomonas bacteria throughout coral bleaching and mortality suggests structural inflexibility of the Pocillopora verrucosa microbiome. *Ecol Evol* 8, 2240–2252. doi:10.1002/ece3.3830.

Pollock, F. J., McMinds, R., Smith, S., Bourne, D. G., Willis, B. L., Medina, M., et al. (2018). Coral-associated bacteria demonstrate phylosymbiosis and cophylogeny. *Nat Commun* 9, 1–13. doi:10.1038/s41467-018-07275-x.

Pollock, F. J., Wada, N., Torda, G., Willis, B. L., and Bourne, D. G. (2017). White Syndrome-Affected Corals Have a Distinct Microbiome at Disease Lesion Fronts. *Appl. Environ. Microbiol.* 83, e02799-16. doi:10.1128/AEM.02799-16.

Pratchett, M. S., McCowan, D., Maynard, J. A., and Heron, S. F. (2013). Changes in Bleaching Susceptibility among Corals Subject to Ocean Warming and Recurrent Bleaching in Moorea, French Polynesia. *PLoS ONE* 8, e70443. doi:10.1371/journal.pone.0070443.

Preston, G. M. (2007). Metropolitan Microbes: Type III Secretion in Multihost Symbionts. *Cell Host & Microbe* 2, 291–294. doi:10.1016/j.chom.2007.10.004.

Price, M. N., Dehal, P. S., and Arkin, A. P. (2010). FastTree 2–approximately maximum-likelihood trees for large alignments. *PloS one* 5, e9490. doi:10.1371/journal.pone.0009490.

Pritchard, L., Glover, R. H., Humphris, S., Elphinstone, J. G., and Toth, I. K. (2015). Genomics and taxonomy in diagnostics for food security: soft-rotting

enterobacterial plant pathogens. *Anal. Methods* 8, 12–24. doi:10.1039/C5AY02550H.

Qi, W., Cascarano, M. C., Schlapbach, R., Katharios, P., Vaughan, L., and Seth-Smith, H. M. B. (2018). Ca. Endozoicomonas cretensis: A Novel Fish Pathogen Characterized by Genome Plasticity. *Genome Biol Evol* 10, 1363–1374. doi:10.1093/gbe/evy092.

Quast, C., Pruesse, E., Yilmaz, P., Gerken, J., Schweer, T., Yarza, P., et al. (2012). The SILVA ribosomal RNA gene database project: improved data processing and web-based tools. *Nucleic Acids Research* 41, D590–D596. doi:10.1093/nar/gks1219.

R Core Team (2019). R: A language and environment for statistical computing. Available at: https://www.R-project.org/.

Rädecker, N., Pogoreutz, C., Voolstra, C. R., Wiedenmann, J., and Wild, C. (2015). Nitrogen cycling in corals: the key to understanding holobiont functioning? *Trends in Microbiology* 23, 490–497. doi:10.1016/j.tim.2015.03.008.

Raimundo, I., Silva, R., Meunier, L., Valente, S. M., Lago-Lestón, A., Keller-Costa, T., et al. (2021). Functional metagenomics reveals differential chitin degradation and utilization features across free-living and host-associated marine microbiomes. *Microbiome* 9, 43. doi:10.1186/s40168-020-00970-2.

Raina, J.-B., Tapiolas, D. M., Forêt, S., Lutz, A., Abrego, D., Ceh, J., et al. (2013). DMSP biosynthesis by an animal and its role in coral thermal stress response. *Nature* 502, 677–680. doi:10.1038/nature12677.

Raina, J.-B., Tapiolas, D., Willis, B. L., and Bourne, D. G. (2009). Coral-Associated Bacteria and Their Role in the Biogeochemical Cycling of Sulfur. *AEM* 75, 3492–3501. doi:10.1128/AEM.02567-08.

Reaka-Kudla, M. L. (1997). "The global biodiversity of coral reefs: a comparison with rain forests," in *Biodiversity II: understanding and protecting our biological resources*, eds. M. L. Reaka-Kudla, D. E. Wilson, and E. O. Wilson (Washington, D.C.: Joseph Henry Press), 83–108.

Reshef, L., Koren, O., Loya, Y., Zilber-Rosenberg, I., and Rosenberg, E. (2006). The Coral Probiotic Hypothesis. *Environmental Microbiology* 8, 2068–2073. doi:10.1111/j.1462-2920.2006.01148.x.

Rice, M. M., Maher, R. L., Vega Thurber, R., and Burkepile, D. E. (2019). Different nitrogen sources speed recovery from corallivory and uniquely alter the microbiome of a reef-building coral. *PeerJ* 7, e8056. doi:10.7717/peerj.8056.

Rideout, J. R., He, Y., Navas-Molina, J. A., Walters, W. A., Ursell, L. K., Gibbons, S. M., et al. (2014). Subsampled open-reference clustering creates consistent, comprehensive OTU definitions and scales to billions of sequences. *PeerJ* 2, e545. doi:10.7717/peerj.545.

Ritchie, K. (2006). Regulation of microbial populations by coral surface mucus and mucus-associated bacteria. *Marine Ecology Progress Series* 322, 1–14. doi:10.3354/meps322001.

Ritchie, K. B., Dennis, J. H., McGrath, T., and Smith, G. (1994). Bacteria associated with bleached and nonbleached areas of Montastrea annularis. In *Proceedings of the 5th Symposium of the National History of the Bahamas*, vol. 5. (Bahamian Field Station: San Salvador, Bahamas: Kass LB), 75–80.

Robbins, S. J., Singleton, C. M., Chan, C. X., Messer, L. F., Geers, A. U., Ying, H., et al. (2019). A genomic view of the reef-building coral Porites lutea and its microbial symbionts. *Nature Microbiology* 4, 2090–2100. doi:10.1038/s41564-019-0532-4.

Rogers, C., and Miller, J. (2006). Permanent phase shifts or reversible declines in coral cover? Lack of recovery of two coral reefs inSt. John, US Virgin Islands. *Marine Ecology Progress Series* 306, 103–114. doi:10.3354/meps306103.

Rognes, T., Flouri, T., Nichols, B., Quince, C., and Mahé, F. (2016). VSEARCH: a versatile open source tool for metagenomics. *PeerJ* 4, e2584. doi:10.7717/peerj.2584.

Rohwer, F., Seguritan, V., Azam, F., and Knowlton, N. (2002). Diversity and distribution of coral-associated bacteria. *Mar Ecol Prog Ser* 243, 1–10. doi:10.3354/meps243001.

Rosenberg, E., and Kushmaro, A. (2011). "Microbial Diseases of Corals: Pathology and Ecology," in *Coral Reefs: An Ecosystem in Transition*, eds. Z. Dubinsky and N. Stambler (Dordrecht: Springer Netherlands), 451–464. doi:10.1007/978-94-007-0114-4_26.

Röthig, T., Ochsenkühn, M. A., Roik, A., Merwe, R. van der, and Voolstra, C. R. (2016). Long-term salinity tolerance is accompanied by major restructuring of the coral bacterial microbiome. *Molecular Ecology* 25, 1308–1323. doi:10.1111/mec.13567.

Royston, J. P. (1982). An Extension of Shapiro and Wilk's W Test for Normality to Large Samples. *Journal of the Royal Statistical Society. Series C (Applied Statistics)* 31, 115–124. doi:10.2307/2347973.

Rua, C. P. J., Trindade-Silva, A. E., Appolinario, L. R., Venas, T. M., Garcia, G. D., Carvalho, L. S., et al. (2014). Diversity and antimicrobial potential of culturable heterotrophic bacteria associated with the endemic marine sponge Arenosclera brasiliensis. *PeerJ* 2, e419. doi:10.7717/peerj.419.

Russell, J. A., Dubilier, N., and Rudgers, J. A. (2014). Nature's microbiome: introduction. *Molecular Ecology* 23, 1225–1237. doi:10.1111/mec.12676.

Savary, R., Barshis, D. J., Voolstra, C. R., Cárdenas, A., Evensen, N. R., Banc-Prandi, G., et al. (2021). Fast and pervasive transcriptomic resilience and acclimation of extremely heat-tolerant coral holobionts from the northern Red Sea. *Proc Natl Acad Sci USA* 118, e2023298118. doi:10.1073/pnas.2023298118.

Schmitz-Esser, S., Tischler, P., Arnold, R., Montanaro, J., Wagner, M., Rattei, T., et al. (2010). The Genome of the Amoeba Symbiont "Candidatus Amoebophilus asiaticus" Reveals Common Mechanisms for Host Cell Interaction among Amoeba-Associated Bacteria. *Journal of Bacteriology* 192, 1045–1057. doi:10.1128/JB.01379-09.

Schreiber, L., Kjeldsen, K. U., Funch, P., Jensen, J., Obst, M., López-Legentil, S., et al. (2016a). Endozoicomonas Are Specific, Facultative Symbionts of Sea Squirts. *Front Microbiol* 7, 1042. doi:10.3389/fmicb.2016.01042.

Schreiber, L., Kjeldsen, K. U., Obst, M., Funch, P., and Schramm, A. (2016b). Description of Endozoicomonas ascidiicola sp. nov., isolated from Scandinavian ascidians. *Systematic and Applied Microbiology* 39, 313–318. doi:10.1016/j.syapm.2016.05.008.

Seemann, T. (2014). Prokka: rapid prokaryotic genome annotation. *Bioinformatics* 30, 2068–2069. doi:10.1093/bioinformatics/btu153.

Shaffer, M., Borton, M. A., McGivern, B. B., Zayed, A. A., La Rosa, S. L., Solden, L. M., et al. (2020). DRAM for distilling microbial metabolism to automate the curation of microbiome function. *Nucleic Acids Research* 48, 8883–8900. doi:10.1093/nar/gkaa621.

Shantz, A. A., and Burkepile, D. E. (2014). Context-dependent effects of nutrient loading on the coral–algal mutualism. *Ecology* 95, 1995–2005. doi:10.1890/13-1407.1.

Sharp, K. H., Sneed, J. M., Ritchie, K. B., Mcdaniel, L., and Paul, V. J. (2015). Induction of Larval Settlement in the Reef Coral Porites astreoides by a Cultivated Marine Roseobacter Strain. *The Biological Bulletin* 228, 98–107. doi:10.1086/BBLv228n2p98.

Shaver, E. C., Shantz, A. A., McMinds, R., Burkepile, D. E., Thurber, R. L. V., and Silliman, B. R. (2017). Effects of predation and nutrient enrichment on the success and microbiome of a foundational coral. *Ecology* 98, 830–839. doi:10.1002/ecy.1709.

Shi, P. J., Sand Hu, H. S., and Xiao, H. J. (2013). Logistic Regression is a better Method of Analysis Than Linear Regression of Arcsine Square Root Transformed Proportional Diapause Data of Pieris melete (Lepidoptera: Pieridae). *Florida Entomologist* 96, 1183–1185. doi:10.1653/024.096.0361.

Shinzato, C., Shoguchi, E., Kawashima, T., Hamada, M., Hisata, K., Tanaka, M., et al. (2011). Using the Acropora digitifera genome to understand coral responses to environmental change. *Nature* 476, 320–323. doi:10.1038/nature10249.

Smith, J. E., Hunter, C. L., and Smith, C. M. (2010). The effects of top–down versus bottom–up control on benthic coral reef community structure. *Oecologia* 163, 497–507. doi:10.1007/s00442-009-1546-z.

Smith, J. E., Shaw, M., Edwards, R. A., Obura, D., Pantos, O., Sala, E., et al. (2006). Indirect effects of algae on coral: algae-mediated, microbe-induced coral mortality. *Ecology Letters* 9, 835–845. doi:10.1111/j.1461-0248.2006.00937.x.

Souza, C. P., Almeida, B. C., Colwell, R. R., and Rivera, I. N. G. (2011). The importance of chitin in the marine environment. *Mar Biotechnol (NY)* 13, 823–830. doi:10.1007/s10126-011-9388-1.

Sully, S., Burkepile, D. E., Donovan, M. K., Hodgson, G., and Woesik, R. van (2019). A global analysis of coral bleaching over the past two decades. *Nat Commun* 10, 1–5. doi:10.1038/s41467-019-09238-2.

Sunagawa, S., DeSantis, T. Z., Piceno, Y. M., Brodie, E. L., DeSalvo, M. K., Voolstra, C. R., et al. (2009). Bacterial diversity and White Plague Disease-associated community changes in the Caribbean coral *Montastraea faveolata*. *The ISME Journal* 3, 512–521. doi:10.1038/ismej.2008.131.

Sunda, W., Kieber, D. J., Kiene, R. P., and Huntsman, S. (2002). An antioxidant function for DMSP and DMS in marine algae. *Nature* 418, 317–320. doi:10.1038/nature00851.

Sweet, M., Burn, D., Croquer, A., and Leary, P. (2013). Characterisation of the Bacterial and Fungal Communities Associated with Different Lesion Sizes of Dark Spot Syndrome Occurring in the Coral Stephanocoenia intersepta. *PLOS ONE* 8, e62580. doi:10.1371/journal.pone.0062580.

Sweet, M., and Bythell, J. (2015). White syndrome in Acropora muricata: nonspecific bacterial infection and ciliate histophagy. *Mol. Ecol.* 24, 1150–1159. doi:10.1111/mec.13097.

Szmant, A. M. (2002). Nutrient enrichment on coral reefs: Is it a major cause of coral reef decline? *Estuaries* 25, 743–766. doi:10.1007/BF02804903.

Tandon, K., Chiang, P.-W., Chen, W.-M., and Tang, S.-L. (2018). Draft Genome Sequence of Endozoicomonas acroporae Strain Acr-14T, Isolated from Acropora Coral. *Genome Announc* 6. doi:10.1128/genomeA.01576-17.

Tandon, K., Lu, C.-Y., Chiang, P.-W., Wada, N., Yang, S.-H., Chan, Y.-F., et al. (2020). Comparative genomics: Dominant coral-bacterium Endozoicomonas acroporae metabolizes dimethylsulfoniopropionate (DMSP). *The ISME Journal*. doi:10.1038/s41396-020-0610-x.

Tatusov, R. L., Galperin, M. Y., Natale, D. A., and Koonin, E. V. (2000). The COG database: a tool for genome-scale analysis of protein functions and evolution. *Nucleic Acids Res* 28, 33–36. doi:10.1093/nar/28.1.33.

Teplitski, M., and Ritchie, K. (2009). How feasible is the biological control of coral diseases? *Trends in Ecology & Evolution* 24, 378–385. doi:10.1016/j.tree.2009.02.008.

Thurber, R. V., Willner-Hall, D., Rodriguez-Mueller, B., Desnues, C., Edwards, R. A., Angly, F., et al. (2009). Metagenomic analysis of stressed coral holobionts. *Environmental Microbiology* 11, 2148–2163. doi:10.1111/j.1462-2920.2009.01935.x.

Tracy, A. M., Koren, O., Douglas, N., Weil, E., and Harvell, C. D. (2015). Persistent shifts in Caribbean coral microbiota are linked to the 2010 warm thermal anomaly. *Environmental Microbiology Reports* 7, 471–479. doi:10.1111/1758-2229.12274.

Trapon, M. L., Pratchett, M. S., and Penin, L. (2011). Comparative Effects of Different Disturbances in Coral Reef Habitats in Moorea, French Polynesia. *Journal of Marine Biology*. doi:10.1155/2011/807625.

Van Alstyne, K. L., Schupp, P., and Slattery, M. (2006). The distribution of dimethylsulfoniopropionate in tropical Pacific coral reef invertebrates. *Coral Reefs* 25, 321–327. doi:10.1007/s00338-006-0114-9.

van Hooidonk, R., Maynard, J. A., and Planes, S. (2013). Temporary refugia for coral reefs in a warming world. *Nature Climate Change* 3, 508–511. doi:10.1038/nclimate1829.

van Oppen, M. J. H., and Blackall, L. L. (2019). Coral microbiome dynamics, functions and design in a changing world. *Nature Reviews Microbiology* 17, 557–567. doi:10.1038/s41579-019-0223-4.

Vega Thurber, R. L., Burkepile, D. E., Fuchs, C., Shantz, A. A., McMinds, R., and Zaneveld, J. R. (2014). Chronic nutrient enrichment increases prevalence and severity of coral disease and bleaching. *Global Change Biology* 20, 544–554. doi:10.1111/gcb.12450.

Vermeij, M. J. A., Moorselaar, I. van, Engelhard, S., Hörnlein, C., Vonk, S. M., and Visser, P. M. (2010). The Effects of Nutrient Enrichment and Herbivore Abundance on the Ability of Turf Algae to Overgrow Coral in the Caribbean. *PLOS ONE* 5, e14312. doi:10.1371/journal.pone.0014312.

Vezzulli, L., Pezzati, E., Huete-Stauffer, C., Pruzzo, C., and Cerrano, C. (2013). 16SrDNA Pyrosequencing of the Mediterranean Gorgonian Paramuricea clavata Reveals a Link among Alterations in Bacterial Holobiont Members, Anthropogenic Influence and Disease Outbreaks. *PLOS ONE* 8, e67745. doi:10.1371/journal.pone.0067745.

Vinebrooke, R. D., Cottingham, K. L., Norberg, J., Scheffer, M., Dodson, S. I., Maberly, S. C., et al. (2004). Impacts of multiple stressors on biodiversity and ecosystem functioning: the role of species co-tolerance. *Oikos* 104, 451–457. doi:10.1111/j.0030-1299.2004.13255.x.

Wang, G. (2006). Diversity and biotechnological potential of the sponge-associated microbial consortia. *Journal of Industrial Microbiology & Biotechnology* 33, 545–551. doi:10.1007/s10295-006-0123-2.

Wang, L., Shantz, A. A., Payet, J. P., Sharpton, T. J., Foster, A., Burkepile, D. E., et al. (2018). Corals and Their Microbiomes Are Differentially Affected by Exposure to Elevated Nutrients and a Natural Thermal Anomaly. *Frontiers in Marine Science* 5, 101. doi:10.3389/fmars.2018.00101.

Webster, N. S., Negri, A. P., Botté, E. S., Laffy, P. W., Flores, F., Noonan, S., et al. (2016). Host-associated coral reef microbes respond to the cumulative pressures of ocean warming and ocean acidification. *Scientific Reports* 6, 19324. doi:10.1038/srep19324.

Wegley, L., Edwards, R., Rodriguez-Brito, B., Liu, H., and Rohwer, F. (2007). Metagenomic analysis of the microbial community associated with the coral Porites astreoides. *Environmental Microbiology* 9, 2707–2719. doi:10.1111/j.1462-2920.2007.01383.x.

Weis, V. (2008). Cellular mechanisms of Cnidarian bleaching: stress causes the collapse of symbiosis. J Exp Biol 211: 3059-3066. *The Journal of experimental biology* 211, 3059–66. doi:10.1242/jeb.009597.

Weiss, S., Xu, Z. Z., Peddada, S., Amir, A., Bittinger, K., Gonzalez, A., et al. (2017). Normalization and microbial differential abundance strategies depend upon data characteristics. *Microbiome* 5, 27. doi:10.1186/s40168-017-0237-y.

Welsh, R. M., Rosales, S. M., Zaneveld, J. R., Payet, J. P., McMinds, R., Hubbs, S. L., et al. (2017). Alien vs. predator: bacterial challenge alters coral microbiomes unless controlled by *Halobacteriovorax* predators. *PeerJ* 5, e3315. doi:10.7717/peerj.3315.

Welsh, R. M., Zaneveld, J. R., Rosales, S. M., Payet, J. P., Burkepile, D. E., and Thurber, R. V. (2016). Bacterial predation in a marine host-associated microbiome. *ISME J* 10, 1540–1544. doi:10.1038/ismej.2015.219.

Wiedenmann, J., D'Angelo, C., Smith, E. G., Hunt, A. N., Legiret, F.-E., Postle, A. D., et al. (2013). Nutrient enrichment can increase the susceptibility of reef corals to bleaching. *Nature Climate Change* 3, 160–164. doi:10.1038/nclimate1661.

Willis, A. D., and Martin, B. D. (2020). Estimating diversity in networked ecological communities. *Biostatistics*. doi:10.1093/biostatistics/kxaa015.

Wipperman, M. F., Fitzgerald, D. W., Juste, M. A. J., Taur, Y., Namasivayam, S., Sher, A., et al. (2017). Antibiotic treatment for Tuberculosis induces a profound dysbiosis of the microbiome that persists long after therapy is completed. *Scientific Reports* 7, 10767. doi:10.1038/s41598-017-10346-6.

Wooldridge, S. A. (2009). Water quality and coral bleaching thresholds: Formalising the linkage for the inshore reefs of the Great Barrier Reef, Australia. *Marine Pollution Bulletin* 58, 745–751. doi:10.1016/j.marpolbul.2008.12.013.

Wright, R. M., Kenkel, C. D., Dunn, C. E., Shilling, E. N., Bay, L. K., and Matz, M. V. (2017). Intraspecific differences in molecular stress responses and coral pathobiome contribute to mortality under bacterial challenge in Acropora millepora. *Sci Rep* 7. doi:10.1038/s41598-017-02685-1.

Xia, Y., and Sun, J. (2017). Hypothesis testing and statistical analysis of microbiome. *Genes & Diseases* 4, 138–148. doi:10.1016/j.gendis.2017.06.001.

Yang, S.-H., Tandon, K., Lu, C.-Y., Wada, N., Shih, C.-J., Hsiao, S. S.-Y., et al. (2019). Metagenomic, phylogenetic, and functional characterization of predominant endolithic green sulfur bacteria in the coral Isopora palifera. *Microbiome* 7, 3. doi:10.1186/s40168-018-0616-z.

Yano, K., Shibata, S., Chen, W.-L., Sato, S., Kaneko, T., Jurkiewicz, A., et al. (2009). CERBERUS, a novel U-box protein containing WD-40 repeats, is required for formation of the infection thread and nodule development in the legume–Rhizobium symbiosis. *The Plant Journal* 60, 168–180. doi:10.1111/j.1365-313X.2009.03943.x.

Zaneveld, J. R., Burkepile, D. E., Shantz, A. A., Pritchard, C. E., McMinds, R., Payet, J. P., et al. (2016). Overfishing and nutrient pollution interact with temperature to disrupt coral reefs down to microbial scales. *Nat Commun* 7, 11833. doi:10.1038/ncomms11833.

Zaneveld, J. R., McMinds, R., and Vega Thurber, R. (2017). Stress and stability: applying the Anna Karenina principle to animal microbiomes. *Nature Microbiology* 2, 1–8. doi:10.1038/nmicrobiol.2017.121.

Ziegler, M., Grupstra, C. G. B., Barreto, M. M., Eaton, M., BaOmar, J., Zubier, K., et al. (2019). Coral bacterial community structure responds to environmental change in a host-specific manner. *Nat Commun* 10, 1–11. doi:10.1038/s41467-019-10969-5.

Ziegler, M., Roik, A., Porter, A., Zubier, K., Mudarris, M. S., Ormond, R., et al. (2016). Coral microbial community dynamics in response to anthropogenic impacts near a major city in the central Red Sea. *Mar. Pollut. Bull.* 105, 629–640. doi:10.1016/j.marpolbul.2015.12.045.

Ziegler, M., Seneca, F. O., Yum, L. K., Palumbi, S. R., and Voolstra, C. R. (2017). Bacterial community dynamics are linked to patterns of coral heat tolerance. *Nature Communications* 8, 14213. doi:10.1038/ncomms14213.

Zielinski, F. U., Pernthaler, A., Duperron, S., Raggi, L., Giere, O., Borowski, C., et al. (2009). Widespread occurrence of an intranuclear bacterial parasite in vent and seep bathymodiolin mussels. *Environmental Microbiology* 11, 1150–1167. doi:10.1111/j.1462-2920.2008.01847.x.

APPENDICES

Appendix A: Ch. 2 Supplementary Material

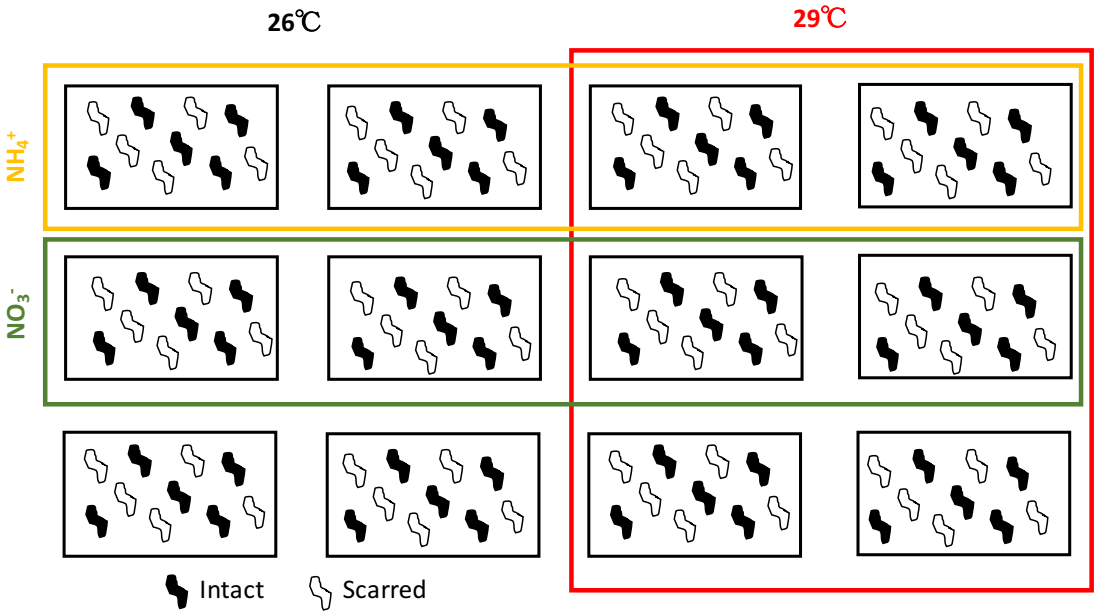

Supplementary Figure 2.1. Tank experimental design. Each tank contained two treatments and each of the twelve treatments was repeated in two tanks, resulting in 10 replicates per treatment. For this study, 6 replicates per treatment were randomly chosen for microbial analyses (3 for each treatment per tank).

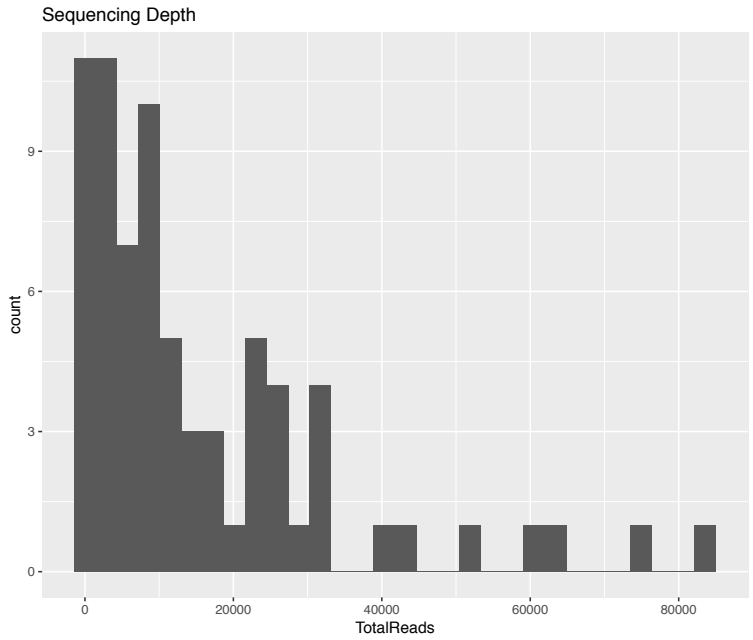

Supplementary Figure 2.2. Histogram of sequencing depth after filtering out OTUs that 1) failed to align with PyNAST to the GreenGenes database, 2) were annotated as mitochondrial or chloroplast sequences, or 3) had less than 100 counts across the entire dataset.

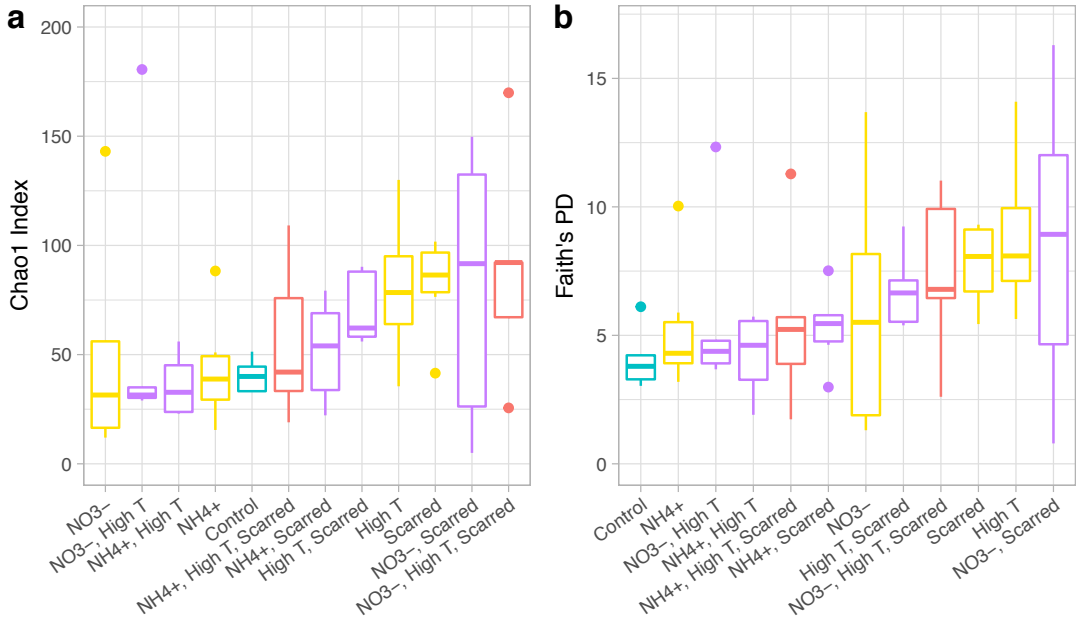

Supplementary Figure 2.3. a) Chao1 index and b) Faith's phylogenetic distance by treatment in order of increasing medians. Colors represent the number of stressors: none=teal, single=yellow, double=purple, triple=red.

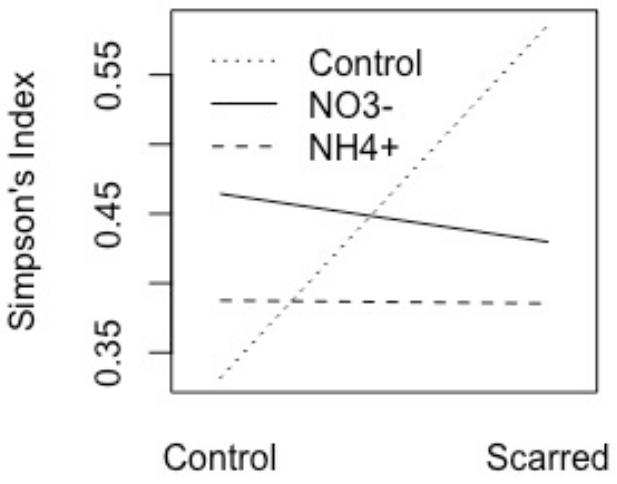

Supplementary Figure 2.4. Interaction plot for Simpson's index by nutrients and scarring treatments. The interaction nutrients:scarring was significant in the linear mixed effects model (Supplementary Table 2.4).

Supplementary Table 2.1. Resulting mapping file after filtering. OTUs were filtered from the dataset if they 1) failed to align with PyNAST to the GreenGenes database, 2) were annotated as mitochondrial or chloroplast sequences, or 3) had less than 100 counts across the entire dataset. Next, samples with less than 1000 reads were discarded (grey-colored sample rows).

#SampleID	Tank	Nutrient	Temperature	Scarring	Colony	Treatment	Stress	Seq Depth
m.ch.15	D	Control	Control	Control	C5	Control	none	12930
m.ch.14	D	Control	Control	Control	C4	Control	none	40274
m.ch.11	D	Control	Control	Control	C1	Control	none	73948
m.ch.19	L	Control	Control	Control	C9	Control	none	4
m.ch.18	L	Control	Control	Control	C8	Control	none	11320
m.ch.17	L	Control	Control	Control	C7	Control	none	24526
m.ch.35	F	Control	High T	Control	C5	High T	single	250
m.ch.34	F	Control	High T	Control	C4	High T	single	22203
m.ch.31	F	Control	High T	Control	C1	High T	single	64340
m.ch.39	G	Control	High T	Control	C9	High T	single	585
m.ch.38	G	Control	High T	Control	C8	High T	single	4562
m.ch.37	G	Control	High T	Control	C7	High T	single	7570
m.ch.21	F	Control	High T	Scarred	C4	High T, scarred	double	5
m.ch.24	F	Control	High T	Scarred	C4	High T, scarred	double	8192
m.ch.25	F	Control	High T	Scarred	C5	High T, scarred	double	17118
m.ch.27	G	Control	High T	Scarred	C7	High T, scarred	double	1501
m.ch.28	G	Control	High T	Scarred	C8	High T, scarred	double	3083
m.ch.29	G	Control	High T	Scarred	C9	High T, scarred	double	26644
m.ch.95	E	NH4+	Control	Control	C5	NH4+	single	4602
m.ch.94	E	NH4+	Control	Control	C4	NH4+	single	24321
m.ch.91	E	NH4+	Control	Control	C1	NH4+	single	52777
m.ch.98	K	NH4+	Control	Control	C8	NH4+	single	8199
m.ch.99	K	NH4+	Control	Control	C9	NH4+	single	21860
m.ch.97	K	NH4+	Control	Control	C7	NH4+	single	24625
m.ch.111	C	NH4+	High T	Control	C1	NH4+, High T	double	86
m.ch.115	C	NH4+	High T	Control	C5	NH4+, High T	double	2859
m.ch.114	C	NH4+	High T	Control	C4	NH4+, High T	double	7614
m.ch.117	J	NH4+	High T	Control	C7	NH4+, High T	double	1
m.ch.118	J	NH4+	High T	Control	C8	NH4+, High T	double	2151
m.ch.119	J	NH4+	High T	Control	C9	NH4+, High T	double	5455
m.ch.105	C	NH4+	High T	Scarred	C5	NH4+, High T, scarred	triple	1616
m.ch.101	C	NH4+	High T	Scarred	C1	NH4+, High T, scarred	triple	17469

m.ch.104	C	NH4+	High T	Scarred	C4	NH4+, High T, scarred	triple	20733
m.ch.107	J	NH4+	High T	Scarred	C7	NH4+, High T, scarred	triple	4
m.ch.108	J	NH4+	High T	Scarred	C8	NH4+, High T, scarred	triple	1962
m.ch.109	J	NH4+	High T	Scarred	C9	NH4+, High T, scarred	triple	15391
m.ch.84	E	NH4+	Control	Scarred	C4	NH4+, scarred	double	3058
m.ch.85	E	NH4+	Control	Scarred	C5	NH4+, scarred	double	10134
m.ch.81	E	NH4+	Control	Scarred	C1	NH4+, scarred	double	32454
m.ch.89	K	NH4+	Control	Scarred	C9	NH4+, scarred	double	1691
m.ch.88	K	NH4+	Control	Scarred	C8	NH4+, scarred	double	8458
m.ch.87	K	NH4+	Control	Scarred	C7	NH4+, scarred	double	31459
m.ch.54	A	NO3-	Control	Control	C4	NO3-	single	8
m.ch.55	A	NO3-	Control	Control	C5	NO3-	single	4442
m.ch.51	A	NO3-	Control	Control	C1	NO3-	single	43207
m.ch.57	H	NO3-	Control	Control	C7	NO3-	single	13249
m.ch.59	H	NO3-	Control	Control	C9	NO3-	single	26058
m.ch.58	H	NO3-	Control	Control	C8	NO3-	single	27945
m.ch.71	B	NO3-	High T	Control	C1	NO3-, High T	double	0
m.ch.74	B	NO3-	High T	Control	C4	NO3-, High T	double	9623
m.ch.75	B	NO3-	High T	Control	C5	NO3-, High T	double	30273
m.ch.79	I	NO3-	High T	Control	C9	NO3-, High T	double	1070
m.ch.77	I	NO3-	High T	Control	C7	NO3-, High T	double	1139
m.ch.78	I	NO3-	High T	Control	C8	NO3-, High T	double	9360
m.ch.61	B	NO3-	High T	Scarred	C1	NO3-, High T, scarred	triple	5912
m.ch.65	B	NO3-	High T	Scarred	C5	NO3-, High T, scarred	triple	7723
m.ch.64	B	NO3-	High T	Scarred	C4	NO3-, High T, scarred	triple	10287
m.ch.68	I	NO3-	High T	Scarred	C8	NO3-, High T, scarred	triple	2
m.ch.69	I	NO3-	High T	Scarred	C9	NO3-, High T, scarred	triple	17725
m.ch.67	I	NO3-	High T	Scarred	C7	NO3-, High T, scarred	triple	23411
m.ch.44	A	NO3-	Control	Scarred	C4	NO3-, scarred	double	4904
m.ch.45	A	NO3-	Control	Scarred	C5	NO3-, scarred	double	21913
m.ch.41	A	NO3-	Control	Scarred	C1	NO3-, scarred	double	83601
m.ch.47	H	NO3-	Control	Scarred	C7	NO3-, scarred	double	9385
m.ch.48	H	NO3-	Control	Scarred	C8	NO3-, scarred	double	10564
m.ch.49	H	NO3-	Control	Scarred	C9	NO3-, scarred	double	15834
m.ch.4	D	Control	Control	Scarred	C4	Scarred	single	2334
m.ch.1	D	Control	Control	Scarred	C1	Scarred	single	5642
m.ch.5	D	Control	Control	Scarred	C5	Scarred	single	9368
m.ch.9	L	Control	Control	Scarred	C9	Scarred	single	3509

m.ch.7	L	Control	Control	Scarred	C7	Scarred	single	32292
m.ch.8	L	Control	Control	Scarred	C8	Scarred	single	59707

Supplementary Table 2.2. Effects of temperature, nutrients, and scarring on relative abundance of the most abundant OTU, family Endozoicimonaceae. Generalized linear mixed-effects model of raw counts with an offset for sequencing depth of the most abundant OTU in the dataset. Fixed (temperature, nutrients, and scarring) and random (tank and colony) effects are included in the model. The resulting formula in the R language was: glmer(Endozoicimonaceae ~ offset(log(sequencing_depth)) + temp * nutrient * corallivory + (1 | tank) + (1 | colony), family = "poisson").

	OTU, family Endozoicimonaceae			
Effect	**Estimate**	**Std. Error**	**z value**	**P**
(Intercept)	-0.07	0.07	-1.04	0.30
High Temp	**-0.46**	**0.07**	**-6.21**	**<0.001**
Nutrient - NH4+	-0.14	0.07	-1.91	0.06
Nutrient - NO3-	**-0.15**	**0.07**	**-1.96**	**<0.05**
Scarred	**-0.52**	**0.01**	**-88.02**	**<0.001**
High Temp:Nutrient - NH4+	**0.44**	**0.11**	**4.13**	**<0.001**
High Temp: Nutrient - NO3-	**0.43**	**0.11**	**4.09**	**<0.001**
High Temp: Scarred	**0.82**	**0.01**	**89.18**	**<0.001**
Nutrient - NH4+:Scarred	**0.57**	**0.01**	**75.70**	**<0.001**
Nutrient - NO3-:Scarred	**0.39**	**0.01**	**52.45**	**<0.001**
High Temp:Nutrient - NH4+:Scarred	**-0.99**	**0.01**	**-68.72**	**<0.001**
High Temp:Nutrient - NO3-:Scarred	**-0.90**	**0.01**	**-68.72**	**<0.001**

Supplementary Table 2.3. Effects of temperature, nutrients, and scarring on relative abundance of most abundant OTUs. Zero-inflated negative binomial regression for unrarefied count data with an offset for sequencing depth. The offset is included to account for the uneven sequencing depth across the unrarefied table. A single zero-inflation parameter is modeled for all observations. The resulting formula in the R language was: glmmTMB(taxon counts ~ offset(log(sequencing depth)) + temperature*nutrient*temperature + (1|tank) + (1|colony), ziformula = ~1, family = nbinom2).

	OTU, family Desulfovibrionaceae			
Count model coefficients (negbin with log link):	**Estimate**	**Std. Error**	**z value**	**P**
(Intercept)	**-6.84**	**0.86**	**-7.98**	**<0.001**
temphigh	**5.49**	**1.08**	**5.09**	**<0.001**
nutrientNH4+	**3.4**	**1.07**	**3.17**	**<0.01**
nutrientNO3-	**5.46**	**1.26**	**4.35**	**<0.001**
corallivoryScarred	**4.93**	**1.08**	**4.59**	**<0.001**
temphigh:nutrientNH4+	**-6.69**	**1.42**	**-4.71**	**<0.001**
temphigh:nutrientNO3-	**-7.24**	**1.53**	**-4.72**	**<0.001**
temphigh:corallivoryScarred	**-7.8**	**1.39**	**-5.62**	**<0.001**
nutrientNH4+:corallivoryScarred	**-5.84**	**1.54**	**-3.78**	**<0.001**
nutrientNO3-:corallivoryScarred	**-6.71**	**1.56**	**-4.31**	**<0.001**
temphigh:nutrientNH4+:corallivoryScarred	**7.51**	**2.02**	**3.72**	**<0.001**
temphigh:nutrientNO3-:corallivoryScarred	**9.81**	**1.97**	**4.98**	**<0.001**
Zero-inflation parameter (binomial with logit link):	**-1.06**	**0.32**	**-3.26**	**<0.01**
	OTU, family Amoebophilaceae			
Count model coefficients (negbin with log link):	**Estimate**	**Std. Error**	**z value**	**P**
(Intercept)	**-6.18**	**0.591**	**-10.456**	**<0.001**
temphigh	**2.68**	**0.84**	**3.19**	**<0.01**
nutrientNH4+	0.9	0.79	1.14	0.26
nutrientNO3-	0.49	0.8	0.61	0.54
corallivoryScarred	**1.69**	**0.77**	**2.2**	**<0.05**
temphigh:nutrientNH4+	-2.22	1.2	-1.84	0.07
temphigh:nutrientNO3-	-0.33	1.14	-0.29	0.77
temphigh:corallivoryScarred	-2.2	1.15	-1.92	0.06
nutrientNH4+:corallivoryScarred	-1.35	1.08	-1.25	0.21
nutrientNO3-:corallivoryScarred	-0.79	1.12	-0.71	0.48
temphigh:nutrientNH4+:corallivoryScarred	**3.34**	**1.64**	**2.04**	**<0.05**
temphigh:nutrientNO3-:corallivoryScarred	-0.53	1.71	-0.31	0.75
Zero-inflation parameter (binomial with logit link):	**-1.79**	**0.44**	**-4.05**	**<0.001**

	OTU, Enterobacteriaceae			
Count model coefficients (negbin with log link):	**Estimate**	**Std. Error**	**z value**	**P**
(Intercept)	**-5.48**	**0.5007**	**-10.95**	**<0.001**
temphigh	1.08	0.81	1.32	0.19
nutrientNH4+	0.99	0.75	1.32	0.19
nutrientNO3-	-0.11	0.92	-0.13	0.9
corallivoryScarred	**2.38**	**0.7068**	**3.37**	**<0.001**
temphigh:nutrientNH4+	2	1.26	1.59	0.11
temphigh:nutrientNO3-	-0.32	1.25	-0.26	0.8
temphigh:corallivoryScarred	-1.56	1.08	-1.45	0.15
nutrientNH4+:corallivoryScarred	**-2.08**	**1.03**	**-2.02**	**<0.05**
nutrientNO3-:corallivoryScarred	**-3.12**	**1.2734**	**-2.45**	**<0.05**
temphigh:nutrientNH4+:corallivoryScarred	0.99	1.63	0.61	0.54
temphigh:nutrientNO3-:corallivoryScarred	3.21	1.7	1.89	0.06
Zero-inflation parameter (binomial with logit link):	**-1.12**	**0.33**	**-3.44**	**<0.001**
	OTU, Moraxellaceae			
Count model coefficients (negbin with log link):	**Estimate**	**Std. Error**	**z value**	**P**
(Intercept)	**-5.99**	**0.68**	**-8.84**	**<0.001**
temphigh	-0.69	1.02	-0.67	0.5
nutrientNH4+	**1.95**	**0.9**	**2.17**	**<0.05**
nutrientNO3-	1.42	0.9	1.57	0.12
corallivoryScarred	1.39	0.86	1.61	0.11
temphigh:nutrientNH4+	2.51	1.45	1.73	0.08
temphigh:nutrientNO3-	0.13	1.32	0.1	0.92
temphigh:corallivoryScarred	0.46	1.27	0.36	0.72
nutrientNH4+:corallivoryScarred	**-2.95**	**1.23**	**-2.39**	**<0.05**
nutrientNO3-:corallivoryScarred	**-3.22**	**1.21**	**-2.67**	**<0.05**
temphigh:nutrientNH4+:corallivoryScarred	-0.12	1.86	-0.06	0.95
temphigh:nutrientNO3-:corallivoryScarred	1.61	1.74	0.92	0.36
Zero-inflation parameter (binomial with logit link):	**-1.15**	**0.35**	**-3.26**	**<0.01**

Supplementary Table 2.4. Effects of temperature, nutrients, and scarring on microbial community alpha diversity metrics. Linear mixed model of factors affecting coral microbial community richness (Chao1), alpha diversity (Simpson's), and phylogenetic relatedness (Faith's PD) using fixed effects (temperature, nutrients, scarring) and random effects (tank and colony). Chao1 and Faith's PD were log-transformed, while Simpson's Index was arcsine-transformed to improve normality. The resulting formula in the R language was: lmer(alpha diversity metric ~ temperature * nutrients * scarring + (1|tank) + (1|colony)). P-values were approximated with the lmerTest package in R.

	Chao1 Index			
Effect	**Estimate**	**Std. Error**	**t value**	**P**
(Intercept)	**3.69**	**0.28**	**13.01**	**<0.001**
High Temp	0.57	0.42	1.38	0.17
Nutrient - NH4+	-0.06	0.37	-0.16	0.88
Nutrient - NO3-	-0.12	0.39	-0.31	0.76
Scarred	0.68	0.37	1.81	0.08
High Temp:Nutrient - NH4+	-0.7	0.58	-1.21	0.23
High Temp: Nutrient - NO3-	-0.34	0.57	-0.59	0.56
High Temp: Scarred	-0.69	0.56	-1.23	0.22
Nutrient - NH4+:Scarred	-0.46	0.52	-0.89	0.38
Nutrient - NO3-:Scarred	-0.38	0.53	-0.72	0.48
High Temp:Nutrient - NH4+:Scarred	0.79	0.78	1.01	0.32
High Temp:Nutrient - NO3-:Scarred	0.92	0.78	1.18	0.24
	Faith's Phylogenetic Diversity			
Effect	**Estimate**	**Std. Error**	**t value**	**P**
(Intercept)	**1.38**	**0.24**	**5.8**	**<0.001**
High Temp	**0.76**	**0.36**	**2.14**	**<0.05**
Nutrient - NH4+	0.21	0.32	0.64	0.52
Nutrient - NO3-	0.09	0.34	0.26	0.79
Scarred	**0.65**	**0.32**	**2.04**	**<0.05**
High Temp:Nutrient - NH4+	**-0.99**	**0.49**	**-2.01**	**<0.05**
High Temp: Nutrient - NO3-	-0.58	0.49	-1.19	0.24
High Temp: Scarred	-0.9	0.48	-1.87	0.07
Nutrient - NH4+:Scarred	-0.6	0.44	-1.36	0.18
Nutrient - NO3-:Scarred	-0.33	0.45	-0.72	0.48
High Temp:Nutrient - NH4+:Scarred	1.04	0.67	1.55	0.13
High Temp:Nutrient - NO3-:Scarred	0.81	0.67	1.21	0.23
	Simpson's Index			

Effect	Estimate	Std. Error	t value	P
(Intercept)	**0.32**	**0.13**	**2.45**	**<0.05**
High Temp	**0.62**	**0.19**	**3.21**	**<0.01**
Nutrient - NH4+	0.29	0.17	1.66	0.1
Nutrient - NO3-	0.3	0.18	1.66	0.1
Scarred	**0.67**	**0.17**	**3.82**	**<0.001**
High Temp:Nutrient - NH4+	-0.5	0.27	-1.84	0.07
High Temp: Nutrient - NO3-	-0.41	0.27	-1.55	0.13
High Temp: Scarred	**-0.84**	**0.26**	**-3.22**	**<0.01**
Nutrient - NH4+:Scarred	**-0.72**	**0.24**	**-2.98**	**<0.01**
Nutrient - NO3-:Scarred	**-0.63**	**0.25**	**-2.54**	**<0.05**
High Temp:Nutrient - NH4+:Scarred	**0.92**	**0.37**	**2.53**	**<0.05**
High Temp:Nutrient - NO3-:Scarred	**0.74**	**0.36**	**2.03**	**<0.05**

Supplementary Table 2.5. Effects of treatment combination on microbial community dissimilarity with pairwise treatment comparisons. PERMANOVA results for differences between treatments based on dissimilarity measures with the formula: adonis(distance matrix ~ treatment) and p-values for pairwise treatment comparisons.

Effect = Treatment	**DF**	**Sum Sq**	**F**	**R^2**	**P**
Weighted Unifrac	**11**	**1.28**	**1.61**	**0.26**	**<0.05**

Comparison	**P**
NH4+, High T, Scarred vs Control	**0.008**
NH4+, High T, Scarred vs High T	0.381
NH4+, High T, Scarred vs High T, Scarred	0.31
NH4+, High T, Scarred vs NH4+, Scarred	0.088
NH4+, High T, Scarred vs NO3-	0.624
NH4+, High T, Scarred vs NH4+	0.13
NH4+, High T, Scarred vs NO3-, High T	0.83
NH4+, High T, Scarred vs NO3-, High T, Scarred	0.537
NH4+, High T, Scarred vs Scarred	0.772
NH4+, High T, Scarred vs NO3-, Scarred	0.34
NH4+, High T, Scarred vs NH4+, High T	0.868
Control vs High T	**0.006**
Control vs High T, Scarred	**0.008**
Control vs NH4+, Scarred	0.123
Control vs NO3-	0.171
Control vs NH4+	**0.03**
Control vs NO3-, High T	**0.012**
Control vs NO3-, High T, Scarred	0.059
Control vs Scarred	**0.006**
Control vs NO3-, Scarred	0.15
Control vs NH4+, High T	0.074
High T vs High T, Scarred	0.058
High T vs NH4+, Scarred	**0.02**
High T vs NO3-	0.201
High T vs NH4+	**0.022**
High T vs NO3-, High T	0.212
High T vs NO3-, High T, Scarred	0.166
High T vs Scarred	0.535
High T vs NO3-, Scarred	0.136
High T vs NH4+, High T	0.212
High T, Scarred vs NH4+, Scarred	0.2

High T, Scarred vs NO3-	0.647
High T, Scarred vs NH4+	0.229
High T, Scarred vs NO3-, High T	0.35
High T, Scarred vs NO3-, High T, Scarred	0.919
High T, Scarred vs Scarred	0.114
High T, Scarred vs NO3-, Scarred	0.672
High T, Scarred vs NH4+, High T	0.285
NH4+, Scarred vs NO3-	0.375
NH4+, Scarred vs NH4+	0.899
NH4+, Scarred vs NO3-, High T	0.061
NH4+, Scarred vs NO3-, High T, Scarred	0.327
NH4+, Scarred vs Scarred	**0.024**
NH4+, Scarred vs NO3-, Scarred	0.505
NH4+, Scarred vs NH4+, High T	0.14
NO3- vs NH4+	0.771
NO3- vs NO3-, High T	0.565
NO3- vs NO3-, High T, Scarred	0.829
NO3- vs Scarred	0.307
NO3- vs NO3-, Scarred	0.949
NO3- vs NH4+, High T	0.427
NH4+ vs NO3-, High T	0.088
NH4+ vs NO3-, High T, Scarred	0.486
NH4+ vs Scarred	**0.022**
NH4+ vs NO3-, Scarred	0.698
NH4+ vs NH4+, High T	0.149
NO3-, High T vs NO3-, High T, Scarred	0.637
NO3-, High T vs Scarred	0.694
NO3-, High T vs NO3-, Scarred	0.371
NO3-, High T vs NH4+, High T	0.403
NO3-, High T, Scarred vs Scarred	0.335
NO3-, High T, Scarred vs NO3-, Scarred	0.686
NO3-, High T, Scarred vs NH4+, High T	0.356
Scarred vs NO3-, Scarred	0.148
Scarred vs NH4+, High T	0.416
NO3-, Scarred vs NH4+, High T	0.351

Supplementary Table 2.6. Effects of temperature, nutrients, and scarring on microbial community dissimilarity. PERMANOVA results for differences between groups based Weighted Unifrac dissimilarity measures with the formula: adonis(distance matrix ~ temperature * nutrient * scarring).

	Weighted Unifrac				
Effect	**DF**	**Sum Sq**	**F**	**R^2**	**P**
Temperature	**1**	**0.25**	**3.39**	**0.05**	**<0.05**
Nutrient	2	0.14	0.97	0.03	0.37
Scarring	1	0.04	0.60	0.01	0.61
Temperature:Nutrients	2	0.18	1.23	0.04	0.25
Temperature:Scarring	1	0.18	2.46	0.04	0.05
Nutrients:Scarring	2	0.11	0.73	0.02	0.60
Temperature:Nutrient:Scarring	**2**	**0.39**	**2.68**	**0.08**	**<0.05**

Supplementary Table 2.7. Effects of treatment combination on microbial community group dispersion. PERMDISP results for differences within treatments based on two dissimilarity measures with the formula: betadisper(distance matrix ~ treatment).

Effect = Treatment	**DF**	**Sum Sq**	**F**	**P**
Weighted Unifrac	**11**	**0.55**	**2.19**	**<0.05**
Comparison				**P**
NH4+, High T, Scarred vs Control				**0.016**
NH4+, High T, Scarred vs High T				0.944
NH4+, High T, Scarred vs High T, Scarred				0.153
NH4+, High T, Scarred vs NH4+, Scarred				0.09
NH4+, High T, Scarred vs NO3-				0.736
NH4+, High T, Scarred vs NH4+				0.115
NH4+, High T, Scarred vs NO3-, High T				0.577
NH4+, High T, Scarred vs NO3-, High T, Scarred				0.588
NH4+, High T, Scarred vs Scarred				0.793
NH4+, High T, Scarred vs NO3-, Scarred				0.54
NH4+, High T, Scarred vs NH4+, High T				0.729
Control vs High T				**0.005**
Control vs High T, Scarred				**0.001**
Control vs NH4+, Scarred				**0.016**
Control vs NO3-				**0.003**
Control vs NH4+				**0.012**
Control vs NO3-, High T				**0.001**
Control vs NO3-, High T, Scarred				**0.025**
Control vs Scarred				**0.001**
Control vs NO3-, Scarred				0.105
Control vs NH4+, High T				**0.004**
High T vs High T, Scarred				0.057
High T vs NH4+, Scarred				**0.037**
High T vs NO3-				0.753
High T vs NH4+				0.077
High T vs NO3-, High T				0.489
High T vs NO3-, High T, Scarred				0.592
High T vs Scarred				0.826
High T vs NO3-, Scarred				0.545
High T vs NH4+, High T				0.598
High T, Scarred vs NH4+, Scarred				0.682
High T, Scarred vs NO3-				0.13

High T, Scarred vs NH4+	0.982
High T, Scarred vs NO3-, High T	**0.003**
High T, Scarred vs NO3-, High T, Scarred	0.361
High T, Scarred vs Scarred	**0.013**
High T, Scarred vs NO3-, Scarred	0.58
High T, Scarred vs NH4+, High T	**0.022**
NH4+, Scarred vs NO3-	0.09
NH4+, Scarred vs NH4+	0.733
NH4+, Scarred vs NO3-, High T	**0.013**
NH4+, Scarred vs NO3-, High T, Scarred	0.267
NH4+, Scarred vs Scarred	**0.01**
NH4+, Scarred vs NO3-, Scarred	0.459
NH4+, Scarred vs NH4+, High T	**0.021**
NO3- vs NH4+	0.146
NO3- vs NO3-, High T	0.778
NO3- vs NO3-, High T, Scarred	0.764
NO3- vs Scarred	0.827
NO3- vs NO3-, Scarred	0.09
NO3- vs NH4+, High T	0.417
NH4+ vs NO3-, High T	0.057
NH4+ vs NO3-, High T, Scarred	0.34
NH4+ vs Scarred	**0.015**
NH4+ vs NO3-, Scarred	0.565
NH4+ vs NH4+, High T	**0.031**
NO3-, High T vs NO3-, High T, Scarred	0.888
NO3-, High T vs Scarred	0.436
NO3-, High T vs NO3-, Scarred	0.806
NO3-, High T vs NH4+, High T	0.18
NO3-, High T, Scarred vs Scarred	0.565
NO3-, High T, Scarred vs NO3-, Scarred	0.897
NO3-, High T, Scarred vs NH4+, High T	0.323
Scarred vs NO3-, Scarred	0.52
Scarred vs NH4+, High T	0.373
NO3-, Scarred vs NH4+, High T	0.322

Supplementary Table 2.8. Effects of stressors on the differences in abundance of bacterial taxa. Results of a negative binomial generalized linear model (glm) fitted with the R package DESeq2. Prior to analysis, the unrarefied OTU table was pre-filtered in phyloseq to excluded all rare taxa that were only present in fewer than 15 samples. The formula in the R language was: ~ temperature * nutrient * scarring. Wald post-hoc tests were performed to identify significant changes and differentially abundant taxa were identified as significant with Benjamini-Hochberg FDR p-values less than 0.05.

OTU ID	baseMean	log2 Fold Change	lfcSE	stat	pval	padj	Taxonomy	Contrast
150582	36.83	10.61	3.05	3.47	0.001	0.009	k__Bacteria p__Proteobacteria c__Alphaproteobacteria o__ c__Alphaproteobacteria g__ s__	Control vs High
369965	14.43	11.70	3.83	3.05	0.002	0.024	k__Bacteria p__Proteobacteria c__Alphaproteobacteria NA c__Alphaproteobacteria NA NA	Control vs High
321533	197.96	5.87	1.87	3.14	0.002	0.024	k__Bacteria p__Bacteroidetes c__Cytophagia o__Cytophagales f__[Amoebophilaceae] g__SGUS912 s__	Control vs High
2932342	956.20	10.65	2.45	4.35	0.000	0.000	k__Bacteria p__Proteobacteria c__Deltaproteobacteria o__Desulfovibrionales f__Desulfovibrionaceae g__ s__	Control vs High
OTU121	1.46	7.13	2.76	2.58	0.010	0.043	k__Bacteria p__Proteobacteria c__Deltaproteobacteria o__Desulfovibrionales f__Desulfovibrionaceae g__ s__	Control vs High
OTU80	4.12	7.36	2.73	2.70	0.007	0.036	k__Bacteria p__Proteobacteria c__Deltaproteobacteria o__Desulfovibrionales f__Desulfovibrionaceae g__ s__	Control vs High
OTU123	2.07	5.66	1.92	2.95	0.003	0.024	k__Bacteria p__Proteobacteria c__Gammaproteobacteria o__Oceanospirillales f__Endozoicimonaceae g__ s__	Control vs High
1010113	122.68	18.49	3.91	4.73	0.000	0.000	k__Bacteria p__Proteobacteria c__Gammaproteobacteria o__Enterobacteriales f__Enterobacteriaceae NA NA	Control vs High
165867	40.49	8.02	2.97	2.70	0.007	0.036	k__Bacteria p__Proteobacteria c__Alphaproteobacteria o__Rhizobiales f__Hyphomicrobiaceae NA NA	Control vs High
428807	20.49	-15.27	4.25	-3.59	0.000	0.007	k__Bacteria p__Proteobacteria c__Alphaproteobacteria o__Rhizobiales f__Hyphomicrobiaceae g__ s__	Control vs High
800197	36.52	9.91	3.58	2.77	0.006	0.034	k__Bacteria p__Proteobacteria c__Alphaproteobacteria o__Rhodobacterales f__Hyphomonadaceae g__Hyphomonas s__	Control vs High
933546	36.50	-14.00	3.12	-4.49	0.000	0.000	k__Bacteria p__Proteobacteria c__Betaproteobacteria o__Neisseriales f__Neisseriaceae g__ s__	Control vs High
60398	103.95	5.41	1.95	2.78	0.005	0.034	k__Bacteria p__Proteobacteria c__Alphaproteobacteria o__Rhodobacterales f__Rhodobacteraceae NA NA	Control vs High
146037	5.31	12.35	4.20	2.94	0.003	0.024	k__Bacteria p__Proteobacteria c__Alphaproteobacteria o__Rhodobacterales f__Rhodobacteraceae NA NA	Control vs High
163471	13.31	7.08	2.60	2.72	0.006	0.036	k__Bacteria p__Proteobacteria c__Alphaproteobacteria o__Rhodobacterales f__Rhodobacteraceae NA NA	Control vs High

816411	66.85	5.60	1.86	3.01	0.003	0.024	k__Bacteria p__Proteobacteria c__Alphaproteobacteria o__Rhodobacterales f__Rhodobacteraceae g__Roseivivax s__	Control vs High
904675	15.56	15.13	3.71	4.08	0.000	0.001	k__Bacteria p__Proteobacteria c__Alphaproteobacteria o__Rhodobacterales f__Rhodobacteraceae NA NA	Control vs High
1123147	11.28	7.70	2.54	3.02	0.002	0.024	k__Bacteria p__Proteobacteria c__Alphaproteobacteria o__Rhodobacterales f__Rhodobacteraceae NA NA	Control vs High
3180137	59.37	6.70	2.26	2.97	0.003	0.024	k__Bacteria p__Proteobacteria c__Alphaproteobacteria o__Rhodobacterales f__Rhodobacteraceae g__ s__	Control vs High
431378	8.41	6.57	2.49	2.64	0.008	0.037	k__Bacteria p__Proteobacteria c__Alphaproteobacteria o__Rhodobacterales f__Rhodobacteraceae NA NA	Control vs High
4327730	21.68	6.68	2.33	2.87	0.004	0.029	k__Bacteria p__Proteobacteria c__Alphaproteobacteria o__Rhodobacterales f__Rhodobacteraceae NA NA	Control vs High
4420764	11.33	9.51	3.59	2.65	0.008	0.037	k__Bacteria p__Proteobacteria c__Alphaproteobacteria o__Rhodobacterales f__Rhodobacteraceae g__ s__	Control vs High
144589	13.01	11.48	4.32	2.66	0.008	0.037	k__Bacteria p__Proteobacteria c__Alphaproteobacteria o__Sphingomonadales f__Sphingomonadaceae g__Novosphingobium s__	Control vs High
833774	5.60	11.10	4.37	2.54	0.011	0.046	k__Bacteria p__Proteobacteria c__Alphaproteobacteria o__Sphingomonadales f__Sphingomonadaceae g__Novosphingobium s__	Control vs High
4445466	12.88	-12.68	4.18	-3.03	0.002	0.024	k__Bacteria p__Firmicutes c__Bacilli o__Lactobacillales f__Streptococcaceae g__Streptococcus s__	Control vs High
369965	14.43	12.01	3.44	3.49	0.000	0.013	k__Bacteria p__Proteobacteria c__Alphaproteobacteria NA c__Alphaproteobacteria NA NA	Control vs NH4
428807	20.49	-15.80	3.83	-4.13	0.000	0.001	k__Bacteria p__Proteobacteria c__Alphaproteobacteria o__Rhizobiales f__Hyphomicrobiaceae g__ s__	Control vs NH4
904675	15.56	-11.72	3.47	-3.38	0.001	0.015	k__Bacteria p__Proteobacteria c__Alphaproteobacteria o__Rhodobacterales f__Rhodobacteraceae NA NA	Control vs NH4
3834498	6.81	-17.92	3.08	-5.82	0.000	0.000	k__Bacteria p__Proteobacteria c__Alphaproteobacteria o__Rhodobacterales f__Rhodobacteraceae g__Roseivivax s__	Control vs NH4
548736	7.03	-16.85	3.23	-5.22	0.000	0.000	k__Bacteria p__Proteobacteria c__Alphaproteobacteria o__Rhodobacterales f__Rhodobacteraceae g__Shimia s__	Control vs NH4
178785	23.84	-19.19	3.57	-5.38	0.000	0.000	k__Bacteria p__Proteobacteria c__Gammaproteobacteria o__Oceanospirillales f__Alcanivoracaceae g__Alcanivorax NA	Control vs NO3
2932342	956.20	9.28	2.31	4.02	0.000	0.001	k__Bacteria p__Proteobacteria c__Deltaproteobacteria o__Desulfovibrionales f__Desulfovibrionaceae g__ s__	Control vs NO3
321405	86.87	-16.32	3.39	-4.82	0.000	0.000	k__Bacteria p__Proteobacteria c__Gammaproteobacteria o__Pseudomonadales f__Moraxellaceae g__Acinetobacter s__lwoffii	Control vs NO3
3633321	359.77	-20.49	2.61	-7.86	0.000	0.000	k__Bacteria p__Proteobacteria c__Gammaproteobacteria o__Pseudomonadales f__Moraxellaceae g__Acinetobacter s__johnsonii	Control vs NO3
1085703	367.78	-7.36	2.47	-2.98	0.003	0.023	k__Bacteria p__Proteobacteria c__Gammaproteobacteria o__Pseudomonadales f__Moraxellaceae g__Acinetobacter s__johnsonii	Control vs NO3

146037	5.31	11.80	3.95	2.99	0.003	0.023	k__Bacteria p__Proteobacteria c__Alphaproteobacteria o__Rhodobacterales f__Rhodobacteraceae NA NA	Control vs NO3
248590	7.31	10.20	3.57	2.86	0.004	0.025	k__Bacteria p__Proteobacteria c__Alphaproteobacteria o__Rhodobacterales f__Rhodobacteraceae g__Pseudoruegeria s__	Control vs NO3
431378	8.41	6.55	2.33	2.81	0.005	0.027	k__Bacteria p__Proteobacteria c__Alphaproteobacteria o__Rhodobacterales f__Rhodobacteraceae NA NA	Control vs NO3
1123147	11.28	7.01	2.41	2.91	0.004	0.024	k__Bacteria p__Proteobacteria c__Alphaproteobacteria o__Rhodobacterales f__Rhodobacteraceae NA NA	Control vs NO3
4420764	11.33	-12.58	3.52	-3.58	0.000	0.004	k__Bacteria p__Proteobacteria c__Alphaproteobacteria o__Rhodobacterales f__Rhodobacteraceae g__ s__	Control vs NO3
4421174	28.55	-21.46	3.93	-5.45	0.000	0.000	k__Bacteria p__Proteobacteria c__Alphaproteobacteria o__Rhodobacterales f__Rhodobacteraceae NA NA	Control vs NO3
144589	13.01	11.96	4.07	2.94	0.003	0.024	k__Bacteria p__Proteobacteria c__Alphaproteobacteria o__Sphingomonadales f__Sphingomonadaceae g__Novosphingobium s__	Control vs NO3
833774	5.60	11.88	4.11	2.89	0.004	0.024	k__Bacteria p__Proteobacteria c__Alphaproteobacteria o__Sphingomonadales f__Sphingomonadaceae g__Novosphingobium s__	Control vs NO3
4445466	12.88	-12.80	3.93	-3.26	0.001	0.011	k__Bacteria p__Firmicutes c__Bacilli o__Lactobacillales f__Streptococcaceae g__Streptococcus s__	Control vs NO3
4393354	25.52	-28.75	3.27	-8.78	0.000	0.000	k__Bacteria p__Proteobacteria c__Gammaproteobacteria o__Vibrionales f__Vibrionaceae g__Vibrio s__	Control vs NO3
1140185	45.17	-18.54	3.47	-5.34	0.000	0.000	k__Bacteria p__Proteobacteria c__Alphaproteobacteria o__Rhodospirillales o__Rhodospirillales NA NA	Control vs NO3
365755	24.16	-11.89	3.29	-3.61	0.000	0.004	k__Bacteria p__Proteobacteria c__Gammaproteobacteria o__Thiohalorhabdales o__Thiohalorhabdales g__ s__	Control vs NO3
150582	36.83	9.60	2.79	3.45	0.001	0.006	k__Bacteria p__Proteobacteria c__Alphaproteobacteria o__ c__Alphaproteobacteria g__ s__	Control vs Scarred
369965	14.43	13.25	3.45	3.84	0.000	0.002	k__Bacteria p__Proteobacteria c__Alphaproteobacteria NA c__Alphaproteobacteria NA NA	Control vs Scarred
OTU5	33.51	-17.58	3.54	-4.97	0.000	0.000	k__Bacteria p__Proteobacteria c__Alphaproteobacteria NA c__Alphaproteobacteria NA NA	Control vs Scarred
321533	197.96	4.24	1.69	2.51	0.012	0.047	k__Bacteria p__Bacteroidetes c__Cytophagia o__Cytophagales f__[Amoebophilaceae] g__SGUS912 s__	Control vs Scarred
2932342	956.20	8.87	2.21	4.01	0.000	0.002	k__Bacteria p__Proteobacteria c__Deltaproteobacteria o__Desulfovibrionales f__Desulfovibrionaceae g__ s__	Control vs Scarred
OTU121	1.46	7.11	2.51	2.83	0.005	0.025	k__Bacteria p__Proteobacteria c__Deltaproteobacteria o__Desulfovibrionales f__Desulfovibrionaceae g__ s__	Control vs Scarred
OTU80	4.12	6.78	2.49	2.72	0.007	0.027	k__Bacteria p__Proteobacteria c__Deltaproteobacteria o__Desulfovibrionales f__Desulfovibrionaceae g__ s__	Control vs Scarred
1010113	122.68	14.13	3.58	3.95	0.000	0.002	k__Bacteria p__Proteobacteria c__Gammaproteobacteria o__Enterobacteriales f__Enterobacteriaceae NA NA	Control vs Scarred

165867	40.49	8.76	2.69	3.26	0.001	0.010	k__Bacteria p__Proteobacteria c__Alphaproteobacteria o__Rhizobiales f__Hyphomicrobiaceae NA NA	Control vs Scarred
149505	22.93	9.48	3.36	2.82	0.005	0.025	k__Bacteria p__Proteobacteria c__Alphaproteobacteria o__Rhodobacterales f__Hyphomonadaceae g__Oceanicaulis s__	Control vs Scarred
220012	148.66	8.61	3.08	2.80	0.005	0.025	k__Bacteria p__Proteobacteria c__Gammaproteobacteria o__Pseudomonadales f__Pseudomonadaceae g__Pseudomonas s__	Control vs Scarred
60398	103.95	5.45	1.76	3.10	0.002	0.015	k__Bacteria p__Proteobacteria c__Alphaproteobacteria o__Rhodobacterales f__Rhodobacteraceae NA NA	Control vs Scarred
135260	5.93	10.03	3.64	2.75	0.006	0.026	k__Bacteria p__Proteobacteria c__Alphaproteobacteria o__Rhodobacterales f__Rhodobacteraceae NA NA	Control vs Scarred
146037	5.31	14.89	3.78	3.94	0.000	0.002	k__Bacteria p__Proteobacteria c__Alphaproteobacteria o__Rhodobacterales f__Rhodobacteraceae NA NA	Control vs Scarred
163471	13.31	7.30	2.36	3.09	0.002	0.015	k__Bacteria p__Proteobacteria c__Alphaproteobacteria o__Rhodobacterales f__Rhodobacteraceae NA NA	Control vs Scarred
539299	32.63	8.95	3.18	2.82	0.005	0.025	k__Bacteria p__Proteobacteria c__Alphaproteobacteria o__Rhodobacterales f__Rhodobacteraceae g__Marivita s__	Control vs Scarred
816411	66.85	6.15	1.68	3.66	0.000	0.004	k__Bacteria p__Proteobacteria c__Alphaproteobacteria o__Rhodobacterales f__Rhodobacteraceae g__Roseivivax s__	Control vs Scarred
904675	15.56	13.88	3.37	4.11	0.000	0.002	k__Bacteria p__Proteobacteria c__Alphaproteobacteria o__Rhodobacterales f__Rhodobacteraceae NA NA	Control vs Scarred
1123147	11.28	7.14	2.32	3.07	0.002	0.015	k__Bacteria p__Proteobacteria c__Alphaproteobacteria o__Rhodobacterales f__Rhodobacteraceae NA NA	Control vs Scarred
3180137	59.37	6.79	2.04	3.32	0.001	0.008	k__Bacteria p__Proteobacteria c__Alphaproteobacteria o__Rhodobacterales f__Rhodobacteraceae g__ s__	Control vs Scarred
431378	8.41	5.69	2.29	2.49	0.013	0.048	k__Bacteria p__Proteobacteria c__Alphaproteobacteria o__Rhodobacterales f__Rhodobacteraceae NA NA	Control vs Scarred
4327730	21.68	6.40	2.11	3.03	0.002	0.016	k__Bacteria p__Proteobacteria c__Alphaproteobacteria o__Rhodobacterales f__Rhodobacteraceae NA NA	Control vs Scarred
4404049	8.86	11.01	3.08	3.58	0.000	0.004	k__Bacteria p__Proteobacteria c__Alphaproteobacteria o__Rhodobacterales f__Rhodobacteraceae g__Rhodovulum s__	Control vs Scarred
4420764	11.33	8.95	3.26	2.74	0.006	0.026	k__Bacteria p__Proteobacteria c__Alphaproteobacteria o__Rhodobacterales f__Rhodobacteraceae g__ s__	Control vs Scarred
4456340	20.14	5.49	2.11	2.60	0.009	0.038	k__Bacteria p__Proteobacteria c__Alphaproteobacteria o__Rhodobacterales f__Rhodobacteraceae g__Rhodovulum s__	Control vs Scarred
144589	13.01	11.43	3.91	2.92	0.003	0.021	k__Bacteria p__Proteobacteria c__Alphaproteobacteria o__Sphingomonadales f__Sphingomonadaceae g__Novosphingobium s__	Control vs Scarred
833774	5.60	11.00	3.96	2.78	0.005	0.026	k__Bacteria p__Proteobacteria c__Alphaproteobacteria o__Sphingomonadales f__Sphingomonadaceae g__Novosphingobium s__	Control vs Scarred
365755	24.16	-11.33	3.14	-3.60	0.000	0.004	k__Bacteria p__Proteobacteria c__Gammaproteobacteria o__Thiohalorhabdales o__Thiohalorhabdales g__ s__	Control vs Scarred

2932342	956.20	-14.58	3.30	-4.42	0.000	0.000	k__Bacteria p__Proteobacteria c__Deltaproteobacteria o__Desulfovibrionales f__Desulfovibrionaceae g__ s__	High:scarred
OTU80	4.12	-9.60	3.64	-2.64	0.008	0.045	k__Bacteria p__Proteobacteria c__Deltaproteobacteria o__Desulfovibrionales f__Desulfovibrionaceae g__ s__	High:scarred
OTU123	2.07	-7.98	2.63	-3.03	0.002	0.018	k__Bacteria p__Proteobacteria c__Gammaproteobacteria o__Oceanospirillales f__Endozoicimonaceae g__ s__	High:scarred
1010113	122.68	-19.41	5.25	-3.70	0.000	0.003	k__Bacteria p__Proteobacteria c__Gammaproteobacteria o__Enterobacteriales f__Enterobacteriaceae NA NA	High:scarred
933546	36.50	16.98	4.10	4.14	0.000	0.001	k__Bacteria p__Proteobacteria c__Betaproteobacteria o__Neisseriales f__Neisseriaceae g__ s__	High:scarred
5826	19.30	-11.80	4.04	-2.92	0.004	0.022	k__Bacteria p__Proteobacteria c__Alphaproteobacteria o__Rhodobacterales f__Rhodobacteraceae g__Rhodovulum s__	High:scarred
60398	103.95	-7.39	2.62	-2.82	0.005	0.028	k__Bacteria p__Proteobacteria c__Alphaproteobacteria o__Rhodobacterales f__Rhodobacteraceae NA NA	High:scarred
146037	5.31	-16.88	5.61	-3.01	0.003	0.018	k__Bacteria p__Proteobacteria c__Alphaproteobacteria o__Rhodobacterales f__Rhodobacteraceae NA NA	High:scarred
163471	13.31	-10.05	3.47	-2.89	0.004	0.023	k__Bacteria p__Proteobacteria c__Alphaproteobacteria o__Rhodobacterales f__Rhodobacteraceae NA NA	High:scarred
808046	39.28	-22.34	4.51	-4.95	0.000	0.000	k__Bacteria p__Proteobacteria c__Alphaproteobacteria o__Rhodobacterales f__Rhodobacteraceae g__ s__	High:scarred
816411	66.85	-7.83	2.50	-3.13	0.002	0.016	k__Bacteria p__Proteobacteria c__Alphaproteobacteria o__Rhodobacterales f__Rhodobacteraceae g__Roseivivax s__	High:scarred
904675	15.56	-27.14	5.02	-5.41	0.000	0.000	k__Bacteria p__Proteobacteria c__Alphaproteobacteria o__Rhodobacterales f__Rhodobacteraceae NA NA	High:scarred
3180137	59.37	-11.84	3.07	-3.86	0.000	0.002	k__Bacteria p__Proteobacteria c__Alphaproteobacteria o__Rhodobacterales f__Rhodobacteraceae g__ s__	High:scarred
4404049	8.86	-29.01	4.64	-6.26	0.000	0.000	k__Bacteria p__Proteobacteria c__Alphaproteobacteria o__Rhodobacterales f__Rhodobacteraceae g__Rhodovulum s__	High:scarred
4420764	11.33	-14.80	4.83	-3.07	0.002	0.017	k__Bacteria p__Proteobacteria c__Alphaproteobacteria o__Rhodobacterales f__Rhodobacteraceae g__ s__	High:scarred
4421174	28.55	-17.37	5.62	-3.09	0.002	0.017	k__Bacteria p__Proteobacteria c__Alphaproteobacteria o__Rhodobacterales f__Rhodobacteraceae NA NA	High:scarred
144589	13.01	-20.80	5.83	-3.57	0.000	0.004	k__Bacteria p__Proteobacteria c__Alphaproteobacteria o__Sphingomonadales f__Sphingomonadaceae g__Novosphingobium s__	High:scarred
833774	5.60	-20.13	5.90	-3.41	0.001	0.007	k__Bacteria p__Proteobacteria c__Alphaproteobacteria o__Sphingomonadales f__Sphingomonadaceae g__Novosphingobium s__	High:scarred
4393354	25.52	-19.76	4.58	-4.31	0.000	0.000	k__Bacteria p__Proteobacteria c__Gammaproteobacteria o__Vibrionales f__Vibrionaceae g__Vibrio s__	High:scarred
369965	14.43	-20.23	5.31	-3.81	0.000	0.002	k__Bacteria p__Proteobacteria c__Alphaproteobacteria NA c__Alphaproteobacteria NA NA	NH4:high

4478041	6.03	-23.60	6.12	-3.86	0.000	0.002	k__Bacteria p__Cyanobacteria c__Oscillatoriophycideae o__Chroococcales f__Cyanobacteriaceae g__Rhopalodia s__gibba	NH4:high
2932342	956.20	-9.11	3.40	-2.68	0.007	0.043	k__Bacteria p__Proteobacteria c__Deltaproteobacteria o__Desulfovibrionales f__Desulfovibrionaceae g__ s__	NH4:high
165867	40.49	-21.82	4.25	-5.14	0.000	0.000	k__Bacteria p__Proteobacteria c__Alphaproteobacteria o__Rhizobiales f__Hyphomicrobiaceae NA NA	NH4:high
143362	29.69	9.99	3.17	3.15	0.002	0.015	k__Bacteria p__Proteobacteria c__Gammaproteobacteria o__Pseudomonadales f__Moraxellaceae g__Acinetobacter s__	NH4:high
1085703	367.78	10.82	3.42	3.16	0.002	0.015	k__Bacteria p__Proteobacteria c__Gammaproteobacteria o__Pseudomonadales f__Moraxellaceae g__Acinetobacter s__johnsonii	NH4:high
3633321	359.77	9.98	3.62	2.76	0.006	0.037	k__Bacteria p__Proteobacteria c__Gammaproteobacteria o__Pseudomonadales f__Moraxellaceae g__Acinetobacter s__johnsonii	NH4:high
4333705	68.73	12.13	3.21	3.78	0.000	0.002	k__Bacteria p__Proteobacteria c__Gammaproteobacteria o__Pseudomonadales f__Moraxellaceae g__Acinetobacter NA	NH4:high
933546	36.50	16.01	4.22	3.80	0.000	0.002	k__Bacteria p__Proteobacteria c__Betaproteobacteria o__Neisseriales f__Neisseriaceae g__ s__	NH4:high
273239	37.01	-19.63	4.95	-3.97	0.000	0.002	k__Bacteria p__Proteobacteria c__Gammaproteobacteria o__Pseudomonadales f__Pseudomonadaceae g__ s__	NH4:high
548736	7.03	17.60	4.88	3.61	0.000	0.004	k__Bacteria p__Proteobacteria c__Alphaproteobacteria o__Rhodobacterales f__Rhodobacteraceae g__Shimia s__	NH4:high
3180137	59.37	-9.34	3.20	-2.92	0.003	0.026	k__Bacteria p__Proteobacteria c__Alphaproteobacteria o__Rhodobacterales f__Rhodobacteraceae g__ s__	NH4:high
4306551	56.26	-21.50	4.04	-5.32	0.000	0.000	k__Bacteria p__Proteobacteria c__Alphaproteobacteria o__Rhodobacterales f__Rhodobacteraceae NA NA	NH4:high
4327730	21.68	-9.06	3.30	-2.74	0.006	0.037	k__Bacteria p__Proteobacteria c__Alphaproteobacteria o__Rhodobacterales f__Rhodobacteraceae NA NA	NH4:high
4404049	8.86	-19.79	4.81	-4.11	0.000	0.001	k__Bacteria p__Proteobacteria c__Alphaproteobacteria o__Rhodobacterales f__Rhodobacteraceae g__Rhodovulum s__	NH4:high
4421174	28.55	17.18	5.78	2.97	0.003	0.024	k__Bacteria p__Proteobacteria c__Alphaproteobacteria o__Rhodobacterales f__Rhodobacteraceae NA NA	NH4:high
144589	13.01	-17.79	6.01	-2.96	0.003	0.024	k__Bacteria p__Proteobacteria c__Alphaproteobacteria o__Sphingomonadales f__Sphingomonadaceae g__Novosphingobium s__	NH4:high
833774	5.60	-17.47	6.08	-2.88	0.004	0.028	k__Bacteria p__Proteobacteria c__Alphaproteobacteria o__Sphingomonadales f__Sphingomonadaceae g__Novosphingobium s__	NH4:high
369965	14.43	30.00	7.18	4.18	0.000	0.001	k__Bacteria p__Proteobacteria c__Alphaproteobacteria NA c__Alphaproteobacteria NA NA	NH4:high:scarred
4478041	6.03	26.59	8.30	3.20	0.001	0.012	k__Bacteria p__Cyanobacteria c__Oscillatoriophycideae o__Chroococcales f__Cyanobacteriaceae g__Rhopalodia s__gibba	NH4:high:scarred
165867	40.49	20.99	5.69	3.69	0.000	0.003	k__Bacteria p__Proteobacteria c__Alphaproteobacteria o__Rhizobiales f__Hyphomicrobiaceae NA NA	NH4:high:scarred

933546	36.50	-15.72	5.66	-2.78	0.005	0.032	k__Bacteria p__Proteobacteria c__Betaproteobacteria o__Neisseriales f__Neisseriaceae g__ s__	NH4:high:scarred
200552	1298.64	13.70	4.89	2.80	0.005	0.031	k__Bacteria p__Proteobacteria c__Gammaproteobacteria o__Pseudomonadales f__Pseudomonadaceae NA NA	NH4:high:scarred
273239	37.01	26.47	6.67	3.97	0.000	0.002	k__Bacteria p__Proteobacteria c__Gammaproteobacteria o__Pseudomonadales f__Pseudomonadaceae g__ s__	NH4:high:scarred
146037	5.31	30.00	7.93	3.78	0.000	0.003	k__Bacteria p__Proteobacteria c__Alphaproteobacteria o__Rhodobacterales f__Rhodobacteraceae NA NA	NH4:high:scarred
808046	39.28	19.24	6.27	3.07	0.002	0.016	k__Bacteria p__Proteobacteria c__Alphaproteobacteria o__Rhodobacterales f__Rhodobacteraceae g__ s__	NH4:high:scarred
3180137	59.37	15.12	4.36	3.47	0.001	0.005	k__Bacteria p__Proteobacteria c__Alphaproteobacteria o__Rhodobacterales f__Rhodobacteraceae g__ s__	NH4:high:scarred
4306551	56.26	23.72	5.43	4.37	0.000	0.001	k__Bacteria p__Proteobacteria c__Alphaproteobacteria o__Rhodobacterales f__Rhodobacteraceae NA NA	NH4:high:scarred
4327730	21.68	14.29	4.46	3.20	0.001	0.012	k__Bacteria p__Proteobacteria c__Alphaproteobacteria o__Rhodobacterales f__Rhodobacteraceae NA NA	NH4:high:scarred
4421174	28.55	22.33	7.88	2.84	0.005	0.030	k__Bacteria p__Proteobacteria c__Alphaproteobacteria o__Rhodobacterales f__Rhodobacteraceae NA NA	NH4:high:scarred
144589	13.01	30.00	8.13	3.69	0.000	0.003	k__Bacteria p__Proteobacteria c__Alphaproteobacteria o__Sphingomonadales f__Sphingomonadaceae g__Novosphingobium s__	NH4:high:scarred
833774	5.60	30.00	8.23	3.64	0.000	0.003	k__Bacteria p__Proteobacteria c__Alphaproteobacteria o__Sphingomonadales f__Sphingomonadaceae g__Novosphingobium s__	NH4:high:scarred
1040220	6654.92	20.69	6.72	3.08	0.002	0.016	k__Bacteria p__Firmicutes c__Bacilli o__Bacillales f__Staphylococcaceae g__Staphylococcus s__	NH4:high:scarred
4345285	608.03	21.86	7.32	2.99	0.003	0.020	k__Bacteria p__Firmicutes c__Bacilli o__Bacillales f__Staphylococcaceae g__Staphylococcus s__	NH4:high:scarred
4445466	12.88	30.00	7.82	3.84	0.000	0.003	k__Bacteria p__Firmicutes c__Bacilli o__Lactobacillales f__Streptococcaceae g__Streptococcus s__	NH4:high:scarred
4393354	25.52	30.00	6.47	4.63	0.000	0.000	k__Bacteria p__Proteobacteria c__Gammaproteobacteria o__Vibrionales f__Vibrionaceae g__Vibrio s__	NH4:high:scarred
369965	14.43	-24.29	4.76	-5.10	0.000	0.000	k__Bacteria p__Proteobacteria c__Alphaproteobacteria NA c__Alphaproteobacteria NA NA	NH4:scarred
2932342	956.20	-10.81	3.05	-3.54	0.000	0.008	k__Bacteria p__Proteobacteria c__Deltaproteobacteria o__Desulfovibrionales f__Desulfovibrionaceae g__ s__	NH4:scarred
800197	36.52	-12.79	4.49	-2.85	0.004	0.047	k__Bacteria p__Proteobacteria c__Alphaproteobacteria o__Rhodobacterales f__Hyphomonadaceae g__Hyphomonas s__	NH4:scarred
146037	5.31	-19.77	5.28	-3.74	0.000	0.005	k__Bacteria p__Proteobacteria c__Alphaproteobacteria o__Rhodobacterales f__Rhodobacteraceae NA NA	NH4:scarred
3180137	59.37	-9.28	2.83	-3.28	0.001	0.018	k__Bacteria p__Proteobacteria c__Alphaproteobacteria o__Rhodobacterales f__Rhodobacteraceae g__ s__	NH4:scarred

4327730	21.68	-9.12	2.94	-3.11	0.002	0.028	k__Bacteria p__Proteobacteria c__Alphaproteobacteria o__Rhodobacterales f__Rhodobacteraceae NA NA	NH4:scarred
4421174	28.55	-15.92	5.20	-3.06	0.002	0.028	k__Bacteria p__Proteobacteria c__Alphaproteobacteria o__Rhodobacterales f__Rhodobacteraceae NA NA	NH4:scarred
548736	7.03	16.53	4.40	3.76	0.000	0.005	k__Bacteria p__Proteobacteria c__Alphaproteobacteria o__Rhodobacterales f__Rhodobacteraceae g__Shimia s__	NH4:scarred
4445466	12.88	-28.42	5.13	-5.54	0.000	0.000	k__Bacteria p__Firmicutes c__Bacilli o__Lactobacillales f__Streptococcaceae g__Streptococcus s__	NH4:scarred
365755	24.16	12.13	4.27	2.84	0.004	0.047	k__Bacteria p__Proteobacteria c__Gammaproteobacteria o__Thiohalorhabdales o__Thiohalorhabdales g__ s__	NH4:scarred
178785	23.84	17.61	5.11	3.45	0.001	0.007	k__Bacteria p__Proteobacteria c__Gammaproteobacteria o__Oceanospirillales f__Alcanivoracaceae g__Alcanivorax NA	NO3:high
2932342	956.20	-12.60	3.36	-3.75	0.000	0.003	k__Bacteria p__Proteobacteria c__Deltaproteobacteria o__Desulfovibrionales f__Desulfovibrionaceae g__ s__	NO3:high
428807	20.49	22.30	5.83	3.82	0.000	0.003	k__Bacteria p__Proteobacteria c__Alphaproteobacteria o__Rhizobiales f__Hyphomicrobiaceae g__ s__	NO3:high
321405	86.87	18.03	4.83	3.73	0.000	0.003	k__Bacteria p__Proteobacteria c__Gammaproteobacteria o__Pseudomonadales f__Moraxellaceae g__Acinetobacter s__lwoffii	NO3:high
3633321	359.77	22.77	3.69	6.17	0.000	0.000	k__Bacteria p__Proteobacteria c__Gammaproteobacteria o__Pseudomonadales f__Moraxellaceae g__Acinetobacter s__johnsonii	NO3:high
933546	36.50	18.73	4.16	4.50	0.000	0.000	k__Bacteria p__Proteobacteria c__Betaproteobacteria o__Neisseriales f__Neisseriaceae g__ s__	NO3:high
4421174	28.55	28.24	5.75	4.91	0.000	0.000	k__Bacteria p__Proteobacteria c__Alphaproteobacteria o__Rhodobacterales f__Rhodobacteraceae NA NA	NO3:high
144589	13.01	-16.20	5.90	-2.74	0.006	0.050	k__Bacteria p__Proteobacteria c__Alphaproteobacteria o__Sphingomonadales f__Sphingomonadaceae g__Novosphingobium s__	NO3:high
833774	5.60	-16.64	5.99	-2.78	0.005	0.049	k__Bacteria p__Proteobacteria c__Alphaproteobacteria o__Sphingomonadales f__Sphingomonadaceae g__Novosphingobium s__	NO3:high
4445466	12.88	30.00	5.73	5.23	0.000	0.000	k__Bacteria p__Firmicutes c__Bacilli o__Lactobacillales f__Streptococcaceae g__Streptococcus s__	NO3:high
1140185	45.17	14.51	4.98	2.91	0.004	0.035	k__Bacteria p__Proteobacteria c__Alphaproteobacteria o__Rhodospirillales o__Rhodospirillales NA NA	NO3:high
365755	24.16	-15.96	4.78	-3.34	0.001	0.009	k__Bacteria p__Proteobacteria c__Gammaproteobacteria o__Thiohalorhabdales o__Thiohalorhabdales g__ s__	NO3:high
2932342	956.20	18.68	4.59	4.07	0.000	0.002	k__Bacteria p__Proteobacteria c__Deltaproteobacteria o__Desulfovibrionales f__Desulfovibrionaceae g__ s__	NO3:high:scarred
1010113	122.68	30.00	7.32	4.10	0.000	0.002	k__Bacteria p__Proteobacteria c__Gammaproteobacteria o__Enterobacteriales f__Enterobacteriaceae NA NA	NO3:high:scarred
428807	20.49	-22.70	7.83	-2.90	0.004	0.035	k__Bacteria p__Proteobacteria c__Alphaproteobacteria o__Rhizobiales f__Hyphomicrobiaceae g__ s__	NO3:high:scarred
933546	36.50	-17.77	5.61	-3.17	0.002	0.016	k__Bacteria p__Proteobacteria c__Betaproteobacteria o__Neisseriales f__Neisseriaceae g__ s__	NO3:high:scarred

337713	13.70	29.92	8.02	3.73	0.000	0.004	k__Bacteria p__Planctomycetes c__Planctomycetia o__Pirellulales f__Pirellulaceae g__ s__	NO3:high:scarred
200552	1298.64	13.97	4.91	2.84	0.004	0.039	k__Bacteria p__Proteobacteria c__Gammaproteobacteria o__Pseudomonadales f__Pseudomonadaceae NA NA	NO3:high:scarred
808046	39.28	21.75	6.22	3.50	0.000	0.008	k__Bacteria p__Proteobacteria c__Alphaproteobacteria o__Rhodobacterales f__Rhodobacteraceae g__ s__	NO3:high:scarred
904675	15.56	30.00	6.98	4.30	0.000	0.002	k__Bacteria p__Proteobacteria c__Alphaproteobacteria o__Rhodobacterales f__Rhodobacteraceae NA NA	NO3:high:scarred
4404049	8.86	24.17	6.39	3.78	0.000	0.004	k__Bacteria p__Proteobacteria c__Alphaproteobacteria o__Rhodobacterales f__Rhodobacteraceae g__Rhodovulum s__	NO3:high:scarred
144589	13.01	26.73	8.05	3.32	0.001	0.010	k__Bacteria p__Proteobacteria c__Alphaproteobacteria o__Sphingomonadales f__Sphingomonadaceae g__Novosphingobium s__	NO3:high:scarred
833774	5.60	27.10	8.16	3.32	0.001	0.010	k__Bacteria p__Proteobacteria c__Alphaproteobacteria o__Sphingomonadales f__Sphingomonadaceae g__Novosphingobium s__	NO3:high:scarred
4393354	25.52	17.81	6.46	2.76	0.006	0.046	k__Bacteria p__Proteobacteria c__Gammaproteobacteria o__Vibrionales f__Vibrionaceae g__Vibrio s__	NO3:high:scarred
593848	3284.32	17.19	5.06	3.39	0.001	0.010	k__Bacteria p__Proteobacteria c__Gammaproteobacteria o__Xanthomonadales f__Xanthomonadaceae g__Stenotrophomonas s__	NO3:high:scarred
OTU5	33.51	22.02	4.94	4.46	0.000	0.000	k__Bacteria p__Proteobacteria c__Alphaproteobacteria NA c__Alphaproteobacteria NA NA	NO3:scarred
2932342	956.20	-11.56	3.12	-3.70	0.000	0.002	k__Bacteria p__Proteobacteria c__Deltaproteobacteria o__Desulfovibrionales f__Desulfovibrionaceae g__ s__	NO3:scarred
1010113	122.68	-23.35	5.08	-4.59	0.000	0.000	k__Bacteria p__Proteobacteria c__Gammaproteobacteria o__Enterobacteriales f__Enterobacteriaceae NA NA	NO3:scarred
3633321	359.77	12.60	3.48	3.63	0.000	0.003	k__Bacteria p__Proteobacteria c__Gammaproteobacteria o__Pseudomonadales f__Moraxellaceae g__Acinetobacter s__johnsonii	NO3:scarred
337713	13.70	-23.61	5.46	-4.32	0.000	0.000	k__Bacteria p__Planctomycetes c__Planctomycetia o__Pirellulales f__Pirellulaceae g__ s__	NO3:scarred
200552	1298.64	-13.12	3.38	-3.89	0.000	0.001	k__Bacteria p__Proteobacteria c__Gammaproteobacteria o__Pseudomonadales f__Pseudomonadaceae NA NA	NO3:scarred
220012	148.66	-12.72	4.36	-2.92	0.003	0.024	k__Bacteria p__Proteobacteria c__Gammaproteobacteria o__Pseudomonadales f__Pseudomonadaceae g__Pseudomonas s__	NO3:scarred
256116	494.08	-11.43	3.38	-3.38	0.001	0.006	k__Bacteria p__Proteobacteria c__Gammaproteobacteria o__Pseudomonadales f__Pseudomonadaceae g__ s__	NO3:scarred
146037	5.31	-15.96	5.30	-3.01	0.003	0.019	k__Bacteria p__Proteobacteria c__Alphaproteobacteria o__Rhodobacterales f__Rhodobacteraceae NA NA	NO3:scarred
4404049	8.86	-11.52	4.27	-2.70	0.007	0.045	k__Bacteria p__Proteobacteria c__Alphaproteobacteria o__Rhodobacterales f__Rhodobacteraceae g__Rhodovulum s__	NO3:scarred
4421174	28.55	22.62	5.26	4.30	0.000	0.000	k__Bacteria p__Proteobacteria c__Alphaproteobacteria o__Rhodobacterales f__Rhodobacteraceae NA NA	NO3:scarred

144589	13.01	-14.67	5.47	-2.68	0.007	0.045	k__Bacteria p__Proteobacteria c__Alphaproteobacteria o__Sphingomonadales f__Sphingomonadaceae g__Novosphingobium s__	NO3:scarred
4393354	25.52	29.63	4.35	6.81	0.000	0.000	k__Bacteria p__Proteobacteria c__Gammaproteobacteria o__Vibrionales f__Vibrionaceae g__Vibrio s__	NO3:scarred
593848	3284.32	-10.54	3.46	-3.05	0.002	0.019	k__Bacteria p__Proteobacteria c__Gammaproteobacteria o__Xanthomonadales f__Xanthomonadaceae g__Stenotrophomonas s__	NO3:scarred
1140185	45.17	18.35	4.62	3.97	0.000	0.001	k__Bacteria p__Proteobacteria c__Alphaproteobacteria o__Rhodospirillales o__Rhodospirillales NA NA	NO3:scarred
365755	24.16	30.00	4.45	6.74	0.000	0.000	k__Bacteria p__Proteobacteria c__Gammaproteobacteria o__Thiohalorhabdales o__Thiohalorhabdales g__ s__	NO3:scarred

Supplementary Table 2.9. Comparison of differential abundance analysis results from OTU tables summarized at the Family, Genus, and OTU levels. Family and Genus tables were obtained using the tax_glom function in phyloseq on the unrarefied input data to DESeq2 analysis presented in Supplementary Table S8. All results are presented as log-fold changes that were significant at an adjusted p-value of <0.05. Significant families are labeled at the family level. Significant genera are listed under their corresponding family and labeled by Genus. Significant OTUs are listed under their corresponding genus and are labeled by Species.

Taxonomy			Comparison										
Family	Genus	Species	Control vs. High T	Control vs. Scar	Control vs. NO3	Control vs. NH4	High T: Scar	NO3: Scar	NH4: Scar	NO3: High T	NH4: High T	NO3:High T :Scar	NH4:High T :Scar
c__Alphaproteobacteria			-	30.00	-24.25	22.61	-	24.00	30.00	30.00	-30.00	30.00	
	g__		-20.55	-	-	-15.52	23.49	-30.00	30.00	30.00	-	NA	NA
		s__	11.70	13.25	-	12.01	-	-	-24.29	-	-20.23	-	30.00
		s__	-	-17.58	-	-	-	22.02	-	-	-	-	-
		s__	10.61	9.60	-	-	-	-	-	-	-	-	-
c__Alphaproteobacteria; o__BD7-3			-30.00	21.60	-30.00	-	21.56	-30.00	-30.00	-	-30.00	-	
	g__		-	-	-	-15.65	30.00	-30.00	-28.93	26.82	-	NA	NA
c__Gammaproteobacteria; o__Thiohalorhabdales			-16.09	-	-30.00	30.00	-	-30.00	30.00	-30.00	-	-	
	g__		-	-16.26	-30.00	-	30.00	-	27.33	-30.00	-	NA	NA
		s__	-	-11.33	-11.89	-	-	30.00	12.13	-15.96	-	-	-
f__[Amoebophilaceae]			30.00	30.00	30.00	30.00	-30.00	30.00	24.78	-	-	-30.00	
	g__SGUS912		-	30.00	30.00	30.00	-30.00	30.00	-30.00	-	-30.00	NA	NA
		s__	5.87	4.24	-	-	-	-	-	-	-	-	-
f__Alcanivoracaceae			30.00	30.00	-30.00	30.00	-30.00	-30.00	-30.00	-30.00	-	-30.00	
	g__Alcanivorax		-	-	-30.00	-	-	-30.00	-30.00	-	-	NA	NA

		NA	-	-	-19.19	-	-	-	-	17.61	-	-	-
f__Cohaesibacteraceae			-30.00	-30.00	-30.00	-22.68	-	-21.08	-22.08	-	-	30.00	
	g__Cohaesibacter		-	-	-	-	-	-30.00	-	-	-	NA	NA
f__Cyanobacteriaceae			17.39	-	-25.91	-30.00	-	-	-	-	-	30.00	
	g__Rhopalodia		-	-	-30.00	-30.00	-27.12	-	-	24.90	-	NA	NA
		s__gibba	-	-	-	-	-	-	-	-	-23.60	-	26.59
f__Desulfovibrionaceae			30.00	30.00	30.00	30.00	-30.00	-30.00	-	25.29	-	-	
	g__		-	-	30.00	30.00	-	-30.00	-30.00	-	-30.00	NA	NA
		s__	10.65	8.87	9.28	-	-14.58	-11.56	-10.81	-12.60	-9.11	18.68	-
		s__	7.13	7.11	-	-	-	-	-	-	-	-	-
		s__	7.36	6.78	-	-	-9.60	-	-	-	-	-	-
f__Endozoicimonaceae			30.00	30.00	30.00	30.00	-30.00	30.00	30.00	25.30	-	-30.00	
	g__		-	30.00	30.00	30.00	-30.00	30.00	-	-	-30.00	NA	NA
		s__	5.66	-	-	-	-7.98	-	-	-	-	-	-
f__Enterobacteriaceae			30.00	30.00	30.00	30.00	-30.00	30.00	26.07	-	-	-30.00	
	NA		-	30.00	30.00	30.00	-30.00	30.00	-30.00	-	-28.47	NA	NA
		NA	18.49	14.13	-	-	-19.41	-23.35	-	-	-	30.00	-
f__Enterobacteriaceae	g__Klebsiella		-	30.00	30.00	30.00	-30.00	30.00	-30.00	-	-24.38	NA	NA
f__Flavobacteriaceae			20.27	-	-	-21.56	30.00	-	-	30.00	-	30.00	
	g__Ascidianibacter		-	-	-	-24.46	-	-26.07	30.00	30.00	-21.61	NA	NA
	NA		-	-	-	-30.00	30.00	-30.00	-	-30.00	-	NA	NA
f__Hyphomicrobiaceae			30.00	24.64	-30.00	30.00	-30.00	-	30.00	30.00	-30.00	30.00	

	NA		27.37	-	-	16.34	-24.81	-30.00	30.00	-	-30.00	NA	NA
		NA	8.02	8.76	-	-	-	-	-	-	-21.82	-	20.99
	g__		-30.00	-	-	-30.00	21.94	-30.00	-	-	-	NA	NA
		s__	-15.27	-	-	-15.80	-	-	-	22.30	-	-22.70	-
f__Hyphomonadaceae			-	-30.00	-30.00	30.00	30.00	27.37	-30.00	30.00	25.64	30.00	
	g__Oceanicaulis		-	21.76	-30.00	-30.00	30.00	-	-	-	-	NA	NA
		s__	-	9.48	-	-	-	-	-	-	-	-	-
	g__Hyphomonas		-30.00	-	-	23.67	-	-27.36	-30.00	-	25.59	NA	NA
		s__	9.91	-	-	-	-	-	-12.79	-	-	-	-
f__Moraxellaceae			20.94	30.00	30.00	30.00	-30.00	30.00	25.91	30.00	-	-30.00	
	g__Acinetobacter		-	30.00	30.00	30.00	-30.00	30.00	-29.38	-	-	NA	NA
		NA	-	-	-	-	-	-	-	-	12.13	-	-
		s__	-	-	-	-	-	-	-	-	9.99	-	-
		s__johnsonii	-	-	-7.36	-	-	-	-	-	10.82	-	-
		s__johnsonii	-	-	-20.49	-	-	12.60	-	22.77	9.98	-	-
		s__lwoffii	-	-	-16.32	-	-	-	-	18.03	-	-	-
f__Neisseriaceae			21.37	23.72	30.00	30.00	-30.00	-30.00	30.00	30.00	-	-30.00	
	g__		30.00	-	-	27.49	-	-30.00	30.00	30.00	-30.00	NA	NA
		s__	-14.00	-	-	-	16.98	-	-	18.73	16.01	-17.77	-15.72
f__Pirellulaceae			23.11	-30.00	-30.00	-15.49	-30.00	-30.00	-30.00	-	30.00	30.00	
	g__		-17.21	-	-13.14	-13.67	-	-30.00	-	-	-	NA	NA

		s__	-	-	-	-	-	-23.61	-	-	-	29.92	-
f__Propionibacteriaceae			-19.56	30.00	30.00	30.00	-30.00	-30.00	-	-	30.00	-30.00	
	g__Propionibacterium		-26.02	-	30.00	15.30	-30.00	-30.00	-	-	30.00	NA	NA
f__Pseudomonadaceae			30.00	30.00	30.00	30.00	-30.00	-30.00	22.97	22.87	-	-	
	NA		-	-	30.00	-	-	-30.00	-	-25.74	-	NA	NA
		NA	-	-	-	-	-	-13.12	-	-	-	13.97	13.70
f__Pseudomonadaceae	g__Pseudomonas		-	-	18.28	-	-30.00	-30.00	30.00	-30.00	-	NA	NA
		s__	-	8.61	-	-	-	-12.72	-	-	-	-	-
	g__		-	-	30.00	-	-	-30.00	-	-	-	NA	NA
		s__	-	-	-	-	-	-11.43	-	-	-	-	-
		s__	-	-	-	-	-	-	-	-	-19.63	-	26.47
f__Rhodobacteraceae			30.00	30.00	30.00	30.00	-30.00	30.00	27.87	22.98	-	-30.00	
	g__Dinoroseobacter		-20.94	30.00	30.00	-30.00	-30.00	30.00	-	-	-	NA	NA
	NA		-	30.00	30.00	30.00	-30.00	30.00	-28.29	-	-28.38	NA	NA
		NA	5.41	5.45	-	-	-7.39	-	-	-	-	-	-
		NA	-	10.03	-	-	-	-	-	-	-	-	-
		NA	12.35	14.89	11.80	-	-16.88	-15.96	-19.77	-	-	-	30.00
		NA	7.08	7.30	-	-	-10.05	-	-	-	-	-	-
		NA	6.57	5.69	6.55	-	-	-	-	-	-	-	-
		NA	15.13	13.88	-	-11.72	-27.14	-	-	-	-	30.00	-
		NA	7.70	7.14	7.01	-	-	-	-	-	-	-	-
		NA	-	-	-	-	-	-	-	-	-21.50	-	23.72

		NA	6.68	6.40	-	-	-	-	-9.12	-	-9.06	-	14.29
		NA	-	-	-21.46	-	-17.37	22.62	-15.92	28.24	17.18	-	22.33
	g__Marivita		-	30.00	30.00	-30.00	-30.00	30.00	-	-	-30.00	NA	NA
		s__	-	8.95	-	-	-	-	-	-	-	-	-
	g__Shimia		21.07	-25.77	-	-15.17	-30.00	-	30.00	30.00	30.00	NA	NA
		s__	-	-	-	-16.85	-	-	16.53	-	17.60	-	-
	g__Roseivivax		-	-	30.00	-	-	-30.00	30.00	-	-	NA	NA
		s__	5.60	6.15	-	-	-7.83	-	-	-	-	-	-
		s__	-	-	-	-17.92	-	-	-	-	-	-	-
	g__Anaerospora		-30.00	-20.26	-30.00	-30.00	-	-	-25.12	30.00	25.00	NA	NA
	g__Pseudorueger ia		-27.30	-24.06	28.58	-22.38	-	-30.00	-	-30.00	-	NA	NA
		s__	-	-	10.20	-	-	-	-	-	-	-	-
	g__		-	30.00	30.00	-	-30.00	30.00	-	-	-	NA	NA
		s__	-	-	-	-	-22.34	-	-	-	-	21.75	19.24
		s__	6.70	6.79	-	-	-11.84	-	-9.28	-	-9.34	-	15.12
		s__	9.51	8.95	-12.58	-	-14.80	-	-	-	-	-	-
	g__Rhodovulu m		-30.00	-	-27.92	30.00	30.00	-26.19	-23.96	-	-30.00	NA	NA
		s__	-	-	-	-	-11.80	-	-	-	-	-	-
		s__	-	11.01	-	-	-29.01	-11.52	-	-	-19.79	24.17	-
		s__	-	5.49	-	-	-	-	-	-	-	-	-
	g__Jannaschia		-18.38	-	-	20.57	-30.00	-30.00	28.32	30.00	24.72	NA	NA
o__Rhodospirillales	NA	NA	-	-	-18.54	-	-	18.35	-	14.51	-	-	-
f__Sphingomonadaceae			-	-	-	-30.00	-	-30.00	-	-30.00	-	30.00	

	g__Novosphingobium		-16.79	-	-	-30.00	-	-30.00	-	-	-	NA	NA
		s__	11.48	11.43	11.96	-	-20.80	-14.67	-	-16.20	-17.79	26.73	30.00
		s__	11.10	11.00	11.88	-	-20.13	-	-	-16.64	-17.47	27.10	30.00
f__Staphylococcaceae			30.00	30.00	-30.00	30.00	-30.00	-30.00	-30.00	-30.00	-	-	
	g__Staphylococcus		-	-	-27.12	30.00	-	-30.00	-30.00	-	-	NA	NA
		s__	-	-	-	-	-	-	-	-	-	-	20.69
		s__	-	-	-	-	-	-	-	-	-	-	21.86
f__Streptococcaceae			30.00	-30.00	-	30.00	-	-30.00	-30.00	30.00	-30.00	-30.00	
	g__Streptococcus		-	-26.70	-	-	27.88	-30.00	-30.00	30.00	-30.00	NA	NA
		s__	-12.68	-	-12.80	-	-	-	-28.42	30.00	-	-	30.00
f__Synechococcaceae			22.18	30.00	30.00	-	-30.00	-30.00	-30.00	27.97	30.00	-30.00	
	g__Synechococcus		-	-	29.08	-	-30.00	-30.00	-30.00	-	30.00	NA	NA
f__Vibrionaceae			30.00	-30.00	-30.00	30.00	-30.00	-	-30.00	-30.00	-30.00	-	
	g__Vibrio		-	-30.00	-30.00	30.00	-	-	-29.01	-30.00	-28.70	NA	NA
		s__	-	-	-28.75	-	-19.76	29.63	-	-	-	17.81	30.00
o__Acidimicrobiales; f__wb1_P06			-	-	-30.00	30.00	-30.00	-30.00	30.00	-26.28	30.00	30.00	
	g__		-	-	-	30.00	-	-30.00	-	-30.00	-	NA	NA
f__Xanthomonadaceae			30.00	30.00	-	30.00	-30.00	-30.00	-	30.00	-	-	
	g__Stenotrophomonas		-	-	-24.05	-	-24.97	-30.00	-	27.36	-	NA	NA
		s__	-	-	-	-	-	-10.54	-	-	-	17.19	-
c: Alphaproteobactieria; NA			28.84	-30.00	-30.00	-18.68	-	29.95	-30.00	30.00	30.00	30.00	

	NA		-16.77	-13.23	-	-11.87	27.57	-26.58	-30.00	26.51	-	NA	NA
o__Rhodospirillales; NA			-	-30.00	-16.67	-30.00	29.21	-30.00	-30.00	28.63	-28.40	-30.00	
	NA		-	-	-26.08	-	-	-	-	-	-	NA	NA

Appendix B: Ch. 3 Supplementary Material

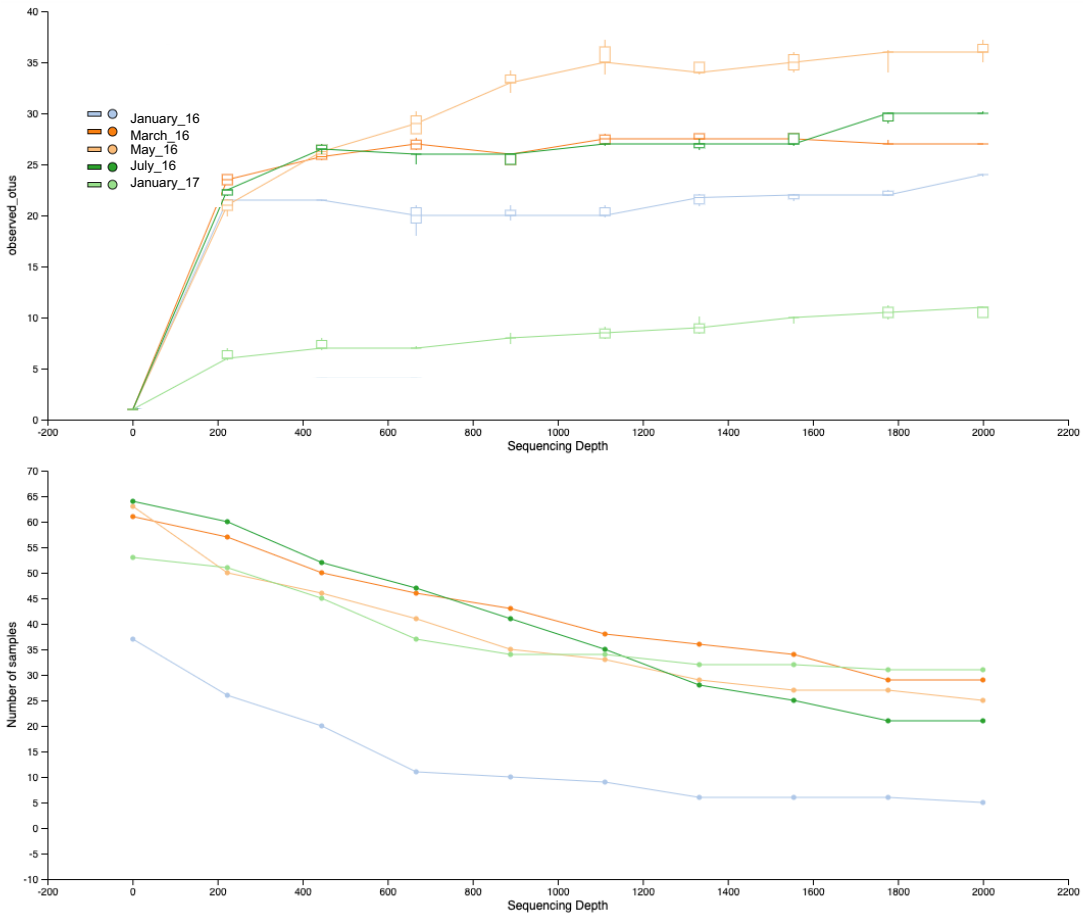

Supplementary Figure 3.1. Alpha rarefaction curves visualized using the q2-diversity plugin for Observed OTUs and Number of samples, colored by sampling month.

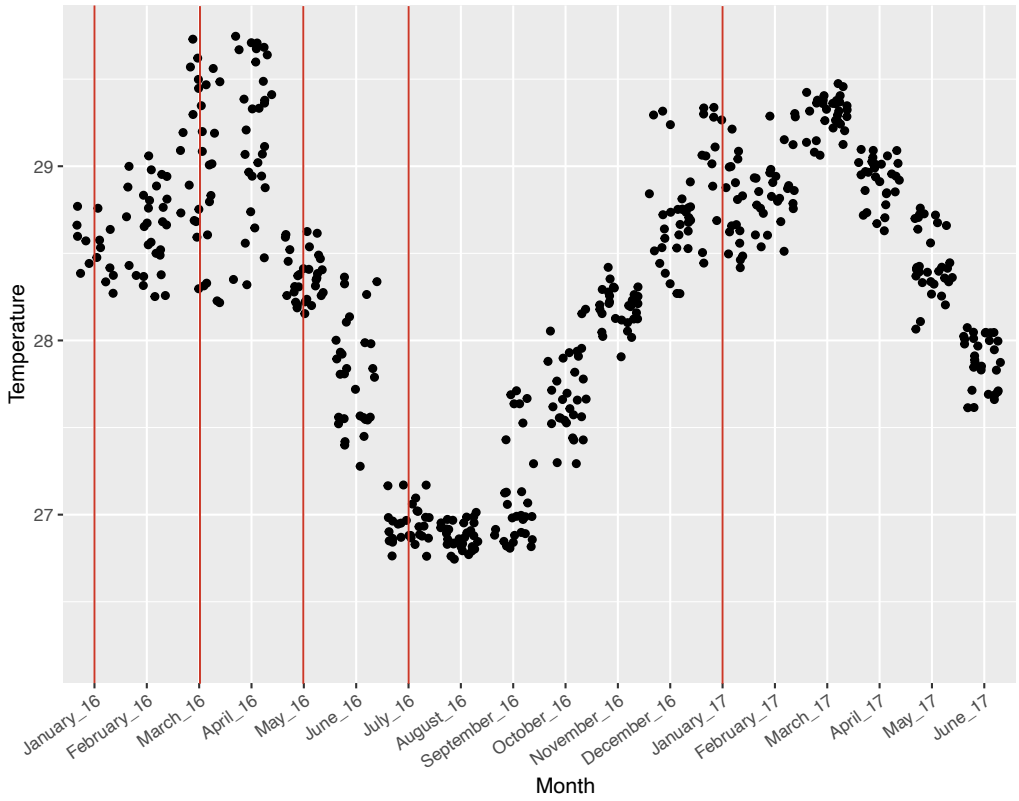

Supplementary Figure 3.2. Average daily temperature from January 2016 to June 2017. The five sampling months included in this study are approximately marked with red vertical lines.

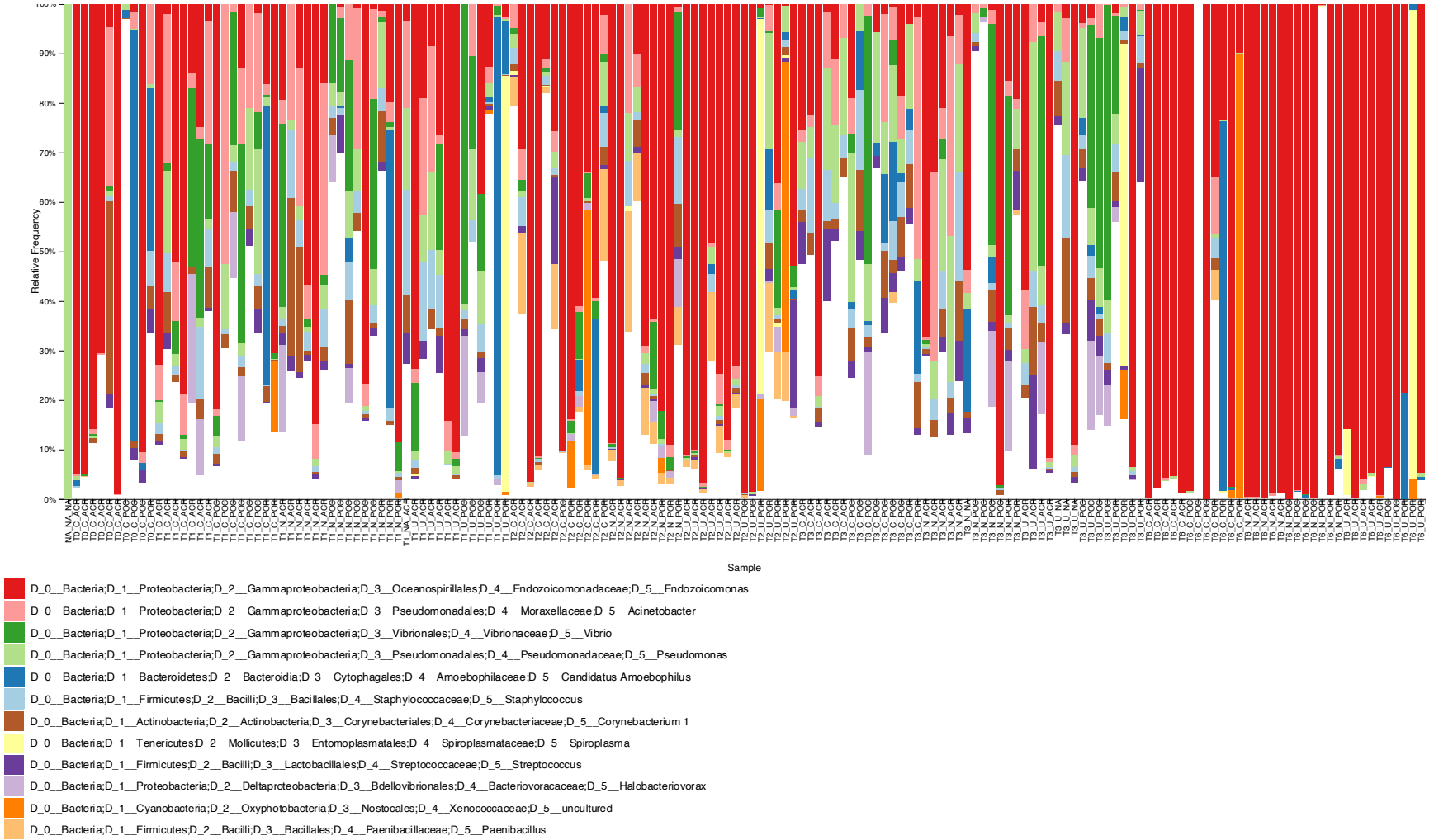

Supplementary Figure 3.3. Relative abundance of top twelve most abundant genera in the dataset for each sample.

Supplementary Table 3.1. Metadata file after filtering. sOTUs were filtered from the dataset if they were annotated as mitochondrial or chloroplast sequences. Corals that were observed to be bleached during time sampling are noted in the Bleached column. Grey-colored sample rows were discarded due to insufficient sequencing depth at an alpha rarefaction level of 881 reads or because of incomplete metadata. In all analyses, "Time" represents the month of sampling (T0-Jan 2016, T1-March 2016, T2-May 2016, T3-July 2016, T4-Jan 2017), and BL represents whether or not the coral bleached (Y/N).

Sample ID	Plot	Tag	Genus	Treatment	Nutrient	Time	Individual	Seq depth	BL
Jan2016.acr36	11	36	ACR	C	control	T0	ACR_36	2	N
March2016.poc211	Q	211	POC	U	nutrient	T1	POC_211	12	N
Jan2016.poc113	4	113	POC	C	control	T0	POC_113	21	N
Jan2016.poc59	10	59	POC	C	control	T0	POC_59	22	N
Jan2016.poc1	17	1	POC	C	control	T0	POC_1	27	N
Jan2016.poc67	2H	67	POC	C	control	T0	POC_67	28	N
March2016.poc135	16	135	POC	U	nutrient	T1	POC_135	32	N
May2016.135poc	16	135	POC	U	nutrient	T2	POC_135	36	N
May2016.55poc	4H	55	POC	C	control	T2	POC_55	37	N
Jan2016.poc55	4H	55	POC	C	control	T0	POC_55	39	N
May2016.43poc	4H	43	POC	C	control	T2	POC_43	39	N
May2016.125poc	1	125	POC	N	nutrient	T2	POC_125	57	Y
May2016.113poc	4	113	POC	U	nutrient	T2	POC_113	61	N
Jan2016.acr84	8	84	ACR	C	control	T0	ACR_84	70	N
July2016.por215	O	215	POR	N	nutrient	T3	POR_215	72	N
May2016.154poc	U	154	POC	C	control	T2	POC_154	82	N
Jan2016.poc120	3	120	POC	C	control	T0	POC_120	88	N
May2016.120poc	3	120	POC	N	nutrient	T2	POC_120	91	Y
May2016.134acr	16	134	ACR	N	nutrient	T2	ACR_134	95	N
May2016.59poc	10	59	POC	N	nutrient	T2	POC_59	96	N
May2016.236poc	C	236	POC	N	nutrient	T2	POC_236	108	N
May2016.215poc	O	215	POC	N	nutrient	T2	POC_215	134	N
Jan2016.acr134	16	134	ACR	C	control	T0	ACR_134	139	N
July2016.acr88	8	88	ACR	U	nutrient	T3	ACR_88	148	N
Jan2016.poc17	14	17	POC	C	control	T0	POC_17	163	N
May2016.162poc	15	162	POC	U	nutrient	T2	POC_162	164	Y
Jan2017.por220	P	220	POR	N	nutrient	T4	POR_220	166	N
Jan2016.poc211	Q	211	POC	C	control	T0	POC_211	169	N
Jan2017.por267	N	267	POR	N	nutrient	T4	POR_267	173	N

March2016.poc81	3H	81	POC	C	control	T1	POC_81	177	N
May2016.67poc	2H	67	POC	C	control	T2	POC_67	187	Y
March2016.poc128	2	128	POC	U	nutrient	T1	POC_128	189	N
July2016.294.1	E	294	NA	N	nutrient	T3	NA_294	211	Y
July2016.acr60	10	60	ACR	N	nutrient	T3	ACR_60	222	N
March2016.por154	U	154	POR	C	control	T1	POR_154	228	N
July2016.acr18	14	18	ACR	U	nutrient	T3	ACR_18	228	N
July2016.por280	I	280	POR	C	control	T3	POR_280	237	N
Jan2016.acr129	9	129	ACR	C	control	T0	ACR_129	242	N
July2016.228.1	K	228	POR	U	nutrient	T3	POR_228	246	N
Jan2017.por275	G	275	POR	C	control	T4	POR_275	246	N
Jan2017.poc162	15	162	POC	U	nutrient	T4	POC_162	253	N
Jan2016.acr88	8	88	ACR	C	control	T0	ACR_88	259	N
May2016.128poc	2	128	POC	U	nutrient	T2	POC_128	276	Y
March2016.por220	P	220	POR	N	nutrient	T1	POR_220	277	N
May2016.294por	E	294	POC	N	nutrient	T2	POC_294	307	Y
March2016.por240	B	240	POR	N	nutrient	T1	POR_240	308	N
May2016.231poc	D	231	POR	N	nutrient	T2	POR_231	314	N
March2016.por246	L	246	POR	U	nutrient	T1	POR_246	319	N
July2016.acr90	1H	90	ACR	C	control	T3	ACR_90	320	N
July2016.por154	U	154	POR	C	control	T3	POR_154	336	N
Jan2017.poc220	P	220	POC	N	nutrient	T4	POC_220	336	N
March2016.por236	C	236	POR	N	nutrient	T1	POR_236	360	N
Jan2016.acr66	2H	66	ACR	C	control	T0	ACR_66	366	N
Jan2017.poc81	3H	81	POC	C	control	T4	POC_81	379	N
Jan2016.acr64	2H	64	ACR	C	control	T0	ACR_64	381	N
Jan2017.poc148	X	148	POC	C	control	T4	POC_148	393	N
Jan2016.acr18	14	18	ACR	C	control	T0	ACR_18	396	N
Jan2016.poc128	2	128	POC	C	control	T0	POC_128	404	N
July2016.por211	Q	211	POR	U	nutrient	T3	POR_211	409	N
March2016.por271	T	271	POR	C	control	T1	POR_271	410	N
July2016.acr134	16	134	ACR	N	nutrient	T3	ACR_134	424	N
Jan2017.por154	U	154	POR	C	control	T4	POR_154	430	N
March2016.por228	K	228	POR	U	nutrient	T1	POR_228	438	N
May2016.105poc	1H	105	POC	C	control	T2	POC_105	438	N
July2016.poc17	14	17	POC	U	nutrient	T3	POC_17	443	N
Jan2017.por243	A	243	POR	U	nutrient	T4	POR_243	450	N
Jan2017.por236	C	236	POR	N	nutrient	T4	POR_236	452	N

Jan2016.poc43	4H	43	POC	C	control	T0	POC_43	458	N
May2016.220poc	P	220	POC	N	nutrient	T2	POC_220	459	N
Jan2016.poc154	U	154	POR	C	control	T0	POR_154	463	N
Jan2016.poc220	P	220	POC	C	control	T0	POC_220	487	N
Jan2017.por228	K	228	POR	U	nutrient	T4	POR_228	487	N
May2016.215por	O	215	POR	N	nutrient	T2	POR_215	494	N
Jan2016.acr68	2H	68	ACR	C	control	T0	ACR_68	506	N
Jan2016.poc231	D	231	POC	C	control	T0	POC_231	513	N
Jan2016.poc162	15	162	POC	C	control	T0	POC_162	514	N
March2016.por251	M	251	POR	U	nutrient	T1	POR_251	520	N
May2016.228por	K	228	POR	U	nutrient	T2	POR_228	520	N
Jan2016.acr161	15	161	ACR	C	control	T0	ACR_161	535	N
Jan2016.acr127	2	127	ACR	C	control	T0	ACR_127	547	N
Jan2017.por211	Q	211	POR	U	nutrient	T4	POR_211	553	N
May2016.243por	A	243	POR	U	nutrient	T2	POR_243	556	N
May2016.240por	B	240	POR	N	nutrient	T2	POR_240	560	N
Jan2017.por240	B	240	POR	N	nutrient	T4	POR_240	563	N
July2016.por275	G	275	POR	C	control	T3	POR_275	570	N
Jan2017.poc231	D	231	POC	N	nutrient	T4	POC_231	586	N
Jan2017.poc154	U	154	POC	C	control	T4	POC_154	590	N
July2016.por267	N	267	POR	N	nutrient	T3	POR_267	602	N
July2016.por236	C	236	POR	N	nutrient	T3	POR_236	605	N
Jan2017.por294	E	294	POC	N	nutrient	T4	POC_294	613	N
Jan2016.poc125	1	125	POC	C	control	T0	POC_125	618	N
March2016.por243	A	243	POR	U	nutrient	T1	POR_243	618	N
March2016.por215	O	215	POR	N	nutrient	T1	POR_215	624	N
March2016.poc17	14	17	POC	U	nutrient	T1	POC_17	662	N
July2016.294.2	E	294	NA	N	nutrient	T3	NA_294	664	N
July2016.poc59	10	59	POC	N	nutrient	T3	POC_59	666	N
March2016.poc59	10	59	POC	N	nutrient	T1	POC_59	685	N
May2016.275por	G	275	POR	C	control	T2	POR_275	704	N
July2016.por260	S	260	POR	C	control	T3	POR_260	716	N
July2016.poc162	15	162	POC	U	nutrient	T3	POC_162	722	Y
May2016.148poc	X	148	POC	C	control	T2	POC_148	723	N
Jan2017.por251	M	251	POR	U	nutrient	T4	POR_251	742	N
May2016.291por	T	291	POR	C	control	T2	POR_291	772	N
July2016.220.1	P	220	NA	N	nutrient	T3	NA_220	778	N
March2016.por260	S	260	POR	C	control	T1	POR_260	791	N

Jan2016.acr76	9	76	ACR	C	control	T0	ACR_76	796	N
July2016.acr36	11	36	ACR	U	nutrient	T3	ACR_36	805	N
Jan2017.por291	T	291	POR	C	control	T4	POR_291	809	N
Jan2017.poc113	4	113	POC	U	nutrient	T4	POC_113	819	N
July2016.por276	H	276	POR	C	control	T3	POR_276	829	N
March2016.por280	I	280	POR	C	control	T1	POR_280	840	N
May2016.66acr	2H	66	ACR	C	control	T2	ACR_66	844	Y
May2016.1poc	17	1	POC	U	nutrient	T2	POC_1	849	N
May2016.220por	P	220	POR	N	nutrient	T2	POR_220	851	N
negative	NA	NA	NA	NA	NA	NA	NA	852	N
July2016.acr161	15	161	ACR	N	nutrient	T3	ACR_161	881	N
July2016.por291	T	291	POR	C	control	T3	POR_291	933	N
July2016.acr68	2H	68	ACR	C	control	T3	ACR_68	934	N
May2016.17poc	14	17	POC	U	nutrient	T2	POC_17	935	N
July2016.acr135	16	135	ACR	U	nutrient	T3	ACR_135	938	N
Jan2016.acr135	16	135	ACR	C	control	T0	ACR_135	940	N
May2016.81poc	3H	81	POC	C	control	T2	POC_81	962	N
March2016.acr161	15	161	ACR	N	nutrient	T1	ACR_161	973	N
March2016.poc220	P	220	POC	N	nutrient	T1	POC_220	994	N
July2016.poc67	2H	67	POC	C	control	T3	POC_67	999	N
March2016.por231	D	231	POR	N	nutrient	T1	POR_231	1001	N
July2016.poc81	3H	81	POC	C	control	T3	POC_81	1025	N
July2016.220.2	P	220	NA	N	nutrient	T3	NA_220	1032	N
March2016.por202	Y	202	POR	U	nutrient	T1	POR_202	1039	N
March2016.poc43	4H	43	POC	C	control	T1	POC_43	1065	N
May2016.154por	U	154	POR	C	control	T2	POR_154	1128	N
Jan2016.acr30	12	30	ACR	C	control	T0	ACR_30	1139	N
July2016.acr66	2H	66	ACR	C	control	T3	ACR_66	1154	N
July2016.acr2	17	2	ACR	U	nutrient	T3	ACR_2	1163	N
Jan2016.poc148	X	148	POC	C	control	T0	POC_148	1166	N
July2016.poc148	X	148	POC	C	control	T3	POC_148	1178	N
Jan2017.por271	T	271	POR	C	control	T4	POR_271	1180	N
May2016.127acr	2	127	ACR	N	nutrient	T2	ACR_127	1192	N
Jan2017.por280	I	280	POR	C	control	T4	POR_280	1196	N
Jan2016.poc236	C	236	POC	C	control	T0	POC_236	1201	N
March2016.acr84	8	84	ACR	N	nutrient	T1	ACR_84	1219	N
March2016.acr18	14	18	ACR	U	nutrient	T1	ACR_18	1220	N
July2016.acr82	3H	82	ACR	C	control	T3	ACR_82	1236	N

May2016.251por	M	251	POR	U	nutrient	T2	POR_251	1241	N
July2016.poc105	1H	105	POC	C	control	T3	POC_105	1255	N
July2016.acr56	4H	56	ACR	C	control	T3	ACR_56	1277	N
July2016.poc43	4H	43	POC	C	control	T3	POC_43	1287	N
May2016.30acr	12	30	ACR	N	nutrient	T2	ACR_30	1297	N
July2016.poc231	D	231	POC	N	nutrient	T3	POC_231	1337	N
July2016.por240	B	240	POR	N	nutrient	T3	POR_240	1350	N
July2016.acr44	4H	44	ACR	C	control	T3	ACR_44	1362	N
May2016.161acr	15	161	ACR	N	nutrient	T2	ACR_161	1450	N
March2016.poc125	1	125	POC	N	nutrient	T1	POC_125	1456	N
May2016.18acr	14	18	ACR	U	nutrient	T2	ACR_18	1467	Y
March2016.poc113	4	113	POC	U	nutrient	T1	POC_113	1491	N
July2016.acr129	9	129	ACR	N	nutrient	T3	ACR_129	1590	N
March2016.acr88	8	88	ACR	U	nutrient	T1	ACR_88	1608	N
July2016.acr76	9	76	ACR	U	nutrient	T3	ACR_76	1646	N
Jan2017.por276	H	276	POR	C	control	T4	POR_276	1646	N
March2016.acr36	11	36	ACR	U	nutrient	T1	ACR_36	1653	N
July2016.por231	D	231	POR	N	nutrient	T3	POR_231	1653	N
March2016.acr82	3H	82	ACR	C	control	T1	ACR_82	1698	N
July2016.acr64	2H	64	ACR	C	control	T3	ACR_64	1724	N
March2016.acr35	11	35	ACR	NA	nutrient	T1	ACR_35	1740	N
March2016.por267	N	267	POR	N	nutrient	T1	POR_267	1771	N
May2016.poc211	Q	211	POC	U	nutrient	T2	POC_211	1908	N
Jan2016.por154	U	154	POC	C	control	T0	POC_154	1925	N
May2016.280por	I	280	POR	C	control	T2	POR_280	1995	N
May2016.129acr	9	129	ACR	N	nutrient	T2	ACR_129	2021	N
July2016.acr84	8	84	ACR	N	nutrient	T3	ACR_84	2022	N
March2016.poc67	2H	67	POC	C	control	T1	POC_67	2031	N
July2016.251.1	M	251	NA	U	nutrient	T3	NA_251	2073	N
May2016.260por	S	260	POR	C	control	T2	POR_260	2122	Y
May2016.236por	C	236	POR	N	nutrient	T2	POR_236	2122	N
May2016.202por	Y	202	POR	U	nutrient	T2	POR_202	2127	N
July2016.acr127	2	127	ACR	N	nutrient	T3	ACR_127	2143	N
July2016.poc113	4	113	POC	U	nutrient	T3	POC_113	2202	N
Jan2016.acr2	17	2	ACR	C	control	T0	ACR_2	2219	N
Jan2017.acr127	2	127	ACR	N	nutrient	T4	ACR_127	2254	N
July2016.por271	T	271	POR	C	control	T3	POR_271	2272	N
May2016.276por	H	276	POR	C	control	T2	POR_276	2315	N

March2016.poc1	17	1	POC	U	nutrient	T1	POC_1	2317	N
Jan2017.por260	S	260	POR	C	control	T4	POR_260	2341	N
March2016.poc154	U	154	POC	C	control	T1	POC_154	2359	N
May2016.271por	T	271	POR	C	control	T2	POR_271	2374	N
July2016.poc55	4H	55	POC	C	control	T3	POC_55	2406	N
July2016.poc211	Q	211	POC	U	nutrient	T3	POC_211	2418	N
March2016.acr44	4H	44	ACR	C	control	T1	ACR_44	2467	N
May2016.76acr	9	76	ACR	U	nutrient	T2	ACR_76	2472	Y
March2016.por291	T	291	POR	C	control	T1	POR_291	2486	N
July2016.por202	Y	202	POR	U	nutrient	T3	POR_202	2486	N
May2016.82acr	3H	82	ACR	C	control	T2	ACR_82	2559	N
May2016.211por	Q	211	POR	U	nutrient	T2	POR_211	2588	N
March2016.poc231	D	231	POC	N	nutrient	T1	POC_231	2603	N
July2016.por243	A	243	POR	U	nutrient	T3	POR_243	2633	N
March2016.poc236	C	236	POC	N	nutrient	T1	POC_236	2660	N
May2016.64acr	2H	64	ACR	C	control	T2	ACR_64	2727	Y
Jan2017.acr82	3H	82	ACR	C	control	T4	ACR_82	2733	N
Jan2016.poc105	1H	105	POC	C	control	T0	POC_105	2751	N
March2016.acr68	2H	68	ACR	C	control	T1	ACR_68	2795	N
March2016.acr66	2H	66	ACR	C	control	T1	ACR_66	2863	N
Jan2017.acr76	9	76	ACR	U	nutrient	T4	ACR_76	2886	N
May2016.68acr	2H	68	ACR	C	control	T2	ACR_68	2936	N
May2016.84acr	8	84	ACR	N	nutrient	T2	ACR_84	2968	N
July2016.acr30	12	30	ACR	N	nutrient	T3	ACR_30	3056	N
Jan2017.por202	Y	202	POR	U	nutrient	T4	POR_202	3130	N
March2016.por211	Q	211	POR	U	nutrient	T1	POR_211	3148	N
May2016.294poc	E	294	POR	N	nutrient	T2	POR_294	3187	N
May2016.246por	L	246	POR	U	nutrient	T2	POR_246	3195	N
Jan2017.poc125	1	125	POC	N	nutrient	T4	POC_125	3407	N
May2016.90acr	1H	90	ACR	C	control	T2	ACR_90	3430	N
March2016.poc162	15	162	POC	U	nutrient	T1	POC_162	3508	N
Jan2017.poc17	14	17	POC	U	nutrient	T4	POC_17	3554	N
March2016.acr56	4H	56	ACR	C	control	T1	ACR_56	3556	N
Jan2017.294	E	294	POR	N	nutrient	T4	POR_294	3652	N
March2016.poc148	X	148	POC	C	control	T1	POC_148	3663	N
May2016.88acr	8	88	ACR	U	nutrient	T2	ACR_88	3666	Y
Jan2017.acr44	4H	44	ACR	C	control	T4	ACR_44	3717	N
March2016.poc120	3	120	POC	N	nutrient	T1	POC_120	3732	N

March2016.acr76	9	76	ACR	U	nutrient	T1	ACR_76	3839	N
May2016.267por	N	267	POR	N	nutrient	T2	POR_267	4027	N
May2016.2acr	17	2	ACR	U	nutrient	T2	ACR_2	4155	Y
May2016.56acr	4H	56	ACR	C	control	T2	ACR_56	4226	N
May2016.135acr	16	135	ACR	U	nutrient	T2	ACR_135	4263	N
Jan2017.poc59	10	59	POC	N	nutrient	T4	POC_59	4269	N
March2016.por276	H	276	POR	C	control	T1	POR_276	4276	N
July2016.poc154	U	154	POC	C	control	T3	POC_154	4277	N
July2016.poc236	C	236	POC	N	nutrient	T3	POC_236	4285	N
May2016.44acr	4H	44	ACR	C	control	T2	ACR_44	4415	N
Jan2017.acr30	12	30	ACR	N	nutrient	T4	ACR_30	4445	N
May2016.254por	V	254	POR	U	nutrient	T2	POR_254	4505	N
May2016.36acr	11	36	ACR	U	nutrient	T2	ACR_36	4509	N
Jan2017.poc120	3	120	POC	N	nutrient	T4	POC_120	4512	N
Jan2017.acr88	8	88	ACR	U	nutrient	T4	ACR_88	4518	N
March2016.acr127	2	127	ACR	N	nutrient	T1	ACR_127	4601	N
July2016.poc128	2	128	POC	U	nutrient	T3	POC_128	4602	N
May2016.60acr	10	60	ACR	N	nutrient	T2	ACR_60	4633	N
Jan2017.poc236	C	236	POC	N	nutrient	T4	POC_236	4660	N
Jan2016.acr90	1H	90	ACR	C	control	T0	ACR_90	4716	N
July2016.poc1	17	1	POC	U	nutrient	T3	POC_1	4741	N
March2016.acr62	10	62	ACR	U	nutrient	T1	ACR_62	4874	N
March2016.acr90	1H	90	ACR	C	control	T1	ACR_90	5020	N
July2016.acr62	10	62	ACR	U	nutrient	T3	ACR_62	5024	N
March2016.por294	E	294	POR	N	nutrient	T1	POR_294	5060	N
March2016.poc105	1H	105	POC	C	control	T1	POC_105	5061	N
May2016.62acr	10	62	ACR	U	nutrient	T2	ACR_62	5214	Y
March2016.acr129	9	129	ACR	N	nutrient	T1	ACR_129	5260	N
Jan2017.poc43	4H	43	POC	C	control	T4	POC_43	5405	N
July2016.poc125	1	125	POC	N	nutrient	T3	POC_125	5623	N
July2016.228.2	K	228	NA	U	nutrient	T3	NA	5886	N
July2016.251.2	M	251	NA	U	nutrient	T3	NA	5947	N
Jan2017.por231	D	231	POR	N	nutrient	T4	POR_231	5948	N
July2016.por246	L	246	POR	U	nutrient	T3	POR_246	6163	N
July2016.por254	V	254	POR	U	nutrient	T3	POR_254	6230	N
Jan2017.por246	L	246	POR	U	nutrient	T4	POR_246	6279	N
March2016.poc55	4H	55	POC	C	control	T1	POC_55	6387	N
March2016.acr60	10	60	ACR	N	nutrient	T1	ACR_60	6509	N

Jan2017.acr161	15	161	ACR	N	nutrient	T4	ACR_161	6782	N
Jan2017.acr68	2H	68	ACR	C	control	T4	ACR_68	7035	N
Jan2017.poc105	1H	105	POC	C	control	T4	POC_105	7306	N
Jan2016.acr56	4H	56	ACR	C	control	T0	ACR_56	7527	N
Jan2017.acr66	2H	66	ACR	C	control	T4	ACR_66	7691	N
Jan2017.acr36	11	36	ACR	U	nutrient	T4	ACR_36	7956	N
March2016.por254	V	254	POR	U	nutrient	T1	POR_254	8044	N
Jan2017.por215	O	215	POR	N	nutrient	T4	POR_215	8133	N
March2016.poc294	E	294	POC	N	nutrient	T1	POC_294	8342	N
Jan2017.acr60	10	60	ACR	N	nutrient	T4	ACR_60	8660	N
March2016.acr2	17	2	ACR	U	nutrient	T1	ACR_2	8821	N
Jan2017.acr62	10	62	ACR	U	nutrient	T4	ACR_62	9246	N
Jan2017.acr18	14	18	ACR	U	nutrient	T4	ACR_18	9287	N
Jan2016.acr62	10	62	ACR	C	control	T0	ACR_62	10270	N
Jan2017.acr84	8	84	ACR	N	nutrient	T4	ACR_84	11143	N
Jan2017.poc211	Q	211	POC	U	nutrient	T4	POC_211	11175	N
March2016.acr64	2H	64	ACR	C	control	T1	ACR_64	11658	N
July2016.poc120	3	120	POC	N	nutrient	T3	POC_120	12018	N
March2016.acr30	12	30	ACR	N	nutrient	T1	ACR_30	13211	N
Jan2017.por254	V	254	POR	U	nutrient	T4	POR_254	13389	N
Jan2017.acr64	2H	64	ACR	C	control	T4	ACR_64	13391	N
Jan2017.poc67	2H	67	POC	C	control	T4	POC_67	13415	N
positive	NA	NA	NA	NA	NA	NA	NA	16702	N

Supplementary Table 3.2. Results of linear mixed effects model for alpha diversity measures. Chao1 was square root transformed, Simpson's diversity was asine-transformed, and Faith's phylogenetic diversity was square-root transformed. Fixed effects include time (month), treatment, coral genus, and their interaction with individual colony as a random effect.

Chao1 Index

	Sum Sq	Mean Sq	NumDF	DenDF	F value	P value
time	**93.769**	**23.4423**	**4**	**112.611**	**16.2339**	**<0.001**
treatment	2.208	1.1041	2	64.734	0.7646	0.46967
genus	**36.13**	**18.065**	**2**	**60.601**	**12.5101**	**<0.001**
time:treatment	8.496	1.4161	6	108.476	0.9806	0.442004
time:genus	**31.671**	**4.5244**	**7**	**109.454**	**3.1332**	**<0.01**
treatment:genus	2.346	0.5864	4	63.145	0.4061	0.803568
time:treatment:genus	23.01	2.0918	11	106.065	1.4486	0.162311

Simpson's Diversity Index

	Sum Sq	Mean Sq	NumDF	DenDF	F value	P value
time	**5.254**	**1.31349**	**4**	**122**	**20.644**	**<0.001**
treatment	0.3201	0.16007	2	122	2.5158	0.0849819
genus	**1.2623**	**0.63115**	**2**	**122**	**9.9197**	**<0.001**
time:treatment	0.4495	0.07491	6	122	1.1774	0.3228048
time:genus	**1.545**	**0.22071**	**7**	**122**	**3.4689**	**<0.01**
treatment:genus	0.4254	0.10635	4	122	1.6715	0.1609088
time:treatment:genus	0.5002	0.04547	11	122	0.7147	0.7226143

Faith's Phylogenetic Distance

	Sum Sq	Mean Sq	NumDF	DenDF	F value	P value
time	**12.9433**	**3.2358**	**4**	**110.5**	**27.5172**	**<0.001**
treatment	0.0865	0.0432	2	58.345	0.3678	0.693877
genus	**2.6773**	**1.3387**	**2**	**54.212**	**11.384**	**<0.001**
time:treatment	0.454	0.0757	6	105.63	0.6435	0.6952
time:genus	**2.5583**	**0.3655**	**7**	**106.752**	**3.108**	**<0.01**
treatment:genus	0.1031	0.0258	4	56.88	0.2193	0.926618
time:treatment:genus	1.2752	0.1159	11	102.769	0.9858	0.464253

Supplementary Table 3.3. Results of linear mixed effects model for alpha diversity measures for Acropora samples. Chao1 was square root transformed, Simpson's diversity was asine-transformed, and Faith's phylogenetic diversity was square-root transformed. For each coral host, time (month) is the fixed effect with individual colony as a random effect.

Chao1 Index

	Sum Sq	Mean Sq	NumDF	DenDF	F value	P value
time	**95.305**	**23.826**	**4**	**57.938**	**18.476**	**<0.001**
contrast	estimate	SE	df	t.ratio	p.value	
T0-T1	-0.872	0.554	62	-1.573	0.5203	
T0-T2	**-1.89**	**0.551**	**60.4**	**-3.428**	**0.0094**	
T0-T3	-1.14	0.569	60.5	-2.004	0.2763	
T0-T4	1.353	0.58	65.2	2.333	0.1478	
T1-T2	-1.018	0.37	51.4	-2.753	0.0598	
T1-T3	-0.268	0.397	54.1	-0.676	0.9609	
T1-T4	**2.225**	**0.396**	**52.7**	**5.625**	**<.0001**	
T2-T3	0.75	0.397	54	1.887	0.3365	
T2-T4	**3.243**	**0.397**	**54.1**	**8.164**	**<.0001**	
T3-T4	**2.493**	**0.423**	**56**	**5.899**	**<.0001**	

Simpson's diversity index

	Sum Sq	Mean Sq	NumDF	DenDF	F value	P value
time	**1.5725**	**0.39312**	**4**	**69**	**7.483**	**<0.001**
contrast	estimate	SE	df	t.ratio	p.value	
T0-T1	-0.26514	0.1093	65.2	-2.425	0.1215	
T0-T2	-0.12405	0.1091	63.7	-1.137	0.7865	
T0-T3	-0.25712	0.1126	63.8	-2.284	0.1635	
T0-T4	0.11236	0.1134	68.1	0.991	0.8585	
T1-T2	0.14109	0.0745	52	1.894	0.3332	
T1-T3	0.00801	0.0796	55.4	0.101	1	
T1-T4	**0.3775**	**0.0795**	**53.8**	**4.75**	**<0.001**	
T2-T3	-0.13308	0.0796	55.4	-1.672	0.4593	
T2-T4	**0.23641**	**0.0796**	**55.4**	**2.97**	**<0.05**	
T3-T4	**0.36948**	**0.0843**	**57.7**	**4.38**	**<0.001**	

Faith's phylogenetic diversity

	Sum Sq	Mean Sq	NumDF	DenDF	F value	P value
time	**9.4057**	**2.3514**	**4**	**57.532**	**23.265**	**<0.001**
contrast	estimate	SE	df	t.ratio	p.value	

T0-T1	-0.1516	0.154	63.3	-0.985	0.861
T0-T2	-0.3863	0.153	61.7	-2.521	0.0992
T0-T3	-0.2976	0.158	61.8	-1.882	0.3376
T0-T4	**0.5972**	**0.16**	**66.5**	**3.721**	**0.0036**
T1-T2	-0.2347	0.103	51.6	-2.268	0.1718
T1-T3	-0.146	0.111	54.6	-1.317	0.6822
T1-T4	**0.7488**	**0.111**	**53.1**	**6.773**	**<.0001**
T2-T3	0.0887	0.111	54.5	0.799	0.9297
T2-T4	**0.9835**	**0.111**	**54.6**	**8.868**	**<.0001**
T3-T4	**0.8948**	**0.118**	**56.7**	**7.594**	**<.0001**

Supplementary Table 3.4. Results of linear mixed effects model for alpha diversity measures for Porites samples. Chao1 was square root transformed, Simpson's diversity was asine-transformed, and Faith's phylogenetic diversity was square-root transformed. For each coral host, time (month) is the fixed effect with individual colony as a random effect.

Chao1 Index

	Sum Sq	Mean Sq	NumDF	DenDF	F value	P value
time	**29.364**	**9.7881**	**3**	**35**	**4.3538**	**<0.05**
contrast	estimate	SE	df	t.ratio	p.value	
T1-T2	-0.367	0.692	28.9	-0.531	0.9509	
T1-T3	0.341	0.773	30.1	0.442	0.9707	
T1-T4	1.829	0.731	29.2	2.503	0.0804	
T2-T3	0.709	0.693	32	1.022	0.7381	
T2-T4	**2.196**	**0.64**	**26.7**	**3.431**	**0.01**	
T3-T4	1.487	0.726	29.2	2.048	0.1941	

Simpson's diversity index

	Sum Sq	Mean Sq	NumDF	DenDF	F value	P value
time	**1.0871**	**0.36238**	**3**	**26.172**	**5.105**	**<0.05**
contrast	estimate	SE	df	t.ratio	p.value	
T1-T2	-0.0868	0.127	25.9	-0.683	0.9027	
T1-T3	-0.2636	0.143	27.1	-1.846	0.2745	
T1-T4	0.23	0.135	26.1	1.708	0.34	
T2-T3	-0.1768	0.13	30.1	-1.355	0.5362	
T2-T4	0.3168	0.117	24.9	2.704	0.0554	
T3-T4	**0.4936**	**0.135**	**27.3**	**3.666**	**0.0055**	

Faith's phylogenetic diversity

	Sum Sq	Mean Sq	NumDF	DenDF	F value	P value
time	**3.6302**	**1.2101**	**3**	**35**	**8.2033**	**<0.001**
contrast	estimate	SE	df	t.ratio	p.value	
T1-T2	-0.3411	0.177	28.9	-1.924	0.2405	
T1-T3	-0.0534	0.198	30.1	-0.27	0.993	
T1-T4	0.4579	0.187	29.2	2.447	0.0903	
T2-T3	0.2877	0.178	32	1.619	0.3824	
T2-T4	**0.799**	**0.164**	**26.7**	**4.874**	**0.0002**	
T3-T4	**0.5113**	**0.186**	**29.2**	**2.749**	**0.0473**	

Supplementary Table 3.5. Results of linear mixed effects model for alpha diversity measures for Pocillopora samples. Chao1 was square root transformed, Simpson's diversity was asine-transformed, and Faith's phylogenetic diversity was square-root transformed. For each coral host, time (month) is the fixed effect with individual colony as a random effect.

Chao1 Index

	Sum Sq	Mean Sq	NumDF	DenDF	F value	P value
time	52.895	13.224	4	41	11.724	**<0.001**
contrast	estimate	SE	df	t.ratio	p.value	
T0-T1	0.2457	0.623	36.9	0.395	0.9947	
T0-T2	**2.6156**	**0.853**	**41**	**3.067**	**<0.05**	
T0-T3	0.2574	0.623	36.9	0.413	0.9936	
T0-T4	**2.673**	**0.667**	**38.7**	**4.005**	**<0.01**	
T1-T2	**2.37**	**0.698**	**41**	**3.395**	**<0.05**	
T1-T3	0.0118	0.39	29.2	0.03	1	
T1-T4	**2.4273**	**0.457**	**35.4**	**5.307**	**<0.001**	
T2-T3	**-2.3582**	**0.693**	**39.8**	**-3.404**	**<0.05**	
T2-T4	0.0574	0.731	38.3	0.078	1	
T3-T4	**2.4156**	**0.457**	**33.7**	**5.286**	**<0.001**	

Simpson's diversity index

	Sum Sq	Mean Sq	NumDF	DenDF	F value	P value
time	4.653	1.1632	4	41	17.74	**<0.001**
contrast	estimate	SE	df	t.ratio	p.value	
T0-T1	-0.2863	0.1501	36.9	-1.908	0.3314	
T0-T2	0.3926	0.2056	41	1.909	0.3288	
T0-T3	-0.2012	0.1502	36.9	-1.339	0.6689	
T0-T4	**0.5166**	**0.1609**	**38.7**	**3.21**	**0.0212**	
T1-T2	**0.6789**	**0.1683**	**41**	**4.034**	**0.0021**	
T1-T3	0.0851	0.0941	29.2	0.905	0.8928	
T1-T4	**0.8029**	**0.1103**	**35.4**	**7.28**	**<.0001**	
T2-T3	**-0.5938**	**0.167**	**39.8**	**-3.555**	**0.0083**	
T2-T4	0.124	0.1762	38.3	0.704	0.9544	
T3-T4	**0.7178**	**0.1102**	**33.7**	**6.515**	**<.0001**	

Faith's phylogenetic diversity

	Sum Sq	Mean Sq	NumDF	DenDF	F value	P value

time	8.4266	2.1067	4	35.845	18.986	**<0.001**

contrast	estimate	SE	df	t.ratio	p.value
T0-T1	-0.0448	0.196	35.9	-0.228	0.9994
T0-T2	0.6947	0.271	40.9	2.563	0.0965
T0-T3	-0.033	0.197	35.9	-0.168	0.9998
T0-T4	**1.0173**	**0.211**	**37.9**	**4.822**	**0.0002**
T1-T2	**0.7396**	**0.222**	**41**	**3.327**	**0.0151**
T1-T3	0.0118	0.123	28.9	0.096	1
T1-T4	**1.0621**	**0.145**	**35**	**7.349**	**<.0001**
T2-T3	**-0.7278**	**0.22**	**39.5**	**-3.309**	**0.0162**
T2-T4	0.3226	0.231	37.8	1.394	0.6354
T3-T4	**1.0503**	**0.144**	**33.3**	**7.285**	**<.0001**

Supplementary Table 3.6. Results of PERMANOVA test on log-transformed data.

Weighted Unifrac

	DF	SumsOfSqs	MeadSps	F.model	R2	P value
time	**4**	**1.2145**	**0.303621**	**16.8018**	**0.27017**	**<0.001**
genus	**2**	**0.323**	**0.161494**	**8.9368**	**0.07185**	**<0.001**
treatment	2	0.0506	0.025282	1.3991	0.01125	0.13
time:genus	**7**	**0.3318**	**0.047402**	**2.6231**	**0.07381**	**<0.001**
time:treatment	6	0.1072	0.017862	0.9885	0.02384	0.467
genus:treatment	4	0.0853	0.021319	1.1798	0.01897	0.223
time:genus:treatment	11	0.1783	0.016212	0.8971	0.03967	0.706
Residuals	122	2.2046	0.018071	0.49043		
Total	158	4.4953	1			

Bray Curtis

time	**4**	**9.19**	**2.2975**	**8.04**	**0.1473**	**<0.001**
genus	**2**	**7.16**	**3.5802**	**12.5291**	**0.11477**	**<0.001**
treatment	2	0.666	0.3331	1.1656	0.01068	0.175
time:genus	**7**	**4.477**	**0.6396**	**2.2381**	**0.07176**	**<0.001**
time:treatment	6	1.664	0.2773	0.9704	0.02667	0.548
genus:treatment	4	1.413	0.3533	1.2362	0.02265	0.061
time:genus:treatment	11	2.956	0.2688	0.9405	0.04739	0.742
Residuals	122	34.862	0.2858	0.55879		
Total	158	62.388	1			

Binary Jaccard

time	**4**	**7.155**	**1.78886**	**4.9183**	**0.10519**	**<0.001**
genus	**2**	**3.711**	**1.85573**	**5.1022**	**0.05456**	**<0.001**
treatment	2	0.765	0.3824	1.0514	0.01124	0.293
time:genus	**7**	**4.417**	**0.63104**	**1.735**	**0.06494**	**<0.001**
time:treatment	6	2.141	0.35679	0.981	0.03147	0.575
genus:treatment	4	1.584	0.39609	1.089	0.02329	0.103
time:genus:treatment	11	3.876	0.35234	0.9687	0.05698	0.747
Residuals	122	44.373	0.36371	0.65233		
Total	158	68.023	1			

Unweighted Unifrac

time	**4**	**6.805**	**1.70134**	**9.53**	**0.18398**	**<0.001**
genus	**2**	**1.772**	**0.88592**	**4.9625**	**0.0479**	**<0.001**
treatment	2	0.36	0.18016	1.0092	0.00974	0.428
time:genus	**7**	**2.555**	**0.36496**	**2.0443**	**0.06907**	**<0.001**

time:treatment	6	0.979	0.16315	0.9139	0.02646	0.76
genus:treatment	4	0.765	0.19128	1.0715	0.02069	0.262
time:genus:treatment	11	1.973	0.17933	1.0045	0.05333	0.471
Residuals	122	21.78	0.17852	0.58882		
Total	158	36.989	1			

Supplementary Table 3.7. Results of PERMANOVA test on log-transformed Acropora samples.

Weighted Unifrac

	DF	SumsOfSqs	MeadSps	F.model	R2	P value
time	**4**	**0.66617**	**0.166544**	**11.6312**	**0.40329**	**<0.001**
treatment	2	0.03558	0.017791	1.2425	0.02154	0.224
time:treatment	6	0.07664	0.012774	0.8921	0.0464	0.62
Residuals	61	0.87344	0.014319	0.52877		
Total	73	1.65184	1			

pairs	F.Model	R2	p.value	p.adjusted
T2vsT4	29.700393	0.48136473	0.001	0.00166667
T2vsT1	6.924297	0.16131416	0.001	0.00166667
T2vsT0	2.659881	0.10365912	0.01	0.01222222
T2vsT3	6.319737	0.16492121	0.001	0.00166667
T4vsT1	34.992387	0.52233378	0.001	0.00166667
T4vsT0	8.293103	0.30385344	0.001	0.00166667
T4vsT3	34.467685	0.55176824	0.001	0.00166667
T1vsT0	3.118741	0.11940625	0.011	0.01222222
T1vsT3	1.865581	0.05508782	0.026	0.026
T0vsT3	3.289884	0.1475954	0.003	0.00428571

Bray Curtis

time	**4**	**6.2391**	**1.55976**	**6.0007**	**0.25909**	**<0.001**
treatment	2	0.5526	0.27628	1.0629	0.02295	0.32
time:treatment	6	1.4338	0.23896	0.9193	0.05954	0.694
Residuals	61	15.8557	0.25993	0.65843		
Total	73	24.0811	1			

pairs	F.Model	R2	p.value	p.adjusted
T2vsT4	9.984557	0.23781499	0.001	0.00125
T2vsT1	6.296198	0.14885966	0.001	0.00125
T2vsT0	2.682971	0.10446496	0.003	0.00333333
T2vsT3	6.22109	0.1627659	0.001	0.00125
T4vsT1	10.07452	0.23944467	0.001	0.00125
T4vsT0	2.783407	0.12777647	0.01	0.01
T4vsT3	12.487271	0.30842462	0.001	0.00125
T1vsT0	2.70445	0.10521332	0.001	0.00125
T1vsT3	2.863831	0.08214333	0.001	0.00125
T0vsT3	3.047904	0.13824008	0.001	0.00125

Binary Jaccard

time	**4**	**6.2391**	**1.55976**	**6.0007**	**0.25909**	**<0.001**
treatment	2	0.5526	0.27628	1.0629	0.02295	0.32
time:treatment	6	1.4338	0.23896	0.9193	0.05954	0.694
Residuals	61	15.8557	0.25993	0.65843		
Total	73	24.0811	1			

pairs	F.Model	R2	p.value	p.adjusted
T2vsT4	7.06125	0.18077379	0.001	0.001
T2vsT1	3.731878	0.09392654	0.001	0.001
T2vsT0	2.329828	0.09197962	0.001	0.001
T2vsT3	3.370859	0.09530047	0.001	0.001
T4vsT1	6.142269	0.16103576	0.001	0.001
T4vsT0	2.507156	0.1165731	0.001	0.001
T4vsT3	6.46004	0.18746468	0.001	0.001
T1vsT0	2.025964	0.08095447	0.001	0.001
T1vsT3	1.74891	0.05182124	0.001	0.001
T0vsT3	1.853044	0.08886203	0.001	0.001

time	**4**	**3.9373**	**0.98433**	**5.7143**	**0.24891**	**<0.001**
treatment	2	0.3774	0.18871	1.0955	0.02386	0.285
time:treatment	6	0.9958	0.16597	0.9635	0.06296	0.59
Residuals	61	10.5077	0.17226	0.66428		
Total	73	15.8183	1			

pairs	F.Model	R2	p.value	p.adjusted
T2vsT4	13.810587	0.30147152	0.001	0.00125
T2vsT1	5.814479	0.1390542	0.001	0.00125
T2vsT0	3.054234	0.11722603	0.001	0.00125
T2vsT3	4.624833	0.12627587	0.001	0.00125
T4vsT1	10.880576	0.25374137	0.001	0.00125
T4vsT0	3.675883	0.16210539	0.001	0.00125
T4vsT3	9.118935	0.24566802	0.001	0.00125
T1vsT0	2.189224	0.08691114	0.001	0.00125
T1vsT3	1.334358	0.04002952	0.076	0.076
T0vsT3	1.525398	0.07431758	0.032	0.03555556

Supplementary Table 3.8. Results of PERMANOVA test on log-transformed Pocillopora samples.

Weighted Unifrac

	DF	SumsOfSqs	MeadSps	F.model	R2	P value
time	**4**	**0.57773**	**0.144432**	**7.5592**	**0.42704**	**0.001**
treatment	2	0.03684	0.018418	0.964	0.02723	0.445
time:treatment	5	0.08869	0.017737	0.9283	0.06555	0.539
Residuals	34	0.64963	0.019107	0.48018		
Total	45	1.35288	1			

pairs	F.Model	R2	p.value	p.adjusted
T1vsT4	19.128918	0.46509655	0.001	0.00333333
T1vsT3	1.595076	0.05389668	0.046	0.0575
T1vsT0	3.195115	0.15821228	0.001	0.00333333
T1vsT2	6.716841	0.29567673	0.003	0.005
T4vsT3	16.996966	0.43585355	0.001	0.00333333
T4vsT0	6.553898	0.37335855	0.003	0.005
T4vsT2	2.247687	0.18351932	0.064	0.064
T3vsT0	2.411899	0.12424848	0.005	0.00714286
T3vsT2	6.371049	0.28478992	0.002	0.005
T0vsT2	3.728349	0.42715396	0.061	0.064

Bray Curtis

time	**4**	**4.339**	**1.08474**	**3.5716**	**0.25606**	**0.001**
treatment	2	0.6977	0.34885	1.1486	0.04118	0.212
time:treatment	5	1.5821	0.31642	1.0419	0.09337	0.385
Residuals	34	10.3261	0.30371	0.60939		
Total	45	16.9449	1			

pairs	F.Model	R2	p.value	p.adjusted
T1vsT4	7.008595	0.24160409	0.001	0.00333333
T1vsT3	1.808582	0.06067321	0.003	0.006
T1vsT0	2.196253	0.1144105	0.001	0.00333333
T1vsT2	3.604514	0.18386142	0.005	0.00833333
T4vsT3	6.79094	0.23587072	0.001	0.00333333
T4vsT0	2.899966	0.20863118	0.008	0.01142857
T4vsT2	1.051122	0.09511451	0.284	0.284
T3vsT0	1.539664	0.08304703	0.023	0.02875
T3vsT2	3.655503	0.18597859	0.003	0.006
T0vsT2	2.450416	0.32889651	0.048	0.05333333

Binary Jaccard

time	**4**	**3.4414**	**0.86035**	**2.23508**	**0.18006**	**0.001**
treatment	2	0.7518	0.37592	0.97661	0.03934	0.526
time:treatment	5	1.8314	0.36629	0.95157	0.09583	0.732
Residuals	34	13.0876	0.38493	0.68477		
Total	45	19.1122	1			

pairs	F.Model	R2	p.value	p.adjusted
T1vsT4	3.8818	0.14998186	0.001	0.00333333
T1vsT3	1.51435	0.05130894	0.003	0.005
T1vsT0	1.596156	0.0858326	0.002	0.005
T1vsT2	2.219733	0.12183127	0.001	0.00333333
T4vsT3	3.61696	0.14119397	0.001	0.00333333
T4vsT0	1.674519	0.13211694	0.046	0.046
T4vsT2	1.811528	0.15336946	0.023	0.02875
T3vsT0	1.265128	0.06926469	0.016	0.02285714
T3vsT2	2.194035	0.12059091	0.003	0.005
T0vsT2	1.8108	0.26587187	0.034	0.03777778

Unweighted UniFrac

time	**4**	**3.3057**	**0.82643**	**4.6235**	**0.31407**	**0.001**
treatment	2	0.2917	0.14585	0.816	0.02771	0.755
time:treatment	5	0.8506	0.17012	0.9518	0.08082	0.568
Residuals	34	6.0774	0.17875	0.5774		
Total	45	10.5254	1			

pairs	F.Model	R2	p.value	p.adjusted
T1vsT4	10.024873	0.31303396	0.001	0.00333333
T1vsT3	1.934523	0.06462516	0.004	0.00571429
T1vsT0	2.10979	0.11040364	0.002	0.004
T1vsT2	4.220946	0.20874127	0.002	0.004
T4vsT3	9.708327	0.30617595	0.001	0.00333333
T4vsT0	3.715848	0.25250656	0.003	0.005
T4vsT2	3.315848	0.24901518	0.007	0.00875
T3vsT0	1.552555	0.08368418	0.019	0.02111111
T3vsT2	4.504046	0.21966621	0.001	0.00333333
T0vsT2	2.997002	0.3747657	0.025	0.025

Supplementary Table 3.9. Results of PERMANOVA test on log-transformed Porites samples.

Weighted Unifrac

	DF	SumsOfSqs	MeadSps	F.model	R2	P value
time	**3**	**0.28514**	**0.095047**	**3.7653**	**0.24889**	**0.001**
treatment	2	0.06562	0.032812	1.2998	0.05728	0.179
time:treatment	6	0.11332	0.018886	0.7482	0.09891	0.918
Residuals	27	0.68156	0.025243	0.59492		
Total	38	1.14564	1			

pairs	F.Model	R2	p.value	p.adjusted
T2vsT4	5.261274	0.2003434	0.001	0.003
T2vsT3	4.282257	0.1839279	0.001	0.003
T2vsT1	2.302459	0.1080842	0.014	0.016
T4vsT3	5.570315	0.2582399	0.002	0.004
T4vsT1	2.418475	0.131307	0.016	0.016
T3vsT1	2.6301	0.158153	0.003	0.0045

Bray Curtis

time	**3**	**2.6322**	**0.87741**	**2.72924**	**0.19196**	**0.001**
treatment	2	0.8301	0.41506	1.29106	0.06054	0.096
time:treatment	6	1.57	0.26167	0.81393	0.11449	0.952
Residuals	27	8.6801	0.32149	0.63301		
Total	38	13.7125	1			

pairs	F.Model	R2	p.value	p.adjusted
T2vsT4	3.224088	0.1330943	0.001	0.002
T2vsT3	3.617719	0.1599506	0.001	0.002
T2vsT1	2.683913	0.1237744	0.002	0.003
T4vsT3	3.109527	0.1627213	0.001	0.002
T4vsT1	1.931079	0.1076945	0.011	0.011
T3vsT1	1.853642	0.1169221	0.006	0.0072

Binary Jaccard

time	**3**	**2.5989**	**0.86631**	**2.27407**	**0.16358**	**0.001**
treatment	2	0.8787	0.43934	1.15327	0.05531	0.092
time:treatment	6	2.1241	0.35402	0.92932	0.1337	0.873
Residuals	27	10.2856	0.38095	0.64741		
Total	38	15.8874	1			

pairs	F.Model	R2	p.value	p.adjusted
T2vsT4	2.632823	0.1114053	0.001	0.001

T2vsT3	2.697185	0.1243104	0.001	0.001
T2vsT1	2.363079	0.1106151	0.001	0.001
T4vsT3	2.324874	0.1268699	0.001	0.001
T4vsT1	1.880113	0.1051511	0.001	0.001
T3vsT1	1.584559	0.1016749	0.001	0.001

Unweighted UniFrac

time	**3**	**1.9068**	**0.6356**	**3.3035**	**0.22029**	**0.001**
treatment	2	0.471	0.2355	1.224	0.05442	0.165
time:treatment	6	1.0832	0.18054	0.9383	0.12514	0.666
Residuals	27	5.1948	0.1924	0.60015		
Total	38	8.6558	1			

pairs	F.Model	R2	p.value	p.adjusted
T2vsT4	5.123261	0.19611873	0.001	0.002
T2vsT3	3.56089	0.15783463	0.001	0.002
T2vsT1	2.928764	0.13355811	0.001	0.002
T4vsT3	3.62265	0.18461576	0.002	0.003
T4vsT1	2.595251	0.13956527	0.005	0.006
T3vsT1	1.327452	0.08660615	0.119	0.119

Supplementary Table 3.10. PERMDISP tests on log-transformed data by coral genus, time (month), and treatment.

Coral Genus

Bray Curtis					
	DF	SumSq	MeanSq	F value	P value
Groups	**2**	**0.05326**	**0.02663**	**4.9107**	**0.008546**
Residuals	156	0.84596	0.0054228		
Binary Jaccard					
Groups	**2**	**0.014802**	**0.0074012**	**5.8797**	**0.003453**
Residuals	156	0.196368	0.0012588		
Weighted Unifrac					
Groups	**2**	**0.017018**	**0.008509**	**4.766**	**0.009793**
Residuals	156	0.278516	0.0017854		
Unweighted Unifrac					
Groups	2	0.00878	0.0043891	1.2122	0.3003
Residuals	156	0.56482	0.0036207		

Sampling Time

Bray Curtis					
	DF	SumSq	MeanSq	F value	P value
Groups	4	0.04926	0.0123156	1.9559	0.104
Residuals	154	0.96967	0.0062966		
Binary Jaccard					
Groups	**4**	**0.03093**	**0.0077337**	**3.6094**	**0.007657**
Residuals	154	0.32996	0.0021426		
Weighted Unifrac					
Groups	4	0.01348	0.0033702	1.3571	0.2515
Residuals	154	0.38244	0.0024834		
Unweighted Unifrac					
Groups	4	0.01177	0.002943	0.7568	0.555
Residuals	154	0.59889	0.0038889		

Treatment

Bray Curtis					
	DF	SumSq	MeanSq	F value	P value
Groups	2	0.00349	0.0017451	0.6031	0.5484
Residuals	156	0.45143	0.0028938		
Binary Jaccard					
Groups	2	0.001608	0.00080415	0.6647	0.5159

Residuals	156	0.18874	0.00120987		
Weighted Unifrac					
Groups	2	0.000918	0.00045911	0.2487	0.7801
Residuals	156	0.287964	0.00184592		
Unweighted Unifrac					
Groups	2	0.0136	0.0068015	1.9263	0.1491
Residuals	156	0.55082	0.0035309		

Supplementary Table 3.11. PERMDISP tests on log-transformed data for individual coral hosts.

Acropora: Sampling Time

Bray Curtis					
	DF	SumSq	MeanSq	F value	P value
Groups	**4**	**0.33385**	**0.083463**	**5.6635**	**0.0005309**
Residuals	69	1.01685	0.014737		
Binary Jaccard					
Groups	**4**	**0.091041**	**0.0227603**	**6.0968**	**0.0002923**
Residuals	69	0.257587	0.0037331		
Weighted Unifrac					
Groups	4	0.050386	0.0125966	13.009	6.01E-08
Residuals	69	0.06681	0.0009683		
Unweighted Unifrac					
Groups	**4**	**0.08746**	**0.0218643**	**4.6078**	**0.002347**
Residuals	69	0.32741	0.0047451		

Acropora: Treatment

Bray Curtis					
	DF	SumSq	MeanSq	F value	P value
Groups	2	0.02917	0.014585	2.303	0.1074
Residuals	71	0.44964	0.006333		
Binary Jaccard					
Groups	2	0.005069	0.0025344	2.012	0.1413
Residuals	71	0.089433	0.0012596		
Weighted Unifrac					
Groups	2	0.002433	0.0012167	0.9642	0.3862
Residuals	71	0.0896	0.001262		
Unweighted Unifrac					
Groups	2	0.004147	0.0020735	0.6191	0.5413
Residuals	71	0.237797	0.0033492		

Pocillopora: Sampling Time

Bray Curtis					
	DF	SumSq	MeanSq	F value	P value
Groups	4	0.2111	0.052776	2.0402	0.1066
Residuals	41	1.0606	0.025868		
Binary Jaccard					
Groups	4	0.03689	0.0092235	1.0397	0.3985

Residuals	41	0.36371	0.0088709		
Weighted Unifrac					
Groups	4	0.007684	0.0019209	0.5907	0.6713
Residuals	41	0.133337	0.0032521		
Unweighted Unifrac					
Groups	4	0.04495	0.0112387	1.2209	0.3168
Residuals	41	0.37742	0.0092054		

Porites: Sampling Time

Bray Curtis					
	DF	SumSq	MeanSq	F value	P value
Groups	3	0.04789	0.015964	1.5618	0.216
Residuals	35	0.35775	0.010221		
Binary Jaccard					
Groups	**3**	**0.023946**	**0.007982**	**4.8591**	**0.006266**
Residuals	35	0.057495	0.0016427		
Weighted Unifrac					
Groups	**3**	**0.0208**	**0.0069333**	**3.4593**	**0.02657**
Residuals	35	0.070148	0.0020042		
Unweighted Unifrac					
Groups	3	0.015814	0.0052712	1.3784	0.2654
Residuals	35	0.133842	0.003824		

Supplementary Table 3.12. Results of differential abundance analysis with ANCOM by month using an unrarefied OTU table summarized to genus. Of the 366 genera in the OTU table, ANCOM only analyzed genera with a prevalence of 90% across samples (prev.cut=0.9). W statistics and detection threshold are presented for those genera with sufficient prevalence. Only genera with a significant (TRUE) W statistic at the 0.9 detection level are considered significant and highlighted in grey.

Coral host	W stat	detected_0.9	detected_0.8	detected_0.7	detected_0.6	Phylum	Class	Order	Family	Genus
All	41	TRUE	TRUE	TRUE	TRUE	p__Proteobacteria	c__Alphaproteobacteria	o__Reyranellales	f__Reyranellaceae	g__Reyranella
All	38	TRUE	TRUE	TRUE	TRUE	p__Proteobacteria	c__Gammaproteobacteria	o__Pseudomonadales	f__Moraxellaceae	g__Acinetobacter
All	39	TRUE	TRUE	TRUE	TRUE	p__Proteobacteria	c__Gammaproteobacteria	o__Pseudomonadales	f__Pseudomonadaceae	g__Pseudomonas
All	40	TRUE	TRUE	TRUE	TRUE	p__Proteobacteria	c__Gammaproteobacteria	o__Xanthomonadales	f__Xanthomonadaceae	g__Pseudoxanthomonas
All	40	TRUE	TRUE	TRUE	TRUE	p__Proteobacteria	c__Alphaproteobacteria	o__Sphingomonadales	f__Sphingomonadaceae	g__Sphingomonas
All	38	TRUE	TRUE	TRUE	TRUE	p__Proteobacteria	c__Gammaproteobacteria	o__Alteromonadales	f__Alteromonadaceae	g__Alteromonas
All	39	TRUE	TRUE	TRUE	TRUE	p__Proteobacteria	c__Gammaproteobacteria	o__Vibrionales	f__Vibrionaceae	g__Vibrio
All	41	TRUE	TRUE	TRUE	TRUE	p__Proteobacteria	c__Gammaproteobacteria	o__Oceanospirillales	f__Endozoicomonadaceae	g__Endozoicomonas
All	38	TRUE	TRUE	TRUE	TRUE	p__Cyanobacteria	c__Oxyphotobacteria	o__Synechococcales	f__Cyanobiaceae	g__Synechococcus CC9902
All	40	TRUE	TRUE	TRUE	TRUE	p__Cyanobacteria	c__Oxyphotobacteria	o__Synechococcales	f__Cyanobiaceae	g__Prochlorococcus MIT9313
All	41	TRUE	TRUE	TRUE	TRUE	p__Firmicutes	c__Bacilli	o__Bacillales	f__Paenibacillaceae	g__Paenibacillus
All	38	TRUE	TRUE	TRUE	TRUE	p__Actinobacteria	c__Actinobacteria	o__Corynebacteriales	f__Corynebacteriaceae	g__Corynebacterium 1
All	41	TRUE	TRUE	TRUE	TRUE	p__Firmicutes	c__Bacilli	o__Lactobacillales	f__Streptococcaceae	g__Streptococcus
All	37	TRUE	TRUE	TRUE	TRUE	p__Firmicutes	c__Bacilli	o__Bacillales	f__Staphylococcaceae	g__Staphylococcus

All	14	FALSE	FALSE	FALSE	FALSE	p__Proteobacteria	c__Gammaproteobacteria	o__Pseudomonadales	f__Moraxellaceae	g__Psychrobacter
All	19	FALSE	FALSE	FALSE	FALSE	p__Proteobacteria	c__Gammaproteobacteria	o__Oceanospirillales	f__Alcanivoracaceae	g__Alcanivorax
All	34	FALSE	TRUE	TRUE	TRUE	p__Proteobacteria	c__Alphaproteobacteria	o__SAR11 clade	f__Clade I	g__Clade Ia
All	28	FALSE	FALSE	FALSE	TRUE	p__Proteobacteria	c__Alphaproteobacteria	o__Rhizobiales	f__Beijerinckiaceae	g__Methylobacterium
All	24	FALSE	FALSE	FALSE	FALSE	p__Proteobacteria	c__Deltaproteobacteria	o__Bdellovibrionales	f__Bacteriovoracaceae	g__Halobacteriovorax
All	25	FALSE	FALSE	FALSE	TRUE	p__Bacteroidetes	c__Bacteroidia	o__Flavobacteriales	f__Flavobacteriaceae	g__NS5 marine group
All	24	FALSE	FALSE	FALSE	FALSE	p__Proteobacteria	c__Alphaproteobacteria	o__Rhodobacterales	f__Rhodobacteraceae	g__Paracoccus
All	30	FALSE	FALSE	TRUE	TRUE	p__Proteobacteria	c__Alphaproteobacteria	o__Rhodobacterales	f__Rhodobacteraceae	g__uncultured
All	22	FALSE	FALSE	FALSE	FALSE	p__Proteobacteria	c__Alphaproteobacteria	o__Rhodobacterales	f__Rhodobacteraceae	g__Ruegeria
All	30	FALSE	FALSE	TRUE	TRUE	p__Proteobacteria	c__Alphaproteobacteria	o__Rhodobacterales	f__Rhodobacteraceae	g__HIMB11
All	23	FALSE	FALSE	FALSE	FALSE	p__Proteobacteria	c__Gammaproteobacteria	o__Enterobacteriales	f__Enterobacteriaceae	g__Pantoea
All	18	FALSE	FALSE	FALSE	FALSE	p__Proteobacteria	c__Gammaproteobacteria	o__Oceanospirillales	f__Halomonadaceae	g__Halomonas
All	27	FALSE	FALSE	FALSE	TRUE	p__Proteobacteria	c__Gammaproteobacteria	o__Alteromonadales	f__Idiomarinaceae	g__Idiomarina
All	24	FALSE	FALSE	FALSE	FALSE	p__Bacteroidetes	c__Bacteroidia	o__Cytophagales	f__Amoebophilaceae	g__Candidatus Amoebophilus
All	31	FALSE	FALSE	TRUE	TRUE	p__Bacteroidetes	c__Bacteroidia	o__Flavobacteriales	f__Weeksellaceae	g__Cloacibacterium
All	24	FALSE	FALSE	FALSE	FALSE	p__Proteobacteria	c__Gammaproteobacteria	o__Pasteurellales	f__Pasteurellaceae	g__Haemophilus
All	30	FALSE	FALSE	TRUE	TRUE	p__Proteobacteria	c__Gammaproteobacteria	o__Alteromonadales	f__Pseudoalteromonadaceae	g__Pseudoalteromonas
All	19	FALSE	FALSE	FALSE	FALSE	p__Firmicutes	c__Clostridia	o__Clostridiales	f__Family XI	g__Anaerococcus

All	22	FALSE	FALSE	FALSE	FALSE	p__Actinobacteria	c__Actinobacteria	o__Micrococcales	f__Micrococcaceae	g__Kocuria
All	29	FALSE	FALSE	TRUE	TRUE	p__Actinobacteria	c__Actinobacteria	o__Actinomycetales	f__Actinomycetaceae	g__Actinomyces
All	18	FALSE	FALSE	FALSE	FALSE	p__Actinobacteria	c__Actinobacteria	o__Micrococcales	f__Micrococcaceae	g__Rothia
All	34	FALSE	TRUE	TRUE	TRUE	p__Actinobacteria	c__Acidimicrobiia	o__Actinomarinales	f__Actinomarinaceae	g__Candidatus Actinomarina
All	23	FALSE	FALSE	FALSE	FALSE	p__Actinobacteria	c__Actinobacteria	o__Micrococcales	f__Brevibacteriaceae	g__Brevibacterium
All	24	FALSE	FALSE	FALSE	FALSE	p__Actinobacteria	c__Actinobacteria	o__Corynebacteriales	f__Corynebacteriaceae	g__Corynebacterium
All	21	FALSE	FALSE	FALSE	FALSE	p__Actinobacteria	c__Actinobacteria	o__Micrococcales	f__Micrococcaceae	g__Micrococcus
All	23	FALSE	FALSE	FALSE	FALSE	p__Actinobacteria	c__Actinobacteria	o__Corynebacteriales	f__Corynebacteriaceae	g__Lawsonella
All	36	FALSE	TRUE	TRUE	TRUE	p__Actinobacteria	c__Actinobacteria	o__Propionibacteriales	f__Propionibacteriaceae	g__Cutibacterium
All	20	FALSE	FALSE	FALSE	FALSE	p__Firmicutes	c__Negativicutes	o__Selenomonadales	f__Veillonellaceae	g__Veillonella
ACR	40	TRUE	TRUE	TRUE	TRUE	p__Proteobacteria	c__Alphaproteobacteria	o__Reyranellales	f__Reyranellaceae	g__Reyranella
ACR	39	TRUE	TRUE	TRUE	TRUE	p__Proteobacteria	c__Gammaproteobacteria	o__Pseudomonadales	f__Moraxellaceae	g__Acinetobacter
ACR	38	TRUE	TRUE	TRUE	TRUE	p__Proteobacteria	c__Gammaproteobacteria	o__Pseudomonadales	f__Pseudomonadaceae	g__Pseudomonas
ACR	39	TRUE	TRUE	TRUE	TRUE	p__Proteobacteria	c__Gammaproteobacteria	o__Xanthomonadales	f__Xanthomonadaceae	g__Pseudoxanthomonas
ACR	38	TRUE	TRUE	TRUE	TRUE	p__Proteobacteria	c__Alphaproteobacteria	o__Sphingomonadales	f__Sphingomonadaceae	g__Sphingomonas
ACR	37	TRUE	TRUE	TRUE	TRUE	p__Proteobacteria	c__Gammaproteobacteria	o__Alteromonadales	f__Alteromonadaceae	g__Alteromonas
ACR	39	TRUE	TRUE	TRUE	TRUE	p__Proteobacteria	c__Gammaproteobacteria	o__Vibrionales	f__Vibrionaceae	g__Vibrio
ACR	41	TRUE	TRUE	TRUE	TRUE	p__Proteobacteria	c__Gammaproteobacteria	o__Oceanospirillales	f__Endozoicomonadaceae	g__Endozoicomonas

ACR	41	TRUE	TRUE	TRUE	TRUE	p__Firmicutes	c__Bacilli	o__Bacillales	f__Paenibacillaceae	g__Paenibacillus
ACR	37	TRUE	TRUE	TRUE	TRUE	p__Actinobacteria	c__Actinobacteria	o__Corynebacteriales	f__Corynebacteriaceae	g__Corynebacterium 1
ACR	38	TRUE	TRUE	TRUE	TRUE	p__Firmicutes	c__Bacilli	o__Bacillales	f__Staphylococcaceae	g__Staphylococcus
ACR	9	FALSE	FALSE	FALSE	FALSE	p__Proteobacteria	c__Gammaproteobacteria	o__Pseudomonadales	f__Moraxellaceae	g__Psychrobacter
ACR	13	FALSE	FALSE	FALSE	FALSE	p__Proteobacteria	c__Gammaproteobacteria	o__Oceanospirillales	f__Alcanivoracaceae	g__Alcanivorax
ACR	14	FALSE	FALSE	FALSE	FALSE	p__Proteobacteria	c__Alphaproteobacteria	o__SAR11 clade	f__Clade I	g__Clade Ib
ACR	16	FALSE	FALSE	FALSE	FALSE	p__Proteobacteria	c__Alphaproteobacteria	o__SAR11 clade	f__Clade I	g__Clade Ia
ACR	13	FALSE	FALSE	FALSE	FALSE	p__Proteobacteria	c__Alphaproteobacteria	o__Rhizobiales	f__Beijerinckiaceae	g__Methylobacterium
ACR	32	FALSE	FALSE	TRUE	TRUE	p__Tenericutes	c__Mollicutes	o__Entomoplasmatales	f__Entomoplasmatales Incertae Sedis	g__Candidatus Hepatoplasma
ACR	13	FALSE	FALSE	FALSE	FALSE	p__Bacteroidetes	c__Bacteroidia	o__Flavobacteriales	f__Flavobacteriaceae	g__NS5 marine group
ACR	15	FALSE	FALSE	FALSE	FALSE	p__Bacteroidetes	c__Bacteroidia	o__Flavobacteriales	f__Cryomorphaceae	g__uncultured
ACR	11	FALSE	FALSE	FALSE	FALSE	p__Proteobacteria	c__Alphaproteobacteria	o__Rhodobacterales	f__Rhodobacteraceae	g__Paracoccus
ACR	21	FALSE	FALSE	FALSE	FALSE	p__Proteobacteria	c__Alphaproteobacteria	o__Rhodobacterales	f__Rhodobacteraceae	g__uncultured
ACR	11	FALSE	FALSE	FALSE	FALSE	p__Proteobacteria	c__Alphaproteobacteria	o__Rhodobacterales	f__Rhodobacteraceae	g__Ruegeria
ACR	14	FALSE	FALSE	FALSE	FALSE	p__Proteobacteria	c__Alphaproteobacteria	o__Rhodobacterales	f__Rhodobacteraceae	g__HIMB11
ACR	18	FALSE	FALSE	FALSE	FALSE	p__Proteobacteria	c__Gammaproteobacteria	o__Alteromonadales	f__Shewanellaceae	g__Shewanella
ACR	13	FALSE	FALSE	FALSE	FALSE	p__Proteobacteria	c__Gammaproteobacteria	o__Enterobacteriales	f__Enterobacteriaceae	g__Pantoea
ACR	13	FALSE	FALSE	FALSE	FALSE	p__Proteobacteria	c__Gammaproteobacteria	o__Oceanospirillales	f__Halomonadaceae	g__Halomonas

ACR	13	FALSE	FALSE	FALSE	FALSE	p__Proteobacteria	c__Gammaproteobacteria	o__Alteromonadales	f__Idiomarinaceae	g__Idiomarina
ACR	15	FALSE	FALSE	FALSE	FALSE	p__Proteobacteria	c__Gammaproteobacteria	o__Pasteurellales	f__Pasteurellaceae	g__Haemophilus
ACR	12	FALSE	FALSE	FALSE	FALSE	p__Proteobacteria	c__Gammaproteobacteria	o__Alteromonadales	f__Pseudoalteromonadaceae	g__Pseudoalteromonas
ACR	29	FALSE	FALSE	TRUE	TRUE	p__Cyanobacteria	c__Oxyphotobacteria	o__Synechococcales	f__Cyanobiaceae	g__Synechococcus CC9902
ACR	23	FALSE	FALSE	FALSE	FALSE	p__Cyanobacteria	c__Oxyphotobacteria	o__Synechococcales	f__Cyanobiaceae	g__Prochlorococcus MIT9313
ACR	16	FALSE	FALSE	FALSE	FALSE	p__Firmicutes	c__Clostridia	o__Clostridiales	f__Family XI	g__Anaerococcus
ACR	18	FALSE	FALSE	FALSE	FALSE	p__Actinobacteria	c__Actinobacteria	o__Micrococcales	f__Micrococcaceae	g__Kocuria
ACR	16	FALSE	FALSE	FALSE	FALSE	p__Actinobacteria	c__Actinobacteria	o__Actinomycetales	f__Actinomycetaceae	g__Actinomyces
ACR	13	FALSE	FALSE	FALSE	FALSE	p__Actinobacteria	c__Actinobacteria	o__Micrococcales	f__Micrococcaceae	g__Rothia
ACR	15	FALSE	FALSE	FALSE	FALSE	p__Actinobacteria	c__Acidimicrobiia	o__Actinomarinales	f__Actinomarinaceae	g__Candidatus Actinomarina
ACR	15	FALSE	FALSE	FALSE	FALSE	p__Actinobacteria	c__Actinobacteria	o__Micrococcales	f__Brevibacteriaceae	g__Brevibacterium
ACR	14	FALSE	FALSE	FALSE	FALSE	p__Proteobacteria	c__Gammaproteobacteria	o__Betaproteobacteriales	f__Hydrogenophilaceae	g__Hydrogenophilus
ACR	17	FALSE	FALSE	FALSE	FALSE	p__Actinobacteria	c__Actinobacteria	o__Micrococcales	f__Micrococcaceae	g__Micrococcus
ACR	13	FALSE	FALSE	FALSE	FALSE	p__Actinobacteria	c__Actinobacteria	o__Corynebacteriales	f__Corynebacteriaceae	g__Lawsonella
ACR	35	FALSE	TRUE	TRUE	TRUE	p__Actinobacteria	c__Actinobacteria	o__Propionibacteriales	f__Propionibacteriaceae	g__Cutibacterium
ACR	31	FALSE	FALSE	TRUE	TRUE	p__Firmicutes	c__Bacilli	o__Lactobacillales	f__Streptococcaceae	g__Streptococcus
POC	32	TRUE	TRUE	TRUE	TRUE	p__Bacteroidetes	c__Bacteroidia	o__Cytophagales	f__Amoebophilaceae	g__Candidatus Amoebophilus
POC	32	TRUE	TRUE	TRUE	TRUE	p__Proteobacteria	c__Gammaproteobacteria	o__Oceanospirillales	f__Endozoicomonadaceae	g__Endozoicomonas

POC	7	FALSE	FALSE	FALSE	FALSE	p__Proteobacteria	c__Gammaproteobacteria	o__Pseudomonadales	f__Moraxellaceae	g__Psychrobacter
POC	13	FALSE	FALSE	FALSE	FALSE	p__Proteobacteria	c__Gammaproteobacteria	o__Pseudomonadales	f__Moraxellaceae	g__Acinetobacter
POC	4	FALSE	FALSE	FALSE	FALSE	p__Proteobacteria	c__Alphaproteobacteria	o__Rhizobiales	f__Beijerinckiaceae	g__Methylobacterium
POC	27	FALSE	TRUE	TRUE	TRUE	p__Proteobacteria	c__Gammaproteobacteria	o__Pseudomonadales	f__Pseudomonadaceae	g__Pseudomonas
POC	6	FALSE	FALSE	FALSE	FALSE	p__Proteobacteria	c__Gammaproteobacteria	o__Xanthomonadales	f__Xanthomonadaceae	g__Stenotrophomonas
POC	1	FALSE	FALSE	FALSE	FALSE	p__Proteobacteria	c__Deltaproteobacteria	o__Bdellovibrionales	f__Bacteriovoracaceae	g__Halobacteriovorax
POC	5	FALSE	FALSE	FALSE	FALSE	p__Proteobacteria	c__Alphaproteobacteria	o__Sphingomonadales	f__Sphingomonadaceae	g__Sphingomonas
POC	6	FALSE	FALSE	FALSE	FALSE	p__Proteobacteria	c__Alphaproteobacteria	o__Rhodobacterales	f__Rhodobacteraceae	g__Ruegeria
POC	6	FALSE	FALSE	FALSE	FALSE	p__Proteobacteria	c__Gammaproteobacteria	o__Enterobacteriales	f__Enterobacteriaceae	g__Pantoea
POC	5	FALSE	FALSE	FALSE	FALSE	p__Proteobacteria	c__Gammaproteobacteria	o__Oceanospirillales	f__Halomonadaceae	g__Halomonas
POC	9	FALSE	FALSE	FALSE	FALSE	p__Bacteroidetes	c__Bacteroidia	o__Flavobacteriales	f__Weeksellaceae	g__Cloacibacterium
POC	7	FALSE	FALSE	FALSE	FALSE	p__Bacteroidetes	c__Bacteroidia	o__Cytophagales	f__Cyclobacteriaceae	g__Fulvivirga
POC	5	FALSE	FALSE	FALSE	FALSE	p__Proteobacteria	c__Gammaproteobacteria	o__Pasteurellales	f__Pasteurellaceae	g__Haemophilus
POC	12	FALSE	FALSE	FALSE	FALSE	p__Proteobacteria	c__Gammaproteobacteria	o__Vibrionales	f__Vibrionaceae	g__Vibrio
POC	8	FALSE	FALSE	FALSE	FALSE	p__Cyanobacteria	c__Oxyphotobacteria	o__Synechococcales	f__Cyanobiaceae	g__Synechococcus CC9902
POC	5	FALSE	FALSE	FALSE	FALSE	p__Firmicutes	c__Clostridia	o__Clostridiales	f__Family XI	g__Anaerococcus
POC	3	FALSE	FALSE	FALSE	FALSE	p__Actinobacteria	c__Actinobacteria	o__Actinomycetales	f__Actinomycetaceae	g__Actinomyces
POC	5	FALSE	FALSE	FALSE	FALSE	p__Actinobacteria	c__Actinobacteria	o__Micrococcales	f__Micrococcaceae	g__Rothia

POC	5	FALSE	FALSE	FALSE	FALSE	p__Actinobacteria	c__Actinobacteria	o__Micrococcales	f__Brevibacteriaceae	g__Brevibacterium
POC	7	FALSE	FALSE	FALSE	FALSE	p__Proteobacteria	c__Gammaproteobacteria	o__Betaproteobacteriales	f__Burkholderiaceae	g__Acidovorax
POC	5	FALSE	FALSE	FALSE	FALSE	p__Actinobacteria	c__Actinobacteria	o__Micrococcales	f__Micrococcaceae	g__Micrococcus
POC	5	FALSE	FALSE	FALSE	FALSE	p__Actinobacteria	c__Actinobacteria	o__Corynebacteriales	f__Corynebacteriaceae	g__Lawsonella
POC	26	FALSE	TRUE	TRUE	TRUE	p__Actinobacteria	c__Actinobacteria	o__Corynebacteriales	f__Corynebacteriaceae	g__Corynebacterium 1
POC	6	FALSE	FALSE	FALSE	FALSE	p__Actinobacteria	c__Actinobacteria	o__Propionibacteriales	f__Nocardioidaceae	g__Nocardioides
POC	5	FALSE	FALSE	FALSE	FALSE	p__Actinobacteria	c__Actinobacteria	o__Propionibacteriales	f__Propionibacteriaceae	g__Cutibacterium
POC	24	FALSE	FALSE	TRUE	TRUE	p__Firmicutes	c__Bacilli	o__Lactobacillales	f__Streptococcaceae	g__Streptococcus
POC	25	FALSE	FALSE	TRUE	TRUE	p__Firmicutes	c__Bacilli	o__Bacillales	f__Staphylococcaceae	g__Staphylococcus
POC	5	FALSE	FALSE	FALSE	FALSE	p__Firmicutes	c__Clostridia	o__Clostridiales	f__Clostridiaceae 1	g__Clostridium sensu stricto 1
POC	6	FALSE	FALSE	FALSE	FALSE	p__Firmicutes	c__Negativicutes	o__Selenomonadales	f__Veillonellaceae	g__Veillonella
POC	5	FALSE	FALSE	FALSE	FALSE	p__Firmicutes	c__Bacilli	o__Bacillales	f__Bacillaceae	g__Bacillus
POC	6	FALSE	FALSE	FALSE	FALSE	p__Fusobacteria	c__Fusobacteriia	o__Fusobacteriales	f__Fusobacteriaceae	g__Fusobacterium
POR	61	TRUE	TRUE	TRUE	TRUE	p__Proteobacteria	c__Alphaproteobacteria	o__Reyranellales	f__Reyranellaceae	g__Reyranella
POR	60	TRUE	TRUE	TRUE	TRUE	p__Firmicutes	c__Bacilli	o__Bacillales	f__Paenibacillaceae	g__Paenibacillus
POR	59	TRUE	TRUE	TRUE	TRUE	p__Firmicutes	c__Bacilli	o__Lactobacillales	f__Streptococcaceae	g__Streptococcus
POR	11	FALSE	FALSE	FALSE	FALSE	p__Actinobacteria	c__Acidimicrobiia	o__Microtrichales	f__Microtrichaceae	g__Sva0996 marine group
POR	11	FALSE	FALSE	FALSE	FALSE	p__Planctomycetes	c__Planctomycetacia	o__Pirellulales	f__Pirellulaceae	g__Rubripirellula

POR	1	FALSE	FALSE	FALSE	FALSE	p__Proteobacteria	c__Gammaproteobacteria	o__Pseudomonadales	f__Moraxellaceae	g__Psychrobacter
POR	3	FALSE	FALSE	FALSE	FALSE	p__Proteobacteria	c__Gammaproteobacteria	o__Pseudomonadales	f__Moraxellaceae	g__Enhydrobacter
POR	1	FALSE	FALSE	FALSE	FALSE	p__Proteobacteria	c__Gammaproteobacteria	o__Pseudomonadales	f__Moraxellaceae	g__Acinetobacter
POR	15	FALSE	FALSE	FALSE	FALSE	p__Proteobacteria	c__Gammaproteobacteria	o__Oceanospirillales	f__Alcanivoracaceae	g__Alcanivorax
POR	9	FALSE	FALSE	FALSE	FALSE	p__Proteobacteria	c__Alphaproteobacteria	o__SAR11 clade	f__Clade I	g__Clade Ib
POR	9	FALSE	FALSE	FALSE	FALSE	p__Proteobacteria	c__Alphaproteobacteria	o__SAR11 clade	f__Clade I	g__Clade Ia
POR	3	FALSE	FALSE	FALSE	FALSE	p__Proteobacteria	c__Alphaproteobacteria	o__Rhizobiales	f__Beijerinckiaceae	g__Methylobacterium
POR	12	FALSE	FALSE	FALSE	FALSE	p__Proteobacteria	c__Alphaproteobacteria	o__Rhizobiales	f__Xanthobacteraceae	g__Bradyrhizobium
POR	12	FALSE	FALSE	FALSE	FALSE	p__Proteobacteria	c__Alphaproteobacteria	o__Rhizobiales	f__Hyphomicrobiaceae	g__Filomicrobium
POR	50	FALSE	FALSE	TRUE	TRUE	p__Proteobacteria	c__Gammaproteobacteria	o__Pseudomonadales	f__Pseudomonadaceae	g__Pseudomonas
POR	52	FALSE	TRUE	TRUE	TRUE	p__Proteobacteria	c__Gammaproteobacteria	o__Xanthomonadales	f__Xanthomonadaceae	g__Pseudoxanthomonas
POR	55	FALSE	TRUE	TRUE	TRUE	p__Proteobacteria	c__Deltaproteobacteria	o__Bdellovibrionales	f__Bacteriovoracaceae	g__Halobacteriovorax
POR	8	FALSE	FALSE	FALSE	FALSE	p__Verrucomicrobia	c__Verrucomicrobiae	o__Verrucomicrobiales	f__Rubritaleaceae	g__Rubritalea
POR	8	FALSE	FALSE	FALSE	FALSE	p__Bacteroidetes	c__Bacteroidia	o__Flavobacteriales	f__Flavobacteriaceae	g__NS5 marine group
POR	11	FALSE	FALSE	FALSE	FALSE	p__Bacteroidetes	c__Bacteroidia	o__Flavobacteriales	f__Flavobacteriaceae	g__NS4 marine group
POR	11	FALSE	FALSE	FALSE	FALSE	p__Bacteroidetes	c__Bacteroidia	o__Flavobacteriales	f__Cryomorphaceae	g__uncultured
POR	0	FALSE	FALSE	FALSE	FALSE	p__Cyanobacteria	c__Oxyphotobacteria	o__Nostocales	f__Xenococcaceae	g__uncultured
POR	10	FALSE	FALSE	FALSE	FALSE	p__Bacteroidetes	c__Bacteroidia	o__Bacteroidales	f__Porphyromonadaceae	g__Porphyromonas

POR	50	FALSE	FALSE	TRUE	TRUE	p__Proteobacteria	c__Alphaproteobacteria	o__Sphingomonadales	f__Sphingomonadaceae	g__Sphingomonas
POR	10	FALSE	FALSE	FALSE	FALSE	p__Proteobacteria	c__Alphaproteobacteria	o__Rhodobacterales	f__Rhodobacteraceae	g__Paracoccus
POR	6	FALSE	FALSE	FALSE	FALSE	p__Proteobacteria	c__Alphaproteobacteria	o__Rhodobacterales	f__Rhodobacteraceae	g__uncultured
POR	11	FALSE	FALSE	FALSE	FALSE	p__Proteobacteria	c__Alphaproteobacteria	o__Rhodobacterales	f__Rhodobacteraceae	g__Ruegeria
POR	21	FALSE	FALSE	FALSE	FALSE	p__Proteobacteria	c__Alphaproteobacteria	o__Rhodobacterales	f__Rhodobacteraceae	g__HIMB11
POR	12	FALSE	FALSE	FALSE	FALSE	p__Proteobacteria	c__Gammaproteobacteria	o__Enterobacteriales	f__Enterobacteriaceae	g__Pantoea
POR	10	FALSE	FALSE	FALSE	FALSE	p__Proteobacteria	c__Gammaproteobacteria	o__Oceanospirillales	f__Halomonadaceae	g__Halomonas
POR	14	FALSE	FALSE	FALSE	FALSE	p__Proteobacteria	c__Gammaproteobacteria	o__Oceanospirillales	f__Saccharospirillaceae	g__Oleibacter
POR	12	FALSE	FALSE	FALSE	FALSE	p__Bacteroidetes	c__Bacteroidia	o__Cytophagales	f__Cyclobacteriaceae	g__Ekhidna
POR	0	FALSE	FALSE	FALSE	FALSE	p__Bacteroidetes	c__Bacteroidia	o__Cytophagales	f__Amoebophilaceae	g__Candidatus Amoebophilus
POR	9	FALSE	FALSE	FALSE	FALSE	p__Bacteroidetes	c__Bacteroidia	o__Flavobacteriales	f__Weeksellaceae	g__Cloacibacterium
POR	5	FALSE	FALSE	FALSE	FALSE	p__Bacteroidetes	c__Bacteroidia	o__Flavobacteriales	f__Weeksellaceae	g__Chryseobacterium
POR	8	FALSE	FALSE	FALSE	FALSE	p__Proteobacteria	c__Gammaproteobacteria	o__Pasteurellales	f__Pasteurellaceae	g__Haemophilus
POR	12	FALSE	FALSE	FALSE	FALSE	p__Proteobacteria	c__Gammaproteobacteria	o__Alteromonadales	f__Alteromonadaceae	g__Alteromonas
POR	10	FALSE	FALSE	FALSE	FALSE	p__Proteobacteria	c__Gammaproteobacteria	o__Vibrionales	f__Vibrionaceae	g__uncultured
POR	54	FALSE	TRUE	TRUE	TRUE	p__Proteobacteria	c__Gammaproteobacteria	o__Vibrionales	f__Vibrionaceae	g__Vibrio
POR	2	FALSE	FALSE	FALSE	FALSE	p__Proteobacteria	c__Gammaproteobacteria	o__Alteromonadales	f__Pseudoalteromonadaceae	g__Pseudoalteromonas
POR	0	FALSE	FALSE	FALSE	FALSE	p__Proteobacteria	c__Gammaproteobacteria	o__Oceanospirillales	f__Endozoicomonadaceae	g__Endozoicomonas

POR	23	FALSE	FALSE	FALSE	FALSE	p__Cyanobacteria	c__Oxyphotobacteria	o__Synechococcales	f__Cyanobiaceae	g__Synechococcus CC9902
POR	51	FALSE	FALSE	TRUE	TRUE	p__Cyanobacteria	c__Oxyphotobacteria	o__Synechococcales	f__Cyanobiaceae	g__Prochlorococcus MIT9313
POR	11	FALSE	FALSE	FALSE	FALSE	p__Firmicutes	c__Clostridia	o__Clostridiales	f__Family XI	g__Anaerococcus
POR	13	FALSE	FALSE	FALSE	FALSE	p__Acidobacteria	c__Blastocatellia (Subgroup 4)	o__Blastocatellales	f__Blastocatellaceae	g__Blastocatella
POR	31	FALSE	FALSE	FALSE	FALSE	p__Actinobacteria	c__Actinobacteria	o__Micrococcales	f__Micrococcaceae	g__Kocuria
POR	8	FALSE	FALSE	FALSE	FALSE	p__Actinobacteria	c__Actinobacteria	o__Actinomycetales	f__Actinomycetaceae	g__Actinomyces
POR	7	FALSE	FALSE	FALSE	FALSE	p__Actinobacteria	c__Actinobacteria	o__Micrococcales	f__Micrococcaceae	g__Rothia
POR	11	FALSE	FALSE	FALSE	FALSE	p__Firmicutes	c__Clostridia	o__Clostridiales	f__Lachnospiraceae	g__Epulopiscium
POR	9	FALSE	FALSE	FALSE	FALSE	p__Actinobacteria	c__Acidimicrobiia	o__Actinomarinales	f__Actinomarinaceae	g__Candidatus Actinomarina
POR	11	FALSE	FALSE	FALSE	FALSE	p__Firmicutes	c__Clostridia	o__Clostridiales	f__Family XI	g__Peptoniphilus
POR	7	FALSE	FALSE	FALSE	FALSE	p__Actinobacteria	c__Actinobacteria	o__Corynebacteriales	f__Nocardiaceae	g__Rhodococcus
POR	6	FALSE	FALSE	FALSE	FALSE	p__Actinobacteria	c__Actinobacteria	o__Corynebacteriales	f__Corynebacteriaceae	g__Corynebacterium
POR	13	FALSE	FALSE	FALSE	FALSE	p__Proteobacteria	c__Gammaproteobacteria	o__Betaproteobacteriales	f__Neisseriaceae	g__Neisseria
POR	13	FALSE	FALSE	FALSE	FALSE	p__Actinobacteria	c__Actinobacteria	o__Corynebacteriales	f__Dietziaceae	g__Dietzia
POR	3	FALSE	FALSE	FALSE	FALSE	p__Actinobacteria	c__Actinobacteria	o__Corynebacteriales	f__Corynebacteriaceae	g__Lawsonella
POR	57	FALSE	TRUE	TRUE	TRUE	p__Actinobacteria	c__Actinobacteria	o__Corynebacteriales	f__Corynebacteriaceae	g__Corynebacterium 1
POR	9	FALSE	FALSE	FALSE	FALSE	p__Actinobacteria	c__Actinobacteria	o__Corynebacteriales	f__Corynebacteriaceae	g__Turicella
POR	9	FALSE	FALSE	FALSE	FALSE	p__Actinobacteria	c__Actinobacteria	o__Propionibacteriales	f__Propionibacteriaceae	g__Cutibacterium

POR	2	FALSE	FALSE	FALSE	FALSE	p__Tenericutes	c__Mollicutes	o__Entomoplasmatales	f__Spiroplasmataceae	g__Spiroplasma
POR	9	FALSE	FALSE	FALSE	FALSE	p__Firmicutes	c__Bacilli	o__Lactobacillales	f__Carnobacteriaceae	g__Dolosigranulum
POR	57	FALSE	TRUE	TRUE	TRUE	p__Firmicutes	c__Bacilli	o__Bacillales	f__Staphylococcaceae	g__Staphylococcus
POR	8	FALSE	FALSE	FALSE	FALSE	p__Firmicutes	c__Clostridia	o__Clostridiales	f__Clostridiaceae 1	g__Clostridium sensu stricto 1
POR	8	FALSE	FALSE	FALSE	FALSE	p__Firmicutes	c__Negativicutes	o__Selenomonadales	f__Veillonellaceae	g__Veillonella
POR	11	FALSE	FALSE	FALSE	FALSE	p__Firmicutes	c__Bacilli	o__Bacillales	f__Bacillaceae	g__Bacillus

Appendix A: Ch. 4 Supplementary Material

Supplementary Figure 4.1. Three sampling sites included in the Tara expedition around the island of Mo'orea in French Polynesia. At each site, a coral fragment was collected from each of three colonies of *Pocillopora meandrina*.

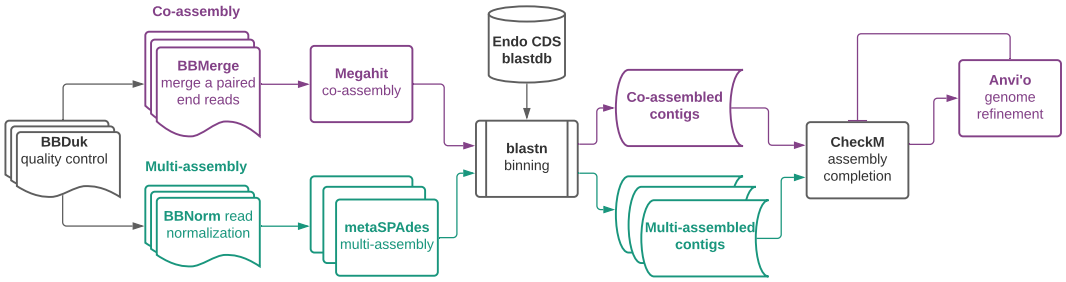

Supplementary Figure 4.2. Bioinformatic pipeline for co-assembly (i.e. reads from all samples assembled together) and multi-assembly (i.e. reads from each sample assembled individually). Our *Endozoicomonas* MAG, *E. meandrina* was the product of Anvi'o refined co-assembled contigs.

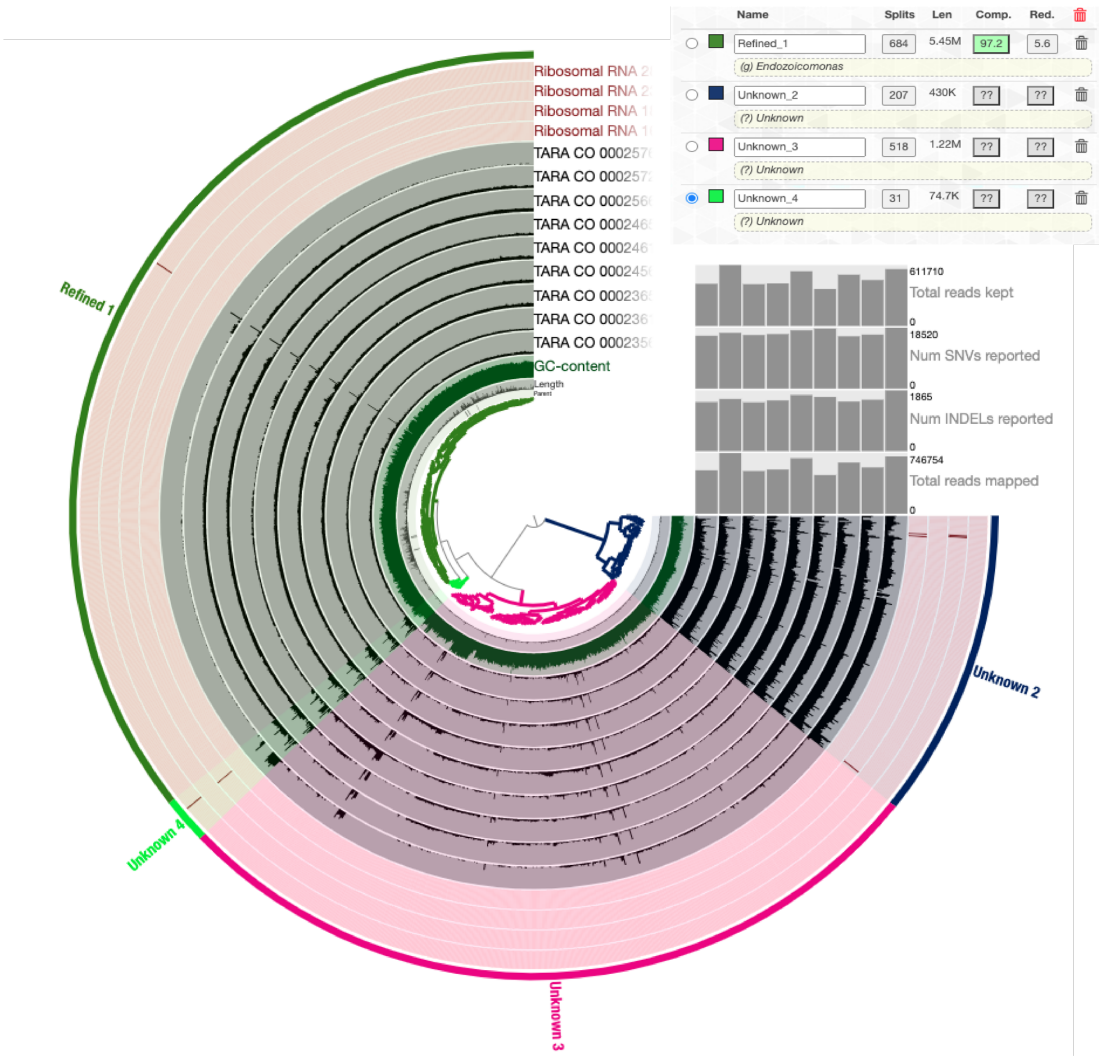

Supplementary Figure 4.3. Anvi-refine interface showing the manual selection of the *Endozoicomonas* genome from blast-identified contigs. All contigs identified as *Endozoicomonas* by blast are included in the figure. The dendrogram in the center shows the hierarchical clustering of the contigs based on coverage across samples. Each sample has a ring with the read coverage per contig. Grey barplots show sample-specific statistics. The outer four rings show the presence of ribosomal RNA genes: 28S, 23S, 18S, and 16S. The collection of contigs were 'binned' manually based on the dendrogram. Each bin was assessed for completeness, redundancy, and taxonomy in the upper right box. Refined 1 represents the *Endozoicomonas* genome.

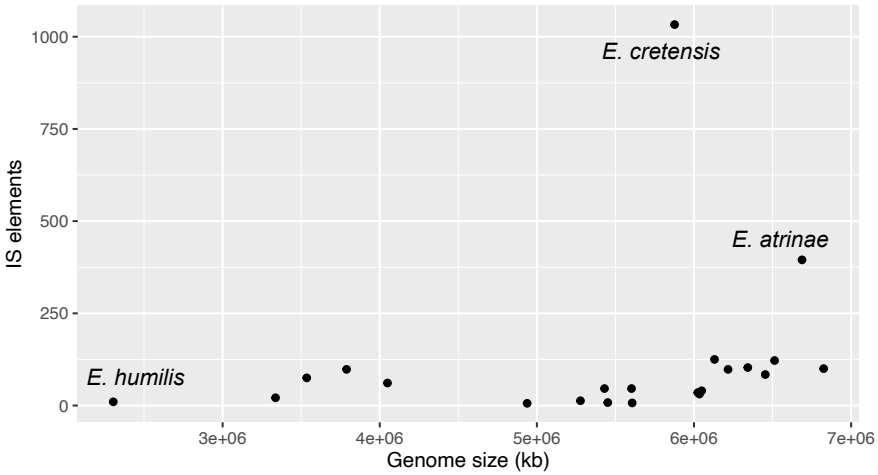

Supplementary Figure 4.4. Relationship between number of IS elements and genome size.

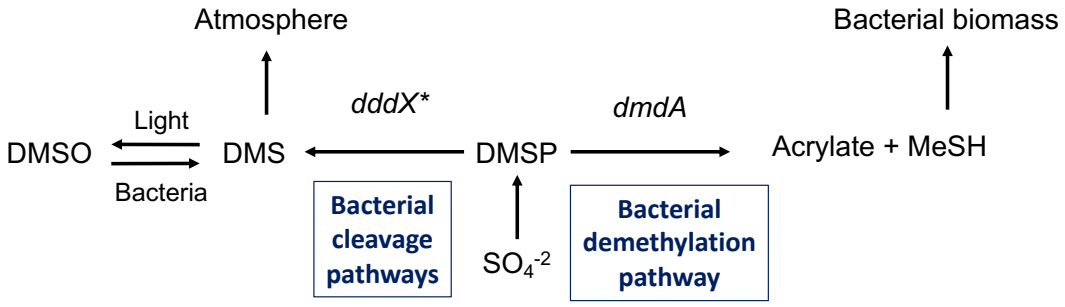

Supplementary Figure 4.5. Pathways for DMSP degradation in coral-associated bacteria. The demethylation pathway is shown on the right, and various different cleavage routes on the left utilizing the genes: *dddP*, *dddY*, *dddQ*, *dddW*, *dddK*, *dddL*, and *dddD*. Abbreviations: DMSP, dimethylsulfoniopropionate; DMS, dimethylsulfide; DMSO, dimethyl sulfoxide; MeSH, methanethiol.

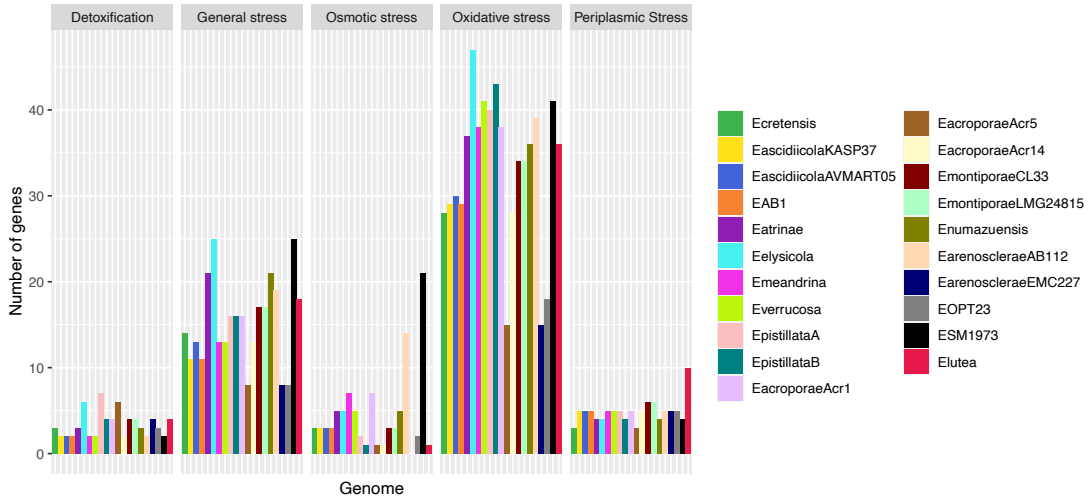

Supplementary Figure 4.6. Distribution of genes assigned to the Stress Response subsystem by RAST (Rapid Annotation using Subsystem Technology) across *Endozoicomonas* genomes.

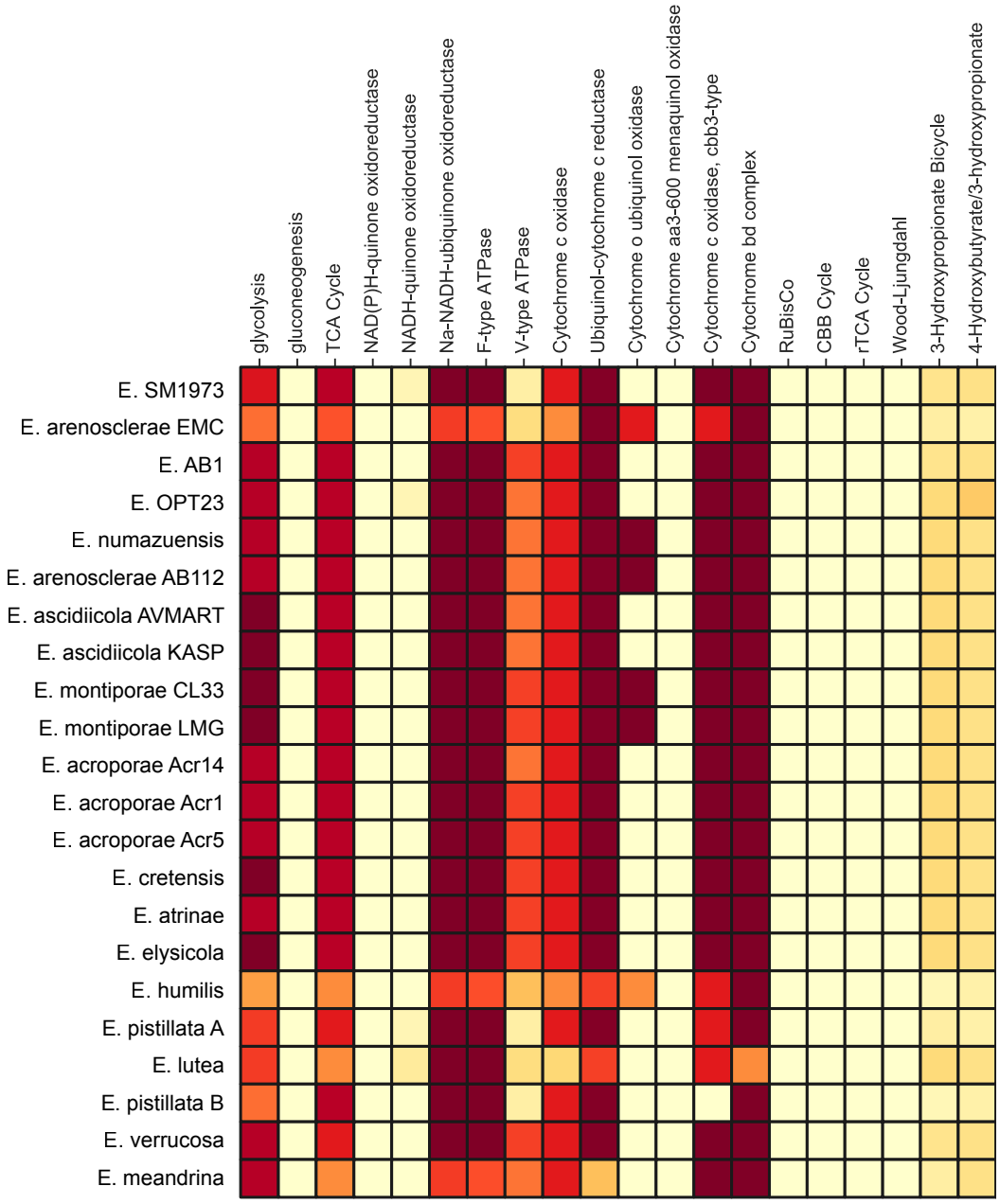

Supplementary Figure 4.7. Metabolic pathway completion based on KEGG Orthologs.

Supplementary Table 4.1. Sample statistics for read quality filtering and assembly. Number of raw, quality-controlled (QC), normalized (Norm), and merged (Merge) reads are reported. Normalized reads were used for multi-assembly, while merged reads were used for co-assembly. The number of scaffolds (Scaff.) assembled by metaSPAdes and the number of *Endozoicomonas* contigs identified by blast (contigs) are reported. CheckM completion (Comp), contamination (Contam), and strain heterogeneity (Het) statistics are also reported for each individual assembly.

				Multi-assembly							Co-assembly	
Sample	Raw PE	QC PE	QC SE	Norm PE	Norm SE	Scaff.	Contigs	Comp	Contam	Het	Merge PE	Merge M
T2356	209,103,298	189,641,290	8,388,071	131,277,950	7,317,094	145,581	1,052	12.97	0.95	0.00	143,344,068	23,148,611
T2361	259,514,350	237,233,764	9,383,948	140,271,880	7,940,648	143,244	1,264	21.41	2.33	8.33	156,019,158	40,607,303
T2365	201,234,712	182,504,078	7,806,544	130,534,940	6,863,509	141,682	2,199	37.90	1.93	5.56	130,312,488	26,095,795
T2456	241,898,388	221,920,620	8,589,076	136,781,852	7,362,214	112,512	2,120	40.17	3.93	5.63	127,399,672	47,260,474
T2461	260,477,368	239,679,490	8,888,849	141,159,704	7,512,646	164,275	2,796	52.22	6.28	4.62	138,148,788	50,765,351
T2465	221,523,886	204,285,358	6,702,494	136,449,456	5,594,698	131,936	1,588	19.49	1.23	5.00	96,832,326	53,726,516
T2566	223,522,020	204,226,970	8,194,873	130,682,284	7,100,327	113,365	2,866	61.97	5.16	2.13	129,591,448	37,317,761
T2572	222,605,972	202,842,452	8,511,129	131,008,474	7,357,686	106,595	2,552	47.88	4.34	13.89	124,557,330	39,142,561
T2576	288,780,618	263,693,022	10,850,759	137,950,326	9,197,792	128,450	450	4.18	1.67	4.55	120,581,260	71,555,881

Supplementary Table 4.2. Availability of genome assemblies.

Genome	GenBank accession	Publication
Endozoicomonas numazuensis DSM 25634	GCA_000722635.1	(Neave et al., 2014)
Endozoicomonas sp. OPT23	GCA_009653635.1	(Alex and Antunes, 2019)
Endozoicomonas elysicola DSM 22380	GCA_000710775.1	(Neave et al., 2014)
Endozoicomonas acroporae Acr-1	GCA_010994335.1	(Tandon et al., 2020)
Endozoicomonas acroporae Acr-5	GCA_010994325.1	(Tandon et al., 2020)
Endozoicomonas montiporae CL-33	GCA_001583435.1	(Ding et al., 2016)
Endozoicomonas montiporae LMG24815	GCA_000722565.1	(Neave et al., 2014)
Endozoicomonas atrinae WP70	GCA_001647025.2	(Hyun et al., 2014)
Endozoicomonas arenosclerae AB112	GCA_001562015.1	(Appolinario et al., 2016)
Endozoicomonas sp. SM1973	GCA_013425485.1	NA
Endozoicomonas ascidiicola AVMART05	GCA_001646945.1	(Schreiber et al., 2016b)
Endozoicomonas acroporae Acr-14	GCA_002864045.1	(Tandon et al., 2018)
Endozoicomonas ascidiicola KASP37	GCA_001646955.1	(Schreiber et al., 2016b)
Ca. Endozoicomonas cretensis	GCA_900299555.1	(Qi et al., 2018)
Endozoicomonas meandrina	See Data Availability	Present study
Endozoicomonas sp. strain AB1	GCA_001729985.1	(Miller et al., 2016)
Endozoicomonas verrucosa	NA*	(Neave et al., 2017a)
Endozoicomonas arenosclerae E-MC227	GCA_001562005.1	(Appolinario et al., 2016)
Endozoicomonas humilis	NA*	(Neave et al., 2017a)
Endozoicomonas lutea	GCA_012267545.1	(Robbins et al., 2019)
Endozoicomonas pistillata (Type B)	NA*	(Neave et al., 2017a)
Endozoicomonas pistillata (Type A)	NA*	(Neave et al., 2017a)

*Assemblies previously had a RAST ID but are no longer hosted on the RAST server.